NASW-4435

IN 1-22 141676

P- 3 25

COMET NUCLEUS AND ASTEROID SAMPLE RETURN MISSIONS

FINAL REPORT

By the 1991-92 Senior Spacecraft Design Students
Penn State Department of Aerospace Engineering

Sponsored by the USRA Advanced Design Program

June 1992

EXECUTIVE SUMMARY

Introduction

Three Advanced Design Projects have been completed this academic year at Penn State. At the beginning of the fall semester the students were organized into eight groups and given their choice of either a comet nucleus or an asteroid sample return mission. Once a mission had been chosen, the students developed conceptual designs. These were evaluated at the end of the fall semester and combined into three separate mission plans, including a comet nucleus sample return (CNSR), a single asteroid sample return (SASR), and a multiple asteroid sample return (MASR). To facilitate the work required for each mission, the class was reorganized in the spring semester by combining groups to form three mission teams. An integration team consisting of two members from each group was formed for each mission so that communication and information exchange would be easier among the groups.

The types of projects designed by the students evolved from numerous discussions with Penn State faculty and mission planners at the Johnson Space Center Human/Robotic Spacecraft Office. Robotic sample return missions are widely considered valuable precursors to manned missions in that they can provide details about a site's environment and scientific value. For example, a sample return from an asteroid might reveal valuable resources that, once mined, could be utilized for propulsion[1,2]. These missions are also more adaptable when considering the risk to humans visiting unknown and potentially dangerous locations, such as a comet nucleus.

Comet Nucleus Sample Return Mission (CNSR)

Background

Presently, much of the scientific community's understanding of the universe has come from remote observation of the cosmos, but technological advances within the past thirty years

have allowed for the study of retrieved cosmic materials on Earth. These Earth-returned samples have proved to be of immense scientific value, providing many answers and potential paths of inquiry.

Although comets have been observed for many centuries, a mystery still shrouds the composition of the comet nucleus. Comets are thought to have been formed simultaneously with the Sun and planets and therefore consist of the most chemically primitive solid matter known to have survived in the planetary system[3]. Thus, the examination of a sample from a comet nucleus would greatly add to knowledge of the Solar System's origin.

Mission Objectives

A CNSR mission is proposed to return a comet nucleus sample in its own environment to Earth for study. The primary mission objective consists of three phases: rendezvous with a short period comet, acquisition of a 10 kg sample from the nucleus, and maintenance of the sample composition and crystalline structure for return to Earth. The secondary objective for the CNSR mission is to monitor comet activity through perihelion by using a penetrator equipped with scientific instrumentation.

The comet Wild 2 was determined to be the most suitable target because of its low inclination to the ecliptic plane, its short orbital period, and its recent change in perihelion distance. An encounter with Jupiter changed Wild 2's perihelion distance from 6.2 AU to 1.6 AU. Consequently, the now short-period comet has the crystalline structure of a long-period comet[4]. A tethered coring unit will reach the comet nucleus and extract a sample that will be housed in a protective environment so that it may be returned to Earth in an unaltered state. Upon rendezvous with the comet, a sampling probe will extract a two meter core sample from a target site where undisturbed material maintains a temperature less than 130 K[3]. The comet must have a relatively low mean temperature to retain its volatile material — any material above that temperature is believed to have experienced too much heating to be of great scientific value.

The last phase of the primary objective is to maintain, as best as possible, the sample's undisturbed state during the transit to Earth. This involves monitoring and controlling the sample's pressure and temperature, as well as keeping it physically stable. A chemically or physically altered comet sample would lead to false conclusions and a distorted picture of the origins of the Solar System.

The secondary objective of the CNSR mission is to obtain as much information as possible on the activity of Wild 2. This ensures that the sample is representative of the comet and allows it to be placed in the proper context with respect to other comets investigated only by remote sensing. Sufficient characterization of the sampled comet also eliminates the need for multiple samples. To fully characterize the comet, a penetrator will be left behind to monitor the comet through perihelion. Characterization of the comet includes the determination of size, shape, density, and surface temperature distribution. The penetrator will monitor temperature and gas production changes of the comet until perihelion.

Mission Profile

The spacecraft will be launched on an Atlas IIA equipped with a Centaur IIA to inject the spacecraft into a low parking orbit and to provide the necessary Earth escape velocity (see Figure 1). The upper stage will then separate from the spacecraft, systems will be checked, and instrument booms and solar arrays deployed (see Figure 2 for spacecraft configuration). After Earth escape additional correction maneuvers during interplanetary cruise will insure accurate targeting for Wild 2.

At 100 to 200 km from Wild 2, the comet approach maneuvers reduce the relative velocity to 2 m/s. The comet's exact size and spin rate will then be determined and during the global characterization phase the surface will be mapped for candidate sampling sites. Candidate sites will be mapped in detail from an altitude of 50 km, and the coma gas and dust will be analyzed. While the spacecraft awaits final site selection it will return to an altitude of 100 km.

After a target site has been selected, the spacecraft will return to a low, *forced* synchronous orbit at 0.5 km above the selected site, reducing contamination of the surface by the thruster plumes. A sampling probe powered by liquid propellant rocket thrusters will then be jettisoned from the spacecraft to impact the target site. Because the spacecraft and the sampling penetrator are connected, a synchronous orbit must be maintained during extraction. Drilling commands will be sent from the spacecraft through cabling enclosed in the tether. After extraction, the tether will be used to retrieve the specimen from the sampling penetrator. Finally, a monitoring penetrator will be deployed and anchored into the comet to monitor Wild 2's activity. This penetrator will be equipped with scientific instrumentation to observe comet activity and return data. An optical communication system powered by a radioisotope thermoelectric generator (RTG) will relay the information to Earth. The RTG will also provide power for the scientific instrumentation.

After the sample has been safely retrieved, it will be returned to the spacecraft and hermetically sealed within multi-layer insulation. Once the sample has been secured in a thermally controlled environment, the spacecraft will depart from the comet leaving behind the monitoring probe. Heat pipes and phase change materials will be used to direct heat from the other spacecraft subsystems away from the sample.

The spacecraft will leave the comet and be placed on a direct Earth return trajectory. The Earth return trajectory will contain no additional maneuvers except those needed for navigational corrections. Upon arrival at Earth the spacecraft's relative velocity will be reduced, and it will be placed into a circular Space Shuttle accessible orbit and remain there no longer than approximately two weeks. The sample will then be retrieved by the Shuttle and returned to the surface in a thermally safe environment.
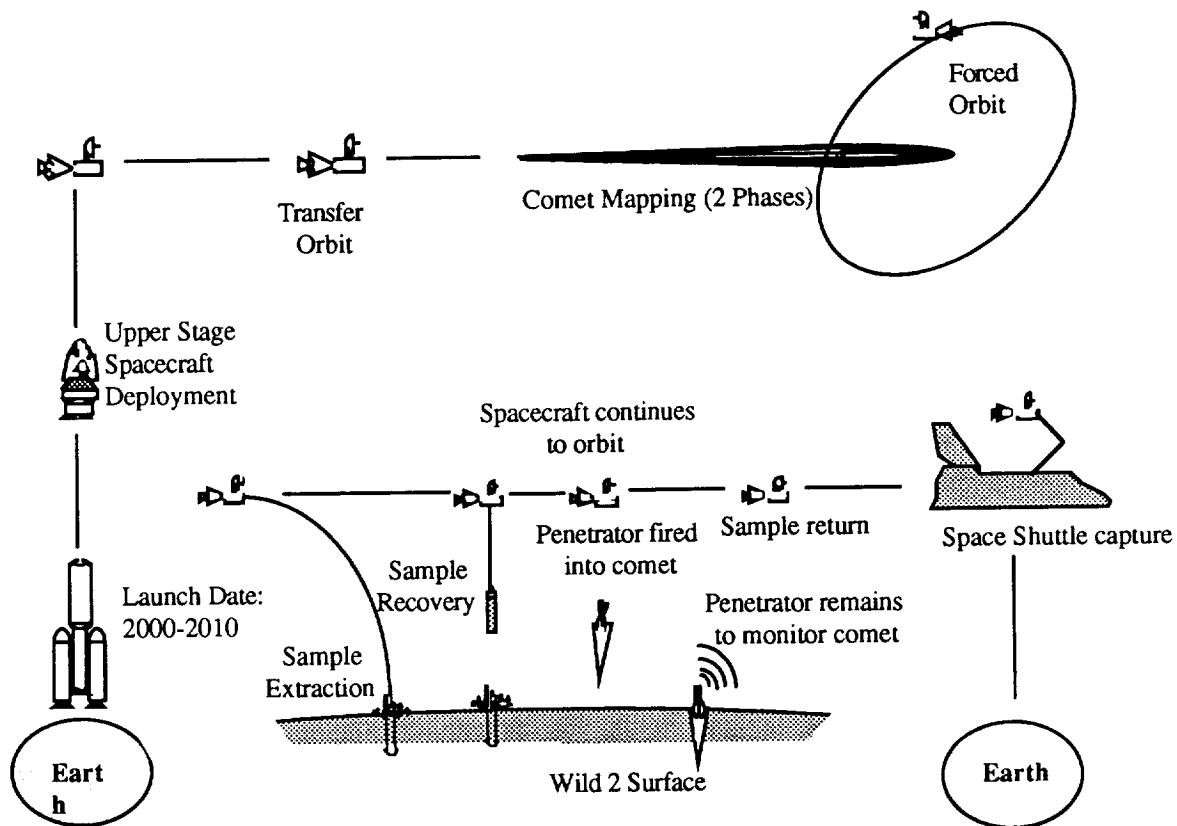
Figure 1: CNSR Mission Profile
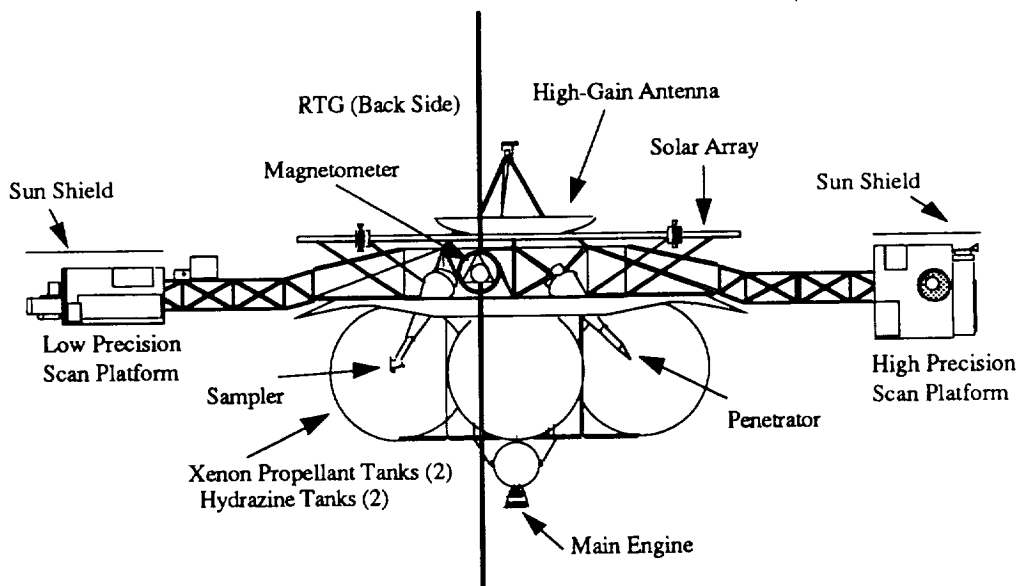
Figure 2: CNSR Spacecraft Configuration

Overall Mass, Power, and Cost Budgets

The spacecraft will have a total mass of 5149 kg (see Table 1) and require a total operating power of 528 Watts (see Table 2). A cost model[5] was applied to the mission estimating a total cost of 1.88 billion FY92 dollars (see Table 3).

Table 1:   Spacecraft Mass Budget

Element	Mass (kg)
Spacecraft Structure	**1309**
Bus	801
Booms (truss structure)	102
Fasteners & joints (10%)	90
Deployment mech. (10%)	90
Contingency (25%)	225
Sampler	**95**
Penetrator	**262**
Power	**93**
Solar Array	10
RTG	83
GN&C	**77**
Scientific Instruments	**134**
Communication	**7**
Computer	**12**
TOTAL	**1990**
10% Electric wiring	199
10% Mass Margin	199
Thermal (8% Dry Mass)	**159**
TOTAL DRY MASS	**2547**
Propulsion	**2602**
Propellant	2312
Tankage (10%)	231
Valves, tubing (25% of tank mass	57
TOTAL WET MASS	**5149**

Table 2: Power Budget

Spacecraft Component	Power (W)
GN&C	20
Mapping	150
Communications	122
Computer System	50
Structure	50
Thermal	40
Sample Extraction	27
AVG. POWER	459
Margin (15%)	69
TOTAL AVG. POWER	528

Table 3: Cost Estimation[5]

Mission Component	Cost ($M)
Computer	47.97
Communications	17.83
Power	135.31
Sampler	240.13
Penetrator	368.00
Thermal	123.04
Propulsion	0.51
GN&C	129.33
Scientific Instruments	209.26
Structure	524.38
Launch System	85.00
TOTAL	1880.76

Single Asteroid Sample Return Mission (SASR)

Mission Objectives

The primary objective of this mission is to extract a core sample from a target asteroid and return this sample to Earth for detailed compositional analysis. Secondary mission objectives entail performing a wide variety of scientific observations that will enable humankind to better understand the physical nature of asteroids, their possible origin, and their effect on the interplanetary environment.

Mission Profile

The mission designers selected 433 Eros as the target asteroid because of its accessibility, its relatively large size, and its well-known orbital parameters. In addition, at least three launch windows will exist for a mission to Eros between 1992 and 2010[6].

Figure 3 illustrates the mission profile. The spacecraft will begin the mission with the landing struts, instrument booms, and high-gain antenna collapsed enabling it to fit in the

launch vehicle shroud and withstand all launch forces. An Atlas IIA launch vehicle will propel the spacecraft into Low Earth Orbit (LEO). While in LEO, the spacecraft will perform checks of all systems. A Centaur will then inject the vehicle into the required transfer orbit after which the spacecraft will deploy the landing struts, booms, and high-gain antenna. Scientific measurements of the interplanetary environment will begin at this time. At a distance of one million km from Eros, the spacecraft will begin to photograph the asteroid and perform scientific observations. Once the spacecraft descends to an altitude of 2.5 km, it will maintain its position above a location on the surface. A passive/active sensing technique will utilize visual images and laser radar scans to identify a safe landing zone that is within the maneuvering range of the vehicle. The spacecraft will then land at this location and anchor into the surface with barbed spikes. Once secured on Eros, the scientific instruments will perform several observations and then cease operations to allow power to be concentrated on the drilling process. The drill will then proceed to extract a five-foot long core sample. Once this sample is stored on the spacecraft, pyrotechnic charges will separate the vehicle's upper portion from the rest of the spacecraft and depart from the asteroid, leaving the drill and landing struts behind. If enough propellant remains, the spacecraft will perform the maneuvers required to complete a detailed map of Eros. Once the mapping is completed, or discovered to be beyond the capacity of the propulsion system, the spacecraft will begin the voyage back to Earth. On the return trip, the vehicle must again execute a mid-course correction. Upon arrival at Earth, the spacecraft will maneuver into LEO where it will remain until it can be retrieved by the Space Shuttle.
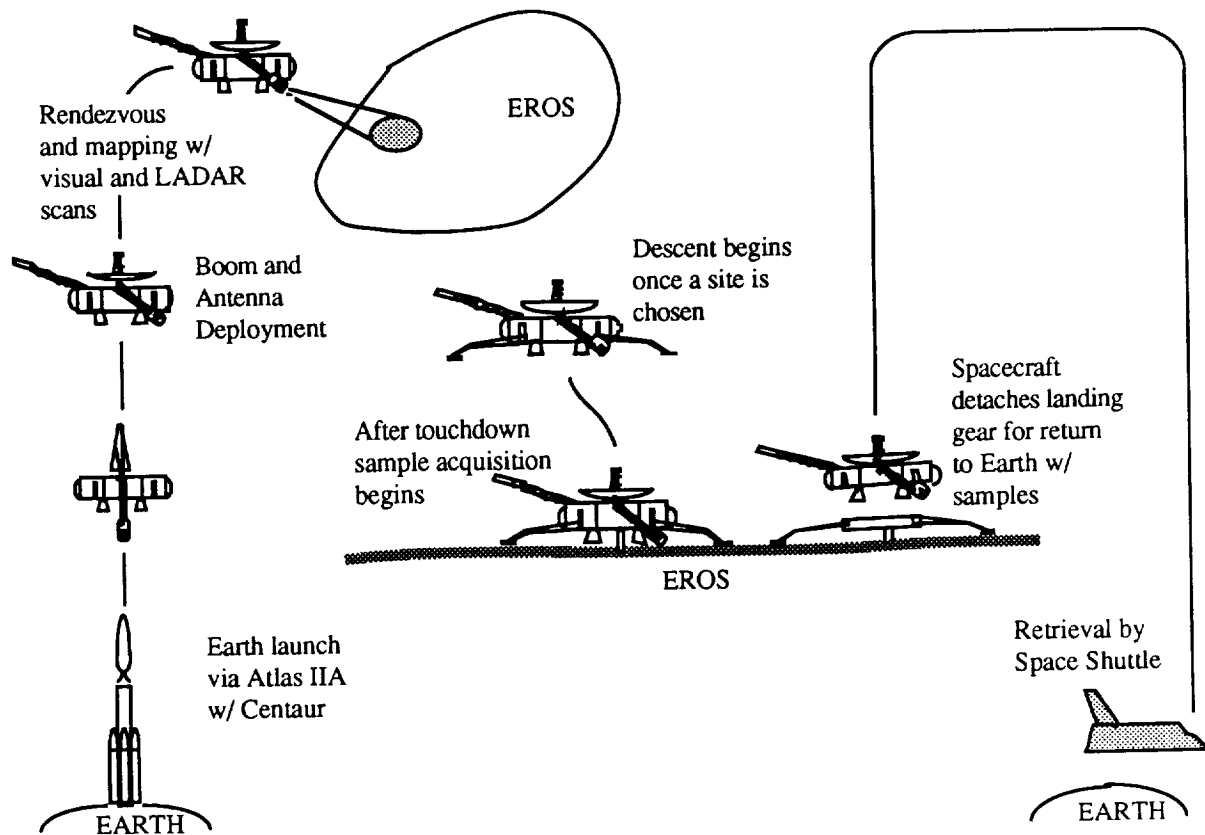
Figure 3: SASR Mission Profile

Spacecraft Description

Figure 4 illustrates the basic spacecraft configuration. The spacecraft structure will be a semimonocoque design constructed chiefly from beryllium. It will use three modular RTGs for general power consumption and will employ three batteries to provide the power required for drill operation. The vehicle will be propelled by four main thrusters that use a bipropellant consisting of monomethylhydrazine and nitrogen tetroxide. Twelve attitude thrusters will utilize hydrazine as a monopropellant. The control system will incorporate three-axis stabilization with momentum wheels. Spacecraft communications will be accomplished by one high-gain antenna and two low-gain antennas that operate in the Ka-band. The scientific payload will include: a visual and infrared mapping spectrometer, an ultraviolet spectrometer, a plasma spectrometer, a magnetometer, a dust analyzer, a laser radar system, and two charge-

coupled device cameras. The thermal subsystem design consists of thermal blankets and heaters for the majority of the spacecraft. Thermal requirements for the drill necessitate the additional use of heat pipes and second-surface mirrors. The electronics will be mounted on cold rails from which heat will be transferred by heat pipes to the second-surface mirrors. In addition, the infrared-sensing instrument will require a radiative cryogenic coolant system. The command and data handling system must be highly autonomous, utilizing higher-order languages, and hybrid architecture.
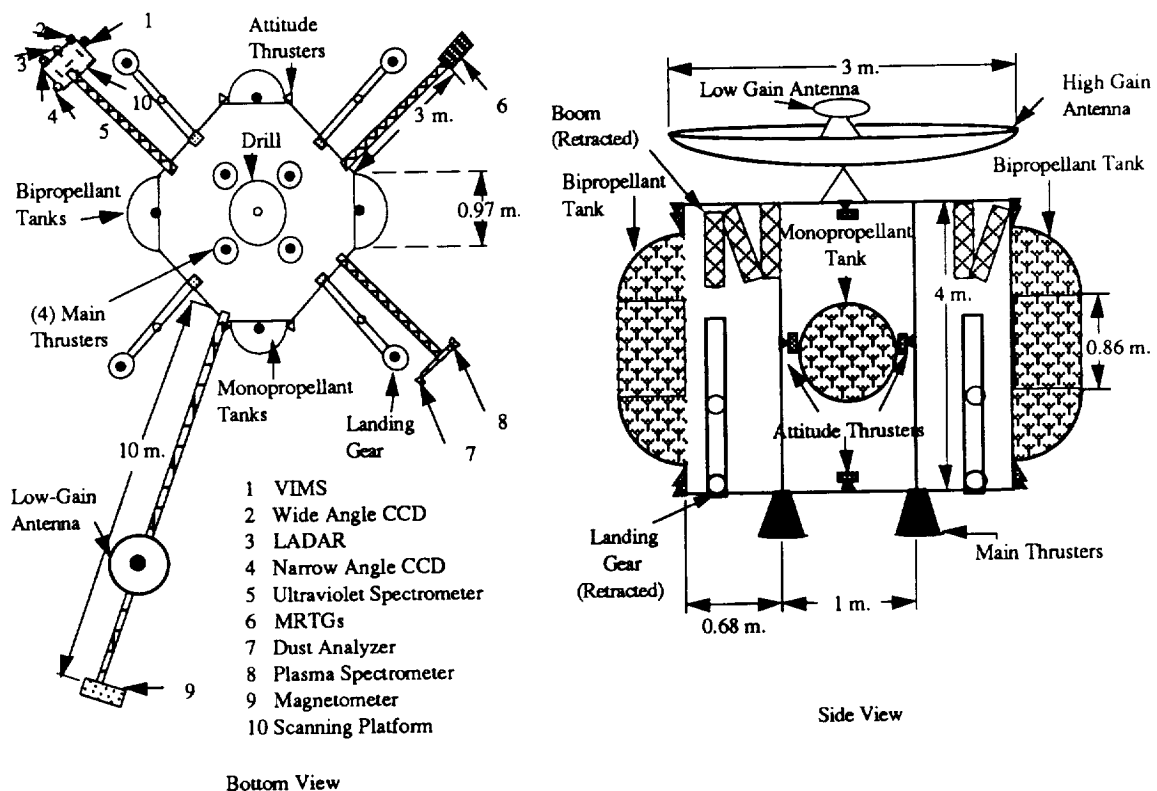
Figure 4: SASR Spacecraft Views

Overall Mass, Peak Power, and Cost Budgets

Table 4 shows the overall spacecraft mass budget and peak power budget. The peak power values are not totaled because all the subsystems will not be simultaneously operating at peak requirements during any particular time of the mission. Table 5 summarizes the overall estimated cost budget for this mission in FY92$M[5,7].

Table 4: Spacecraft Mass and Peak Power Budgets

Subsystem	Mass (kg)	Peak Power (W)
Propulsion	3633.11	150.0
C&DH	121.35	451.1
Drill	450.00	7500.0
Attachment	150.00	181.0
Structure	550.00	N/A
Scientific Payload	116.20	114.2
Communications	32.00	80.0
Power	550.00	
GN&C	200.00	550.0
Thermal	50.00	60.0
TOTAL	**5852.66**	**N/A**

Table 5: Overall Mission Cost Budget[5,7]

Segment Description	Cost (FY92$M)
R & D and Testing	1141.16
First Unit	57.09
Ground Segment	1530.65
Launch Segment	115.70
TOTAL	**2844.60**

Multiple Asteroid Sample Return Mission (MASR)

Mission Objective

The goal of this mission is to return sample material from three asteroids to Earth for scientific analysis. Asteroids Euterpe, Psyche, and Themis will be sampled, covering three major classes of asteroids, S (stony iron), M (metallic), and C (carbonaceous), respectively. The MASR mission utilizes numerous state-of-the-art technologies including a nuclear reactor for the power system, a low-thrust propulsion system, a deployable truss structure, and an optical communications system.

Spacecraft Configuration

The spacecraft configuration consists of a main spacecraft and a tethered lander (see Figures 5 and 6). The spacecraft employs a reactor with shielding and radiator panels separated from the main spacecraft body by an expandable truss. This configuration keeps the harmful radiation from the reactor away from sensitive subsystems like the computer or

scientific instruments. The main spacecraft body contains all required propellant, the lander, and all other subsystems. The tethered lander is stored inside the main spacecraft body and consists primarily of a drill and a small GN&C system.
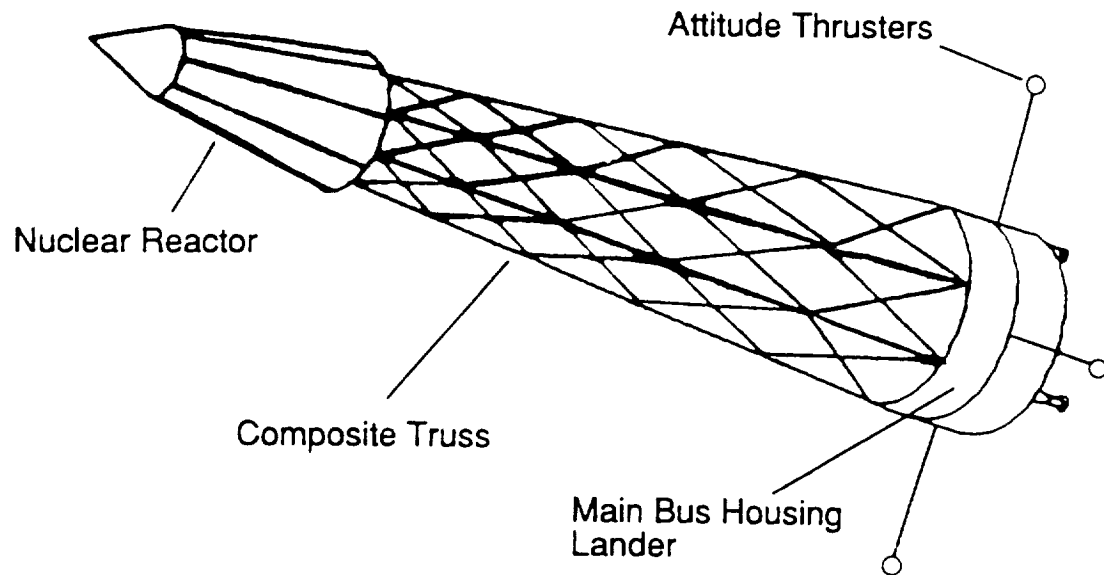
Figure 5: MASR High Technology Spacecraft
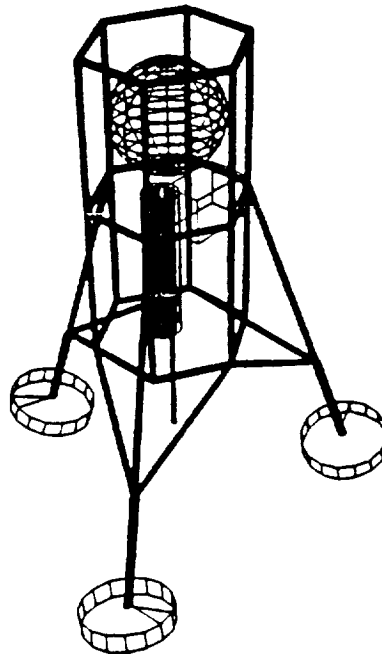
Figure 6: Sampler/Lander

Mission Profile

The following description of the mission plan is summarized in Figure 7. The mission scenario begins by launching the spacecraft into LEO with a Titan IV on March 1, 2002. The Titan IV will be used because it is the only current launch system that can accommodate the spacecraft's mass, 15,800 kg, and size, 16 m long by 4.5 m diameter. During the launch phase, communication with the spacecraft will be through an omnidirectional antenna. Before starting the nuclear reactor, power for the communication and housekeeping systems will be supplied by batteries. Once in LEO, the spacecraft will then deploy the partially collapsible truss structure and optical communications system, again by battery power. The omni antenna will then be switched off and the optical communication system used for the remainder of the mission. The reactor will be powered up and a functional check-out performed on all subsystems. The spacecraft will now rely on the nuclear reactor for power. A series of xenon thrusters will be activated, propelling the spacecraft toward the first target asteroid. The thrusters will cycle through thrust and coast stages to achieve the most efficient trajectory. This thrust profile has been calculated by NASA's QuickTop 2 (QT2) computer program.

Once the main spacecraft detects the asteroid with sensors, the rendezvous and docking (RVD) processor will take control and implement the necessary orbital maneuvers to orient the main spacecraft in the proper attitude. While the main spacecraft is approaching the asteroid, several scientific instruments will be collecting data to determine the best possible landing sites. A mass spectrometer, laser altimeter, and a radiometer will provide a complete map of the asteroid's surface. The main computer system will analyze this data and select the four best sites, three to sample and one as a backup. These landing sites may require additional maneuvering of the main spacecraft. The lander, while still attached to the main spacecraft through a tether, descends toward the asteroid and one of the landing sites. The lander's propulsion system will consist of 12 xenon thrusters powered by the reactor through a cable in the tether. The RVD processor on the main spacecraft will also control the lander during its rendezvous with the asteroid.

The lander attaches itself to the asteroid by drills in the landing pads. Three core samples, from three different locations on the asteroid, will be extracted from the asteroid along with other scientific data. While the lander is maneuvering to the next sampling site the main spacecraft, while orbiting above, will follow it to the next site. This is necessary due to the limited length of the tether. Each sample will be encased in its coring barrel to prevent contamination. All samples and scientific information will be stored on the main spacecraft. Power and communications for the lander will be provided by the main spacecraft through the tether.

After the three samples are taken from the asteroid, the lander will then rendezvous with the main spacecraft. The RVD processor will also control these maneuvers and will dock the lander in the center of the main spacecraft. Once the lander is secure, the main spacecraft will then proceed to the next asteroid. Because of the large amount of data needed to be stored for these RVD maneuvers, data will be transmitted to Earth between asteroid encounters. When the next asteroid is located by the long-range sensors, the rendezvous and sampling scenario will then be repeated.

After the last sample is obtained, the lander will return and dock in its station in the center of the base of the main spacecraft. The main spacecraft will then begin its journey back to Earth. The return leg of the mission is similar to the first leg in that it will consist of a series of thrust and coast periods as calculated by QT2. Along with the thrust and coast periods the program provides the appropriate orbital paths for returning to Earth.

The ship will approach Earth to enter an orbit where it may release the lander, or the sample container alone if feasible. This orbit will be designed such that the Space Shuttle, or its replacement in 2026, will be able to retrieve the samples.

After the sample container or lander is released the main spacecraft will have completed its duties. The reactor will then be shut down using systems that are designed to function independently of the spacecraft. Two proposals have been suggested for dealing with the spacecraft after the mission is complete. The main goal is to eliminate possible contamination

to the environment after the reactor is shut down. One proposed method is to have the main spacecraft thrust into a high nuclear-safe orbit that will not decay for approximately 1000 years. Another solution is to send the spacecraft on an Earth escape trajectory. If reentry were to occur after spending a long time in space, a majority of the radioactivity would have decayed. However, as an added safety feature, the nuclear system will be designed to safely accommodate accidental reentry. The SP-100 has been designed to remain inoperable and to survive the intense heat and aerodynamic forces of reentry and to bury itself on impact in water, soil, or pavement[8].
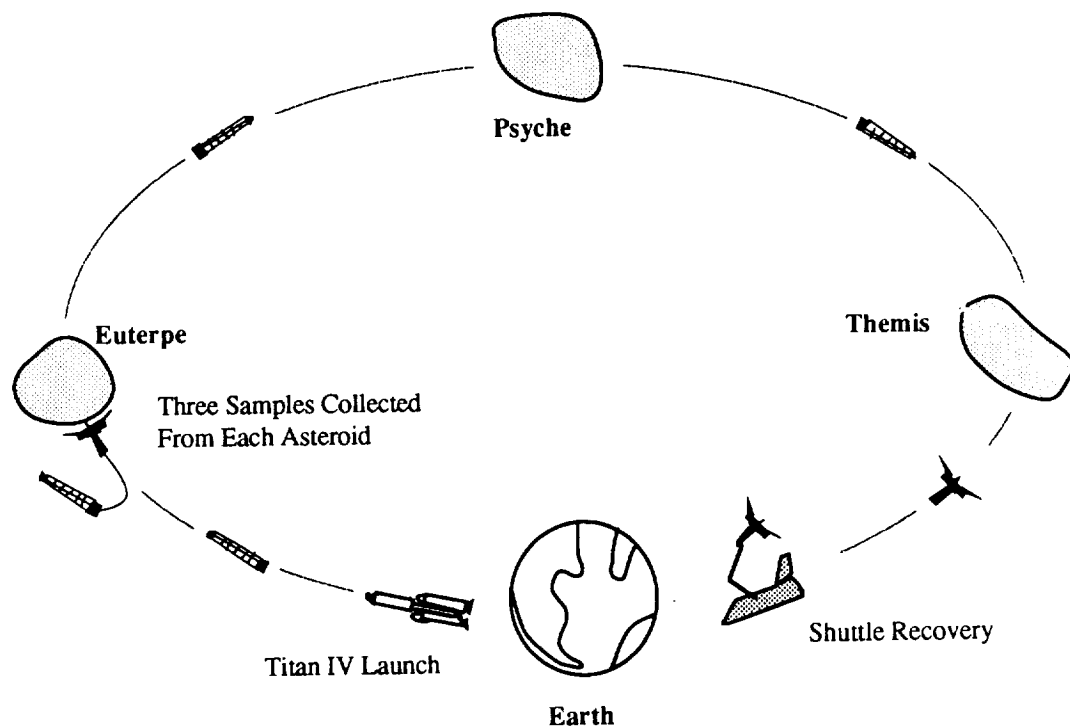
Figure 7: MASR Mission Scenario

Overall Mass, Power, and Cost Budgets

Mass, power, and cost budgets[5] are shown in Table 6. A substantial safety margin is included in each of these categories to ensure a reliable design.

Table 6: Mass, Power, and Cost Budgets

Subsystem	Mass (kg)	Power (W)	Cost[5] ($M)
Communication	52	57	158
Computer	45	89	20
Drill	160	1200	329
GN&C	260	394	34
Landing gear	15	300	69
Launch Vehicle	N/A	N/A	150
Power	6000	N/A	1418
Propulsion	1800	86000	1423
Scientific Inst.	120	250	180
Structure	220	N/A	373
Micromet. Prot.	128	N/A	7
Thermal	125	N/A	16
Margin	400	1,000	50
TOTAL	**9325**	**89290**	**4227**

Conclusion and Recommendations

Three design projects completed by the students have been discussed. There are still some unresolved issues in each of the missions which need to be addressed. First, a redesign of the monitor penetrator in the CNSR mission is required to place the RTG and optical communications package away from the rocket engine. Two members of the SASR team found that the hardness of the asteroid surface cannot be determined. A sampler drill to accommodate this variable should be examined. Using the QT2 trajectory code, the MASR mission length was calculated to be approximately 24 years. Missions of this length cause serious wear on systems. Reducing the length could be as simple as visiting the asteroids in a different order or visiting fewer asteroids.

Samples returned from the Moon by the Apollo astronauts have provided a wealth of information about its composition. Missions that return samples from comets and asteroids are important because they may reveal the intricate building blocks of the Solar System. In addition, asteroids may contain mineral deposits that could be refined for use as propellants.

Perhaps one day humans will visit the asteroids and comets, but until then these robotic missions can provide information of considerable significance to cosmologists and planetary geologists.

References

[1] Barnes-Svarney, Patricia, "Grabbing a Piece of the Rock," *Ad Astra*, v2, n10, October 1990, pp. 7-13.

[2] *International Asteroid Mission*, International Space University 1990 Design Project Final Report, York University, Toronto, Canada, Summer Session, 1990.

[3] Stetson, D.S., Lundy, S.A., and Yen, C.L., "The Mariner Mark II Comet Rendezvous/Asteroid Flyby Mission," AIAA Paper No. 84-2016, AIAA/AAS Astrodynamics Conference, Seattle, WA, August 20-22, 1984.

[4] Feingold, H., Hoffman, S.J., and Soldner, J.K, "A Comet Nucleus Sample Return Mission," AIAA Paper No. 84-2027, AIAA/AAS Astrodynamics Conference, Seattle, WA, August 20-22, 1984.

[5] Cyr, Kelley, "Cost Estimating Methods for Advanced Space Systems," SAWE Paper No. 1856, Index Category No. 29, July 29, 1988.

[6] Lau, C.O., and Hulkower, N.D., "On the Accessibility of Near-Earth Asteroids," AAS Paper No. 85-352, AAS/AIAA Astrodynamics Specialist Conference, Vail, CO, August 12-15, 1985.

[7] Wertz, J.R. and Larson, W.J., *Space Mission Analysis and Design*, Kluwer Academic Publishers, Boston, MA, 1991.

[8] General Electric Space Nuclear Power Tutorial, Conducted at NASA Lewis Research Center, May 29-31, 1991.

Volume I

Comet Nucleus Sample Return Mission

The Pennsylvania State University

Department of Aerospace Engineering

COMET NUCLEUS SAMPLE RETURN MISSION

(Project Snowball)

by

Keith Blystone, Cory Dodson, Robert Grogan, Timothy Hagin,
Johanna Ramos, Thomas Rayer, John Stoll, Diane Wentzel,
Kenneth Whang, Gary Wulkowicz, Travis Zimmerman

June 1992

Abstract

Although comets have been observed for many centuries, little is known about them. A mission is proposed for returning a comet nucleus sample to Earth. Primary goals of this mission consist of three phases: rendezvous with a short period comet, acquisition of a 10 kg sample, and maintenance of sample integrity for Earth return. A secondary goal is to monitor the comet through its orbit to perihelion. Comet selection criteria determined Wild 2 to be the most suitable mission target, using a Hohmann-like transfer for trajectory design. A hybrid electric/chemical propulsion system is proposed because it will reduce the overall propellant mass by 59%. The power subsystem will consist of sets of solar arrays complemented by an RTG. A central heating system, in conjunction with passive devices, will be used in the thermal control subsystem. The spacecraft bus and scan platform boom structures have been modelled using ANSYS, estimating natural frequencies and deflections that would result during launch. An Atlas IIA was selected as the launch system based on mission requirements and size constraints. The present design includes a sampler penetrator which will retrieve a 2m by 5cm diameter specimen to be hermetically sealed and returned to the spacecraft bus for transport to Earth. A separate long-lived monitoring penetrator will be employed to observe and analyze comet material properties and activity through perihelion.

Table of Contents

List of Figures

List of Tables

1.0   Introduction

Past rendezvous missions to observe and gather particle emissions from short period comets have given scientists reason to believe that comets contain material which closely approximates the composition of the primordial solar nebula [1]. The study of this material may help scientists to discover more about the distant past of the planets while at the same time refine the current theories regarding the nature and evolution of the Solar System [1].

A comet nucleus sample return (CNSR) mission is proposed to return a comet sample in its own environment to Earth to be studied by scientists. The mission scenario is presented in Figure 1.1. The primary mission objective consists of three phases: rendezvous with a short period comet, acquisition of a 10 kg sample from the comet nucleus, and maintenance of the sample composition and crystalline structure for return to Earth. The secondary objective for the mission is to monitor comet activity through perihelion by using a penetrator equipped with scientific instrumentation.

The following report details topic information in the Snowball missions. These topics include: mission target; trajectory design; launch vehicle; spacecraft structure; power; propulsion; guidance, navigation, and control; command and control; thermal; science; sample extraction and storage; and the penetrator monitoring unit.

Figure 1.1: Mission Scenario

Forced Orbit

Comet Mapping (2 Phases)

Space Shuttle capture

Earth

Sample return

Penetrator remains to monitor comet

Spacecraft continues to orbit

Penetrator fired into comet

Wild 2 Surface

Transfer Orbit

Sample Recovery

Sample Extraction

Upper Stage Spacecraft Deployment

Launch Date: 2000-2010

Earth
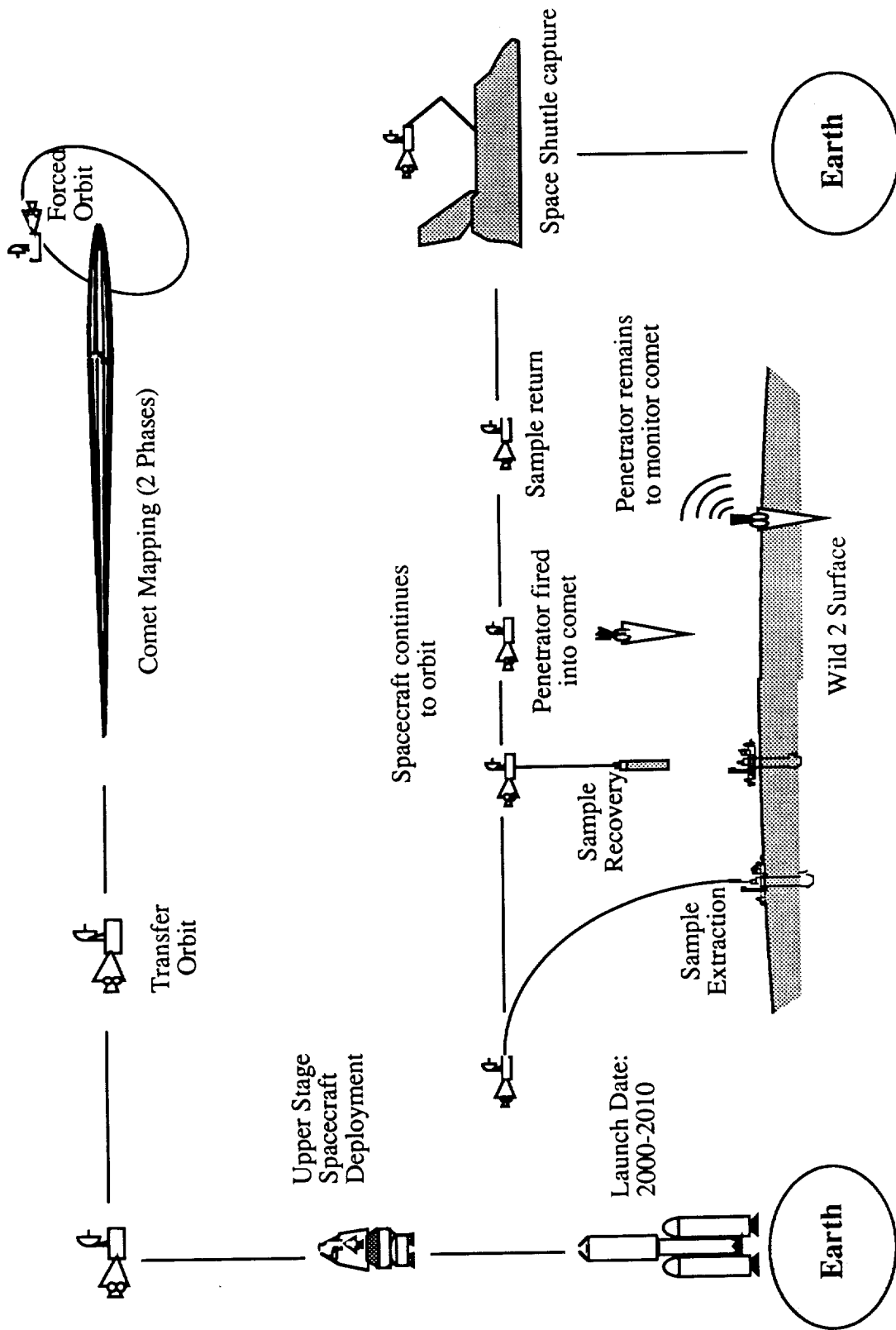
2.0   Mission Target

2.1   Target Selection Criteria

Several criteria have been placed on selection of the mission target. Two primary criteria are that the comet's orbital motion should be well understood and the comet should exhibit both quiescent and active stages. In addition, it is desirable that the spacecraft be able to rendezvous with the comet before it becomes active and that the comet should have a relatively high gas production rate near perihelion. Other criteria are that a good observational history should exist for each comet and that during the rendezvous phase the comet should be easily observed from Earth. Ideally, the comet orbit should not place unnecessary cost burdens upon the launch vehicle, spacecraft, and ground operations [2].

Additional research has produced several other target requirements. The comet should have a well-identified nucleus and a low inclination to the ecliptic plane. The target should also have a short orbital period and small non-gravitational acceleration.

Table 2.1 lists the orbital parameters of the two comets of interest. Note that both comets have a small inclination to the ecliptic plane and a short orbital period making them both reasonable choices. Wild 2 is particularly attractive because its 1974 encounter with Jupiter lowered its perihelion distance from 6.2 AU to 1.6 AU. Thus, it has only recently begun to experience the chemical differentiation induced by significant thermal forces [2].

Table 2.1: Comet Targets (Myers, Mark ,"Trajectory Design For The Comet Rendezvous Asteroid Flyby 1995-1996 Opportunities," Jet Propulsion Laboratory, Pasadena, California, AIAA, 1988)

Orbital Elements	Wild 2	Kopff
Aphelion Dates	7/13/00 12/07/06	9/19/99 3/05/06
Perihelion Dates	9/26/03 2/22/03	12/12/02 5/25/09
Inclination (deg)	3.2	4.7
Period (yrs)	6.41	6.46
Mag. of Gas Production	8.0	8.2
Semi-major Axis	3.45	3.47
Eccentricity	0.54	0.54
Perihelion Radius (AU)	1.59	1.58
Aphelion Radius (AU)	5.31	5.35
No. Days r<1.66 AU	94	98
No. Days r>4.73 AU	894	932

2.2   Target Selection

A calculation, shown in Appendix A, was performed to determine the total ΔV required for a heliocentric Hohmann-like transfer to the specific comets of interest: Kopff and Wild 2. The calculation provided information comparable to that obtained from Reference [2]. The lower velocity required for the transfer to Wild 2 is most attractive in this case, but other trajectories cannot be dismissed.

Interplanetary transfer modes have been considered in detail in References [2] and [3] for various transfer opportunities. Earth (EGA), Jupiter (JGA), Venus-Earth (VEGA), and Venus-Earth-Earth (VEEGA) gravity assists significantly minimize the total ΔV required for comet rendezvous, but limit launch windows to times of correct planetary alignment. Also, gravity assist trajectories require a more complex analysis than direct trajectories.

2.3   The Comet Nucleus

Currently, there is a limited quantity of information about the comet nucleus. Previous comet observation missions have indicated that the comet nucleus is a fairly homogeneous mixture of ices and silicates. The surface may be covered by a layer of nonvolatile silicate which is less than one meter in thickness [4]. Previous studies indicate five comet surface types [5]:

- Active vents with sublimating exposed volatiles
- Mantled areas with gas and dust release
- Mantled areas with outgassing
- Vents with exposed ices in dormant phase
- Inactive areas, containing no ices within a few meters depth

Vents on a comet are described as discrete dust or gas sources. These vents typically release CO, NH_3, CO_2, CH_4, N_2, materials which are more active than water ice [5].

2.4   Conclusions and Recommendations

There are several similar comets suitable as mission targets. The selection of Wild 2 is based primarily on its recently lowered perihelion and low ΔV requirements. Further research into gravity assist trajectories may limit the availability of Wild 2 as a possible target. Thus many more targets should be considered in a detailed gravity assist analysis.

3.0   Trajectory Design

3.1   Requirements

In general, there are an infinite number of paths which a spacecraft may take to a given destination. In order to choose an appropriate trajectory, it is clear that many general parameters of the mission must be analyzed. These parameters include: launch windows, arrival date, deep space maneuvers, propellant limits, mission duration, and launch capability.

3.2   Trajectory Options

Various trajectory options have been considered for transfer to Wild 2, including: Hohmann-like, Earth Gravity Assist (EGA), Venus-Earth Gravity Assist (VEGA), and Venus-Earth-Earth Gravity Assist (VEEGA) transfer modes. Trajectories utilizing Mars or Jupiter flybys are rare and have not been considered at this point. Moreover, VEGA and VEEGA trajectories would limit available launch windows due to waiting for the correct alignment of Earth, Venus, and Wild 2. Gravity assists using both Venus and Earth would also significantly increase flight time. Therefore, the scope of this investigation has been limited to the comparison of a Hohmann-like transfer and EGA.

Appendix A contains a calculation of the required ΔV for a Hohmann-like transfer to Wild 2 at aphelion from a 200 km Earth parking orbit. The launch ΔV to be performed by an upper stage burn, and the post launch ΔV, including navigational allowances, are listed in Table 3.1 for the Hohmann-like transfer. This table contains ΔV allowances for a comet approach sequence, comet exploration, comet escape, and Earth return based on the planned Rosetta and CRAF missions contained in References [2] and [6], respectively.

Table 3.1: ΔV Budget for Hohmann-like Transfer

Event	ΔV (m/s)
• Post Launch and Navigational Allowances	
Interplanetary Maneuver	1493
Inclination Change	406
Comet Approach Sequence	1595
Comet Exploration	189
Comet Escape	10
Earth Return	235
Total Post Launch ΔV and Allowances	3928
• Launch	
Launch	6340
Total Launch and Post Launch ΔV	**10,270**

Table 3.2 contains the ΔV budget for the CRAF Baseline Mission to Wild 2 [2]. The ΔV values are representative of other ΔV-EGA trajectories which have been documented in References [2], [3], and [6].

Table 3.2: ΔV-EGA Trajectory for the CRAF Baseline Mission

Event	ΔV (m/s)
Post Launch and Navigational Allowance	3476
Launch	4350
Total	**7830**

The ΔV-EGA is thus 24% lower than that of the Hohmann-like transfer, this is primarily due to the reduction in required launch ΔV. Since the total required ΔV is directly related to the mass of the spacecraft, it is clear that using an Earth Gravity Assist trajectory would be favorable to the mission.

3.3 Trajectory Analysis

3.3.1 Orbit Alignment Determination

The determination of the heliocentric positions of both Earth and Wild 2 is very critical in mission planning. By knowing the relative positions of each body at points in time, various relations can be determined. One such relationship is the phase angle at departure which is the angle between the radius vectors to the Earth and Wild 2. The requirement that the phase angle at departure be correct severely limits the times when a launch may take place [7].

The orbital elements for both Earth and Wild 2 have been obtained and are listed in Tables 3.3 and 3.4, respectively.

Table 3.3: Orbital Elements of Earth for the Epoch 1969 June 28.0 (Bate, Mueller, White, "Fundamentals of Astrodynamics", Dover Publications, Inc., New York, 1971)

Semi-major axis a (AU)	Orbital eccentricity e	Inclination to ecliptic i	Longitude of ascending node, Ω	Longitude of perihelion π	True longitude at epoch, lo
1.00	.0167	0.00	undefined	102.416	276.117

Table 3.4: Orbital Elements of Wild 2. (Orbital elements obtained through personal correspondence with Jost Jahn, Bodenteich, Germany.

	Perihelion Radius Rp	Eccentricity e	Argument of Periapsis	Longitude of Ascending node	Inclination i	Magnitude of Gas Production
5/6/97	1.5826	.5402	41.77	136.15	3.243	8.1
9/26/03	1.5904	.5387	41.75	136.14	3.240	8.0
2/23/10	1.5981	.5374	41.79	136.09	3.238	8.0
7/20/16	1.5921	.5384	41.70	136.12	3.240	8.0

Using a computer program (Appendix B), these orbital elements have been used to calculate the ecliptic projection of the orbits of Earth and Wild 2 as shown in Figure 3.1. These orbits correspond to the start date of 8/26/03 and continue for one period.
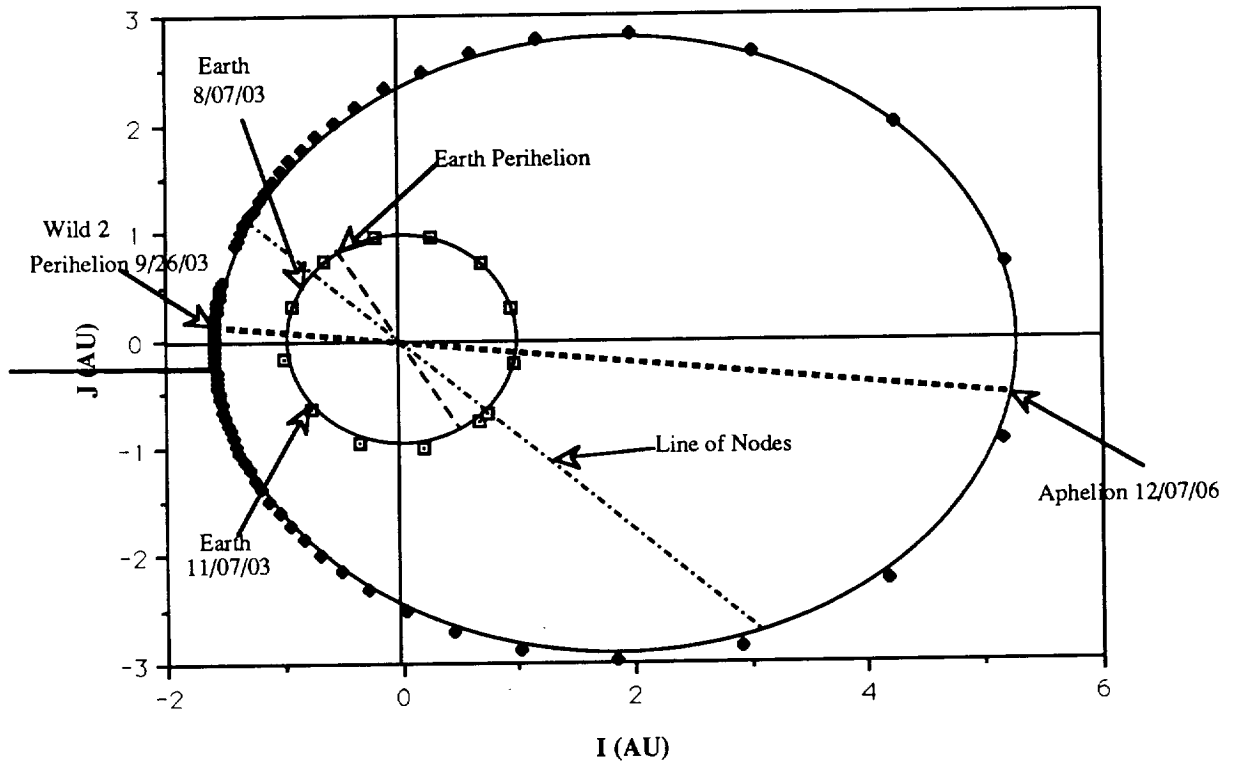
Figure 3.1: Ecliptic Projection of Wild 2 Orbit

Appendix B contains the program used to determine the orbits for a user-defined start date and simulation length. The program utilizes the orbital elements at a given epoch time and calculates both the perifocal and heliocentric coordinate positions. A Newton-Raphson routine was used to determine the eccentric anomaly at each time interval. Due to a coding problem, results had to be corrected by 180°. Future work is needed to correct this error.

3.3.2 The Two-Body Boundary Value Problem

Using the developed program the position of both the Earth and Wild 2 can be determined for any point in time. A constraint placed upon the mission is that the spacecraft must rendezvous with Wild 2 at or near aphelion to avoid damaging debris. Also, at aphelion, the heliocentric speed of Wild 2 is small and the ΔV required to match the spacecraft and comet velocities is minimized. As noted on Figure 3.1, aphelion occurs on 12/07/06. A study of the trajectory design for the CRAF mission conducted at the Jet Propulsion Laboratory mentions that the optimal (in the sense that the total ΔV required to effect comet rendezvous is minimized) launch occurs very near the date that the Earth crosses the comet's periapsis direction [3]. This is obvious since it is closest to a Hohmann transfer which is known to provide the minimum ΔV required for an interplanetary mission. An attempt was made to analyze the total required ΔV for the range of dates, 8/07/03 to 11/07/03, when the Earth is near Wild 2's periapsis.

The analysis program included in Appendix C utilizes Lambert's time-of-flight equation for an elliptical transfer. Fixing the arrival date and location of Wild 2's aphelion, the total required ΔV may be acquired for the set range of launch dates. Total ΔV is a useful comparative measure of mission performance since it is dependent upon the trajectory parameters and is not coupled to either the launch vehicle capability or spacecraft design [3].

Although this analysis was not possible, all is not lost, since the trajectory which has the minimum total ΔV is expected to resemble a Hohmann transfer. Thus, the patched conic approximation provided in Appendix A provides a good estimate for the total required ΔV for preliminary estimates of mission requirements, such as propellant mass.

3.3.3 Injection From Circular Orbits

The mission will begin when the spacecraft is launched from Cape Canaveral into a circular parking orbit. At the appropriate point, an engine restart will be initiated and the spacecraft will move along a hyperbolic path relative to Earth. The asymptotic value of the

relative velocity vector is the departure velocity of the vehicle with respect to the Earth. The sphere of influence of the Earth extends to a distance of half a million miles. Beyond the sphere of influence, the Earth's gravity effects diminish rapidly and solar gravity provides the force field which governs the path of the spacecraft [8].

3.3.4   Non-coplanar Interplanetary Trajectories

The simplified analysis to generate possible trajectories will assume that the orbit of Wild 2 lies in the plane of the ecliptic. Of course, this is not true. In reality, the orbit of Wild 2 is inclined 3.2° to the ecliptic. A good procedure to use when the target lies above the ecliptic is to launch the spacecraft into a transfer orbit which lies in the ecliptic plane and then make a simple mid-course plane change when the true anomaly change remaining to intercept is 90° [7]. This plane change results in additional ΔV constraints and thus, greater propellant expenditures. With this assumption in mind, Wild 2 has a relatively small inclination and its ecliptic projection will be used for the purpose of analysis.

3.4   Maneuver Considerations

Maneuvers may be necessary to correct for the non-gravitational acceleration of the comet nucleus. The non-gravitational forces result from the expulsion of comet gas which acts as a thruster, modifying the orbit about the sun. These forces can slow down or speed up a comet

Orbit perturbations and maneuvers to correct the orbital elements must be considered. Both bodies, the spacecraft and the comet, will be equally affected by the gravitational force of the Sun. Thus, the bodies may be considered to be in a uniform gravitational field, and orbits about the comet may be considered a two-body problem.

Since comets are relatively small as compared to other celestial bodies, an orbit about one may be difficult to achieve or the orbit may be at too low an altitude. A high-altitude synchronous orbit may be forced to correct this problem. To achieve such an orbit,

downward thrusting with respect to Wild 2 may be used to create an artificial gravity force. This poses a problem since it takes propellent to attain this thrust.

3.5 Conclusion and Recommendations

It should be noted that rendezvous missions to targets with orbital properties, such as those of Wild 2, using direct trajectories are, in general, not feasible for sizable payloads, This is because the required high injection energies are not within the capabilities of any current launch vehicles. The direct trajectories have important predictive value for trajectory design using ΔV-EGA, VEGA, and VEEGA trajectory classes [3]. Therefore, if such a mission is to actually be flown, importance should be given to more feasible gravity assist or low thrust options utilizing trajectory optimization software, such as MIDAS or QT2.

4.0   Launch Systems

4.1   Requirements

A typical launch system includes a launch vehicle with one or more stages, which provide required velocity changes to place the spacecraft in orbit and an adequate design envelope which protects it from the ascent environment [9]. The launch system is limited by several constraints including specific orbit, velocity to achieve that orbit, spacecraft size, mass, cost, and availability [9]. Other areas that need to be addressed are fairings, structural and electrical interfaces, and payload environment. The satellite must be designed to withstand the payload environment which is typically exposed to a temperature range of 9° to 37°C. Static pressures are about 79 millibars [9]. The electrical signals must be compatible between the spacecraft bus, payload, launch vehicle, and the launch site. Electrical signals of different frequencies and power levels can combine to form transmissions that can interfere with electrical systems. The satellite structure must also withstand the various load conditions which include venting loads, aerodynamic loads, acceleration loads, vibration loads, and acoustic loads.

4.2   Launch Parameters for the Spacecraft

The spacecraft has an estimated dry mass of 2548 kg and a loaded mass of 5150 kg (see Table 4.1) and uses a Hohmann-like transfer. Final analysis of the spacecraft structure estimate dimensions of the spacecraft to be 2 meters in diameter and 5 meters in height when folded for launch. And finally, an Earth escape orbit must be achieved after the burn has been completed, requiring a velocity of 8.85 km/s based on a Hohmann Transfer orbit (see Appendix A). These requirements limit the choice of launch vehicle, especially by payload capacity and fairing size. The proposed launch vehicle for this mission is an Atlas system, although a Delta II may be possible should the spacecraft mass change, perhaps due to an alternative trajectory design. The option remains, however, to design a new launch system to

meet the requirements of the mission, but the cost implications would probably be unacceptable. It is most beneficial to this mission to design the spacecraft to be compatible with several launch systems to enhance launch availability.

Table 4.1: Mass Budget

Element	Mass (kg)	
Spacecraft Structure	**1309.35**	
Bus		801
Booms (truss structure)		102
Fasteners and joints (10%)		90.3
Deployment mechanisms (10%)		90.3
Contingency (25%)		225.75
Sampler	**95**	
Penetrator	**262**	
Power	**93**	
Solar Array		10
RTG		83
Guidance Navigation & Control	**77**	
Scientific Instruments	**134.9**	
Communication	**7.1**	
Computer	**12**	
TOTAL	**1990.35**	
10% Electronic wiring		199.04
10% Mass Margin		199.04
Thermal Control (8% dry)	**159.23**	
TOTAL DRY MASS	**2547.66**	
Mass Propellant for Hohmann-like transfer	**2602.02**	
Propellant tanks (10%)		2312.6
Valves, tubing (25%) of		231.26
propellant tank mass		57.82
TOTAL WET MASS	**5150**	

4.3   Atlas Commercial Launch Vehicle

Although the Atlas series has several rockets which meet the payload capacity criteria for the CNSR mission, it is presumed that only the Atlas II and Atlas IIA will still be in

production by the time the mission is prepared for launch. Performance parameters are available in Table 4.2 for a low Earth orbit of 185 km at an inclination of 28 degrees assuming the smaller payload fairing is used [10]. The Atlas, primarily used by the Air Force, is capable of low Earth, geosynchronous transfer or geosynchronous Earth orbits and is used equally for each type. From 1958 to 1990, the success rate of this rocket was a fairly high 86.9%, accomplishing 213 of 245 attempts [10]. However these figures do not include data from the Atlas IIA, and IIAS.

Table 4.2: Performance Parameters for Atlas, Delta Launch Systems

Launch System	LEO (kg)	Fairing Dia. (m)	Envelope Length (m)	Compatible Upper Stages
ATLAS I ATLAS II ATLAS IIA ATLAS IIAS	5785 6600 6965 8595	3.3, 4.2	10.4, 12.0	Centaur I Centaur II Centaur IIA Centaur IIA
DELTA II	3990 5045	2.9, 3.05	8.47, 7.92	PAM-D

The Atlas II and Atlas IIA models are compatible with the Centaur IIA upper stage, which is assumed to be part of the launch system. Launch sites for this rocket include both Vandenburg Air Force Base and Cape Canaveral Air Force Station, although the Atlas IIA and IIAS are limited to only the Cape Canaveral site. Financial analysis produces ranges from $80-120 million in 1990 dollars.

4.3.1 Payload Compartment

The payload fairing will protect the spacecraft from the time it is loaded into the payload envelope through atmospheric ascent. The fairing can experience a dynamic pressure of 33520 N/m^2 with a maximum pressure change equal to 5.4 KPa/second. Maximum acoustic levels can reach 137.4 dB with frequencies at a minimum of 10 Hz laterally and 15 Hz longitudinally [10]. The launch system applies both axial and lateral loads to the spacecraft during launch and ascent. Although the maximum loads do not occur simultaneously, they can reach 6 g's axially and ±2 g's laterally.

The Atlas has a choice of two payload fairings (see Table 4.2) each with the capability to add a thermal shield or acoustic blanket for very controlled environments [10]. The estimated dimensions for the spacecraft when in a folded configuration indicate a smaller payload fairing size can be used for this mission. The dynamic envelope, or useable envelope for this fairing has a maximum payload diameter of 2.92 m, maximum cylinder length of 5.33 m, and maximum cone length of 3.84 m with a payload adaptor interface diameter of 0.945 m or 1.21 m [10]. The fairing structure is a skin-stringer shell made of aluminum.

4.3.2 Payload Delivery

The ultimate goal of the launch system is to safely deliver the payload to a desired orbit. To assure this, the Atlas IIA is integrated with a Centaur avionics system for guidance, flight control and sequencing functions [10]. The Inertial Navigation Unit (INU) performs the inertial guidance and attitude control computations for the Atlas and the upper stage, as well as controls the upper stage tank pressure and propellant use [10]. The Remote Control Unit (RCU) provides sequencing for the vehicle and spacecraft. A Power Distribution Unit (PDU) provides changeover capabilities form ground to internal main vehicle power system to meet spacecraft power requirements.

The attitude control system is capable of payload delivery with an accuracy of ±0.5°
in pitch, yaw and roll. For a Low Earth Orbit, the system can deliver the payload to a circular
orbit ±6.5 km and within 0.011° inclination.

4.4   Conclusions and Recommendations

A vast improvement to the launch system would be to lower the margin between the
spacecraft loaded mass and the maximum payload capability. A reduction of only 100 kg in
the spacecraft mass would allow the launch system to be downgraded to a Delta II. This
launch system would still meet the size constraint of the spacecraft, with fairing size options
of 2.9 m and 3.5 m. System cost would drop substantially to $45-50 million using the Delta
system. Finally, since the Atlas IIA was in production during 1991, while the Delta II was
already completed by 1989, there is not a comparable amount of reliable flight data available.

5.0   Spacecraft Structures and Mechanisms

5.1   Requirements [9]

The spacecraft structure and mechanisms subsystem will consist primarily of the spacecraft bus and attachments (see Figures 5.1 and 5.2). This subsystem will mechanically support all spacecraft subsystems and attach the spacecraft to the Atlas II. The spacecraft can be categorized as having two classes of structures. The primary structure, the first class, will be responsible for carrying the spacecraft's major loads and the secondary structure, the second class, will support low-weight components (typically under 10 lbs).

Solar Array Sun Shade
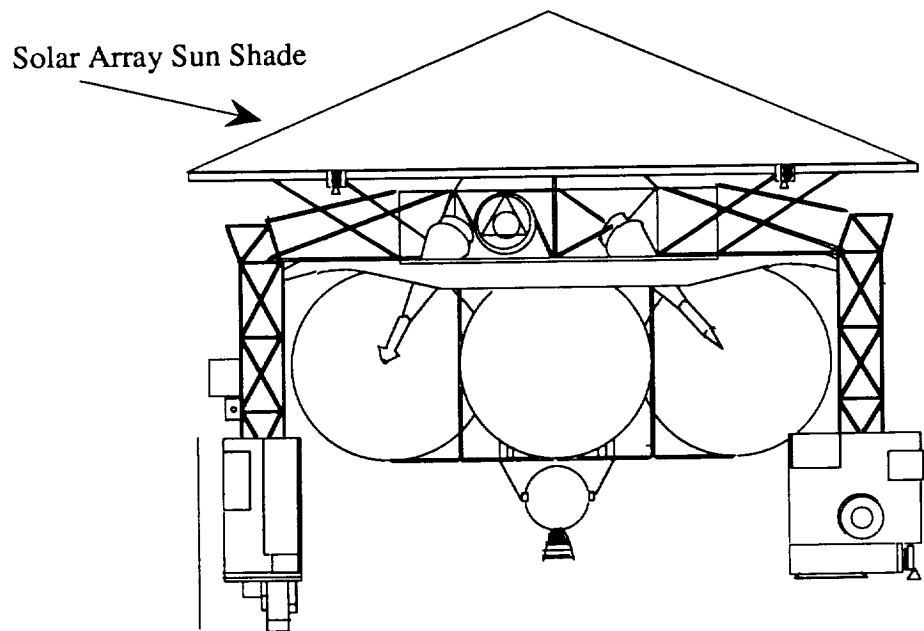
Figure 5.1: CNSR Spacecraft Launch Configuration

Many design parameters for the spacecraft structures and mechanisms subsystem are determined by the launch vehicle. These parameters must be designed to fit within requirements for the payload fairing or dynamic envelope of the launch vehicle. Strength, weight, geometry, and stiffness requirements of the spacecraft and the interface to the launch

booster must be satisfied as well as rigidity and natural frequency requirements. The spacecraft structure must be designed to survive all phases of the design process, including manufacture and assembly, transport and handling, testing, pre-launch testing, and finally, launch, ascent, and mission operations [9].
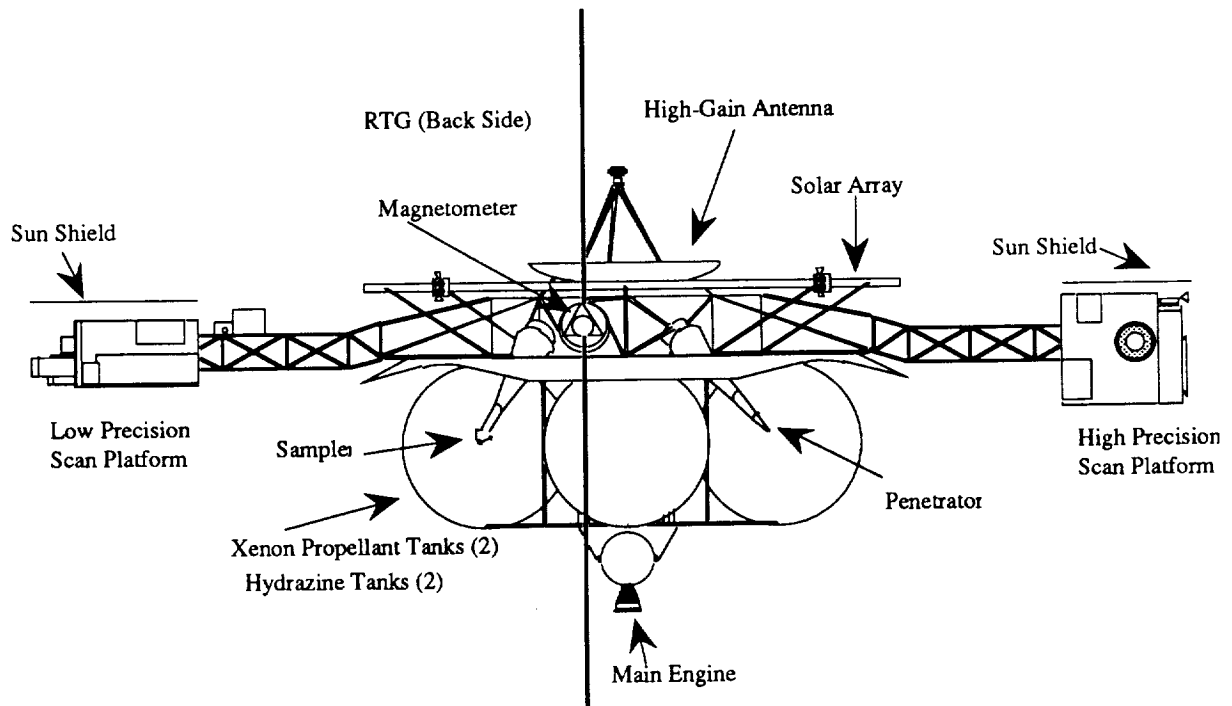
Figure 5.2: Deployed CNSR Spacecraft

5.2 Advanced Composite Materials

The use of advanced composite materials in construction will provide many advantages. Not only do composites achieve very high strength and stiffness at low weight, but they have also proven to have improved damping qualities and to be damage tolerant to impact and fatigue. The potential also exists to tailor material properties to optimize structural efficiency and also to create smart structures for specialized applications.

Of course, composite materials are not perfect. Composites are difficult to manufacture which makes them costly and also difficult to fasten together. Most composite material structures have metal end fittings attached by bonding, but the bond's strength depends on the process and workmanship [9]. Another problem associated with the use of composites for space purposes is outgassing. In order to avoid this problem, special laminates will need to be applied to the composite. Continuing research and increased popularity in the use of advanced composite materials should dictate the need for new manufacturing techniques and mass production. This should make composites relatively inexpensive to use and the advantages will far outweigh the cost. Thus, advanced composite materials will be utilized whenever possible in the spacecraft construction.

5.3   Truss Construction

As shown in Table 5.1, all truss members will be graphite/epoxy (G/E) tubes with beryllium end fittings. The use of G/E will provide a high stiffness to weight ratio along with negligible expansion and contraction resulting from temperature gradients [9]. The use of beryllium provides a way to fasten the tubes together in addition to providing high stiffness. Figure 5.3, which was created on the ANSYS™ finite element package, illustrates one of the instrument support trusses which will be used.

Table 5.1: Spacecraft Materials (Wertz, J.R., and Larson, W.J., *Space Mission Analysis and Design,* Kluwer Academic Publishers, Boston, MA, 1991)

Material	Young's Modulus E (GPa)	Density $\rho * 10E3$ (kg/m^3)	Shear Modulus G (GPa)	Specific Stiffness E/ρ (10^3N m/kg)	Location
G/E	289	1.69	4.1	171	truss
Kevlar	75	1.38	2.1	54.3	bus skin panel
Aluminum Honeycomb Hex 5052	3.1	0.096	N/A	32.3	bus core
Beryllium	293	1.85	138.0	158.4	end fittings; propellant tanks
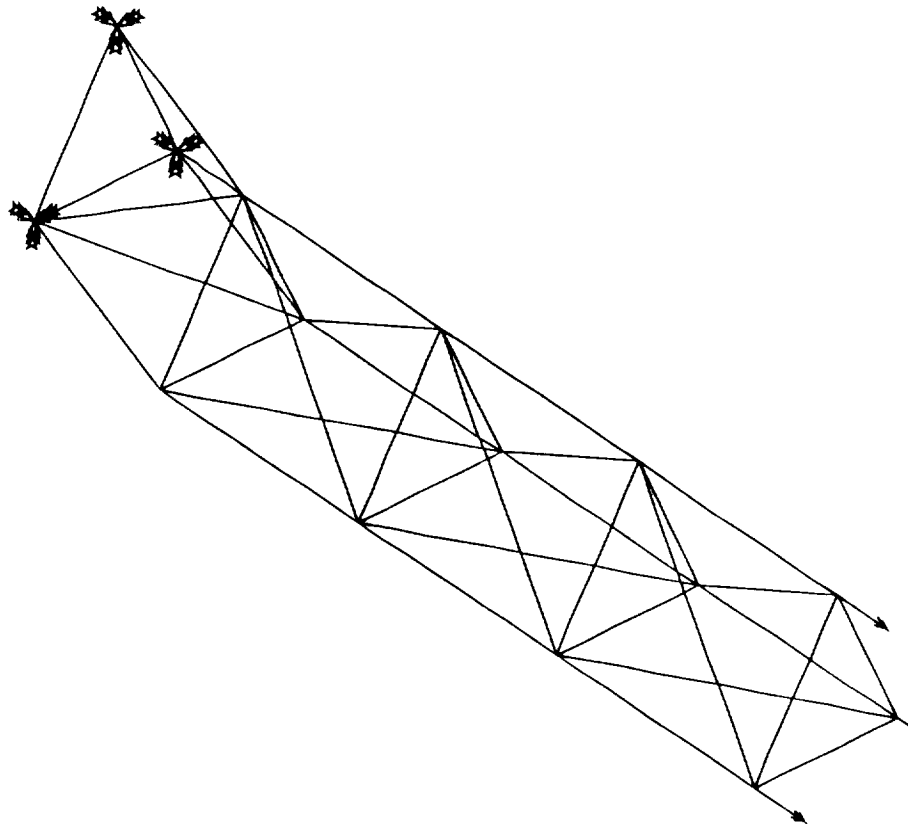
Figure 5.3: Instrument Support Truss

The model was constructed with ANSYS™ using simple beam elements assuming an effective spar radius of 1.9 cm and a flexural rigidity of 3.077×10^4 N m. Analysis was done on the LPSP truss structure for launch configuration. This condition was investigated because of extremely harsh loading conditions experienced during launch, which the LPSP will observe more than the HPSP because of the higher instrument mass being supported. At the time of analysis, the exact launch vehicle was not known so a launch G-force of 7.7 g was assumed, for a worst case scenario. The results of this analysis are provided in Table 5.2. Appendix E shows the truss in each of its first three natural frequencies. None of these determined frequencies match fundamental vibration frequencies of the launch systems under consideration. As a result, there should not be much of a problem for the truss during launch, except for the possibility of acoustical frequencies, which were not investigated.

Table 5.2 ANSYS™ Structure Analysis

Component	Mass (kg)	Maximum Deflection (cm)	1st Natural Frequency (Hz)	2nd Natural Frequency (Hz)	3rd Natural Frequency (Hz)
Truss	51.83	0.0073	85.84	97.45	189.81
Bus	802.91	0.275	---	---	---

5.4   Spacecraft Bus Construction

The spacecraft bus, which will contain many of the delicate and mission-critical instruments, must be designed to withstand impacts from comet debris. The structure will consist of an eight bay bus with sandwich construction skin panels, as shown in Figure 5.4. The skin panels are designed as a sandwich using Kevlar face sheets separated by an aluminum honeycomb core, as shown in Figure 5.5. This type of construction features high strength, stiffness, and impact resistance and is stiffer than skin-only designs of comparable weight [9]. Analysis performed on ANSYS is given in Table 5.1, where reaction forces during launch by the scan platform booms were applied.
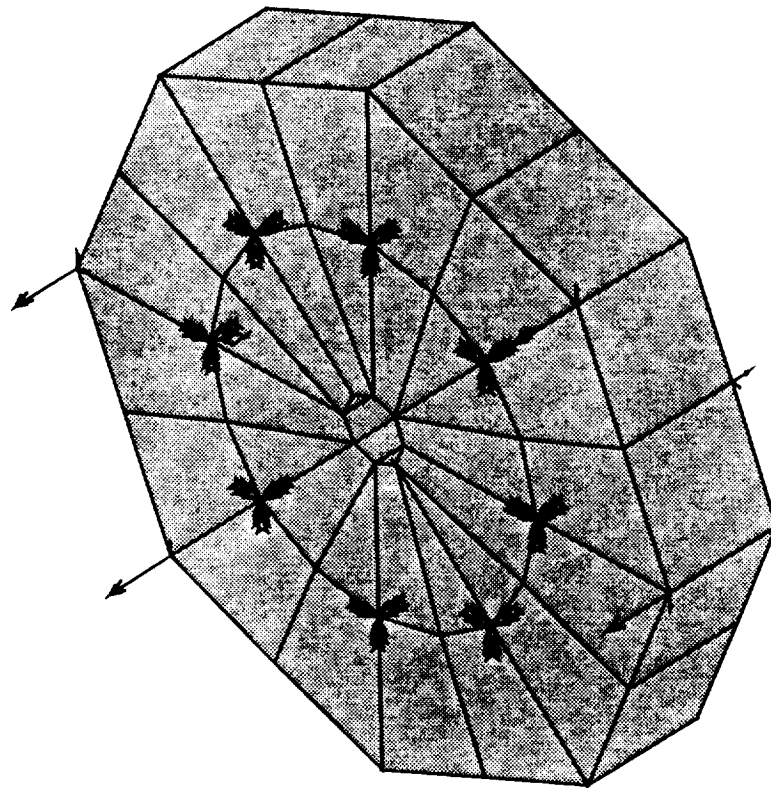
Figure 5.4: Eight-bay Bus Structure
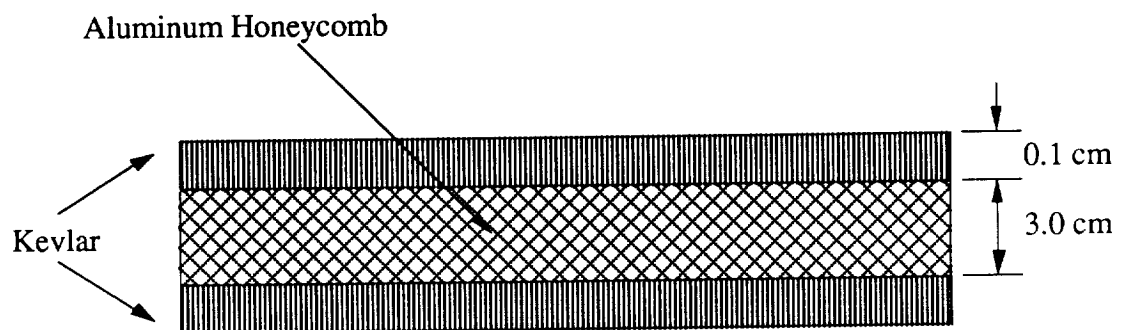
Figure 5.5: Sandwich Construction Skin Panels

It is imperative that the spacecraft design meet the aforementioned requirements as well as additional criteria to be an effective spacecraft bus. The mission calls for a bus that has a positive history of usage. Also, this spacecraft bus would have to change to specifically fit this mission, which means that it can be easily reconfigured. Lastly, this spacecraft bus would have to be cost effective to avoid the burden of additional funding. The spacecraft bus chosen for the Snowball mission, the Mariner Mark II, meets these requirements, as well as structural and geometric requirements determined by the launch vehicle. The Mariner Mark II program was designed at JPL by working with the Solar System Exploration Committee (SSEC). The concept is to make a spacecraft with Voyager and Galileo quality science, and to use inheritance and new technology to keep development costs low [11].

5.5 Tether Construction

The comet sample will be retrieved by means of a tether connecting the sampler with the orbiting spacecraft. The tether must support the mass of the sample in addition to its own mass and any external forces. NASA and the Martin Marietta Corporation have created a tether or a multi-layered cable that is only one-tenth of an inch thick. At its core is a copper-wound, plastic filament that is surrounded for strength with braided Kevlar. The outermost layer is made of Nomex, a synthetic fiber that will protect against oxidation by any ionized gases. The tether can hold up to 1873.7 N without breaking [12]. A tether of larger diameter and similar construction can be developed to support a greater mass.

5.6 Conclusions and Recommendations

Further investigation should be made into the optimization of the scan platform booms with respect to size, strength, and weight. Investigation of the acoustical frequencies encountered during launch should also be analyzed for the truss structure. The spacecraft bus, being off the shelf, cannot be optimized; however, it can be analyzed for full reaction forces during launch to assure survival during launch.

6.0 Power

6.1 Requirements

The power subsystem will consist of the sources to generate electrical power, the storage mechanisms, the wiring for distribution, and the regulators for control purposes. Furthermore, a method to dispose the excess heat within the spacecraft will be necessary. Major considerations concerning this subsystem involve the reliability, lifetime, and heritage of each component. This comet sample return mission will require approximately 528 W of power. Table 6.1 outlines the estimated power needs of the spacecraft.

Table 6.1: Power Budget

Spacecraft Component	Power (W)
Guidance, Navigation, and Control (sensors only)	20
Mapping	150
Communications	122
Computer System	50
Structure	50
Thermal	40
Sample Extraction	27
Average Power	459
Margin (15%)	69
Total average requirements for operating power	528

6.2 Sources

For the comet mission, a method to supply electrical power for the spacecraft's operations is needed. The possible power source options for long duration (5-15 years) space missions are solar, nuclear reactor, and radioisotope [13]. The solar power source can be photovoltaic arrays or solar dynamic systems. Both static and dynamic use of a nuclear reactor or radioisotope comprise the other options. Solar arrays function as power sources by

converting the incident solar radiation into electrical energy. The static power sources convert thermal energy into electric power. For the dynamic power sources either Stirling-cycle, Rankine-cycle, or Brayton-cycle engines generate the electrical power. These engines use a working fluid that is transferred from a heat source, such as solar arrays, radioisotope, or nuclear reactor [9]. Nuclear reactor use has been essentially ruled out for this mission, because is has not been proven reliable and is not fully developed. The power sources for the spacecraft in this comet mission will need to produce power for an extended period of time; the reliability and effectiveness of the various power sources are the main factors in determining the appropriate power source that will meet the needs of this comet mission.

6.2.1 Solar Arrays

Solar arrays are useful for missions up to about ten years. Since the sample return mission will probably take from six to eight years, solar arrays are a viable option. Photovoltaics produce between 26-100 W/kg. In addition, they cost 2500 to 3000 dollars per W [13]. Silicon, gallium-arsenide, or indium phosphide solar cells will be used to construct the arrays. Silicon solar cells cost less than gallium-arsenide cells and indium phosphide cells, mainly because the latter are still in the developmental stages. Using silicon solar cells, however, requires that the solar arrays be more massive and larger than the arrays using gallium-arsenide. Gallium-arsenide does have a higher cell efficiency than the silicon solar cell. Indium phosphide, another option, has an advantage in that it reduces the degrading effects of radiation. The development and reliability of silicon solar cells is more advanced which makes the silicon solar cells an attractive option for the solar arrays for this mission [9].

Recent advancements in solar arrays have brought about ultra-light solar panels called Super-ULP's. These arrays produce 60 W/kg and 100 W/m^2 at 1 AU from the sun [13].

6.2.2   Radioisotope Thermoelectric Generator

A radioisotope thermoelectric generator (RTG) is a static power source option for this comet sample return mission. The RTG works on the principle that the natural decay of the radioisotope gives off heat to generate thermal power. A commonly used radioisotope is plutonium-238 which has a half-life of 87.7 years. An average RTG produces about 8-10 W/kg, and it will cost approximately 16,000-18,000 dollars per W [14]. The RTG is advantageous since it only slightly degrades over time, does not depend on the Sun's radiation, and does not require storage of its power. Since the use of an RTG is more risky than photovoltaics or dynamic power sources, more safety measures and analysis is involved [9].

6.3   Evaluation

Because of this mission's high power requirements, solar arrays will be supplemented by an RTG. Solar arrays have been successfully used for many space missions over the years. They have a strong heritage, and they are reliable and developed for use in space. Another advantage is that solar arrays do not use onboard fuels; the Sun's radiation is not a scarce commodity, though it does decrease rapidly with distance [16]. Some disadvantages for solar cell arrays are their large size, the need for solar intensity, and the danger of dust near the comet [17]. Solar arrays must be used in conjunction with batteries for this comet mission. Since the spacecraft will be farther than 3 AU from the sun during the mission, the spacecraft will also be powered by the stored energy in the batteries.

The other power source is the radioisotope thermoelectric generator. The RTG also has been successfully used in space missions; for example, since 1961 the United States has successfully used 36 RTGs as electrical power sources in 21 space systems [16]. However, many safety concerns still surround the use of RTGs due to the fact that they emit radiative energy.

6.4 Power Source Sizing

For this mission the power subsystem will consist of an RTG, batteries, and either silicon solar cells or the Super ULP's. The spacecraft will unfold the solar arrays after launch and will use them as the power source up to about 3 AU from the Sun. It will approach the comet using the energy stored in the batteries and/or from the RTG. Leaving the comet, the spacecraft will rely upon the stored energy until it is again about 3 AU from the Sun. In addition, the solar arrays on the return trip will help to shadow the comet sample [18].

The power available for the mission will depend on the size of the RTG and the area of the solar array. RTGs can provide between 2.7 and 285 W, depending on their size. A 16.6" x 44.5" RTG with a mass of 56 kg would generate approximately 285 W [19]. The area of the solar array is dependent upon the amount of power needed for the mission and upon the arrays capabilities at its beginning of life (BOL) and end of life (EOL). The array's power per area decreases over time; therefore, the life degradation is the factor between the EOL and BOL power per area. The following shows the calculations used to determine the area of the solar arrays for this mission.

$$P_{BOL} = P_0 \, I_d \cos \theta$$

Since the silicon solar cells have ideal efficiencies of 14%, the ideal solar cell output performance per unit area, P_0, is 190 W/m^2. Accounting for the design and assembly, shadowing, and temperature of the solar array, the inherent degradation, I_d, is nominally 0.77 [9]. The incident angle, θ, varies between 0 to 23.5 degrees. The goal of the attitude control subsystem of the spacecraft is to maintain an incident angle as close as possible to zero degrees. In addition to the control for the solar array, the spacecraft will need to maintain the attitude to protect the comet sample. The beginning of life power per area was calculated to be around 145 W/m^2 for an incident angle around 5 degrees.

$$P_{EOL} = P_{BOL} \, L_d$$

For the comet sample return mission which is expected to take about six years, the life degradation, L_d, would be about 77% for a silicon solar array. The end of life power per area for the mission would be approximately 110 W/m^2.

$$A_{sa} = P_{sa} / P_{EOL}$$

Finally, the area of the solar array using silicon cells was calculated to be around 2.3 m^2 for a power requirement of 528 W with the RTG supplying around 275 W [9]. The mass for the silicon solar arrays would be 5-10 kg, and the RTG will have a mass of 56 kg. The Super-ULP's would also need to be about 2.5 m^2 if they were used, but they would only have a mass of 4.2 kg [15]. The main advantage of the Super-ULP's is that they have a smaller mass than the silicon arrays; however, the silicon solar arrays have a strong heritage. The RTG/solar array combination appears to be an appropriate method of power generation for this mission. Furthermore, recent advancements are being made in the development of more efficient and safer RTGs and in increasing the amount of power a solar array can generate per area.

6.5   Storage

The energy storage will be accomplished with the use of batteries. Since the power demand varies and may not be generated continuously as in photovoltaics, batteries are necessary to store the energy. The main requirement of the battery is to recharge when the spacecraft is near the Sun and discharge at a distance greater than 3 AU [14]. Primary batteries were essentially not considered an acceptable option for this mission, since they cannot be recharged; therefore, secondary batteries will store the energy from the solar arrays. The batteries will either be made of nickel-cadmium, nickel-hydrogen, or sodium-sulfur. The nickel-cadmium battery is the most common secondary battery; however, the nickel-hydrogen battery appears to be better for extended missions [9]. The nickel-hydrogen battery is still under development but expectations are high concerning its performance. The

nickel-cadmium battery, however, is supported by extensive data and by its success in many missions.

6.6   Power for Penetrator

The penetrator can be powered by either batteries or an RTG. A possible option is to mount small arrays on the penetrator which can use the Sun's radiant energy when the comet neared the Sun. A battery could be used to store energy during eclipse periods. Since the penetrator will be in place when the comet is at apogee, the timing to use the solar arrays would be difficult to coordinate. Furthermore, using batteries would limit the amount of the monitoring time. The batteries for use in the penetrator would last approximately ten days [18]. An RTG was elected to be used as the power source for the penetrator. The RTG would produce the necessary amount of power for an extended amount of time. Ideally, monitoring of the comet through one orbital period is desired. However, the length of time the RTG can supply power would determine the amount of monitoring time. Since the penetrator will need 137 W, the RTG is estimated to be 3.3" x 8.7" and have a mass of 27 kg.

6.7   Conclusions and Recommendations

The power for the spacecraft bus and the penetrator together form the power subsystem of the comet nucleus sample return mission. Table 6.2 presents a summary of the power sources for the spacecraft and their sizes.

Table 6.2:   Power Generation Sizing

	Silicon Solar Arrays	RTG
Power Available (W)	253	275
Mass (kg)	5-10	56
Size	2.3 m^2	0.158 m^3

In addition to the RTG and the silicon solar cell arrays for the spacecraft's needs, a smaller RTG will meet the penetrator's requirements. Rocket thrusters will also provide power in the mission, such as the case of the drilling for the sample extraction. The power storage component of the subsystem will be comprised of nickel-cadmium batteries. Depending on the future of this proposed mission, nickel-hydrogen batteries may become available and prove to be more effective for this mission. Furthermore, RTGs are still being technically advanced, and using solely RTGs to generate power may be more efficient.

7.0   Propulsion

7.1   Requirements

The propulsion system will be responsible for providing the necessary ΔV's and attitude control maneuvers to accomplish the mission in the most efficient manner. What follows is a description of the chosen propulsive method and the process taken to arrive at this system.

7.2   Chemical

Chemical combustion systems including liquid, solid, and hybrid rockets are the most common. Although monopropellant engines have excellent handling characteristics, relative stability, and clean product decomposition, they lack performance to provide large velocity changes. In bipropellant engines, a fuel and an oxidizer chemically react with one another. One such example is monomethylhydrazine (MMH) and N_2O_4. This system type is more complex and expensive, but it produces a much higher specific impulse than the monopropellant systems [9].

7.3   Electric

Electric propulsion (EP) systems externally provide electric power to a working fluid to produce useful thrust. An ion engine uses charged particles that are accelerated by an electric field and discharged at a high velocity. Ion thrusters are able to generate exhaust velocities of 30 to 50 km/s, which are one order of magnitude higher than conventional chemical rockets. Hence, one EP-stage is able to generate velocity increments of 15 to 25 km/s with gross payload ratios of 10% to 50% [20]. While developmental risks are high, this method of propulsion seems promising because of its high-specific impulse, but low-thrust capabilities.

7.4 Propulsion Scenario

Selecting a propulsion system for the Snowball mission involves many different parameters including the mass and size of the spacecraft. Though the nuclear options are clearly the way of the future, there are still uncertainties in their development, and at this time they cannot be considered as a viable option.

For the comet sample return mission, a hybrid electric/chemical propulsion system will be used. The first phase of the mission, which includes launch ΔV's and inclination changes, will use an ion electric propulsion system powered by solar arrays. Because of the high potential of solar array damage in near comet operations, the arrays will be shielded for their protection. Chemical propulsion will be used for the remainder of the voyage for all midcourse corrections and rendezvous maneuvers. A similar method was originally planned for the CNSR mission.

The attitude correction thrusters will also use chemical propulsion for the entire voyage. The back-up systems will be supplied by chemical rockets should the electric propulsion fail.

7.5 First Propulsive Phase - Xenon Electric Propulsion

As previously stated, the primary system will use electric propulsion. Specifically, the ESA/German rf-ion thruster RIT 35 xenon or similar type engine will be used. This engine works with an electrodeless, inductive rf-gas discharge and ion-optically optimized three-grid electrostatic accelerator [20]. In an electric propulsion thruster, the propulsive mass (propellant) is ionized and then accelerated to high exhaust velocities by electrostatic Coulomb-forces. Thus, an EP-thruster consists of:

1. The ionizer, i.e., the ion or plasma source (substituting the conventional combustion chamber)
2. The accelerator, i.e., a high-voltage force grid system or a "magnetic nozzle" (substituting the thermodynamic nozzle)
3. The auxiliary and periphery components such as the thruster case and propellant tanks

I - 33

In general, electric propulsion systems consist of 4 components: the electric power source, the thruster electronics, the propellant storage and feed system, and the thruster itself. These will now be detailed.

7.5.1 Electric Power Source

As the primary power source, ultra-light solar panels will be used. One example is the Super-ULPs of MBB, Munich which are capable of generating more than 60 W/kg and 100 W/m^2 of specific power at 1 AU [20]. Unfortunately, solar cells operate effectively only up to 3 AU and a cell deterioration of up to 30% may be expected for this mission [21]. Solar arrays also risk comet dust impact damage on near-comet maneuvers. This second problem can be remedied by retracting the solar arrays when such damage is probable.

7.5.2 Electronics

The thruster electronics must provide the thrust unit with all the required voltage. An automatic control unit must control the system operation from the main bus voltage [20].

7.5.3 Propellant System

The propellant system includes the storage tank, the propellant feed systems, and the flow control unit. Ion thrusters need propellant of a high atomic mass in order to enable sufficient impulse-to-energy or thrust-per-power consumption rates. Xenon propellant has been chosen as the propellant for the electric propulsion phase and its physical features are given in Table 7.1.

Table 7.1: Xenon Propellant Features ("Review: Ion Propulsion Systems", Paper 87-25119, 1987, pp.75-92; [1] Airco Gas Company of Malvern, PA)

Contamination Risk	None
Price	$4.00/liter
Atomic Mass	131.3 AMU

True, it is estimated that the propellant will cost approximately $436,600 for the estimated 642.90 kg [21], but the safety which can be ensured to ground crews and mission operations justify this expenditure. Another substantial factor in choosing electric propulsion is that xenon will reduce the total propellant mass by 58.66%. This is shown in Table 7.2.

Table 7.2: Comparison of EP/Chemical Hybrid System to All-Chemical System ([2]MMH pricing from Olin Research Rocket Company @ $48.40/kg)

Parameter	EP/ Chemical Hybrid Propulsion	All Chemical Propulsion	% Saved By Using Hybrid System
Propellant Mass	2312.60 kg	5594.48 kg	58.66
Propellant Cost[2]	$517,400	$121,800	-76.47

In principle, the required propulsive force could be generated by one single EP-thruster. In practice, a cluster of 6 to 8 engines is preferred because of redundancy and throttling by cluster switching and the possibility of spacecraft maneuvering [20].

7.6   Second Propulsive Phase - Chemical Propulsion

Xenon electric propulsion will not be able to be utilized in near-comet operations. Similar to the CNSR mission, the solar arrays will be covered at about 200 km from the comet to ensure that the arrays do not incur further damage from comet debris impact. These arrays will remain retracted for the remainder of the mission. The second phase will be comprised of mission operations including the comet approach sequence, comet exploration and escape, and the Earth return sequence.

The fuel and oxidizer combination monomethylhydrazine will be used. This combination has a specific impulse of 220 s and the same mass margins were used as those for xenon. It is estimated that 1669.70 kg will cost approximately $80,800. The chemical propulsion expenditures are also depicted in Table 7.2.

7.7 Propellant Budget

The propellant budget is presented in Table 7.3. Allowances have been made for nominal and off-nominal operations which include correction factors. A mission margin and contingency of 5% each have been assumed and residual propellant and loading uncertainty accounted for an additional 2% and 0.5% respectively [9]. It should be noted that the xenon fuel accounted for 27.80% of the total propellant budget. Hence, for mass budget considerations, it is easy to see why electric propulsion was chosen as the primary method. Though an all-chemical system is nearly 4.25 times less expensive than the hybrid system, the advantages of a hybrid propulsion system are certainly made up for in mass considerations by 58.66%. The reduced propellant mass will ultimately reduce launch costs because smaller, less expensive launch rockets would be used.

Table 7.3:   Snowball Propellant Budget

Element	Hohmann Transfer Mass of Xenon-EP Propellant (kg)	Hohmann Transfer Mass of Chemical Propellant (kg)
ΔV Maneuvers	682.987	1218.850
Control Functions	0.000	233.000
Nominal Load	682.987	1451.850
Allowance for Off-Nominal Performance	6.830	14.518
Allowance for Nominal Operations	6.830	14.518
Mission Margin	34.800	74.000
Contingency	34.800	74.000
Total Required Propellant	765.600	1628.000
Residual Propellant	15.312	32.560
Loading Uncertainty	3.828	8.140
Total Propellant of Phase	784.739	1668.700
Total Propellant Load	**2453.439**	

7.8 Attitude Control Thrusters

All attitude and control movements will be accomplished by chemical thrusters. A mass of 233 kg has been incorporated into the propulsion budget at an estimated cost of $11,300. These thrusters have a steady-state pulse of 285 s and a mass of 0.5 kg [9].

7.9 Fuel Tanks

Four spherical fuel tanks will be used for this mission because they are easy to incorporate into the spacecraft bus configuration. Each tank will have a diameter of 1.2 m; three will contain hydrazine and the other xenon. Typically, stainless steel metal propellant tanks are used because of their proven design and compatibility [9]. Because these tanks will be custom made for the Snowball mission, it is difficult to analyze the tank's cost and mass at this time. Temperature control will be accomplished by active and passive thermal control measures.

7.10 Conclusions and Recommendations

Component refinements include placing the main electric and chemical thrusters on the spacecraft bus, positioning the attitude control thrusters, and choosing a specific type of propellant tank. Of the propulsive tasks remaining, determining the placement of the thruster is likely to be the most difficult.

8.0   Guidance, Navigation, and Control

8.1   Requirements

Assuming that the launch vehicle accurately delivers the spacecraft to an initial low Earth orbit, additional correction velocity changes will not be required. As a result, initial orbital maneuvers could be programmed from the ground, requiring no onboard guidance and navigation. Once the spacecraft is out of Earth orbit, however, guidance and control will require onboard equipment for attitude control. The payload pointing direction for this mission will be inertial pointing, due to the comet's non-Earth oriented orbit. This will have an important role in the determination of proper guidance, navigation, and control systems.

8.2   Sensors

The selection of the sensors is dependent upon accuracy as well as the type of referencing, i.e., the inertial fixed direction for the Snowball mission. The following is a description of possible sensors which may be used in conjunction with the mission, and most likely in combination with one another.

8.2.1   Sun Sensors [22]

Sun sensors are the most widely used sensor type; one or more varieties have flown on nearly every satellite. The Sun sensor owes its versatility to several factors. Unlike the Earth, the angular radius of the Sun is nearly orbit independent and sufficiently small (0.267 deg at 1 AU) such that for this mission, a point-source approximation is valid. This simplifies both sensor design and attitude determination algorithms. The Sun, at Wild 2 aphelion, is sufficiently bright to permit the use of simple, reliable equipment without discriminating among sources and with minimal power requirements. Consequently, the Snowball mission is concerned with the orientation and time evolution of the Sun vector in body coordinates. Attitude control systems are frequently based upon the use of a Sun

reference pulse for thruster firings, or more generally, whenever phase angle information is required. Sun sensors are also used to protect sensitive equipment such as star trackers, to provide a reference for onboard attitude control, and to position solar power arrays.

Sun presence detectors are used to protect instrumentation, to activate hardware, and to position the spacecraft. Ideally, Sun presence detectors provide a step function response that indicates when the Sun is within the field of view (FOV) of the detector.

8.2.2 Star Sensors [22]

Star sensors measure star coordinates in the spacecraft frame and provide attitude information when these observed coordinates are compared with known star directions obtained from a star catalog. In general, star sensors are the most accurate of attitude sensors, achieving accuracies to the arc-second range. This impressive capability is not provided without considerable cost, however. Star sensors are heavy, expensive, and require more power than most other attitude sensors. In addition, computer software requirements are extensive, because measurements must be preprocessed and identified before attitudes can be calculated. Star sensors also suffer from both occultation and interference from the Sun, the Earth, and other bright sources. In spite of these disadvantages, the accuracy and versatility of star sensors have led to applications in a variety of different spacecraft attitude environments.

Stray light is a major problem with star sensors. Thus, an effective Sun shade is critical to star sensor performance. Carefully designed light baffles are usually employed to minimize exposure of the optical system to sunlight and light scattered by dust particles, nozzle exhaust, and portions of the spacecraft itself. Even with a well-designed Sun shade, star sensors are typically inoperable within 30 to 60 deg of the Sun.

Gimbaled star trackers are commonly used when the spacecraft must operate at a variety of attitudes. This type of tracker has a very small optical FOV (usually less than 1 deg). The gimbal mounts, however, give the sensor a much larger effective FOV. In

addition, these trackers normally operate on a relatively small number of target stars. A major disadvantage of gimbaled star trackers is that the mechanical action of the gimbals reduces their long-term reliability. Also, the gimbal mount assembly is frequently large and heavy.

Many different types of image definition devices are used in gimbaled star trackers to determine the position of the star with respect to the center position in the small FOV. The electronics assembly causes the gimbals to move so that the star image remains centered in the small FOV. The star's position is then given by the gimbal angle readout positions.

Spacecraft which maintain an inertially fixed direction commonly employ gimbaled star trackers which have a unique target star. The positions of Polaris and Canopus near the north celestial and south ecliptic poles, respectively, make these two stars particularly useful. A Sun/Canopus attitude reference system has been used for Mariner and Surveyor [23]. A serious disadvantage of unique star trackers is that they may occasionally track either the wrong star or particles scattering stray light, such as paint chips from the spacecraft.

8.2.3   Inertial Measurement Units

Inertial measurement units (IMUs) consist of sensors that measure translational motion using accelerometers and rotational motion using gyros. Spacecraft IMUs need these accelerometers only if they must measure velocity, either for guidance and navigation of the spacecraft or for turning off an engine. These units can be gimbaled platforms: gyros and accelerometers mounted on an internal platform that maintains a given inertial orientation in space. These units can also be strapdown systems, which use high-resolution software to resolve the output of the body-referenced sensors into an inertial frame. Strapdown units often use rate gyros that supply rates directly and allow the integration of their output to obtain position data [9]. Rate gyros are the simplest and the least expensive gyros, but their integrated output requires frequent correction for precise attitude determination using other sensors such as Sun sensors and star trackers [22].

IMUs are subject to gyro drift and bias errors. For more than a few hours of use, their information must be updated from an external reference such as the Earth, Sun, or the stars. In the future the IMU gyros of the gas-bearing and laser type will be made smaller, less massive, less costly, and therefore be more commonly used, while a host of new gyros are on the drawing board, such as the fiber-optic gyro [9].

8.2.4 Sensor Determination

The sensor system chosen for the Snowball mission is a fiber optic rotation sensor in combination with a sun sensor and star tracker. The star tracker to be used is the recently upgraded Astros II, a gimbaled star and target tracker. Its advantages include the abilities to simultaneously integrate over a field as it scans and to tolerate a higher amount of stray light (as compared to the former model, Astros I) [24]. The sun sensor for Snowball will be an Adcole two-axis digital sun sensor, a category of acquisition sun sensors. Though sun sensors are not used for high precision navigation corrections, they do serve important functions which include the shielding of more sensitive instrumentation, due to their relative ruggedness. The fiber optic rotation sensor (FORS), which is an IMU, will be placed in parallel with the Astros II star tracker. It includes an integrated optics chip to control rotational motion using gyros. The new technological payoffs of FORS include long life, low mass and power, and a lower recurring cost [24]. The rate gyros used by FORS are the simplest and least expensive in comparison to other IMUs but their output requires frequent correction. This is why it is used in conjunction with a sun sensor and star tracker.

All three of the sensors will be placed on the High-Precision Scan Platform. The Adcole sun sensor requires a 128° by 128° FOV and thus is placed on the outer corner of the platform [22]. Astros II, which is a fragile component, will be sandwiched between other less fragile instruments.

8.3   Actuators

Once the requirements are defined, a method of controlling the spacecraft must be selected from three types: passive, spinners, or three-axis stabilized. Three-axis stabilized control is best suited to the Snowball mission because of the extreme accuracies required for Wild 2 observations. The following is a list of possible actuator controllers which may be used in conjunction with the mission.

8.3.1   Momentum and Reaction Wheels [22]

Devices for the storage of momentum are used on spacecraft for several purposes: to add stability against disturbance torques, to provide a variable momentum to allow operation for Earth-oriented missions, and to transfer momentum to the spacecraft body for the execution of slewing maneuvers.

Because reaction wheels are defined to be a system with nominally zero momentum, they are used primarily for absorbing cyclic torques and temporarily storing momentum from the body during slew, or reorientation, maneuvers. However, secular disturbance torques would eventually saturate the momentum storage capacity. Therefore, a provision is made for periodic momentum dumping through external torques produced by gas jets. Normally, three reaction wheels are used to control a vehicle, with each wheel axis aligned with each of the respective body principal axes; a redundant fourth wheel is also common.

8.3.2   Control Moment Gyros [22]

A gyroscope, or gyro, is any instrument which uses a rapidly spinning mass to sense and respond to changes in the inertial orientation of its spin axis. Two basic types of gyros are used on spacecraft: rate gyros, which are attitude sensors used to measure changes in the spacecraft orientation and were described previously; and control moment gyros (CMGs), which are used to generate control torques to change and maintain the spacecraft's orientation.

Control moment gyros are not attitude sensors like rate gyros, but are used to generate attitude control torques in response to onboard command or ground command. They operate much like reaction wheels except that their spin axis is gimbaled. Torques are generated by commanding a gimbal rotation and thereby changing the spin axis orientation. CMGs may be used in conjunction with rate gyros and an onboard computer as components of an attitude determination and control system. Because of their expense and weight, CMGs are used only on large spacecraft, and will not be considered.

8.3.3 Gas Jets [22]

All jets or thrusters produce thrust by expelling propellent in the opposite direction. The resultant torques and forces are used to control attitude, to control the speed of momentum wheels, and to adjust orbits. Hot-gas jets generally produce a higher thrust level (>5 N) and a greater total impulse or time integral of the force. Cold-gas systems operate more consistently, particularly when the system is operated in a pulsed mode, because there is no chemical reaction which must reach steady state. The lower thrust levels (<1 N) of cold-gas systems may facilitate more precise control than would be available with a high-thrust system.

The propellant supply required for jets is the major limitation on their use since the propellant budget is such an important part of mission planning. Other considerations are the overall weight of the system and the need to position thrusters where the exhaust will not impinge on the spacecraft. In more distant orbits, beyond geosynchronous altitude, jets are the best means of interchanging momentum with the environment. High-thrust or total impulse requirements may indicate the need for a hot-gas system. Otherwise, the cold-gas system may be favored because the hydrazine freezes at about 0° C and may require heaters if lower temperatures will be encountered during the mission.

8.3.4 Actuator Determination

Three-axis control will be required for this mission because of the large and extremely accurate velocity changes that will be required in order to rendezvous with the comet. The control torques about the three axes will be generated from a zero-momentum system and thrusters. This type of system is extremely accurate and allows for unlimited maneuverability. The lifetime of this system is only dependent upon the amount of propellant, which is very important, considering the length of the mission. One drawback of this system is the higher cost compared to others. As accuracy need is increased, costs will increase similarly. Thrusters will be used for momentum dumping of the reaction wheels as well as for the orbital velocity changes. Internal disturbances, such as propellant sloshing, thruster misalignment, and vibration, can be controlled by these means, but will have less of an impact on control. One important internal force which must be taken into consideration is the effects of the penetrator and drill jettison and sample rendezvous with the orbiter.

Since the speed for the reaction wheels will be approximately ±2000 rpm, a fine model is manufactured by Sperry. It produces a high moment of inertia because of its nonorthogonal four-wheel configuration. At its top speed the Sperry momentum wheel can produce over 40 kg m^2/s of angular momentum [22].

Four attitude control thruster clusters are placed on the outer edge of the solar array so as not to impinge on the spacecraft. The thrusters on Snowball will consist of both a hydrazine hot-gas system for orbit corrections and a Freon cold-gas system for attitude and spin rate control. Although single systems can be designed to perform all three functions, this mission requires the ejection of the orbit correction system before all attitude and spin rate control functions are completed. The impulse potential of a hot-gas system was required for the orbit changes, but a simpler cold-gas system sufficed for the other requirements. Also, the low temperature encountered when Snowball will rendezvous with Wild 2 requires the Freon system in case the hydrazine were to freeze up.

8.4 Onboard Computers [22]

In general, onboard attitude control is obtained by combining onboard sensors through a control law, which is implemented via analog logic ar a digital computer. Because attitude control systems are normally chosen for reliability and cost, control laws which are easily implemented with analog systems have been widely used. Sun sensors are well suited for such applications because the sensor output is simply related to an angle which is to be controlled. Reaction wheels, momentum wheels, or jets are preferred torquing devices because in many applications there is a simple relationship between attitude errors and the appropriate torque commands.

Increasingly stringent spacecraft attitude control and autonomy requirements have resulted in the need for onboard computers or digital processors. Digital processors afford several advantages over analog systems, including the capability of processing complex types of data - such as star tracker, gyroscope, or digital Sun sensor data - and of modifying programmed control laws via ground command.

8.5 Conclusions and Recommendations

Navigational problems that might be encountered during this type of mission will be a result of the following comet characteristics [24]:

- Very small orbital radius and orbital speed
- Unknown central-body mass and gravitational harmonic coefficients
- Relatively large ratio of non-gravitational to gravitational accelerations
- ΔV maneuvers as small as 1 cm/s

All of these potential causes for problems are based on the small size of a comet and uncertainties associated with it. This is another deciding factor in the determination of the type of GN&C equipment that will need to be implemented for this mission.

Cost of the GN&C system has roughly been determined as $129 M by a spacecraft system cost model. Maximum power usage for the sensor system is 60 W, while that for the actuator system is 90 W.

9.0   Command and Control

The command and control subsystem is responsible for the operation of the spacecraft. It distributes commands, stores information, and formats data from the spacecraft and the payload. The commands can be transmitted from the ground in real-time, or they can be preprogrammed into onboard computers. Generally, the command and control subsystem can be broken down into the spacecraft's computer and communication systems.

9.1   Computer Systems

9.1.1   Requirements

The computer system is responsible for managing all of the spacecraft's functions and integrating them together. The functions of the onboard software include navigation, housekeeping and health monitoring, command processing, spacecraft subsystem management, payload management, and communications [9].

In designing a computer system, the availability, capability, flexibility, and reliability need to be maximized while cost and risk are minimized. Though a specific computer system has not been chosen for this mission, much of the criteria needed to select an adequate system is presented.

All of the subsystem programs will run continuously whenever the subsystem is powered, and they will be coordinated with a real-time clock. Each of the microprocessors must be capable of accepting and interpreting commands from the ground, and they must be able to synchronize and control the hardware in their respective subsystems. Additionally, they must obtain data from a telemetry downlink and they must be compatible with one another [25].

9.1.2 Capability and Flexibility

Since it is desired that the computer system must be flexible, the spacecraft will probably carry a hybrid machine that contains both a general purpose computer (GP) and a digital differential analyzer (DDA). The GP computer excels in tasks involving numerous decision functions or requiring many discrete solutions of a given problem. The DDA computer is useful for problems that require high iteration speeds such as differential equations. In addition, the DDA is capable of serving as a control element in a closed-loop system [14].

Also, in order to provide maximum flexibility in program development, most of the spacecraft subsystem programs will be completely reprogrammable. The software must be able to modify control algorithms based on flight performance, spacecraft inertial property changes, and structural dynamics. Additionally, the software will be able to adapt sequence changes based on science and engineering data collection [25].

9.1.3 Availability and Cost

To meet reliability requirements, a spacecraft computer system may have to be duplicated or even triplicated. To reduce the cost of computer systems, many spacecraft commonly use commercially available computers rather than a computer system designed specifically for the mission. As long as these off-the-shelf computers can be easily adjusted to accommodate the requirements of the spacecraft, the savings will be great; however, if a system needs to be altered extensively, it may be cheaper to design a computer for the mission [26].

9.1.4 Reliability

The spacecraft's computer system must be very reliable since it controls all of the other subsystems. In case of computer failure, some type of backup system will be required

to ensure the success of the mission. Redundancy techniques range from entire system replication to virtual redundancy.

A functional distribution system with virtual redundancy is being considered for the comet sample return mission. This system is similar to that of the Galileo spacecraft. Galileo has a dual computer system. The attitude control and pointing uses a standard off-the-shelf computer while the command and data system uses another commercially available microprocessor. The dual computer system carries STAR (Self Testing And Repair). This consists of multiple copies of each major component. A special piece of hardware called TARP (Test And Repair Processor) controls the computer system. Five TARPs were onboard, but only three worked at one time. If the TARPs voted that a component had failed, the spare would be activated. If the vote was not unanimous, the dissident TARP would be shut down and a spare would be activated. The advantage of this type of system is that only the minimum number of components would be powered at a given time. A weakness is that if a switch failed to turn off a component, the fault tolerance would be negated [26].

A similar type of system that is being considered is the spacecraft health reasoning prototype (SHARP). Its primary task is the monitoring and diagnosis of spacecraft and ground systems. SHARP applies artificial intelligence as well as conventional computer science techniques to automate and eliminate much of the tedious data processing and analysis associated with monitoring the health and status of the spacecraft. SHARP has not yet been fully developed, but so far, it is living up to its expectations [27].

9.1.5   Specific Design Criteria

Computers for space applications are much different than ground-based systems. The computer system has to be as lightweight and power efficient as possible. In addition, it must be hardened to protect it from damaging ionizing radiation and it must be mounted a safe distance away from the RTGs. Due to the rough flight that the spacecraft may experience, computers must be supported in flexible mounting systems [9].

Using Galileo's computer as an approximation to the one needed for the comet sample return spacecraft, the mass will be about 12 kg. Its volume will be about 12,900 cubic centimeters, and it will consume about 50 W [9]. Galileo's 19 microprocessors have a total of 320 kbytes of random access memory (RAM) and 41 kbytes of read-only memory (ROM) [25].

9.1.6   Conclusions and Recommendations

The comet sample return spacecraft will use a computer system which resembles that of Galileo. A commercially available dual computer system will minimize cost and a virtual redundancy system similar to STAR will provide a desirable degree of reliability. Though a specific system has not been defined, it is hoped that with the requirements that have been presented, an adequate system can be easily chosen.

9.2   Communications

9.2.1   Requirements

The communications subsystem will deal with the transmitted and received signals of the spacecraft. A typical deep space telecommunications system performs three basic functions: telemetry, command, and tracking. The telemetry function involves informing the Earth ground station of the status of spacecraft instruments and systems, of the imaging data, and of the scientific research data. The command function involves the transmission of the commands needed to control specific spacecraft functions such as flight path, mapping, and drilling. The tracking function transmits information on monitoring spacecraft trajectory and navigation, and measuring the local space medium properties [28].

To perform the transmissions that are necessary during the mission, the design of the communications system must take into account the position of the comet probe, the position of the Earth, and the position of the penetrator monitoring unit left behind on the comet

surface. Three main communication systems will be used, the first for communication between Earth and the comet probe, the second for communication between Earth and the penetrator monitoring unit, and a third for relaying commands from the spacecraft probe to the tethered extraction unit. Because of the penetrator monitoring unit's small size, low power, and need for long distance communication, a relatively large high-gain antenna is not a viable option.

For the sample return mission requirements, a high-gain parabolic antenna will be used for the long communication with Earth. The penetrator monitoring unit will employ an independent system for sending its scientific data to Earth. For this task a smaller, lower powered optical communication unit will be implemented. Wiring located inside the tether will be sufficient to transfer commands from the spacecraft's main computer to the extraction probe.

9.2.2   High-Gain Antenna

The basic components of the communications subsystem consist of a receiver, a high-power transmitter, a directional antenna, and an rf diplexer [28]. The rf diplexer allows the antenna to both transmit and receive data.

For communication with Earth, high-gain antennas with minimum side and back lobes should be used to maximize the signal to noise ratio and prevent any electromagnetic interference to the spacecraft instruments [29].

Several beam frequencies are available for use. The National Telecommunications and Information Administration (NTIA) assigns specific frequencies for use with NASA's Deep Space Network (DSN). The allocation of radio frequency bands is defined in terms of radio services, one of which is space research. Deep space communication must take place in bands allocated for space research. The choice of bands is limited at present to the 2-GHz uplink-downlink pair and the 8-GHz downlink [28]. Since the higher frequency downlink will use less power to transmit, the frequency for the transmission from the probe to Earth

will be 8.45 GHz, while communications from Earth to the probe will use a frequency of 2.12 GHz.

The high gain antenna would have a large diameter of 2 m, a mass of 7.1 kg, and a cost of approximately $8M. Along with the antenna, a 4.75 kg transponder costing $4.9M would be needed [30]. The high-gain antenna system should require 122 W [29].

9.2.3 Penetrator Monitoring Unit

While the spacecraft bus' communications with Earth will take place using a high-gain antenna, the penetrator monitoring unit must also have the capability of sending the scientific data of comet behavior independently to Earth. For this assignment a directional high-gain antenna would be too large and require too much power for communication with Earth. To ensure the success of the penetrator monitoring unit, the communication system with Earth must be of modest size, low power and reliable. A recently developed optical communication system (OPTRANSPAC) which satisfies these requirements has a mass of 54 kg and will require 57 W [31].

The system design must minimize the effects of equipment variations during transmission. Realizing that not all transmissions can be made 100% error free, the transmissions will be in the form of an 8-bit error correction code. This will greatly improve the reliability of each transmission and reduce the number of needed retransmitted signals. Data rates will resemble those of the Voyager missions to Saturn at around 30,000 bits per second [32]. They will vary upon the amount of information needed for transmission and the exact distance to Earth [32]. The entire communications system will offer a dependable and proven method of command and data handling.

9.2.4 Sampler Communication

The sampling unit will require a limited amount of commands to the drilling unit. The entire drilling procedure should only take about 30 minutes. Drilling procedures will be

coordinated and monitored from the spacecraft bus' main computer. This communication link will utilize wiring embedded into the sampler's tether.

9.2.5 Conclusions and Recommendations

The use of low-gain antennas to provide a link from the penetrator monitoring unit to the spacecraft bus has been ruled out. This was done because it would require that the spacecraft bus stay in the vicinity of the comet for a prolonged period of time and during its active state. This would endanger the main objective of the mission, to return a comet nucleus sample uncorrupted to Earth. Thus, OPTRANSPAC is the preferred method.

The use of fiber optic cables was also investigated for the communication link between the spacecraft's main computer and the extraction probe. This option was ruled out due to the operating temperatures of the detectors needed for the fiber optic network.

OPTRANSPAC is a low mass, low powered option that was also considered as the main communication link between the spacecraft bus and Earth. A high-gain antenna was chosen instead because of its long history of proven reliability and lower cost than the recently developed OPTRANSPAC.

10.0 Thermal

10.1 Requirements

The design of the thermal-control subsystem is entirely dependent on the other subsystems, including the placement of components within the craft. Throughout the entire mission, all spacecraft components must be maintained within their respective temperature limits. This is a difficult task due to the variation in temperature the craft will experience in travelling from an Earth orbit to Wild 2 near aphelion. Sources of heat are the Sun, the Earth, which both reflects and emits energy, and elements within the craft itself. These internal sources will consist of the transmitter, RTG, batteries, scientific payload, kick motor, and thrusters.

Operating temperatures differ significantly between spacecraft elements. Batteries must be maintained between 5 and 20°C, electronics between 0 and 40°C, while solar cells can operate anywhere from -100 to +100°C. Hydrazine thrusters will be used, and the liquid monopropellant must be maintained between 7 and 35°C. The fuel lines will therefore require heating. Structural members can tolerate a temperature range from -45 to +65°C, but the booms which support the two scan platforms, particularly the one supporting the high precision scan platform (HPSP), must not be subjected to such large temperature gradients. These platforms will permit much smaller temperature variances due to the pointing accuracies required of the devices which they house. The scientific instrumentation itself must also be thermally controlled. The infrared radiometer and mapping spectrometer on the HPSP, for example, ideally operate at less than 120K and will therefore require refrigeration [9].

The thermal-control subsystem will most likely need to employ passive, semi-passive, and active techniques. Passive systems have no mechanically moving parts and therefore require less power. Also, they are generally less massive, and cost less than active methods. Semi-passive systems enhance passive ones through the use of simple temperature-activated

controls to open or close conductive paths. Such non-active techniques, however, may not ensure adequate temperature ranges. Therefore, an optimum combination between active and passive thermal-control systems is sought.

10.2   Passive and Semi-Passive Techniques

To minimize the cost, passive control techniques will be used as much as possible. The most inexpensive means is thermal coatings and paints. These will be applied to the four propellant tanks. Two of the tanks will contain hydrazine, and therefore must be maintained at a higher temperature than the two xenon tanks. The tanks will be pointed away from the Sun, so a coating with a fairly high absorptivity, such as black paint ($\alpha = 0.975$), will be suitable for the hydrazine tanks [9]. The xenon tanks, however, must be kept at low temperatures and would be better suited with silvered or aluminized teflon, or white enamel, which have considerably lower absorptivities. Multi-layer insulation (MLI) blankets, louvers, and radiators will be used on the spacecraft bus.

The high and low precision scan platforms (HPSP and LPSP) and the magnetometer will be protected from solar radiation by Sun shields, composed possibly of OSR (Quartz Over Silver) with very low solar absorptivity and high infrared emissivity [9]. Internal coupling, both conductive and radiative, will be maximized to reduce temperature gradients and simplify the passive thermal control design. Affixed to each scan platform will be a radiator, such as a second surface mirror, which will radiate waste heat to deep space. A central heating system (CHS), designed originally for the CRAF spacecraft, is shown in Figure 10.1 [24]. The CHS will utilize waste RTG heat to minimize the amount of active electrical heating. In the design of the CHS, heat pipes will transfer heat, as needed, to the spacecraft bus and the scan platforms via thermal switches. These switches, which provide direct conduction paths between the equipment mounting plates and the heat sources, whether they are heat pipes or electrical heaters, will be used to control heat flux [9].
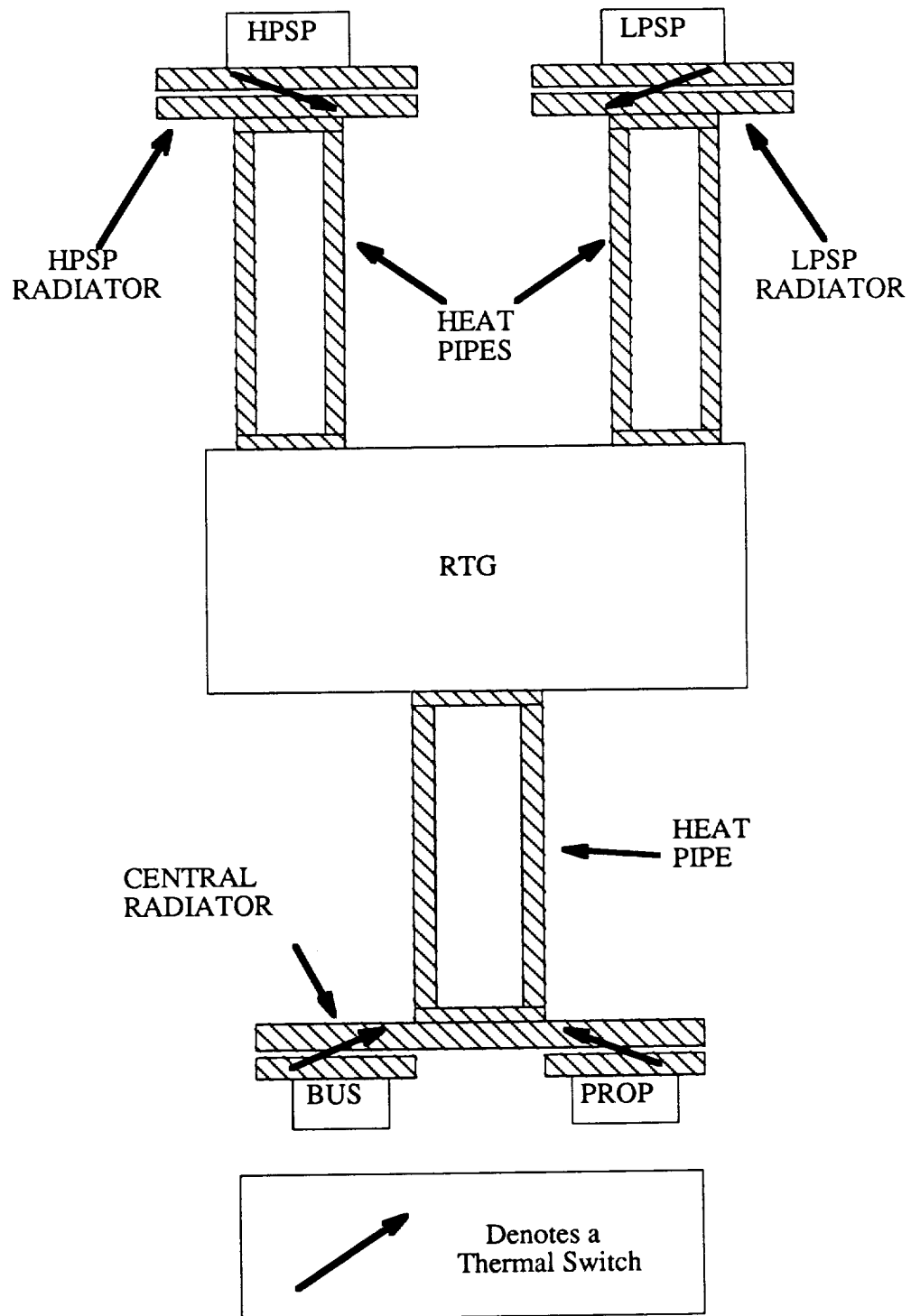
Figure 10.1: Schematic of Thermal Subsystem

10.3 Active Techniques

Present designs minimize the use of active thermal control systems due to their cost and mass penalties, and reliability. They are more prone to failure than are passive methods because of their moving parts. Two prominent active techniques are electrical heaters controlled by thermostats and pumped-loop systems [9]. The only active devices which are planned to be employed are auxiliary electrical heaters, which will be used as back-up thermal control for the CHS.

10.4 Cost

Dr. Robert McMordie of the Martin Marietta Astronautics Group estimates that the thermal-control subsystem accounts for about 3-4% of the total spacecraft dry mass and roughly the same percentage of the cost [9]. This estimate is most likely on the low side for the mission at hand for two reasons. First, this estimate is for satellites in a geocentric orbit in which Earth is a heat source, whereas an interplanetary orbit will result in lower temperatures. Consequently, more heating of electronics will be required. Secondly, one mission objective is to preserve the comet sample's physical and chemical integrity. The sample will therefore need to be well-protected against thermal contamination. These two factors may increase the spacecraft's mass and cost to between 6 and 8 per cent.

10.5 Conclusions and Recommendations

To adequately describe the thermal-control subsystem, the exact configuration of the craft and its space environment must be known. After defining this configuration, the craft can be modeled using a finite element scheme, and the effects of conduction, convection, radiation, and internal heat generation can be better approximated. In the preliminary thermal control design, proven technology, essentially passive in nature, has been chosen because of the extended length of the mission. These approximations allow the locations of the thermal control devices to be determined, and further refinement can be achieved.

11.0   Science Payload

11.1   Requirements

The selection of appropriate landing sites will rely mainly on two characteristics: safety and sample return. The selected sites must be safe for the monitor and drill from landing through departure phases. In addition, these sites must also allow the best chance for returning and examining the most volatile comet materials. To determine these characteristics, the orbiter must make many orbits around the comet. This task would best be broken down into two stages. The first stage would involve a brief overview of the comet while the second stage would involve more detailed analysis of all possible landing sites. These sites must be fairly flat, have a thin crust layer, and have fairly low gas and dust production to insure safe landings for the drilling unit and penetrator.

In order to determine these various comet characteristics, science observing instrumentation will need to be either mounted on a high-precision scan platform (HPSP) or a low-precision scan platform (LPSP), depending on needed accuracy. These instruments will need to be put on such platforms in order to get unobstructed views of the comet and to avoid magnetometer and RTG interference. Both platforms will also require appropriate shielding from the Sun and central heating from waste RTG heat [24]. In addition to solar shielding each of the instruments will have to be protected from dust contamination. In order to accomplish this each instrument will have to be allowed a "dust budget" of allowable contamination. A dust counter will measure the comets dust production rate. If an instrument is in a hazard level then a safety device for that instrument will be triggered (cover closing, power down, etc).

11.2   High Precision Scan Platform

As listed in Table 11.1, the HPSP will contain four scientific instruments plus the star tracker, sun sensor, and FORS. These instruments include a thermal infrared radiometer, a

visual-infrared mapping spectrometer, and wide and narrow angle cameras. Each of these instruments will be used for determining the size and shape of the comet as well as the sub-surface volatility characteristics (see Table 11.2 for detail). Instrument observing positions on this platform will need to be controlled with accuracies within 2 mrad with 1 mrad resolution [24].

Table 11.1: Science Payload Mass and Power Budget (Draper, Ronald F., Comet Rendezvous Asteroid Flyby, Mariner Mark II, Technical Definition and Class "A" Cost Review, JPL D-3384, Volume 1, June 9, 1987.)

Instrument	Mass (kg)	Operating Power (W)	Survival Power (W)	Location *
Ion Mass Spectrometer	4.2	3.5	0.0	LPSP
Scanning Electron Microscope/ Particle Analyzer	12.9	14.0	N/A	LPSP
Ice and Dust Detector	8.9	10.7	1.1	LPSP
Neutral Gas Ion Mass Spectrometer	9.0	16.0	0.3	LPSP
Cometary Dust Environment Spectrometer	5.3	2.9	2.9	LPSP
Superthermal Plasma Investigation of Cometary Environments	13.8	16.5	0.0	LPSP
Thermal Infrared Radiometer	7.8	4.5	0.0	HPSP
Cameras (NA & WA)	36.5	24.3	10.0	HPSP
Visual-Infrared Mapping Spectrometer	18.5	10.4	3.1	HPSP
Coordinated Radio, Electron, and Wave Experiment	13.1	13.0	2.0	HPSP
Magnetometer	4.9	5.8	1.0	Bus/Boom
Totals	**134.9**	**121.6**	**20.4**	

* LPSP=Low Precision Scan Platform
HPSP=High Precision Scan Platform

Table 11.2: HPSP Instrument Objectives and Purposes (Schwehm, G.H., Langevin, Y., "Rosetta/Comet Nucleus Sample Return Mission", ESA Publications Divisions, Netherlands 1991)

Instrument	Objectives	Purpose
Ion Mass Spectrometer	-Determine composition of gas and ions in coma and on surface -Study chemical reactions and ionization processes	-Sample documentation -Site selection
Scanning Electron Microscope/ Particle Analyzer	-Determine cometary dust distribution & dynamics -Imaging individual cometary dust grains	-Site selection -Sample documentation
Ice and Dust Detector	-Characterize grain emission by the comet -Measure integral mass deposition rate on Spacecraft	-Spacecraft ops. -Sample documentation
Neutral Gas Ion Mass Spectrometer	-Determine chemical composition of organic and anorganic volatiles	-Sample documentation
Cometary Dust Environment Spectrometer	-Determine cometary dust distribution & dynamics	-Site selection -Sample documentation
Superthermal Plasma Investigation of	-Characterize plasma velocity distribution around comet	-Site selection -Sample documentation
Cometary Environments	-Determine electron energy-angle distribution and wave forms	

11.3 Low Precision Scan Platform

This platform will support seven scientific instruments, as listed in Table 11.1. These instruments will all be needed in determining a wide variety of comet characteristics. The comet elemental composition, mass and density, dust and gas production rates, composition of the neutral gas and low energy ions in the coma, magnetic field, and density, temperature, and energy spectrum of electrons will all be necessary in determining appropriate landing sites (see Table 11.3 for specific instrument detail). The comet dust environment monitor

will be activated throughout the entire rendezvous with the comet in order to examine dust and gas emission changes, especially while approaching perihelion. Various other imaging objectives will also be achieved with these instruments, such as determining the chemical and physical diversity of the nucleus, activity difference between the nucleus and surface, relation of nucleus surface activity to comet atmosphere, and the properties of dust and ion tails in relation to nucleus activity. All instruments on the LPSP will only need to be controlled to within 17 mrad with 17 mrad knowledge [24].

Table 11.3: LPSP Instrument Objectives and Purposes (Schwehm, G.H., Langevin, Y., "Rosetta/Comet Nucleus Sample Return Mission", ESA Publications Divisions, Netherlands 1991)

Instrument	Objectives	Purpose
Thermal Infrared Radiometer	-Measure temperature profile of core sample -Measure thermal diffusivity of comet surface layers	-Sample documentation
Cameras (NA & WA)	-Comet detection -Global/detailed mapping -Characterize nucleus: shape, rotation, surface features, albedo, volume, density, active sites	-Site selection -Spacecraft operations.
Visual-Infrared Mapping Spectrometer	-Generate thermal map of comet nucleus -Characterization of coma and nucleus absorption and emission	-Site selection -Sample documentation
Coordinated Radio, Electron, and Wave Experiment	-Determine density, temperature and energy spectrum of electrons -Characterize plasma wave spectra and wave forms	-Site selection -Sample documentation

11.4   Conclusions and Recommendations

The next step in completing the science payload substructure would be to budget the power requirements for each instrument throughout all mission phases, especially rendezvous. Most of the science instruments will remain powerless or in a minimal power required state during pre-rendezvous. Once the spacecraft begins to approach aphelion various instruments will be used for their respected tasks and, therefore, burden the spacecraft with different power requirements at different times. An instrument such as the dust counter would obviously remain on throughout the entire rendezvous in order to determine when hazardous dust emission rates occur for each instrument. Information like this should be budgeted for every instrument. The organization of the exact location of each instrument on its respective scan platform should also be developed. In doing this, consideration must be made towards placing each instrument in an area that will allow an unobstructed FOV.

12.0   Sample Extraction

12.1   Requirements

This sample extraction process will take place via a tethered coring system. A 0.5 km long tether, a drive impact tube, and a coring unit housed in a penetrator will be required for this phase of the mission. Each of these must fulfill certain requirements for a successful mission. The tether must have a low mass and high strength, and at the same time, it must be relatively thin to minimize the pre-launch volume. The drive impact tube, necessary for determining the surface density and strength, must house an accelerometer and a low-gain antenna to transmit data back to the spacecraft. The sampler must be designed to withstand the impact with the comet surface. The most important requirement for the sampler will be its ability to control the thermal environment around the sample during the extraction.

12.2   Sampling Process

Once the comet has been sufficiently mapped, and a target site has been selected, the spacecraft will begin the sample extraction phase. This phase will begin by "forcing" an orbit around the comet, and then maintaining a stationary position half a kilometer above the selected target site. Next, a drive impact tube housing an accelerometer and a low-gain antenna will be spring fired at the comet surface. The drive tube is basically a hollow tube that will determine the density and strength of the cometary surface upon impact. Once this information has been relayed to the spacecraft, calculations will be made to determine the necessary velocities needed for the sampling penetrator and the penetrator monitoring unit to sufficiently implant themselves in the surface.

The sampling penetrator will be deployed on a tether from the spacecraft using a spring mechanism. When it has reached a safe distance away from the spacecraft, it will be accelerated to the necessary velocity using a pair of small rocket thrusters. The penetrator will be attached to the tether by a slip-connection to allow for spin stabilization during flight.

The tether, stored on a flywheel driven by an electric motor, will be released freely during the flight of the penetrator. After impact, tension in the tether will be kept to a minimum so that the coring process is not disturbed. Upon completion of the coring, the tether will be retracted by the motor driven flywheel, returning the sample to the spacecraft bus. The penetrator utilizes a liquid propellant, monomethylhydrazine, to control the duration of the in-flight burn and to power the drilling process. The total time for dispatch, sample extraction, and retrieval will be about 30 minutes [18].

12.2.1 Tether

The sampler tether will be about 0.5 kilometers in length and have a mass of approximately 4.1 kg. Its outer diameter is only 2.5 mm, giving it a volume of 0.00245 m^3. The tether consists of five layers: an inner Nomex core, a communication wire, an insulation layer, a Kevlar strength member, and an outer Nomex braid. The tether was initially designed for the Tethered Satellite project (TSS). The TSS tether was designed to tow a 500 kg satellite at a distance of 100 km, and thus it meets the light-weight, high-strength requirement needed for this mission [33]. The motor used to retract the tether and sample will require 10 W.

12.2.2 Anchoring

Because of the near-zero gravity conditions which exist on the comet surface, the penetrator will have to be anchored before the sample extraction process begins. A predetermined velocity for sampler implantation will be calculated using the accelerometer data from the drive impact tube. This velocity must allow sufficient penetration of the surface for a stable coring process, but at the same time cause minimal damage to the comet mantle. The anchoring will be aided by using a series of inverted cones which increase in size starting from the penetrator tip (See Figure 12.1). These cones will also have sharp tabs placed on them to help resist any de-anchoring forces.

I - 63

TETHER

SLIP CONNECTION

INNER
THRUSTERS

OUTER
THRUSTERS

ANCHORING
CONES

1.25 m
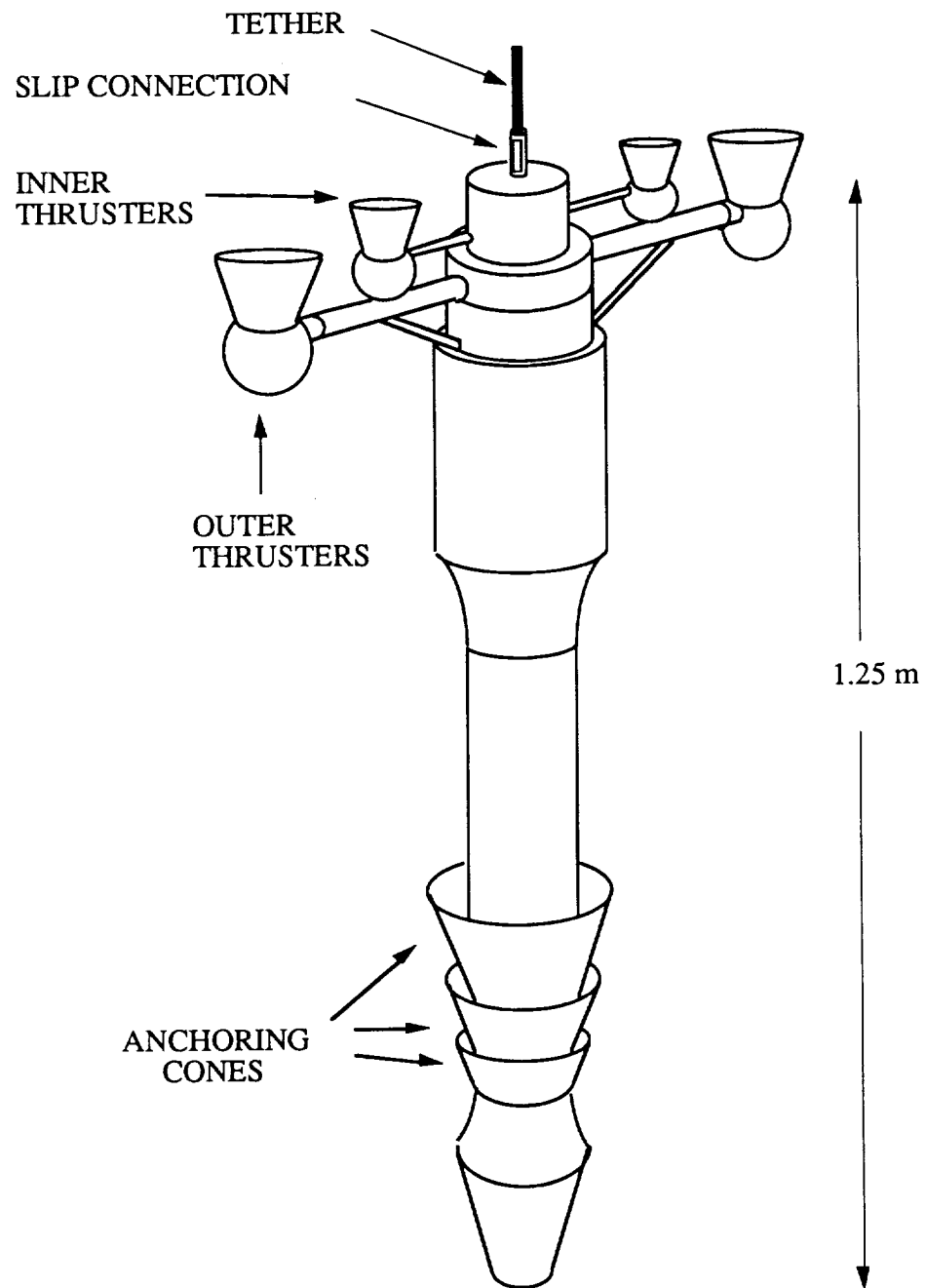
Figure 12.1: Sampler Penetrator

In the event that the sampler is not properly secured, the upper cones, the ones away from where the coring will take place, can be heated causing the ice around them to melt and refreeze to help in anchoring the penetrator. However, the heating would damage and alter the sample, so this would be done only if all else fails.

12.2.3 Drilling

The sampler consists of two parts, an outer coring unit and an inner unit which will contain the sample. The coring unit will have a Beryllium stem and a Tribocor bit [34], while the penetrator will be constructed from a composite material, such as, boron/epoxy or graphite/epoxy. These materials were chosen because of their strength and thermal conductivity.

Once the penetrator has been secured in the surface, the coring process will then begin. The outer rocket thrusters will rotate downward so when they are fired they produce both a rotational and downward force for the coring process. The inner storage unit of the sampler consists of two one-meter sections, one housed inside the other. As the coring progresses deeper, the inner section will telescope out of the larger section, and they will lock together when its maximum length has been reached. This will allow for a two meter long sample to be taken, and it will minimize the pre-launch volume of the penetrator. Once the coring has been finished, the entire inner storage unit of the sampler will be rotated using the inner set of thrusters. This motion is purely rotational and will drive a set of shutter segments to cut off the end of the sample and seal it.

12.2.4 Thermal Disturbance

The primary objective of this mission is to return a comet sample to Earth in as pristine a state as possible to maximize the scientific value of the sample. Initially, it appeared as if the thermal disturbance to the sample was going to be a major concern. However, R.J. Amudsen and B.C. Clark [34], found that the thermal damage caused by the

coring process would be minimal. The temperature of the central portion of the sample never rose more than 1 or 2 degrees above the initial temperature, while the temperature at the edge of the sample only increased 6 degrees. Only a portion of the sample in contact with the coring bit would experience extreme heating and vaporization, but this would be a small fraction of the total sample.

12.3   Conclusions and Recommendations

A remote operation was chosen over a lander for several reasons. First, an attempted landing on a highly irregular cometary surface could damage delicate spacecraft appendages such as solar arrays, antennae, scientific instrumentation, etc. Another potential problem of landing would be the thermal drain on the spacecraft due to the contact with the low temperature cometary surface. Equipment requiring temperatures above that of the surface for operation would need extra insulation and/or would have to be heated. A remote sampler will also lower the propellant mass needed because it eliminates the landing and departing processes.

Although the tether meets the requirements of this mission, it is probably stronger and more massive than needed. It has these excessive characteristics because it was originally constructed to tow an object nearly 50 times more massive at 200 times the distance. Future considerations should examine the possibility of removing one or more of the layers to further decrease the mass and volume of the tether.

Liquid propellant was chosen for the sampler thrusters because of its throttling capability. Using liquid propellant thrusters will require a greater mass due to the need for fuel lines, pumps, etc., but they are necessary to insure that the sampler is not over-accelerated prior to impact. Also, hypergolic properties of monomethylhydrazine will provide high reliability.

Using a cost estimation model, the cost of the penetrator was determined to be 146.0 million dollars [30].

13.0 Sample Storage

13.1 Requirements

The principle objective of this mission is to return to earth a comet sample in a form which is as close to its original state as possible. The most important physical parameter in accomplishing this objective is maintaining its temperature. According to John Wood of the ESA/NASA Science Definition Team this would be best accomplished if the sample could be stored at a temperature less than 130 K [35]. For this reason, the temperature of the sample during extraction, storage, and transport to the terrestrial laboratory are some of the most critical parameters for the success of the mission. Other primary considerations in returning a representative sample are contamination and the preservation of the samples density. These constraints have also heavily influenced the designs of the storage subsystem for this mission.

13.2 Storage in Spacecraft Bus

Precautions taken during the extraction phase of the mission will allow the sample to be returned to the spacecraft bus with a temperature rise of approximately 3 K for the internal portion of the sample and 10 K for the external portion. There the specimen will be hermetically sealed to prevent contamination. It will be stored in multi-layered insulation and strategically placed in the shadow of the solar arrays. With the sample stored inside the craft, a system is needed to remove the heat generated by the other on-board systems. A combination of the multi-layer insulation, heat pipes and a thermally-buffering mass have been chosen for this purpose. The thermally-buffering mass will be minimized through the use of the phase-change material, cis-2-Butene. It was chosen due to its high latent heat of fusion and safety concerns with respect to flammability and toxicity as compared in Table 13.1 [36].

Table 13.1: Phase Change Compounds (Clark, B.C., Amundsen, R.J. and Blanchard, D.P., *Sampling the Cometary Nucleus*, Martin Marietta Denver Aerospace and NASA Johnson Space Center, 1988.)

Compound	M.P. (K)	Hf (J/g)	r (g/cc)	Vapor Pres (psi @ RT)	Flammable	Toxicity
Propene	88	71.4	0.5	154	High	Low
1-Pentene	107.0	82.9	0.6	10.7	High	Low
Isopentane	113.3	71.3	0.6	11.6	High	Med
cis-2-pentene	121.8	101.5	0.7	8.2	High	Low
trans-2-Pentene	133.0	119.2	0.6	11.0	High	Low
cis-2-Butene	134.3	135.1	0.6	20.0	Med	Low
n-Pentane	143.5	116.7	0.6	8.3	Med	Med
1-Heptene	153.5	128.9	0.7	0.9	Expl	Med
1,3-Butadiene	164.3	147.0	0.6	22.0	High	Low

13.3   Storage During Earth Parking Orbit

To eliminate direct reentry, the craft will be placed in a parking orbit and recovered by the Space Shuttle. This increases the costs, but avoids the most thermally difficult phase of the mission during which aerobraking would cause a large heat spike. This heat would need to be dissipated through a series of thermal breaks in the structure. A phase-change buffer outer jacket employing ventable H_2O would be effective as its specific heat and latent heats of fusion and vaporization are extremely high. This layer would buffer the environment experienced by the canister shell to approximately 100° C [36]. Even more difficult than this, however, is minimizing the heat that would occur once in orbit because radiative cooling becomes much more difficult as a result of the infrared albedo of the Earth and its atmosphere. These problems would also cause a dramatic increase in mass and power needs and are therefore the reasons that the parking orbit and recovery by the Shuttle was chosen.

The availability of the Space Shuttle influenced the decision to store the sample inside the craft for added protection. This in turn led to the methods discussed in the previous section. An alternative to direct Shuttle recovery could have been storing the sample at the

Space Station Freedom until the Shuttle was available, but this method was rejected due to the even greater uncertainty of the Space Station's availability.

13.4   Density Preservation

Thermal constraints were not the only problems that needed to be addressed with respect to packaging and storage methods. Another is the possibility that the cometary material may have a very low density. Preservation of this density may prove scientifically valuable since it would allow for the study of the fabric structure. Conversely, many scientists would argue that a greater mass would be more valuable and that the sample should be compressed allowing more mass to be returned. This debate also had to be considered when deciding on the method of reentry since direct reentry would not allow for the volume to be preserved. If direct reentry had been chosen, it would have been more advantageous to compact the sample mechanically, so that the procedure would take place under controlled conditions allowing for easier analysis of the specimen on Earth.

13.5   Contamination

In addition, the selection of all the materials coming in direct contact with the sample must be carefully evaluated such that any contamination of the sample will be able to be recognized and analyzed. This is the reasoning for hermetically sealing the sample before storing it aboard the spacecraft bus. These considerations are of even greater importance when guarding against contamination of the Earth's environment.

13.6   Conclusions and Recommendations

These storage methods are first employed before extraction of the sample by cooling the drill bit through radiative means. Composites are then used to both dissipate the heat and insulate the sample from heat during extraction. Once hermetically sealed, the sample is strategically placed in the spacecraft bus so that it will remain in the shadow of the solar

array. Multi-layer insulation, heat pipes, and a thermally-buffering mass will combine to protect the sample from heat produced by other on-board systems. These systems along with the extra protection from the bus structure will allow a larger window for recovery by the Shuttle. This recovery procedure will also preserve the density of the sample as desired. While the requirements for storage have been satisfied through passive means, it should be realized that failure of this subsystem will compromise the main objective of the mission.

14.0   Penetrator Monitoring Unit

14.1   Requirements

The mission objectives call for complete characterization of the comet. To satisfy this requirement, a penetrator monitoring unit is proposed. Upon designation of the landing site, a rocket-propelled penetrator will be launched toward the comet to monitor its activity and analyze its properties via an array of instruments. Observation through one complete orbit is desired, but would be too costly to achieve, given the harsh environment and technological limits. Present designs do, however, include a unit that will ideally operate through perihelion. The basic concept for this penetrating unit originated from the recently cancelled CRAF mission. The choice to use both a sampling lander and a long-lived penetrator was made to reduce the risk of a failure in one lander/sampler unit, despite the associated mass and propellant penalties, and the increased cost. The penetrator must be durable enough to withstand impact with Wild 2, and it must be self-sufficient with its own power supply, data acquisition and handling system, and communications.

14.2   Deployment

The penetrator will be launched roughly 0.5 km above the comet's surface. To prevent damage to the spacecraft from the rocket's exhaust, a spring mechanism will be used to eject the penetrator to a suitable distance, at which point the rocket will be ignited. A crucial factor in the success of the penetrator will be its ability to hit the planned landing site. Should it hit an area that is not relatively flat, it may not impact properly to carry out the intended observations. To further ensure an acceptable impact angle (less than $30°$ from the normal), the unit may require spin-stabilization. Dr. William Boynton of the University of Arizona, who headed the project to build the penetrator/lander for the CRAF mission, had managed to successfully test a full-size, five-foot long prototype prior to the mission's

C-2

cancellation [37]. At 40 m/s, the model firmly lodged itself into solid ice at various impact angles.

The surface hardness of Wild 2, however, is not precisely known. This uncertainty presents a problem in predetermining the impact speed of the penetrator. Wild 2's surface may resemble anything from lightly packed dirty snow to solid ice laden with rocks. If a penetrator similar to Boynton's is planned to impact fluffy snow at 40 m/s, it may bury itself too deep to transmit data. The surface hardness will have to be estimated prior to the penetrator's launch using data obtained from the drive impact tube, and the unit's speed adjusted accordingly. Consequently, a rocket motor using a solid propellant will be unsuitable. A liquid propellant system, with the added pumps, will be more massive but because of its throttling capability will allow for the required thrust adjustment. One candidate is the Marquardt R-1E, a 110 N hypergolic thruster developed as the Space Shuttle's attitude control/orbit adjust thruster [33]. The R-1E has a dry mass of 3.7 kg, an exit diameter of 15.2 cm, and a length of 28 cm. It uses monomethylhydrazine as fuel and nitrogen tetroxide as an oxidizer to provide a specific impulse of 280 s. Protective casings will provide protection from any possible damage to the RTG and optical communication unit during the penetrator's thruster operation.

14.3   Instrumentation

The penetrator will ideally bury a group of instruments that will monitor and analyze the comet's interior, while several instruments at the rear of the unit will analyze the comet's atmosphere. A preliminary penetrator design can be seen in Figure 14.1. Table 14.1 shows the components and instrumentation included on the penetrator, their masses, and power requirements.
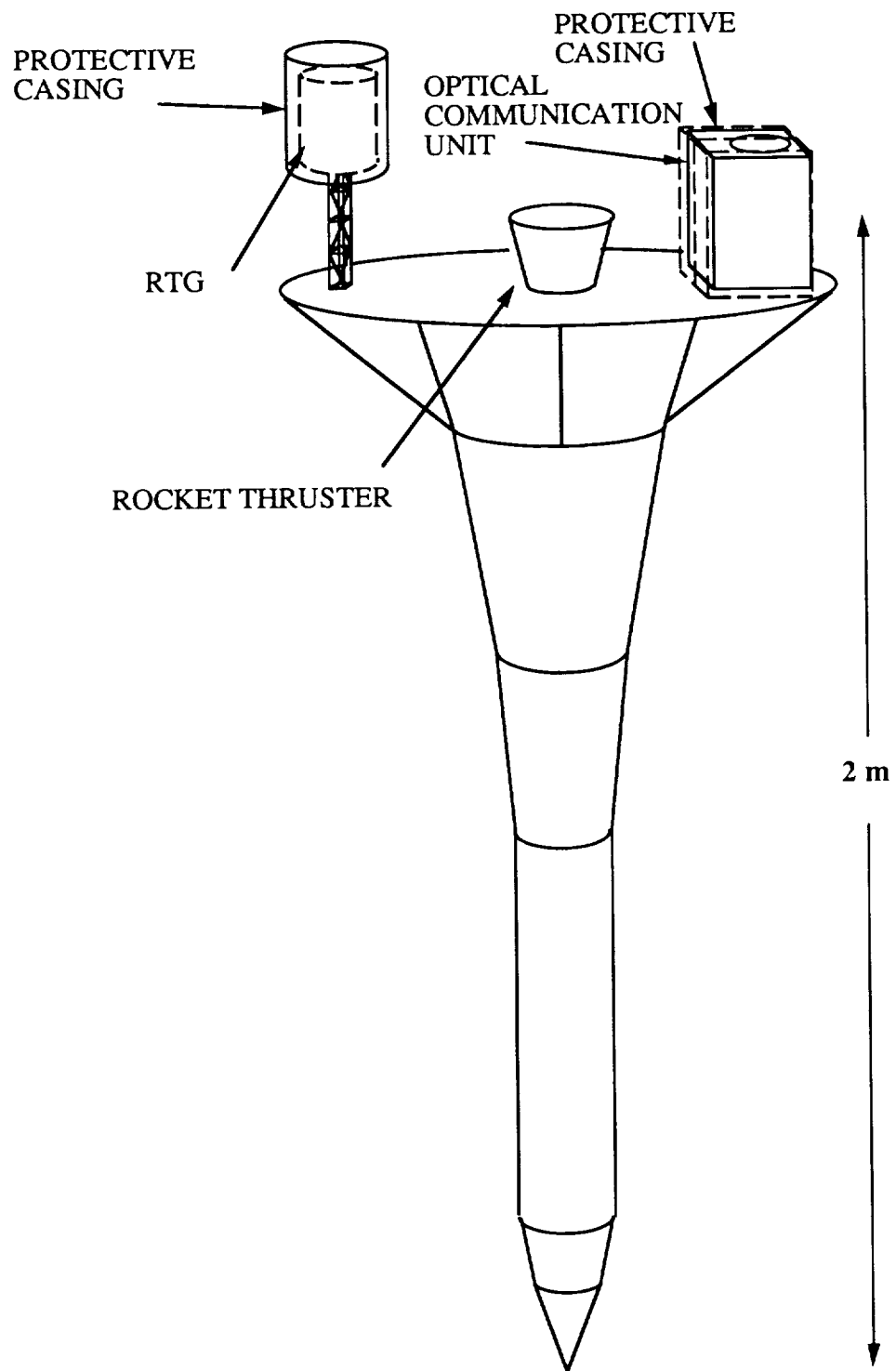
Figure 14.1: Preliminary Penetrator Monitoring Unit Configuration

Table 14.1: Penetrator Monitoring Unit Scientific Instrumentation

Instrument	Mass (kg)	Power Requirement (W)
Gamma-ray Spectrometer	14	4
Neutral Gas and Ion Mass Spectrometer (NGIMS)	9	15
Seismometer	2	3
Temperature Transducer	<0.1	1
Pressure Transducer	<0.1	1
Temperature Probe (3 will be required)	<1.5	3
Calorimeter with gas Chromatograph	3	15
Cometary Dust Environment Monitor (CODEM)	4.2	8
RTG	27	---
Rocket Motor (dry)	~4	---
OPTRANSPAC	52	57
Propellant	60	---
Computer	10	30
Structure	75	---
Totals	262	137

Below the surface, five accelerometers located at various positions along its two meter length will be used to determine the penetrability index (a measure of the surface hardness) of the outer layers, as well as the penetration depth, by measuring deceleration as a function of time. Temperature probes will measure the thermal diffusivity of the nucleus material, and a gamma-ray spectrometer will allow the comet's elements to be identified for comparison with known meteorite types. A seismometer will measure the activity of Wild 2's interior. The CRAF plans included a calorimeter equipped with pressure and temperature transducers and a gas chromatograph. Using this device, analysis of a sample would reveal its molecular composition and allow the formation temperature to be estimated [18]. This device will only be used once and is not required to be used while other instruments are operating. It will, therefore, not tax the power supply.

Above the surface, instruments will monitor atmospheric features. A cometary dust environment monitor (CODEM) will act as a dust counter and measure the gas production rate. Data from the CODEM will provide an understanding of the physical and dynamic properties of small dust particles at the comet's surface [25]. The composition of the dust will be analyzed using a neutral gas and ion mass spectrometer (NGIMS) [18].

14.4 Communications

The feasibility of a station-keeping craft was investigated. Its purpose would be to relay data from the penetrator monitoring unit to Earth, while a separate return unit would deliver the core sample back to Earth. This plan would make the task of designing (and manufacturing) the penetrator somewhat less crucial but would greatly complicate the overall mission. The risk of malfunction that may result in a partitioned craft was deemed unacceptable.

In the present design, the penetrator will transmit directly to Earth. At a maximum operating distance of 4 AU, the minimum parabolic antenna diameter will be 2 m, which is rather large relative to the size of the penetrator. The high-gain antenna at this distance would use 130 W. To reduce the antenna size, it may be possible to store the data and transmit it when the comet is sufficiently close to Earth. A foldable, deployable antenna might reduce the risk of damage from dust particles during the penetrator's deployment and not interfere with experiments above the comet surface, but the question of it surviving the impact still remains. Interference from Wild 2's outgassing and dust production will cause communication problems, especially near perihelion, where its gas production rate is 4×10^{28} s^{-1} [18]. (Wild 2's dust production is unknown, but is believed to be on the order of magnitude of 10^5 g/s, comparable to that of Tempel 2 and Kopff [18].)

Alternatively, an optical communications system could reduce the power required for data transmission. An optical transceiver package (OPTRANSPAC) using a telescope to downlink, with a maximum range of 10 AU and capable of 100 kbs, is 52 kg but requires

only 57 W, as opposed 120 W required by the antenna. Another advantage of this device is that it is much more compact than the antenna and will not be damaged by the rocket exhaust during deployment and have a better chance of surviving impact. Outgassing and dust accumulation may, however, have an effect on the package's performance.

14.5 Power

The choice of the penetrator power supply is a key consideration in fulfilling the mission requirement of comet characterization. Much valuable information can be attained during the perihelion phase, and to achieve this, a long-duration power supply such as an RTG will be required. A 27 kg RTG will supply the estimated 137 W. The RTG will be placed sufficiently far away from the instrumentation to diminish any effects of radiation the unit may cause, and will have a protective casing to avoid possible damage from the rocket's exhaust plume.

14.6 Structure

As seen from Figure 14.1, the penetrator will be cone-shaped, 1.5 to 2 meters of it intended to be below the comet surface. Above the surface will be several instruments, the power supply, and the communications package. The cone will house the aforementioned sub-surface instrumentation, as well as the computer which will oversee its operation and store the data for transmission. Rigidity of the penetrator and its components will be of the utmost importance, since they must accommodate the stresses associated with an impact anywhere from 3 to 40 m/s. Composite materials such as graphite/epoxy, boron/epoxy, or Kevlar-49/epoxy would provide the required rigidity and strength, at minimum mass, for the casing and infrastructure. In addition, composites can be designed to have low thermal conductivities, low (even negative) coefficients of thermal expansion, and high damage and impact resistances. They can be tailored due to their controlled anisotropy, i.e., the ratio of property values in different directions can be easily varied [38]. Approximating the

penetrator body and internal structure as a hollow graphite/epoxy (ρ = 1540 kg/m^3) cone with a height of 2m, a base radius of 0.33m, and thickness of 0.03m, and allowing for a 10% contingency, the penetrator's structural mass is 75 kg.

14.7 Conclusions and Recommendations

Obviously, much more research is needed for the design of a penetrator such as the one proposed here. The unit's long operational life and autonomy dictate that it be fairly massive and require relatively large amounts of power. Moreover, its housing and components must be designed with only mere milliseconds of its life in mind - the time of impact with the comet. A cost estimate was obtained using the 'Cost Estimation of Advanced Space Systems' model developed by Kelley Cyr at NASA's Johnson Space Center. Modelling the penetrator as a combination of first and third generation, planetary components, its cost will be $263 million, in 1992 dollars. The cost of a shorter-lived penetrator was investigated. A battery would replace the RTG, a low-gain antenna would transmit back to a station-keeping craft, and a smaller computer would be used. In this case, the cost was found to be $215 million. It may therefore be more desirable to limit the scope of the penetrator monitoring unit such that its success will be more easily achieved.

15.0   Cost Analysis

A preliminary cost estimate was performed for the Snowball mission using an advanced spacecraft system cost model. Five parameters — mass, launch date, culture, generation, and number of units — were input into the model for each subsystem. Table 15.1 lists the costs of each spacecraft component. The propellant cost was estimated using a computer program which may be found in Appendix D.

Table 15.1:   Mission Cost Analysis [30]

Mission Component	Cost (FY92$M)
Computer	47.97
Communications	17.83
Power	135.31
Sampler	240.13
Penetrator	368.00
Thermal	123.04
Propulsion	0.51
GN&C	129.33
Scientific Instruments	209.26
Structure	524.38
Launch System	85.00
TOTAL	**1880.76**

Up to this point the mission requirements have not dictated strict budget constraints. Thus, this raw analysis is a first iteration of the estimated cost. This is certainly an area that needs much consideration especially if this mission is to ever fly.

16.0   Conclusions and Recommendations

A mission to the comet Wild 2 has been described. The Snowball spacecraft was designed to produce maximum value from a limited amount of resources (specifically mass). The total mass of the spacecraft is approximately 5150 kg and will require 528 W of power distributed throughout various phases of the mission. A final cost estimate of $1880M (FY92) was completed using an advance space systems model.

Before the Snowball mission can be considered anything more than a detailed conceptual design, certain aspects of the mission need to be enhanced or resolved. First, the trajectory design can be better defined through the use of a commercial package such as MIDAS or QUICKTOP. These programs work best with low-thrust scenarios (electric portion of hybrid propulsion system) and give trajectory results for given launch dates and propulsive performance. Also, the scientific instruments require proper placement on the high and low precision scan platforms. This placement must allow for individual instrument field of view requirements and thermal profiles. A power timeline for the entire mission would allow an investigation into peak usage and the interval between peaks. This information could be useful in determining if the current power subsystem is adequate to suit the requirements of the spacecraft. Furthermore, a redesign of the power system may be required if a large surplus is discovered. While the cost model used in the mission analysis gives an excellent approximation to component relative costs, it is not accurate when determining absolute costs. A more detailed cost model could be applied to refine the cost of each spacecraft component.

17.0 References

[1] Carusi, A. and Valsecchi, G., "*Dynamics of Comets -Their Origin and Evolution,*" D. Reidel Publishing Company, Boston, MA, 1985.

[2] Feingold, H., Hoffman, S.J., and Soldner, J.K., "A Comet Nucleus Sample Return Mission," AIAA Paper No. 84-2016, AIAA/AAS Astrodynamics Conference, Seattle, WA, August 1984.

[3] Myers, M., "Trajectory Design For The Comet Rendezvous Asteroid Flyby 1995-1996 Opportunities," Jet Propulsion Laboratory, Pasadena, CA, AIAA, 1988.

[4] Swenson, B.L., Squyres, S.W., and Knought, T.C.D., "Proposed Comet Nucleus Penetrator for the Comet Rendezvous Asteroid Flyby Mission," *Acta Astronautica,* v15 n6-7 1987, pp.471-479.

[5] Schwehm, G.H. and Langevin, Y., "Rosetta/Comet Nucleus Sample Return Mission," ESA Publications Divisions, Netherlands 1991.

[6] Stetson, D.S., Lundy, S.A., and Yen, C.L., "The Mariner Mark II Comet Rendezvous/Asteroid Flyby Mission," AIAA/AAS Astrodynamics Conference. Seattle, WA, August 20-22, 1984.

[7] Bate, R.R., Mueller, D.D., and White, J.E., *Fundamentals of Astrodynamics,* Dover Publications, Inc., New York, 1971, pp. 176,225.

[8] Battin, R.H., *An Introduction to the Mathematics and Methods of Astrodynamics,* AIAA, Inc., New York, 1987.

[9] Wertz, J.R.,and Larson, W.J., *Space Mission Analysis and Design,* Kluwer Academic Publishers, Boston, MA, 1991.

[10] Isakowitz, S.J., *International Reference Guide to Space Launch Systems,* American Institute of Aeronautics and Astronautics, Washington, DC, 1991.

[11] Draper, R.F., "The Mariner Mark II Program," AIAA Paper No. 84-0214, AIAA 22nd Aerospace Sciences Meeting, Reno, NV, January 9-12, 1984.

[12] Rennie, J., "Spacecraft on a String", *Scientific American,* October 1989.

[13] Massie, L.D. "Space Power Systems Requirements and Issues: The Next Decade," *IEEE Aerospace and Electronic Systems Magazines,* December, 1990.

[14] Krassner, G. and Michaels, J. *Introduction to Space Communication Systems,* McGraw Hill Book Company, New York, 1964.

[15] Loeb, J.W., "Ion Propulsion Systems," NASA Technical Report, 1987, pp. 75-92.

[16] Bennett, G.L., "Safety Status of Space Radioisotope and Reactor Power Sources," 25th Intersociety Energy Conversion Engineering Conference, Vol. 1, 1990.

[17] El-Genk, M.S. and Hoover, M.D. "A Summary Overview of Recent Advances in Space Nuclear Power Systems Technology," 25th Intersociety Energy Conversion Engineering Conference, Vol. 1, 1990.

[18] Rolfe, D.J. and Battrick, B. (editors), Symposium on the Diversity and Similarity of Comets, European Space Agency, Paris, 1987, pp. 517-546.

[19] Mastel, E.S., *Radioisotope Power Systems for the Common Lunar Lander Program*, NASA Technical Presentation, Johnson Space Center, July 1991.

[20] Loeb, H.W., "Review: 'Ion Propulsion Systems," Paper 87-25119, 1987, pp. 75-92.

[21] Aldrich Chemical Co., Inc 1990-91 Handbook, Milwaukee, Wisconsin, 1990.

[22] Wertz, J.R., *Spacecraft Attitude Determination and Control*, Dordrecht, Holland: D. Reidel Publishing Company, 1978.

[23] Spacecraft Star Trackers, NASA SP-8026, July 1970.

[24] Draper, R.F., Comet Rendezvous Asteroid Flyby, Mariner Mark II, Technical Definition and Class "A" Cost Review, JPL D-3384, Volume 1, June 9, 1987.

[25] *Galileo: Exploration of Jupiter's System*, NASA, 1985.

[26] Atkinson, D., James, M., and Martin, R., "SHARP", *The International Society for Optical Engineering*, Vol. 1293-pt 2, 1990, pp. 859-869.

[27] Tomayko, J.E., "Lessons Learned in Creating Spacecraft Computer Systems: Implications for using Ada for the Space Station," *Applications for the NASA Space Station*, University of Houston, June 5-6, 1986.

[28] Yuen, J.H. (editor), *Deep Space Telecommunications Systems Engineering*, Jet Propulsion Laboratory and California Institute of Technology, July 1982.

[29] Standing, A.F., *Measurement Techniques for In-Orbit Testing of Satellites*, W. H. Freeman and Company, 1990

[30] Cyr, K., *Cost Estimation of Advanced Space Systems*, NASA Johnson Space Center, 1988.

[31] S. G. Lambert, et al (McDonnell-Douglas Astronautics Co.), *Design and Analysis Study of a Spacecraft Optical Transceiver Package*, NASA Document NAS 1.26:179958, Final Report, 19 August, 1985

[32] *The Deep Space Network*, Jet Propulsion Laboratory, NASA Document NAS 1.12/7:400-333, January 1988

[33] Wilson, A. (editor), *Interavia Space Directory 1989-90*, Geneva, Switzerland, 1989.

[34] Amundsen, R.J. and Clark, B.C., *Study of Sampling Systems for Comets and Mars*, Martin Marietta Denver Aerospace, April, 1987.

[35]   Science Applications, Inc., *Comet Nucleus Sample Return Mission*, NASA Technical Report; NASW-3622, May-August, 1983

[36]   Clark, B.C., Amundsen, R.J., and Blanchard, D.P., *Sampling the Cometary Nucleus*, Martin Marietta Denver Aerospace and Johnson Space Center, 1988.

[37]   Cole, S., "To Spear a Comet", *Air and Space*, August/September, 1990.

[38]   Agarual, B.D. and Broutman, L.J., *Analysis and Performance of Fiber Composites*, Wiley and Sons, New York, pp.12-13.

Appendix A

Model Simplifications:

Earth Orbit is circular about the Sun

Parking Orbit is circular about the Earth

Comet Orbit inclination to the ecliptic is small, therefore inclination change is neglected
transfer is made to comet's apogee from a 200 km parking orbit
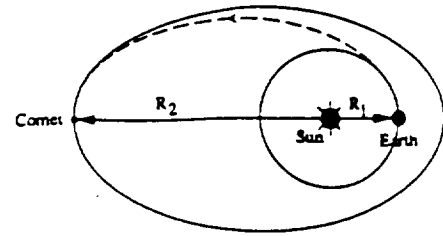
$$\mu_\oplus = 3.9486e5 \frac{km^3}{s^2} \qquad\qquad R1 = 1AU \qquad\qquad Rcirc = 6578km$$

$$v\oplus = 29.79 \frac{km}{s} \qquad\qquad 1AU = 149.6e6km \qquad Vcirc = \sqrt{\frac{\mu\oplus}{Rcirc}} = 7.784 \frac{km}{s}$$

$$\mu sun = 1.327 \frac{km^3}{s^2}$$

Wild 2 Transfer

$$R2 = 5.31AU \qquad\qquad a_t = \frac{R1 + R2}{2} = 3.155AU$$

$$e_2 = .54$$

$$V+ = \sqrt{\mu sun \left(\frac{2}{R1} - \frac{1}{a_t} \right)} = 38.64 \frac{km}{s}$$

$$V_\infty^+ = v^+ - v\oplus = 8.85 \frac{km}{s}$$

injection velocity

$$Vo = \sqrt{V_\infty^{+2} + \frac{2\mu\oplus}{Rcirc}}$$

$$\Delta V1 = Vo - Vcirc = 6.34 \frac{km}{s}$$

$$e_t = 1 - \frac{R1}{a_t} = .683$$

$$Vt2 = \sqrt{\frac{\mu sun(1 - e_t)}{R2}} = 7.277 \frac{km}{s}$$

at comet orbit

$$Vt2 = \sqrt{\frac{\mu sun(1 - e_2)}{R2}} = 8.77 \frac{km}{s}$$

$$\Delta V2 = 1.493 \frac{km}{s}$$

$$\Delta Vtot = 7.83 \frac{km}{s}$$

Kopff Transfer

$$R2 = 5.35AU \qquad\qquad a_t = 3.175AU$$

$$e_2 = .54$$

$$V_\infty^+ = 10.64 \frac{km}{s}$$

$$\Delta V1 = 7.526 \frac{km}{s}$$

$$Vt2 = 7.227 \frac{km}{s}$$

$$\Delta V2 = 1.503 \frac{km}{s}$$

$$\Delta Vtot = 9.029 \frac{km}{s}$$

Appendix B

```
c=================================================================
c Aerospace 401b - Spacecraft Design
c Program to determine the positions of earth and wild 2 for
c specified start date and simulation period
c by Bob Grogan
c=================================================================
      dimension erie(0:500),erip(0:500),whrz(0:500)
      dimension wrie(0:500),wrip(0:500),whrx(0:500),whry(0:500)
      dimension ehrx(0:500),ehry(0:500)
      integer  idiot,noyr,step,m,d,yr
      double precision mu,delta,
     $pi,erie,erip,wrie,wrip,whrx,whry,whrz

c open output file
      open (unit=99, file='earth')
c Month, day, and year for start of simulation
      m   = 3
      d   = 20
      yr  = 2003
c number of years for simulation
      noyr= 6
c step size - entered in days
      step= 30
c initialize input variables
      mu      = 1.327d11
      delta   = .000001d0
      idiot   = 30000

      call earth (m,d,yr,noyr,step,mu,delta,idiot,erie,erip)
      do 7 iii=0,12*noyr
 44   format (2(f6.3,2x),i4)
        ehrx(iii)=cos(102.4*3.1415926/180.)*erie(iii)
     $   -sin(102.4*3.1415926/180.)*erip(iii)
        ehry(iii)=sin(102.4*3.1415926/180.)*erie(iii)
     $   +cos(102.4*3.1415926/180.)*erip(iii)
        write(99,44) ehrx(iii),ehry(iii),iii
 7    continue

      call wild (m,d,yr,noyr,step,mu,delta,idiot,wrie,wrip,
     $whrx,whry,whrz)
      do 8 jjj=0,12*noyr
        write (99,66) wrie(jjj), wrip(jjj),
     $whrx(jjj), whry(jjj) ,whrz(jjj) ,jjj
 8    continue
 66   format (5(f6.3,2x),i4)
      end
c=================================================================
c subroutine earth finds coordinates for earth orbit using
c orbital elements based on epoch 1969 June 28.0
      subroutine earth (m,d,yr,noyr,step,mu,delta,idiot,rie,rip)
      dimension rie(0:500),rip(0:500)
      integer  idiot,t,noyr,step,m,d,yr,tref,interval
      double precision a,eccen,Eo,mu,tau,delta,E,
     $pi,mo,do,yro,to,eepoch,f,r,rie,rip
```

I-84

```
c set orbital elements
      a       = 1.4959956d8
      eccen   = .0167d0
      pi = 3.14159265359d0
      mo = 6.
      do =28.
      yro = 0.
      tref = 1969
      Eepoch = 3.030345d0

c find time of epoch and time of periapsis passage (tau)
      to = 2620800.*mo+86400.*do+31449600.*yro
      tau = to -(eepoch-eccen*dsin(eepoch))/dsqrt(mu/a**3.)

c call subroutine to find coordinates based on orbital elements
      call pfocal(m,d,yr,tref,step,noyr,tau,a,mu,eccen,
     $delta,idiot,rie,rip)
      do 6 ii=0,12*noyr
          rie(ii)=rie(ii)/a
          rip(ii)=rip(ii)/a
 6        continue
      return
      end
c==================================================================
c subroutine finds coordinates for wild 2 using orbital elements
c based on ephermis 2000 and corresponding to perihelion on 9/26/2003
      subroutine wild (m,d,yr,noyr,step,mu,delta,idiot,rie,rip,
     $hrx,hry,hrz)
      dimension rie(0:500),rip(0:500),hrx(0:500),hry(0:500),hrz(0:500)
      integer  idiot,t,noyr,step,m,d,yr,tref,interval
      double precision a,eccen,Eo,mu,tau,delta,E,
     $pi,mo,do,yro,to,eepoch,f,r,rie,rip,thing
     $,R11,R12,R21,r22,r31,r32,hrx,hry,hrz,node,aofp,inc
c set orbital elements
      pi = 3.14159265359d0
      node = 136.139*pi/180.
      aofp = 41.754*pi/180.
      inc = 3.24*pi/180.
      a       = 3.45*1.4959956d8
      thing = 1.4959956d8
      eccen   = .53874d0
      mo = 9.
      do =26.
      yro = 2003.
      tref = 0
      Eepoch = 0d0

c find time of periapsis passage
      to = 2620800.*mo+86400.*do+31449600.*yro
      tau =    to -(eepoch-eccen*dsin(eepoch))/dsqrt(mu/a**3.)

      call pfocal(m,d,yr,tref,step,noyr,tau,a,mu,eccen,
     $delta,idiot,rie,rip)
      do 6 ii=0,12*noyr
          rie(ii)=rie(ii)/thing
          rip(ii)=rip(ii)/thing
 6        continue
```

```fortran
c transform from perifocal to heliocentric coordinate system
      r11 = dcos(node)*dcos(aofp)-dsin(node)*dsin(aofp)*dcos(inc)
      r12 = -dcos(node)*dsin(aofp)-dsin(node)*dcos(aofp)*dcos(inc)
      r21 = dsin(node)*dcos(aofp)+dcos(node)*dsin(aofp)*dcos(inc)
      r22 = -dsin(node)*dsin(aofp)+dcos(node)*dcos(aofp)*dcos(inc)
      r31 = dsin(aofp)*dsin(inc)
      r32 = dcos(aofp)*dsin(inc)
      do 22 jj=0,12*noyr
      hrx(jj)=r11*rie(jj)+r12*rip(jj)
      hry(jj)=r21*rie(jj)+r22*rip(jj)
      hrz(jj)=r31*rie(jj)+r32*rip(jj)
 22   continue
      return
      end
c=================================================================
c subroutine finds perifocal coordinates for given time interval
      subroutine pfocal(m,d,yr,tref,step,noyr,tau,a,mu,eccen,
     $delta,idiot,rie,rip)
      dimension rie(0:500),rip(0:500)
      integer  idiot,t,noyr,step,m,d,yr,tref,interval
      double precision a,eccen,Eo,mu,tau,delta,E,
     $pi,f,r,rie,rip,x,y,ff

      t = 2620800*(m      )+86400*(d    )+31449600*(yr-tref)
      interval = step*86400

      do 5 i=t,t+noyr*31449600,interval
c         initial guess for eccentric anomaly
      Eo=(i-tau)/dsqrt((a**3.)/mu)
      call kepler (a,eccen,Eo,mu,i,tau,delta,idiot,E)
c         true anomaly
      ff=2.*datan(dsqrt((1.+eccen)/(1.-eccen))*dtan(e/2.))
      x=dcos(ff)
      y=dsin(ff)
      f=datan2(y,x)+3.1415926
c         radius magnitude
      r=a*(1.-eccen**2.)/(1.+eccen*dcos(f))
c         components of radius vector
      rie((i-t)/86400/step)=r*dcos(f)
      rip((i-t)/86400/step)=r*dsin(f)
 5    continue

      return
      end
c=================================================================
c subroutine to determine the eccentric anomaly using
c the newton-raphson method to solve kepler's equation
      subroutine kepler (a,eccen,Eo,mu,i,tau,delta,idiot,E)
      integer  idiot,i
      double precision a,eccen,Eo,mu,tau,delta,E,thing,f,fprime

      do 777 j=1,idiot

      f = (i-tau)*dsqrt(mu/a**3.) - Eo + eccen*dsin(Eo)
      fprime = -1 + eccen*dcos(Eo)
      E = Eo - f/fprime

c check for convergence
```

```fortran
      thing = abs( (E-Eo)/E)
      if (thing.le.delta) then
c     write (99,*) '# of iterations - newton-raphson',j
      return
      endif

      Eo = E

777   continue

c prints a warning if solution does not converge for
c given number of iterations
      write (99,*) 'newton-raphson DID NOT CONVERGE'

      return
      end
c==================================================================
```

Appendix C

```
c Aerospace 401b
c Snowball Comet Mission
c Program to calculate the necessary velocities
c for direct elliptical transfer to Wild 2
c by Bob Grogan and
c    Chris Stoll
        double precision mu,pi,delt,a,b,x,y,r1,vc,deltaf,vw2,r2,c,s
        double precision alpha,beta,p,f,g,gt,v1x,v1y,v1,delv1,v2x
        double precision v2y,delv2,totv
        open (unit=99, file='earth')
        open (unit=98, file='what')
      mu=1.327e11
       pi=3.1415926
       delt=9.72628e7
      write (98,*) '   totv','   delv1','   delv2'
       do 666 i=1,10
          read(99,*) a,b

        x=a*1.496e8
        y=b*1.496e8
       r1=sqrt(x**2+y**2)
        vc=sqrt(mu/r1)
      deltaf=pi-asin(y/r1)
        vw2=8.789
         r2=7.9287e8
        c=dsqrt(r1**2+r2**2-2*r1*r2*dcos(deltaf))
         s=.5*(r1+r2+c)
      call fixedp (mu,s,c,delt,a,alpha,beta)

       p=4*a*(s-r1)*(s-r2)*(dsin((alpha-beta)/2))**2/c**2
      F=1-r2*(1-dcos(deltaf))/p
       G=r2*r1*dsin(deltaf)/dsqrt(mu*p)
       Gt=1-r1*(1-dcos(deltaf))/p
       v1x=(r2-F*x)/G
       v1y=-f*y/g
      v1=dsqrt(v1x**2+v1y**2)
       delv1=dsqrt(v1**2+vc**2-2*vc*vc)
      v2x=(gt*r2-x)/G
       v2y=-y/g
       v2=dsqrt(v2x**2+v2y**2)
       delv2=vw2-v2
       totv=delv2+delv1
       write (98,88) totv,delv1,delv2
  88     format (3(f6.2))
            delt=delt+864000
  666    continue

         end

c subroutine to determine the semi-major axis using
c fixed point iteration
        subroutine fixedp (mu,s,c,delt,a,alpha,beta)
        double precision mu,s,c,delt,a,alpha,beta,tof,thing,delta
      double precision xxx
```

I - 88

```
      do 555 a=1.496e9,1.496e30,1.496e8
      alpha=2*dasin(dsqrt(s/(2*a)))
      beta=2*dasin(dsqrt((s-c)/(2*a)))
    tof=dsqrt((a**3)/mu)*((alpha-dsin(alpha))+(beta-dsin(beta)))
c check for convergence
      thing = abs( (delt-tof)/delt)
      delta= 0.01
       if (thing.le.delta) then
         return
       endif
  555  continue

c prints a warning if solution does not converge for
c given number of iterations
      write (*,*) 'fixed point DID NOT CONVERGE'

      return
      end
```

Appendix D

```
      real dv,nl,aon,ano,mm,con,trp,rp,lu,tpop,tpl,mo,p$,ph$,ipro
      character label*30
      dimension dv(2),cfdv(2),nl(2),aon(2),ano(2),mm(2),trp(2),rp(2),
     -lu(2),tpop(2),Isp(2),ipro(2),con(2),p$(2),ph$(2),label(2)

c     print *,'Enter spacecraft dry mass'
c     read *, mo
c     print *,'Enter total delta V for ELECTRIC THRUSTERS (m/s)'
c     read *, dv(2)
c     print *,'Enter total delta V for CHEMICAL THRUSTERS (m/s)'
c     read *, dv(1)
c     print *,'Enter control function delta V for CHEMICAL (m/s)'
c     read *, cfdv(1)

      open (unit = 30, file = 'pout401b', status = 'unknown')

      mo = 2000
      cfdv(1) = 233
      cfdv(2) = 0
      dv(1)    = 2029
      dv(2)    = 8239

 ****  DEFINE ROCKET CONSTANTS

      e = 2.718281828
      cfdv(2) = 0
      Isp(2) = 4077.471967
      Isp(1) = 220.000000
           g = 9.81
      ph$(1) =   48.40
      ph$(2) = 679.12
      label(1) = 'MONO-METHYL HYDRAZINE CHEMICAL PHASE'
      label(2) = 'XENON ELETRICAL PHASE'

 20   format (1x,a33,10x,f20.3)
 40   format (1x,a33)

        do 10,i=1,2
            temp  = 0
            mmt   = 0

            ipro(i)   = mo * (1 - e**(-1*(dv(i)/(g*Isp(i)))) )
            nl(i)  = ipro(i) + cfdv(i)
            temp   = nl(i) / 100
            aon(i) = temp
            ano(i) = temp
            mmt    = nl(i) + aon(i) + ano(i)
            mm(i)  = 0.05 * mmt
            con(i) = mm(i)
            trp(i) = mmt + mm(i) + con(i)
            rp(i)  = 0.02 * trp(i)
            lu(i)  = 0.005 * trp(i)
            tpop(i) = trp(i) + rp(i) + lu(i)
            p$(i) = ph$(i) * tpop(i)
```

```
         write (30,40) label(i)
         write (30,20)
         write (30,20) 'Delta v manuvers',ipro(i)
         write (30,20) 'Control Functions',cfdv(i)
         write (30,20) 'Nominal Load',nl(i)
         write (30,20) 'Allowance for Off Nominal Perf',aon(i)
         write (30,20) 'Allowance for Nominal Operations',ano(i)
         write (30,20) 'Mission Margin',mm(i)
         write (30,20) 'Contingency',con(i)
         write (30,20) 'Total Required Propellant',trp(i)
         write (30,20) 'Residual Propellant',rp(i)
         write (30,20) 'Loading Uncertainty',lu(i)
         write (30,20)
         write (30,20) 'Total Propellant of Phase',tpop(i)
         write (30,20) 'Price of Propellant Phase',p$(i)
         write (30,20)
         write (30,20)
         mo = mo + tpop(1)
10    continue

      tpl = tpop(1) + tpop(2)
      ptp = p$(1) + p$(2)
      write (30,20)
      write (30,20)
      write (30,20) 'TOTAL PROPELLANT LOAD ', tpl
      write (30,20) 'TOTAL PROPELLANT PRICE', ptp

      end
```

Appendix E
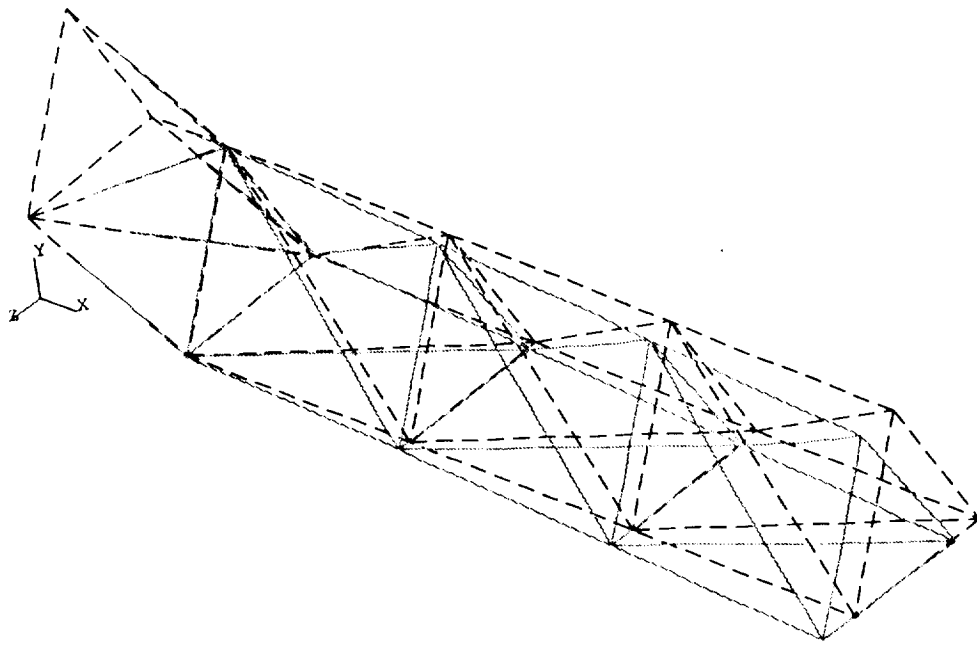
Figure E.1: Platform Truss in Mode 1 (f=85.842 Hz)
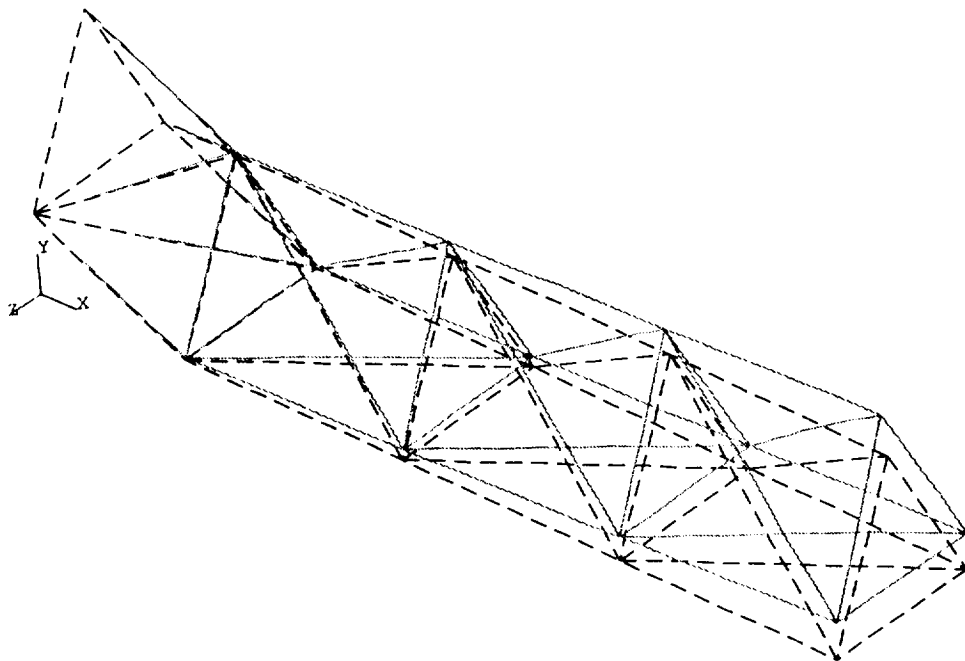
Figure E.2: Platform Truss in Mode 2 (f=97.445 Hz)
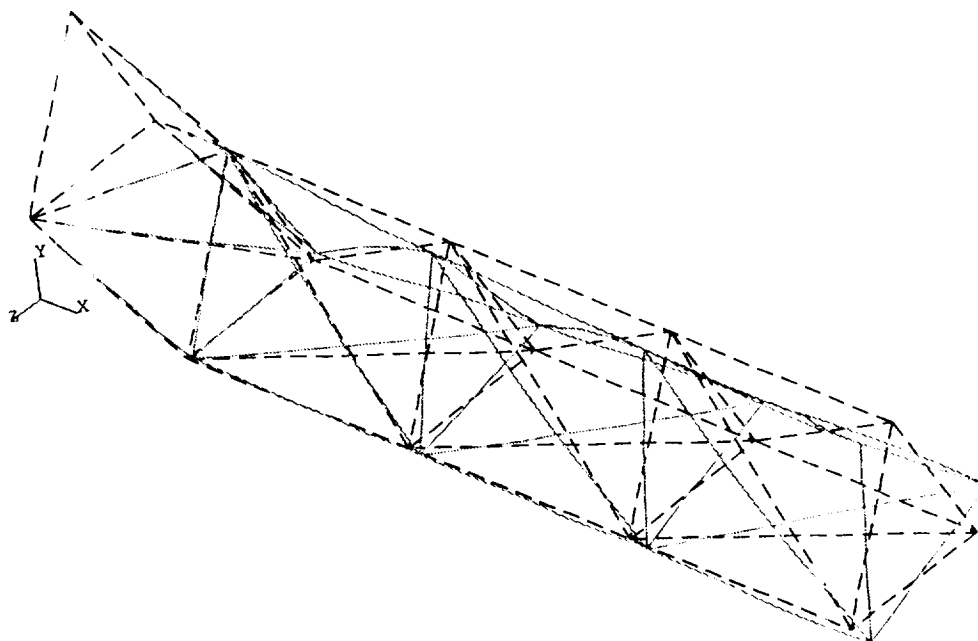
Figure E.3: Platform Truss in Mode 3 (f=189.81 Hz)

Volume II

Single Asteroid Sample Return Mission

The Pennsylvania State University

Department of Aerospace Engineering

SINGLE ASTEROID SAMPLE RETURN MISSION

by

Paolo Angulo, Michael Bobulinski, Robert Buchina, Scott Davis, Keith Dobson, Kenneth Ely, Christopher Flotta, Daniel Harter, Thomas McCallan, Courtenay McMillan, Paul Olah, James Pawloski, Raymond Sedwick, Kurt Stang, Glenn Szydlowski, Gregory Traub, Lance Williard, Milad Youssef, Christopher Zalewski

June 1992

Abstract

This report describes a single asteroid sample return mission. The objective of this mission is to return an asteroid core sample to Earth while performing a variety of scientific observations of the asteroid and its environment. A near-Earth asteroid, 433 Eros, was chosen as the target. Orbital mechanics analysis has determined that it will take approximately 1.5 years to arrive at Eros and another year to return. The current launch date for the mission is January 21, 2000. Utilizing the Atlas IIA launch vehicle, the spacecraft will attain its parking orbit and engage a Centaur IIA upper stage to achieve Earth escape. The spacecraft will have a semimonocoque structural design composed mostly of beryllium. In order to meet the payload volume requirements of the launch vehicle, the spacecraft will have deployable booms, landing gear, and high-gain antenna. Four bipropellant thrusters will control velocity changes and maneuvering. The spacecraft will utilize twelve monopropellant thrusters in conjunction with reaction wheels to maintain navigational stability during transfer to the asteroid. Attitude determination will be accomplished by inertial measurement units with sunsensors and starsensors to establish an inertial reference. Three MOD-RTGs will be used to supply power to the spacecraft, with three independent pressure vessel NiH_2 batteries to supply power to the sampling drill. The spacecraft will employ various instruments to perform scientific observations. These include: a plasma spectrometer, a magnetometer, a dust analyzer, a laser radar system, and several instruments that provide detailed surface analysis of Eros using imaging in the ultraviolet through infrared electromagnetic spectrum. The projected cost for this mission is $2844.6M (FY92).

Table of Contents

List of Figures

List of Tables

1.0 Introduction

Many consider the asteroids to be a great potential supply of mineral resources that could be tapped at some time in the future. Unfortunately, very little information is available about these celestial bodies. During the past two decades, interplanetary probes such as Viking 1 and 2, Pioneer 10 and 11, and Voyager 1 and 2 have provided mankind with much information about several planets and satellites in the solar system. However, all probes launched to date have returned little significant information about the asteroids. In addition, none of these unmanned spacecraft were capable of returning samples to Earth for detailed analysis. Therefore, a design is proposed for a mission that would study an asteroid in detail and return core and surface samples back to Earth.

Scientific missions for asteroid research are becoming important as the world looks for alternative fuel sources, natural resources, and future way stations for deep space travel. Relatively little information is known about asteroids and their specific characteristics. The asteroid 433 Eros was chosen as the target because of its proximity to Earth and numerous launch opportunities in the next several years.

In this mission, the spacecraft will rendezvous with, land on, and anchor itself to Eros, a near-Earth asteroid (see Figure 1.1). It will then drill to obtain core samples, which will be stored onboard for the voyage home. Finally, the spacecraft will return to Earth where the samples will be retrieved. Throughout the mission, the spacecraft will perform many scientific experiments in an effort to obtain as much detailed information as possible.

This report describes the subsystems that are required for the spacecraft to complete its mission. Topics detailed in this report include launch vehicle; spacecraft structure; power; propulsion; guidance, navigation, and control; communications; command and data handling; thermal control; scientific instruments; sample acquisition; and sample retrieval.

Figure 1.1: Mission Scenario

Rendezvous
and mapping w/
visual and LADAR
scans

EROS

Descent begins
once a site is
chosen

Spacecraft
detaches landing
gear for return
to Earth w/
samples

Retrieval by
Space Shuttle

EARTH

EROS

After touchdown
sample acquisition
begins

Boom and
Antenna
Deployment

Earth launch
via Atlas IIA
w/ Centaur

EARTH
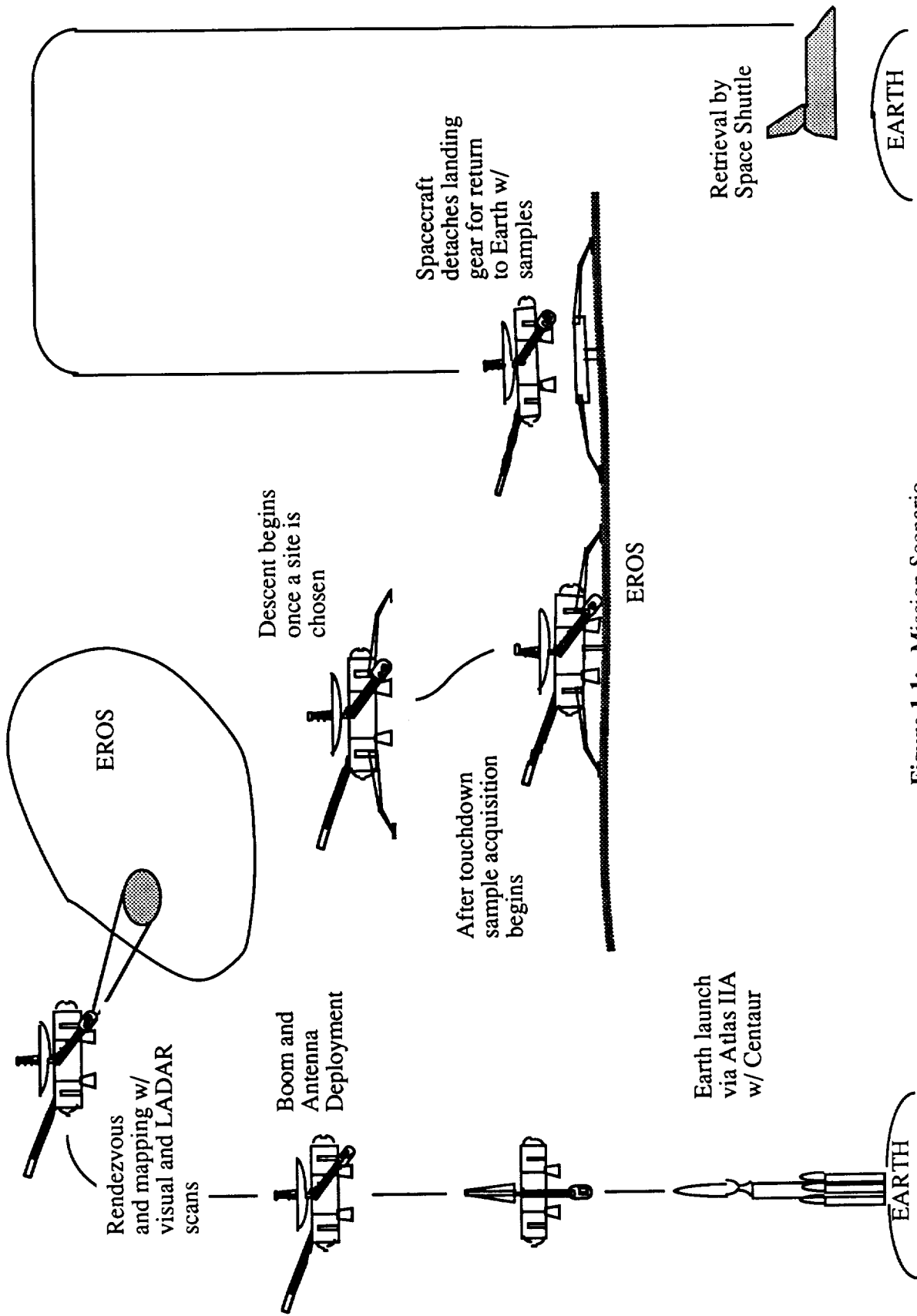
2.0 Launch Vehicle

2.1 Requirements

The launch vehicle is required to lift the spacecraft to an altitude where the propulsion subsystem can take over and propel the spacecraft to the target asteroid. The basis of selection of an appropriate vehicle involved three different criteria. First, the possible boosters were analyzed to determine which ones were able to boost the design mass of the spacecraft. Second, the cost of each remaining booster was investigated to determine which would be the most cost effective of the proposed vehicles. Finally, any additional benefits that would be gained by the different systems were weighed versus their cost. Based on these three criteria, a launch system was chosen according to the current mission profile.

2.2 Atlas IIA

The launch vehicle chosen to provide initial boost for the spacecraft was the Atlas IIA. The Atlas IIA, manufactured by General Dynamics, is capable of boosting a payload of 6760 kg into a 185 km, 28 degree inclination parking orbit. Using the current mission profile, the spacecraft's mass is 5830 kg which is within the Atlas IIA's capabilities. Also, the Atlas IIA is the lowest cost booster, $80-90 million (1990 dollars) per launch, which is able to launch the spacecraft's budgeted mass. At liftoff the Atlas IIA can provide an average of 2.11 million Newtons of thrust, which is sufficient for the current payload specifications. The launch processing time for this vehicle is 71 days, from erection to launch at the Cape Canaveral Air Force Station facility (CCAFS). Figure 2.1 gives a pictorial representation of the launch sequence. The Centaur upper stage, provided with the Atlas IIA, will be used for Earth escape [1].

Flight Sequence

Event	Flight Time (min:sec)			
	Atlas I	Atlas II	Atlas IIA	Atlas IIAS
Liftoff/SRM ignition (1st pair)	00:00	00:00	00:00	00:00
SRM burnout (1st pair)	--	--	--	00:56.0
SRM ignition (2nd pair)	--	--	--	01:06.2
SRM jettison (1st pair)	--	--	--	01:31.7
SRM burnout (2nd pair)	--	--	--	02:02.5
SRM jettison (2nd pair)	--	--	--	02:06.2
Atlas booster engine cutoff (BECO)	02:35.5	02:52.4	02:48.7	02:47.8
Atlas booster package jettison	02:38.5	02:55.5	02:51.8	02:50.9
Insulation panel jettison	03:00.5	--	--	--
Payload fairing jettison	03:40.8	03:46.0	03:52.4	03:37.5
Atlas sustainer engine cutoff (SECO)	04:27.0	04:38.2	04:38.9	04:43.4
Atlas sustainer jettison	04:29.0	04:40.2	04:40.9	04:45.4
Centaur first main engine start (MES1)	04:39.5	04:50.7	04:51.4	04:55.9
Centaur first main eingne cutoff (MECO1)	09:53.2	11:13.3	09:55.1	09:48.1
Centaur second main engine start (MES2)	24:08.7	24:32.5	24:09.4	23:40.4
Centaur second main engine cutoff (MECO2)	25:42.5	26:17.3	25:39.5	25:21.1
Alignment to separation attitude and spin-up	25:44.5	26:19.3	25:41.5	25:23.1
Separate spacecraft	27:57.5	28:32.3	27:54.5	27:36.1
Collision and contamination avoidance maneuver	37:57.5	38:32.3	37:54.5	37:36.1
Satellite first apogee arrival	5.7 hrs	5.7 hrs	5.7 hrs	5.7 hrs

Figure 2.1: Pictorial Representation of the Flight Sequence (Isakowitz, Steven J., *International Reference Guide to Space Launch Systems*, AIAA Publications, Washington, D.C., 1992.)

2.3 Payload Accommodation

Considering the estimated size of the spacecraft, the largest payload fairing available with the Atlas was chosen. This fairing provides a maximum payload diameter of 3.65 meters, a maximum cylinder length of 5.258 meters and a maximum cone length of 5.55 meters. Figure 2.2 illustrates these and other dimensions of the payload fairing. Considering the current configuration, Table 2.1 lists the environment the spacecraft will experience during the launch phase of the mission [1].

Large Payload Fairing

47.5 in
(1206.5 mm)

218.5 in
(5549.9 mm)

14.5 deg

473.0 in
(12014.2 mm)

Dynamic
Envelope

165 in
(4191.0 mm)

143.7 in
(3650 mm)

Adapter
(TBD)

42.0 in
(1066.8 mm)

Equipment
Module
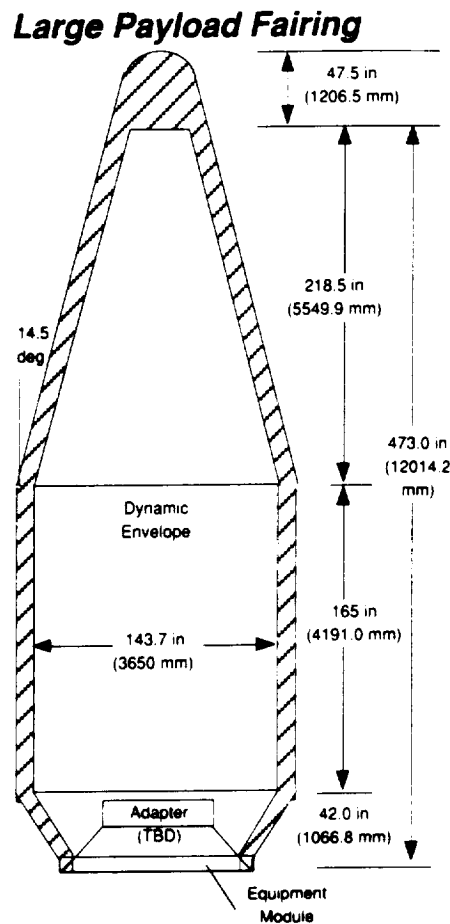
Figure 2.2: Large Payload Fairing (Isakowitz, Steven J., *International Reference Guide to Space Launch Systems*, AIAA Publications, Washington, D.C., 1992.)

Table 2.1: Payload Fairing Environment (Isakowitz, Steven J., *International Reference Guide to Space Launch Systems*, AIAA Publications, Washington, D.C., 1992.)

Maximum Load Factors (not at same time)	+6.0 g axial, ±2.0 g lateral
Maximum Lateral/Longitudinal Payload Freq.	10 Hz / 15 Hz
Maximum Overall Acoustic Level	138.4 dB (1/3 octave)
Maximum Flight Shock	2000 g at 1500 Hz
Maximum Dynamic Pressure on Fairing	700 lb/ft^2 (33520 N/m^2)
Maximum Pressure Change in Fairing (prior to launch)	0.8 psi/s (5.4 kPa/s)

2.4 Conclusions and Recommendations

Based on the current dimensions and mass of the spacecraft, the Atlas IIA was chosen as the primary launch vehicle. If the payload mass should increase beyond the capabilities of the Atlas IIA, the Atlas IIAS may be used with minimal modifications made to the spacecraft adapter and mission design. The IIAS is essentially identical to the IIA, except for the addition of four Castor IVA solid boosters. These additional boosters increase the available spacecraft mass to 8930 kg. The Centaur upper stage and large payload fairing are also available on the Atlas IIAS [1].

3.0 Spacecraft Structure

3.1 Structural Requirements

The structure subsystem must perform many duties during the mission. First and foremost, it must provide strength and rigidity to the spacecraft. It must also protect certain sensitive components, house all subsystems, withstand launch loads, fit within the launch vehicle shroud, and be able to withstand forces exerted by the main thrusters and the attitude thrusters. The structure must provide a stable platform from which the many components, particularly the scientific components, can operate. The structure must also protect the computer system components from the harsh space environment.

Many factors, both external and internal, will influence the design of the spacecraft structure. The spacecraft structure must be designed to withstand a wide variety of forces. The chosen launch vehicle, an Atlas IIA, will impart 6g's of force on the spacecraft during launch. This force will transfer through the launch shroud's support structure which will attach directly to the spacecraft. In addition to this, the structure must withstand the maximum force which occurs during the firing of the main thruster. Yet another load that the structure must withstand will be a moment created by the attitude thrusters. The spacecraft will employ these thrusters periodically in order to reorient itself. Also, the launch vehicle's maximum payload capacity will constrain the size of the spacecraft.

3.2 Critical Phases

3.2.1 Launch

The Atlas IIA launch vehicle presents two payload fairing options; a medium payload fairing and a large payload fairing (see Figure 2.2). Due to the spacecraft's size, the large payload fairing was chosen to house the spacecraft. This fairing has a length of 39.4 ft. (12.0 m), and a diameter of 13.75 ft. (4.2 m). The upper portion of the payload bay is conical in

shape with a length of 218.5 in (5550 mm). The bottom of the payload bay is cylindrical with a length of 165.0 in (4191 mm) and will house the 4.0 m high spacecraft. The conical section will house the folded high-gain antenna.

The spacecraft structure will experience large loads during the launch phase. The structure must be able to withstand the force of lift-off without coming loose in the payload bay. The Atlas launch will impart a 6g axial force and a ± 2g lateral force to the spacecraft. Both the axial and lateral loads will be transferred through the spacecraft adapter. The spacecraft will lie 16.4 in. (416 mm) from each inner wall of the payload fairing, thus defining the spacecraft's maximum deflection due to the lateral launch forces.

3.2.2 Cruise Phase

After departing from the Atlas payload shroud, the spacecraft will deploy the high-gain antenna and the various booms. All of these items will be retracted during launch to conserve payload space. Once the spacecraft successfully deploys these items, the cruise phase will begin.

During the cruise phase, the only severe action that the structure will have to endure will consist of firing main thrusters for orbital maneuvers and the firing the attitude thrusters for attitude maneuvers. These events are critical to the spacecraft's design. The four main thrusters will impart a maximum force of 1.6 kN to the vehicle. Each attitude thruster will impart 0.5 N of thrust and a moment of 0.124 N-m. The spacecraft structure will need to withstand these forces.

3.2.3 Asteroid Departure

Once the spacecraft contacts the asteroid, it will firmly attach itself using barbed spikes located in the landing leg footpads. The drilling will then commence. When the drilling is done, the spacecraft will depart from Eros. To reduce the propellant mass, the legs and drill will detach from the spacecraft and remain on Eros. Pyrotechnic charges will

disconnect the spacecraft's lower and upper sections, leaving the lower section (containing the landing struts and drill) on the surface.

3.3 Placement of Major Components

3.3.1 Placement of the Drill

The placement of the drill is critical to the design of the structure. The drill must be placed in the center of the landing gear, equidistant from each landing strut in order to balance the stresses on the attachment assembly. The entire drill apparatus will connect entirely to the spacecraft's bottom section; thus, the spacecraft can separate its upper and lower sections, leaving the drill on the asteroid along with the landing gear. The drill will require a firm structure to successfully hold it in place and transfer the axial forces needed to drill into the asteroid. The drilling process will require that this structure withstand a 2.22 kN axial force during the drilling process. Therefore, the lower assembly may be quite massive.

3.3.2 Placement of Thrusters

The spacecraft will employ two types of thrusters: the main thrusters, and the attitude thrusters. Four main thrusters will execute orbital maneuvers. These four engines will be placed symmetrically around the spacecraft, so as to provide stability during operation. Each thruster outputs 400 N of thrust, for a total of 1.6 kN thrust. The structure must be designed to distribute these loads over itself.

The spacecraft will utilize three-axis stabilization which will require the use of at least 12 attitude thrusters to provide adequate control. Each of the chosen attitude thrusters outputs 0.5 N of force for a moment of 0.124 N-m. These thrusters must be placed such that little or no exhaust gases affect exterior components such as the propellant tanks, scientific instruments, the antennae, or the power supply.

3.3.3 Placement of Propellant Tanks

Due to the nature of the mission, the spacecraft must carry a significant amount of propellant. Four tanks will store the propellant. Two tanks placed symmetrically opposite each other will store the monopropellant, and the two larger tanks, also located opposite one another, will carry the bipropellant. Since the composition of the fuel and oxidizer are not the same, each bipropellant tank will be divided by a straight wall for separate storage of fuel and oxidizer in the same tank. With this method, the symmetry of the spacecraft will remain intact through the trip.

The bipropellant tanks were initially designed to maximize the volume of the tank while minimizing its surface area. The corresponding sphere that matches the volume of propellant required exceeded the size of one side of the spacecraft. Thus, the tanks were redesigned as a cylinder with spherical end caps. The radius of the end caps are 19.038 in, and the height of the cylindrical section is 33.921 in. The monopropellant tanks were designed similarly. The end cap radius is 19.038 in. and the cylindrical height is 3.455 in. The end cap radius is exactly half of the length of one side of the octagonal spacecraft, which is the maximum allowable dimension.

3.3.4 Placement of Landing Struts and Anchoring Devices

The landing struts and anchors pose another structural design problem. The struts and anchors must firmly attach to the spacecraft structure to provide adequate surface anchoring. They will remain retracted into recessed grooves located along the sides of the spacecraft and will deploy after injection into the transfer orbit to Eros. They also must also be able to separate from the spacecraft as it launches from the asteroid. Therefore, the whole bottom assembly will detach from the spacecraft upon departure from the asteroid. This bottom assembly will act as a launch pad for the spacecraft. The main thrusters, attached to the upper section, protrude through openings in the truss of the bottom assembly allowing them to slide freely from the bottom section.

3.3.5 Placement of Scientific Instruments

Many scientific instruments will require mounting locations on the spacecraft's exterior. Three extended booms will house the scientific instruments. One boom will contain a rotating turntable, which will hold the dust analyzer, and the plasma spectrometer. The longest boom (10 m), will hold the magnetometer. The last boom will hold the HPSP which will accommodate the ultraviolet spectrometer, the wide-angle and narrow-angle CCDs, the laser radar system, and the Visual and Infrared Mapping Spectrometer. These booms must be sturdy enough to support the instrument during impulsive maneuvers, and remain as motionless as possible while the instruments are taking precise data.

3.3.6 Placement of Antennae

Other major components requiring exterior locations are the antennae. The spacecraft will employ one high-gain antenna (HGA) and two low-gain antennae (LGA). To provide adequate communications, the HGA will require an unobstructed view. The HGA will be a deployable structure, similar to the one found on the Galileo spacecraft. While on the asteroid's surface, the antenna must rotate to point at the Earth. Therefore, it will be mounted on a gimballed support.

One LGA will be located directly above the HGA. The other LGA will be placed half-way out on the magnetometer boom. To provide 360° coverage, the LGA will point in opposite directions. Both LGAs are deployable structures.

3.3.7 Placement of Computer System

The extremely sensitive computer system requires significant protection from both the space environment and heat generation. The computer will be placed near the top of the spacecraft close to the HGA. This will ensure the farthest distance from the drill during operation, and the main thrusters during firing.

3.3.8 Placement of Power Supply

Three Modular Radioisotope Thermoelectric Generators (MOD-RTG's) will provide power to all of the spacecraft's systems excluding the drill. Because of the radiation and electric and magnetic fields created by this power supply, it will be located far enough away from all sensitive instrumentation. The MOD-RTGs will be placed on a deployable boom three meters in length, similar to what was done on the Galileo spacecraft.

Three batteries will provide power for the drill. These will be placed near the drill on the bottom assembly, and will be left on the asteroid with the drill.

3.4 Spacecraft Bus

The structure itself requires as light and strong a design as possible. The construction materials must reflect these properties. Beryllium was selected to be the ideal material for the fabrication of the structure due to its high stiffness-to-mass ratio [2].

The spacecraft structure itself will employ a semi-monocoque design, thus providing sufficient strength yet weighing relatively little. The shape of the bus is similar to a cylindrical octagon. The spacecraft will measure 157.5 in. (4.00 m) in height with the length of each octagon side measuring 38.076 in. (0.967 m) in width. The spacecraft will require such a large height to accommodate the drill dimensions. The four propellant tanks will lie half embedded in the structure to save mass, and to maximize the interior surface area. The maximum dimension across the structure will be 130 in (3.302 m) at the bipropellant tanks.

Twelve attitude thrusters will be arrayed around the spacecraft to provide maneuverability around each axis. These thrusters will mount on the faces of the propellant tanks.

The four landing struts will lie on the four remaining faces. They will retract into recessed grooves for storage during launch. Once deployed, they need never retract and therefore can deploy via a one-way system. The four booms carrying the MOD-RTGs and

the various scientific instruments will also remain retracted during launch and deploy during the cruise phase of the mission.

In keeping with symmetry, the spacecraft will have four main rocket motors placed symmetrically about the centrally located drill. The amount of force generated by the drilling process will constrain the choice of drill placement. By placing the drill off-center, the struts would experience uneven loads.

The total mass of the structure is estimated to be roughly 10% of the spacecraft's mass (with propellant) or 550 kg. Figure 3.1 illustrates a bottom view of the spacecraft design and Figure 3.2 depicts a side view.
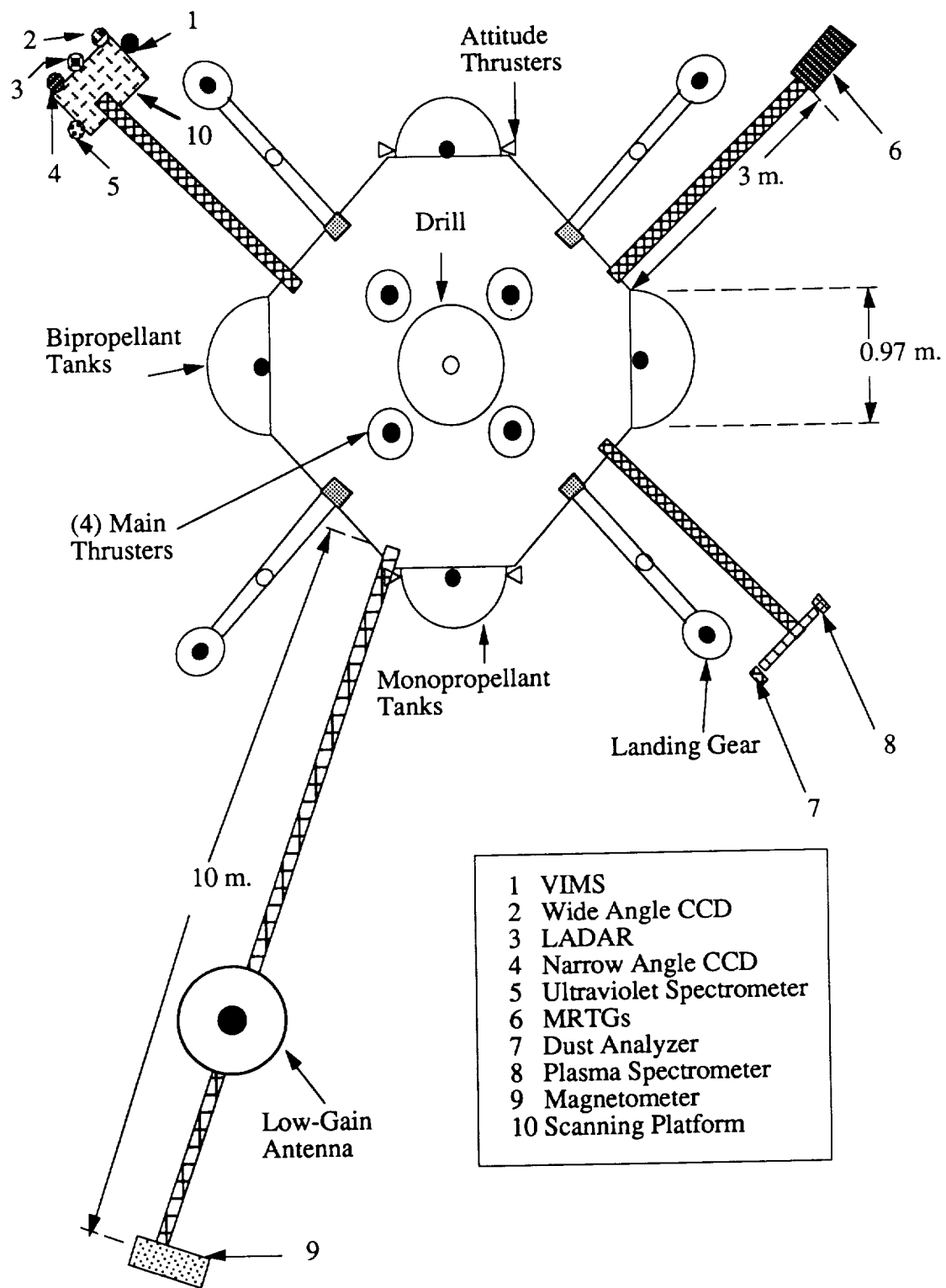
Figure 3.1: Spacecraft Bottom View

Labels in figure:

2 →
3 →
1
10
4 5
Attitude Thrusters
Drill
3 m.
6
0.97 m.
Bipropellant Tanks
(4) Main Thrusters
Monopropellant Tanks
Landing Gear
8
7
10 m.
Low-Gain Antenna
9

1 VIMS
2 Wide Angle CCD
3 LADAR
4 Narrow Angle CCD
5 Ultraviolet Spectrometer
6 MRTGs
7 Dust Analyzer
8 Plasma Spectrometer
9 Magnetometer
10 Scanning Platform
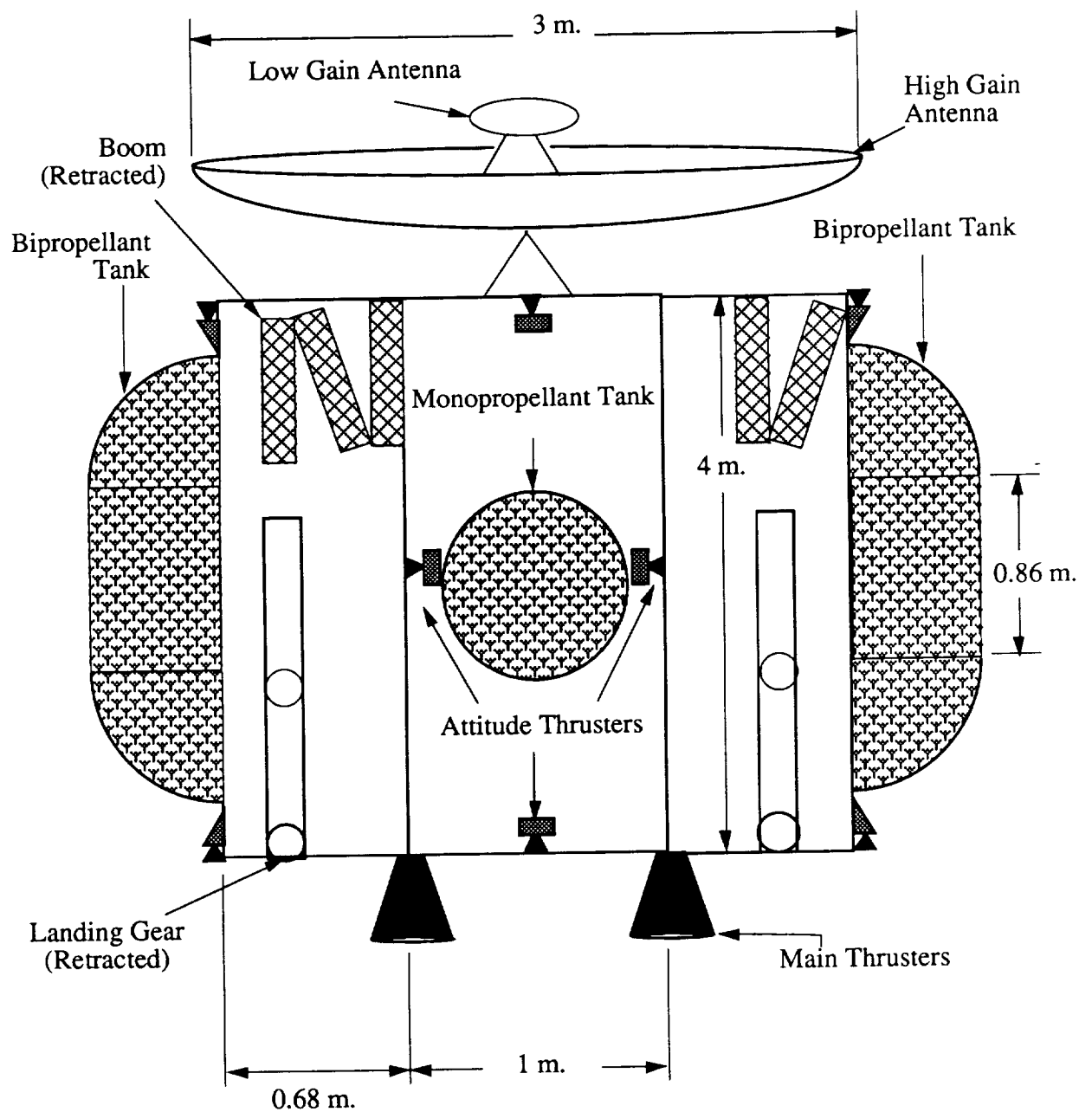
Figure 3.2: Spacecraft Side View

3.5 Conclusions and Recommendations

The spacecraft structure will utilize a semi-monocoque structure constructed chiefly of beryllium. Three scientific booms, an RTG boom, four landing gear, and the antennae, which are retracted during launch, will deploy shortly after leaving the Atlas IIA launch shroud. The structure must withstand the forces of the four main thrusters, along with those of the attitude thrusters on the voyage to Eros and back to Earth. Barbed spikes will attach the spacecraft to the asteroid during drilling. To conserve propellant, the heavy drill, landing gear, and bottom assembly will remain on the asteroid's surface and act as a launch pad. Finally, the Space Shuttle will retrieve the spacecraft from LEO and return it safely to Earth.

The semi-monocoque design must be fully tested to analyze how the forces will affect the structure. These forces are derived from the launch thrust, orbital maneuvers, attitude maneuvers, and drilling process. The stresses on the deployable booms must also be analyzed further.

4.0   Power Subsystem

4.1   Requirements

Generation, regulation, distribution, and storage of all spacecraft electric power is provided by its power subsystem. The determination of the power source was primarily based on the average and peak electrical power needed to successfully complete the mission.

Spacecraft power for can be generated using energy from the Sun, radioisotope decay, or nuclear fission reactors. Electrochemical energy can be stored in numerous devices. The following is a discussion of the various power sources that were investigated in order to determine which type would be most appropriate for this mission.

Table 4.1 lists the final power budget for the asteroid sample return mission. The average power consumption by all subsystems (other than those exclusive to the drilling phase of the mission) will be approximately 1.2 kW. The drilling apparatus requires 7.5 kW of power for a period of four hours.

Table 4.1: Power budget for the mission

System	Power (W)
Attachment to Asteroid	181
C&DH	451
Communications	80
GN&C	550
Propulsion	40
Science Instruments	114
Thermal	60
Subtotal :	1193 W
Drill :	7500 W
Total :	8693 W

4.2   Radioisotope Thermoelectric Generators

Since 1961, Radioisotope Thermoelectric Generators (RTGs) have been providing safe and reliable power to spacecraft designed for long missions. RTGs use thermocouples to convert the heat radiated by the isotope (usually Pu-238) into usable electric power for spacecraft subsystems. Major drawbacks to using RTGs are the availability of the Pu-238 and the cost of a unit, $120,000/W [3].

The Modular Radioisotope Thermoelectric Generator (MOD-RTG) has been chosen as the primary power source for this mission. The MOD-RTG represents the next generation of RTGs. The General Purpose Heat Source Radioisotope Thermoelectric Generators (GPHS-RTGs) were also considered as a power source for this mission, but the MOD-RTG has two distinct advantages over the GPHS-RTG: higher specific power and modularity.

The high specific power of the MOD-RTG is greater than 7.7 Watts/kg. This specific power represents a 45% improvement over the GPHS-RTG. The MOD-RTG can provide spacecraft power ranging from 19 Watts to as high as 340 Watts, depending on the spacecraft's power requirements. Each modularized segment provides a power output of 19 Watts at 30.8 Volts DC [4]. The DC output of the RTGs can be regulated and controlled to provide 2.4 kHz AC for spacecraft systems, if necessary [5]. The power output for the MOD-RTG, shown in Figure 4.1, is 340 Watts and its specific power is 7.9 Watts/kg. This is the configuration that will be used for this mission.

The MOD-RTG utilizes a Multifoil insulation system which surrounds the General Purpose Heat Source. A zirconia powder coating separates each of the 60 foil layers in the MOD-RTG design. The GPHS-RTG design utilizes quartz cloth separators. The multifoil insulation system of the MOD-RTG is lighter than the quartz cloth separators used in the GPHS-RTGs. The resulting weight savings can be seen in Table 4.2.
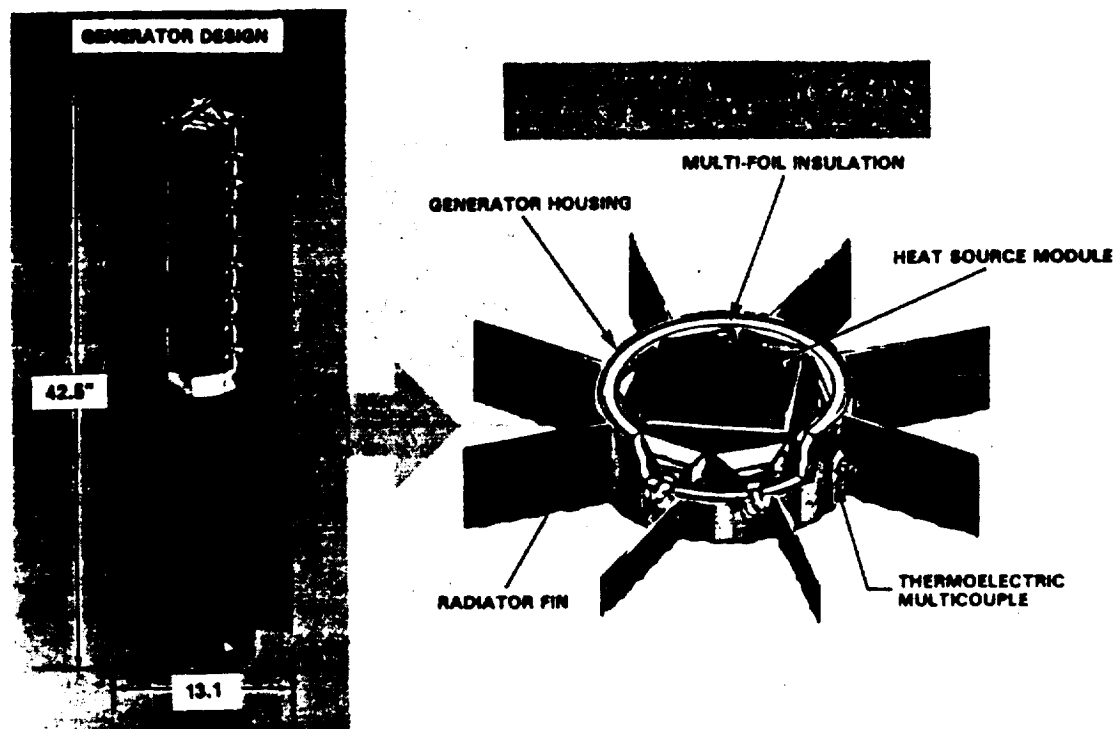
Figure 4.1: Modular RTG Design Parameters (Hartman, Robert F., "Modular RTG Technology Status," Proceeding of 25th IECEC, Vol. 1, 1990, p. 235.)

Table 4.2: MOD-RTG /GPHS-RTG weight comparison (Hartman, Robert F., "Modular RTG Technology Status," Proceeding of 25th IECEC, Vol. 1, 1990, p. 236.)

Major Weight Difference (kg)	MOD-RTG	GPHS-RTG
Multifoil Insulation System	2.2	6.4
Outer Shell	5.7	8.9
T/E Devices (including Mounting Hardware)	2.4	6.2
Heat Source Support System	3.9	4.7
Total RTG Mass	42.2	56.0

The critical design parameters listed in Table 4.3 are for each of the three MOD-RTGs that will be used as the primary power source for this mission.

Table 4.3:   MOD-RTG Design Parameters (Hartman, Robert F., "Modular RTG Technology Status," Proceeding of 25th IECEC, Vol. 1, 1990, p. 236.)

Number of GPHS Modules	18	
Voltage	30.8	Volts
Power Output	340	Watts
Specific Power	7.9	W/kg
Converter Efficiency	7.5	Percent
Length	1.08	M
Overall Diameter	0.33	M
Mass	42.2	kg
Operating Life	5	years
Storage Life	3	years

Three MOD-RTGs are not capable of providing sufficient power for drilling the core sample. It was decided that the solution to this problem would be to have an additional power source on board the spacecraft to use exclusively for the powering of the drill.

4.3   Dynamic Power Systems

To provide all the power necessary to complete the mission with only one power source, Dynamic Power Systems (DPS) were considered. Dynamic Power Systems utilize a heat source to drive an engine in a thermodynamic cycle. The Rankine, Brayton, and Stirling cycles are used to generate electricity in DPS. Unlike RTGs, DPSs have moving parts and use a working fluid to transfer heat. The Free-Piston Stirling Engine (FPSE) requires the smallest radiator area. The FPSE also has the potential for the highest efficiency and lowest overall system mass of the three cycles.

A DPS is capable of producing power over the range of 1kW to 1MW. For this particular mission results from the SP-100 Program carried out by the General Electric Company (GE) may be utilized to develop a power system configuration involving the FPSE.

Utilizing a nuclear reactor as a heat source, the SP-100 system is anticipated to have a mass around 1300 kg and provide 10 to 15 kW of power [5].

Two types of Stirling engine are being developed by GE: a state-of-the-art low temperature engine with superalloy construction, and an advanced Stirling engine operating at higher temperatures with some refractory metal construction. Table 4.4 lists some characteristics of both engines designed to produce power in the 10 kW range.

Table 4.4: Some Characteristics of GE's FPSE, 10 kW net power to user (Darooka, D.K., "Ten Kilowatt to Multimegawatt Modular Space Power System Using Stirling Engines," Proceedings of 25th IECEC, Vol. 5, 1990, p. 226.)

	Low Temp Engine	High Temp Engine
Power Generated by Engine (kWe)	11.14	11.14
Engine Efficiency	29.5%	29.5%
Average Radiator Temperature (K)	505	615
Radiator Area (M^2)	10.24	4.46

The Stirling engine is a reciprocating piston engine which operates at approximately 100 Hz [6]. This generates vibrational forces which could be transmitted to the spacecraft. The engines are usually attached to the rest of the spacecraft by a boom structure; therefore, the magnitude of the forces transferred to the rest of the spacecraft is a function of the boom's structural parameters. Optimization of engine location and orientation were suggested as solutions to minimizing the transfer of vibrational forces.

4.4   SNAP-DYN Systems

Systems for Nuclear Auxiliary Power (SNAP) nuclear reactors coupled with dynamic power converters (SNAP-DYN systems) were another possible power source considered for suppling power for this mission. SNAP-DYN is a space nuclear power system that attains high efficiencies while utilizing only conventional materials and operating at low temperatures. Three different designs of the SNAP-DYN use the organic Rankine cycle (ORC), the closed Brayton cycle (CBC), and the FPSE. Results from ground tests indicate

that the engines operate with efficiencies of 16 to 20 percent and have an expected operational lifetime of 8.3 years (60,000 hours) [7]. Table 4.5 lists some characteristics of the 10 kWe systems. It has been demonstrated that vibrational problems associated with the FPSE can be reduced by using a dynamically balanced, opposed piston engine. The FPSE is an attractive system because of the small area required for its radiator.

Table 4.5: Characteristics of the SNAP-DYN 10 kWe Systems (Determan, W.P., "SNAP-DYN: Concepts for Multikilowatt Space Power Applications," Proceedings of 23rd IECEC, Vol. 3, 1988, p. 210.)

	ORC	CBC	FPSE
Mass (kg)	1571	1551	1562
Main Radiator Area (M^2)	32.9	36.7	23.5
Radiator Temperature (K)	333-361	294-432	371-426
System Efficiencies	16.6	18.1	16.9

4.5   Batteries for the Drill

Batteries must be used for the drill, since RTGs alone cannot supply enough power for drilling. The exact type of drill required for this mission was never thoroughly described. However, it was estimated that the drill would require about 7.5 kW of power for four hours in order to obtain the core sample.

4.5.1   Battery Requirements

A formula for the estimation of the required capacity of the battery is given in Wertz on page 364 [8].

$$Cr = \frac{Pe\ Te}{Cd\ N\ Vd\ n}$$

Assuming the following parameters:

Cr	=	rated battery capacity		
Pe	=	average power load	=	7500 W
Te	=	time required to drill	=	4 hr
Cd	=	limit on battery DOD	=	0.80
N	=	number of batteries	=	1
Vd	=	bus voltage	=	30 V
n	=	transmission efficiency	=	0.90

The rated battery capacity is 1389 A-hrs (amp hours) or about 41 kW-hrs. This battery capacity can be reduced by breaking the drilling time into smaller time increments. After each drilling period, the RTGs could recharge the batteries and the process could be repeated. The number of batteries could also be increased to reduce the individual battery capacity.

In order to make batteries a reliable power source, a large number of cells, wired in series and/or parallel, will be used. Should some of these cells fail during the mission, the batteries would still be able to function independent of one another. The batteries must have a discharge current that is sufficient for running the drill. Also, the batteries must be able to be recharged by the small amount of power provided by the RTGs.

Due to the unique power requirements of the drill, it was difficult to find one particular battery to meet the needs. Even so, an approximation of the battery was obtained by studying three different types of batteries that are currently available or will soon be available. The battery used for this mission may have to be specifically designed for this mission.

4.5.2 IPV NiH$_2$ Rechargeable Battery

Independent Pressure Vessel (IPV) Nickel-Hydrogen (NiH$_2$) batteries are currently being flown on the Hubble Space Telescope and are being planned for use on Space Station Freedom. Nickel-Hydrogen batteries are being used increasingly as replacements for Nickel Cadmium batteries since NiH$_2$ batteries have a higher specific energy. A typical IPV NiH$_2$ battery has a specific energy of 50-60 W-hr/kg while a NiCd only has a specific energy of 30-40W-hr/kg [9]. Still under development is a less massive Common Pressure Vessel (CPV) NiH$_2$, which will offer better performance than an IPV. Nickel-Hydrogen batteries have not been flown on deep space missions yet, but should be developed in time for this mission.

4.5.3 Rechargeable Lithium Battery

The second type of battery considered was a rechargeable lithium battery. Lithium batteries may use different chemicals for the electrolytes, but the one for this battery is organic V_2O_5. The rechargeable lithium system has the advantage of a low self-discharge and high efficiency. This battery is still being developed but it is expected to have a specific energy of 100-140 Wh/kg [9] This battery offers a considerable mass savings when compared to other batteries.

4.5.4 Lithium Thionyl-Chloride Battery

The last type of battery considered was a primary Lithium Thionyl-Chloride (Li/T-Cl) battery. This battery was developed for the Strategic Defense Initiative Office and was successfully flown on a mission in 1988 [10]. Since this is a primary battery, it will not be able to be recharged after being discharged. Also, when compared to a rechargeable battery, a primary battery would not require a recharging systems. A possible problem with primary batteries is that, after time, the battery may lose some of its original charge. This should not be much of a problem with a Lithium Thionyl-Chloride since lithium batteries generally have a long shelf life [11].

4.5.5 Battery Recommendations

Table 4.6 lists some of the important characteristics of the three batteries discussed above. The three types of batteries should all be able to meet the estimated requirements of the drill. However, due to the relatively unknown surface composition of the asteroid, the power requirements for the drill may change once drilling begins. If the drill was required to operate for a longer period of time than anticipated, then the Lithium Thionyl-Chloride battery would not be able to supply the extra power needed. Even though the Li/T-Cl would not require recharging circuits, it lacks the flexibility of rechargeability the other batteries

possess. For this reason, the Lithium Thionyl-Chloride battery would not be a good choice for a mission of this nature.

Table 4.6: Individual Battery Characteristics.

	NiH2[1]	Li[2]	Li/TCl[3]
Amp-hours	88	90	1384
Voltage (V)	28	30	28
Volume (cm^3)	57460	22000	20533
Mass (kg)	71	30	253
Number Req'd	3	3	1
Total Mass (kg)	213	90	253

[1]Standlee, D.,"The Hubble Space Telescope Battery Background", The 1990 NASA Aerospace Battery Workshop, 1990, p. 691-704.

[2]Deligiannis, F., "Performance Characteristics of Lithium Primary Cells after Controlled Storage", Proceedings of the 26th IECEC, vol 3, 1991, p. 395.

[3]Sullivan, Ralph M., et al., "The Delta 181 Lithium Thionyl Chloride Battery", Proceedings of the 26th IECEC, vol 3, 1991, p. 384-386.

Three rechargeable batteries were determined to be necessary for this mission. With three batteries, a failure of one would not jeopardize the mission since the two remaining batteries should still be sufficient to complete the drilling. Five or six recharging cycles are expected to be needed if three batteries of the types listed above are used. Recharging time between cycles is not expected to be more than 3 days.

From Table 4.6, it can be seen that the lithium battery is predicted to have a mass less than one half of an equivalent IPV NiH$_2$ battery. However, lithium batteries are still being developed and it may be several years before a lithium battery suitable for this mission is developed. Nickel-Hydrogen battery technology is currently being used and should be ready for this mission. For this reason, three IPV NiH$_2$ batteries were chosen to be the power source of the drill. If the launch date of the mission were delayed by several years, then lithium batteries may become a good option.

4.6   Power Management and Distribution

The Power Management and Distribution (PMAD) system is broadly defined as the system performing all electrical power system functions other than generation and storage. The PMAD system takes raw power from the source and transforms it into useful power for the various spacecraft loads. The PMAD is also responsible for the regulation of this power.

The previously designed PMAD of the Galileo spacecraft served as a model in the design of the PMAD for this mission. The expected mass of the PMAD is 80 kg/kW or about 96 kg [13]. The wiring harness is expected to weigh between 10% to 25% of the total power systems mass or about 100 kg [8].

4.6.1   PMAD Description

The spacecraft's PMAD system is shown in Figure 4.2. Three MOD-RTGs will provide the power to a 30 Vdc bus. Each output of the RTG is connected to isolation diodes, by-passible through a relay. The isolation diodes provide protection for the spacecraft in case of an internal failure of one of the RTGs. Also, these diodes provide enough of a voltage drop to power the memory keep-alive circuits [14]. The bus regulator consists of a shunt regulator and a capacitor discharge controller. Excess RTG power is diverted by the shunt regulator into external shunt radiators, which may be used to heat various parts of the spacecraft. The discharge controller stores capacitor energy which can be supplied to the bus through transient energy support [14].

The Power Control unit in Figure 4.2 contains all of the control and switching functions as well as some telemetry of the PMAD. This unit contains many redundant features which will help ensure continued operation [14]. The Power Control unit also controls the power from the batteries to the drill. When the batteries need recharging, the Power Controller diverts RTG power into the Recharger unit, which controls the recharging of the batteries.
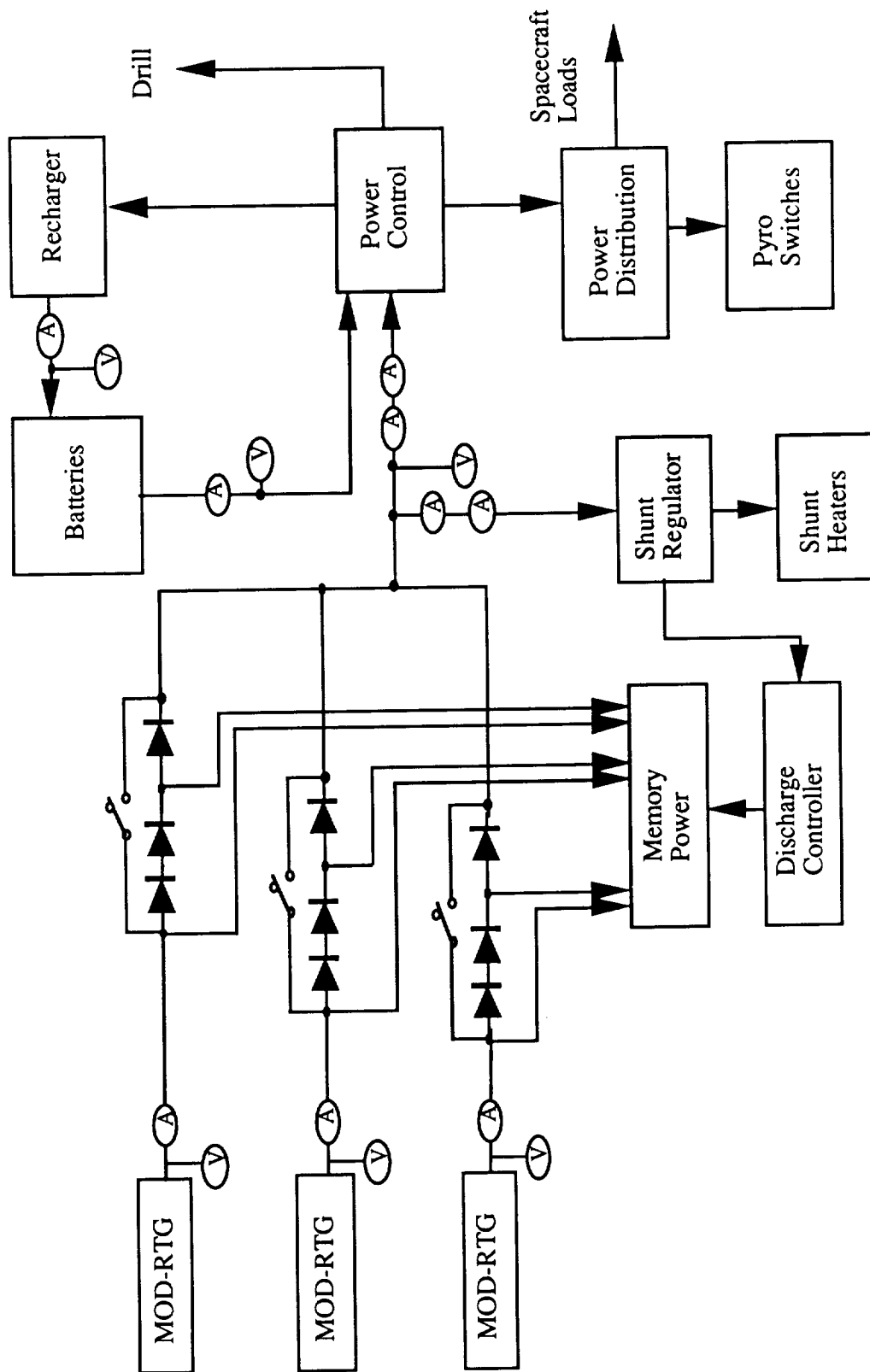
Figure 4.2: PMAD System (based on diagram in Detwiler, R.C. and Smith, R.L., "Galileo Spacecraft Power Management and Distribution System", Proceedings of the 25 IECEC, vol. 1, p. 450.)

The Power Distribution unit handles the distribution of power to the various spacecraft loads. Load switching is accomplished by magnetically latched relays which are arranged for redundancy in the event of a failure. Also connected to the Power Distribution unit is the Pyro Switching unit. This unit controls several pyrotechnic devices which aid in the deployment of booms, and spacecraft launch vehicle separation [14].

4.6.2 Autonomy and Memory Keep-Alive

Not all of the power system's functions can be controlled from the ground due to the time delay involved in transmitting commands. The PMAD must contain a large degree of autonomy and fault protection. The spacecraft must, in the very least, detect a fault, autonomously recover from the fault, transmit telemetry of the fault to Earth, and safe itself while protecting other systems of the spacecraft. The fault protection system must also be able to be reprogrammed in-flight to correct for possible design flaws and to add flexibility to the system [14].

To insure that the computer of this spacecraft has sufficient power at all times, the PMAD provides a memory keep-alive function. The maximum duration of a correctable fault in the power system is on the order of only a few seconds. The short term keep-alive circuits will be able to handle a power disruption lasting only a few seconds. For longer power outages, a centralized and block redundant memory power system with a DC/DC converter is used. The DC/DC converter operates from the small voltage developed across the two series diodes, shown in Figure 4.2 [14].

4.7 Recommendations

The final selection of the power source was three MOD-RTGs and three rechargeable Independent Pressure Vessel NiH_2 batteries for powering the drill. The mass of the RTG and battery system was determined to be much lower than using DPS or SNAP-DYN systems.

For instance, an RTG and battery system (including the PMAD and wire harness) will have a mass of approximately 550 kg while a DPS or SNAP-DYN system will be over 1300 kg.

MOD-RTGs are expected to be flight-ready by 1993, prior to the anticipated launch date of January, 2000. As stated previously, the batteries for the drill should be custom designed for the mission. Of the three types of batteries considered, the IPV NiH_2 batteries appear the best selection and should be ready by the expected launch date. If the mission is postponed a few years, then more efficient batteries, such as rechargeable lithium batteries could be used.

5.0   Propulsion Subsystem

5.1   Requirements

Four areas were considered when choosing the propellants for this mission: mass, storability, performance, and combustibility. Low mass is desired to lessen the gross mass of the spacecraft. It was not considered beneficial to have any kind of cryogenic or possibly corrosive propellants. This would require special refrigeration units or insulation to store these propellants.

The spacecraft had to meet three major performance considerations. Primarily, it must perform a total, out of plane, velocity change of 12 km/s. The attitude mission parameter requires a three-axis stabilization for the spacecraft while enroute to the asteroid. This is maintained through a combination of attitude thrusters and reaction wheels. Once the spacecraft has reached the asteroid, a 90° slew must be performed to properly align the spacecraft with the asteroid.

The combustibility consideration deals with the properties of the propellant, combustion mechanisms, combustion chamber and the nozzle. The combustion chamber and engine nozzles are chosen from other conventional spacecraft with similar mission parameters. A chemical reaction combustion is chosen over other engine classes, such as the electric or nuclear motors. These are not considered advantageous to the mission due to power and mass considerations. Table 5.1 gives specifications for different propellants.

5.2   Propellants

5.2.1   Cold Gas

Cold gas is a propellant that requires no combustion because it produces thrust simply by releasing compressed gas in a given direction. There are 4 types now used in space vehicles; nitrogen, ammonia, freon, and helium. These cold gases produce a low specific

impulse (Isp) and low thrust range compared to other propellants (see Table 5.1). Due to the high density of the cold gas propellant, compared to other kinds of propellants, the spacecraft design must account for a very heavy propulsion system. Even though the cold gas is relatively simple and reliable, it produces a very low performance.

Table 5.1: Propellant Specifications. (Wertz, J.R. and Larson, W.J., eds., *Space Mission Analysis and Design*, Kluwer Academic Publishers, Norwell, MA, 1991.)

PROPELLANT	THRUST RANGE (N)	I_{sp} (sec)
Cold Gas*	0.05 - 200	50 - 75
Solid Propellants	50 - 5×10^6	280 - 300
Liquid Propellants		
Monopropellants	0 - 0.5	150 - 225
Bipropellants	0 - 5×10^6	300 - 430
Water Electrolysis	0 - 500	360

*Data measured at 24 MPa and 273 K

5.2.2 Liquid Propellants

Both monopropellants and bipropellants were considered for this mission. Two specific monopropellants were considered due to their past use in space. The two monopropellants were hydrogen peroxide (H_2O_2) and hydrazine (N_2H_4). The monopropellants' low thrust range is ideal for small attitude corrections (see Table 5.1). The monopropellants are reliable, because of the simple combustion mechanisms. One disadvantage of the monopropellants is that they are slightly heavier than other propellants. This disadvantage is offset, however, by the low cost necessary to produce the monopropellant.

Bipropellants are composed of two different chemical components, a fuel and an oxidizer. Four different oxidizers were considered for this mission: nitrogen tetroxide (N_2O_4), fluorine (F_2), oxy-fluorine (OF_2), and chlorine trifluoride (ClF_5). These oxidizers had the best performance characteristics (see Table 5.1). Even though these bipropellants

have good performance capabilities, the fluorine family (F_2, OF_2, and ClF_5) are extremely toxic and complicated to use. Fluorine derivatives tend to corrode some of the metals on the spacecraft and their high density adds unwanted mass. Nitrogen tetroxide is easier to handle because of its non-corrosive properties.

There are four choices for fuel based on industry use and performance. The four fuel were hydrogen (H_2), hydrazine (N_2H_4), monomethylhydrazine (MMH), and unsymmetrical dimethylhydrazine (UDMH). Hydrazine has the property of being both a fuel and a monopropellant depending on the catalyst. Almost all the fuels have the same properties varying slightly only in storability and cost. Monomethylhydrazine is the fuel mostly used for this type of mission in industry.

Another liquid propellant method considered uses water electrolysis instead of combustion, where two molecules of water are decomposed into molecules of hydrogen (H_2) and oxygen (O_2). This method provides both the oxidizer and fuel components of a bipropellant. Water electrolysis gives a high performance due to its high specific impulse (see Table 5.1). The main disadvantage is that water electrolysis is very complicated to use because it needs a large power supply. At present, this method is in the developmental stage.

5.2.3 Solid Propellants

Solid propellants are not very useful because they cannot be throttled or controlled. This is an important aspect to attitude control and maneuvering control. Another consideration with solid propellants is that they must be designed to burn evenly along the entire length to prevent unsteady thrust from the motor. Also, they produce too much thrust force to be useful for either attitude or maneuvering control.

5.2.4 Other Propellants

Other propellants and propulsion techniques were rejected on the basis of complexity, storage, or power requirements. These techniques included solar conversion and some corrosive liquid propellants.

5.3 Discussion of Propellants

5.3.1 Monopropellant

Due to the major and minor corrections in flight path, orbits, and trajectories, the attitude control subsystem must have large range capacities. It is proposed to use a combination of monopropellant and bipropellant thrusters for this mission. The monopropellant would be hydrazine (N_2H_4), which was chosen for a variety of reasons. It has a low bulk density of only 1.0 g/cm^3. Other characteristics include the fact that it is simple and reliable to use and store, it does not require the extra mass for an oxidizer, and it has a low thrust range. This last is important because it will be used to make the very small attitude changes or corrections such as precision pointing of the communication antenna and sensors.

5.3.2 Bipropellant

The bipropellant suggested is the MON-1 [Mixed Oxides of Nitrogen] /MMH configuration. This was chosen due to its relatively high I_{sp} (see Table 5.1) and its storability [15]. The density of MON-1/MMH is lower than some of the other bipropellants and therefore will not require as much storage volume, which will decrease tank mass. This configuration loses some I_{sp} but gains a slightly more stable propellant compared to other bipropellants. MON-1 is a derivative of nitrogen tetroxide (N_2O_4); however, it contains 0.8% NO, which produces a higher performance than regular N_2O_4.

5.4   Propellant Specifications

5.4.1   Hydrazine (N_2H_4)

The hydrazine must be stored between 274.5 K and 386.4 K, its freezing and boiling points respectively. It can spontaneously ignite with nitric acid, nitrogen tetroxide, and air. It has a positive heat of formation, 0.1256 kJ/kg, and therefore has a better performance than other fuels. As a monopropellant, it can be decomposed with certain catalysts at different temperatures. This decomposition is necessary to combust the propellant efficiently. The catalyst may have to be preheated to work efficiently. Iridium, at room temperature, iron, nickel, and cobalt, at 450 K, all decompose hydrazine well. Care must be taken not to store hydrazine in a tank made of the above materials [16].

5.4.2   Monomethylhydrazine (CH_3NHNH_2)

Monomethylhydrazine (MMH) is a derivative of hydrazine and is used only in rocket engines, usually as an attitude control propellant. MMH is most commonly used with N_2O_4 as an oxidizer and its vapors ignite on contact with air with a flammability of 2.5% to 98% per volume at sea-level conditions. The I_{sp} for MMH is about 1% to 2% lower than with other fuels. This however, is offset by the increased stability and management of the MMH. MMH usually decomposes at about 491 K in atmospheric pressure. MMH, like hydrazine, is very toxic and must be stored at about 300 K. It has a boiling point of 360.6 K, a melting point of 220.7 K, and a heat of vaporization of 790 kJ/kg [16].

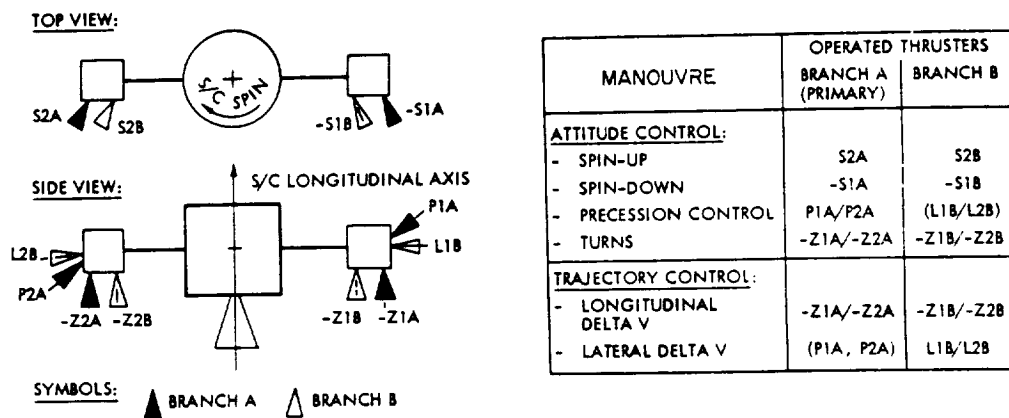### 5.4.3   Nitrogen Tetroxide (N_2O_4)

Nitrogen tetroxide has a boiling point of 294.3 K, a melting point of 261.5 K, and a heat of formation/vaporization of 413 kJ/kg. With a narrow liquid range, the storage tanks must be designed to prevent freezing or evaporation of the nitrogen tetroxide. One of this oxidizer's most attractive points is that it is not as corrosive in its pure state as other

II - 34

oxidizers. There is no problem storing it indefinitely, as long as it is not stored with anything that would make it hypergolic. Like the other propellants, nitrogen tetroxide's fumes are extremely toxic; therefore, special handling procedures are required. N_2O_4 usually uses MMH as its fuel counterpart, like those used in the Titan II missile systems. Even though the chosen oxidizer is MON-1, it still has most of the same properties as nitrogen tetroxide [16].

5.5 Attitude Thruster Engines

5.5.1 Monopropellant Thrusters

It is recommended that 12 monopropellant thrusters and 4 bipropellant thrusters be used on the spacecraft. Figure 5.1 shows a proposed position schematic of the 16 thrusters. The monopropellant thrusters will be used for precise control of the spacecraft, while the bipropellant thrusters will be used for mid-course maneuvers. The monopropellant thrusters used are a variation on the Mark II propulsion module developed by Martin Marietta. These thrusters can carry a maximum of 100 kg of propellant. The thrust nozzles are only 0.4 kg each. The tanks, however, will be designed to carry only 64.7 kg of propellant for each thruster resulting in a total propellant mass of 776.21 kg. An additional 300 kg of propellant will be required to clear debris during the drilling operations, detailed in a later section.

MANOUVRE	OPERATED THRUSTERS	
	BRANCH A (PRIMARY)	BRANCH B
ATTITUDE CONTROL:		
- SPIN-UP	S2A	S2B
- SPIN-DOWN	-S1A	-S1B
- PRECESSION CONTROL	P1A/P2A	(L1B/L2B)
- TURNS	-Z1A/-Z2A	-Z1B/-Z2B
TRAJECTORY CONTROL:		
- LONGITUDINAL DELTA V	-Z1A/-Z2A	-Z1B/-Z2B
- LATERAL DELTA V	(P1A, P2A)	L1B/L2B

Figure 5.1: Thruster configuration and functional capability (Sutton, G.P., *Rocket Propulsion Elements; An Introduction to the Engineering of Rockets*, John Wiley & Sons, New York, New York, 1986.)

Therefore, the total mass will be 1076.21 kg. The main function of these thrusters will be to establish orbit adjustments and attitude control for initial stabilization, sensor alignment, and roll control. Figure 5.2 gives the schematic configuration and specifications on the Mark II propulsion module. The hydrazine and nitrogen are initially pressurized to 2.76 MPa with a chamber pressure of 689 kPa. The propulsion feed temperature will be 422 K with a combustion temperature of 3000 K and an engine thrust of 22 Newtons. Figure 5.3 shows a hydrazine rocket engine with a steady state I_{sp} of 234 seconds and a pulse I_{sp} of 200 seconds.
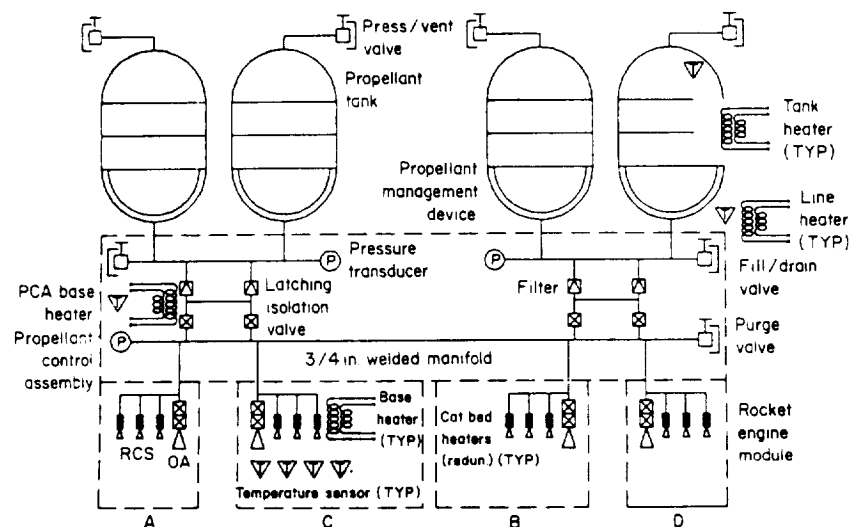
Figure 5.2: Mark II PM fluid schematic (Sutton, G.P., *Rocket Propulsion Elements; An Introduction to the Engineering of Rockets*, John Wiley & Sons, New York, New York, 1986.)
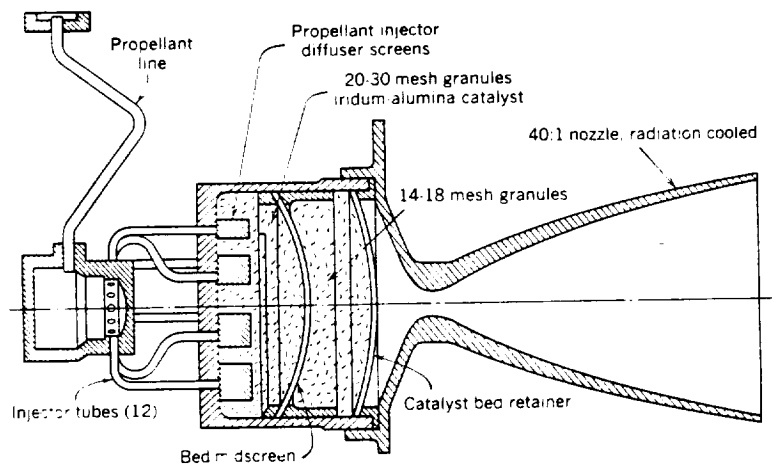
Figure 5.3: A typical attitude control rocket design using hydrazine monopropellant (Sutton, G.P., *Rocket Propulsion Elements; An Introduction to the Engineering of Rockets*, John Wiley & Sons, New York, New York, 1986.)

5.5.2 Bipropellant Thrusters

The bipropellant thrusters, which perform the velocity change and maneuvering control, operate at a propellant feed pressure of 1.7 MPa and chamber pressure of 758 kPa. The propulsion feed temperature is 294K, and the combustion chamber temperature is 3100K. Figure 5.4 illustrates the bipropellant thruster configuration. The bipropellant thruster is similar to that used in the Galileo propulsion module. This thruster class produces thrust for deflection maneuvers, orbit insertion, and periapsis raising maneuvers. The propulsion system utilizes a thrust vectoring system, see Figure 5.5, using a gimballed engine assembly. This system uses two electric actuators to deflect the thrust vector and can cause a deflection on the average of 10 to 15 degrees. The thruster configuration allows for smoother control by dividing the attitude control among a group of thrusters instead of just one or two. The thrusters provide 400 N of thrust each, a specific impulse of about 300 seconds, and a life of about 23 hours [16]. This thruster class is radiation and fuel film cooled to prevent overheating the combustion and nozzle chambers. The thruster uses an unlike stream impingement system as an injector for optimum mixing of the propellant and oxidizer. This

engine was developed by Messerschmitt-Bolkow-Blohm (MBB), has a mass of about 4.5 kg, and will use a total of 2534.1 kg of propellant [16].

Figure 5.4: A typical bipropellant attitude control thruster (Sutton, G.P., *Rocket Propulsion Elements; An Introduction to the Engineering of Rockets*, John Wiley & Sons, New York, New York, 1986.)

Figure 5.5: Gimballed engine assembly (Sutton, G.P., *Rocket Propulsion Elements; An Introduction to the Engineering of Rockets*, John Wiley & Sons, New York, New York, 1986.)
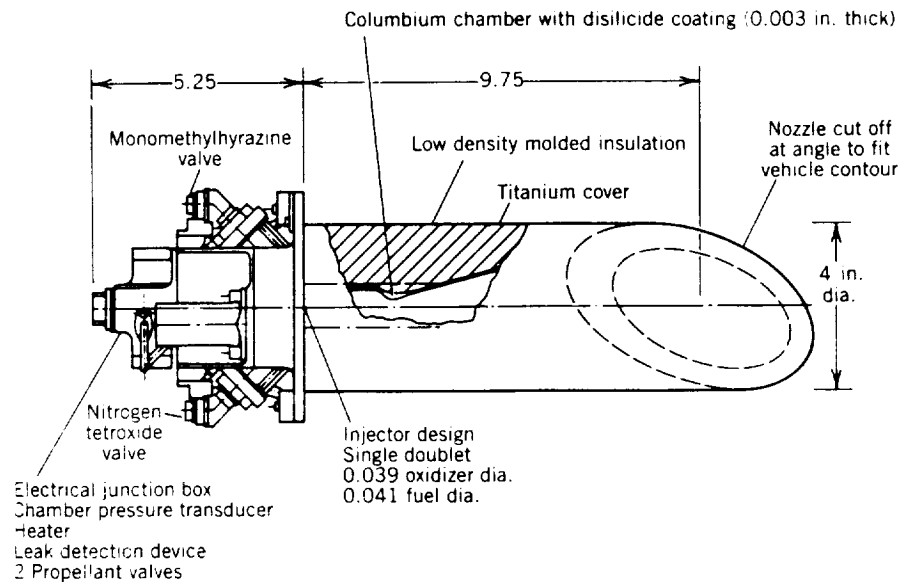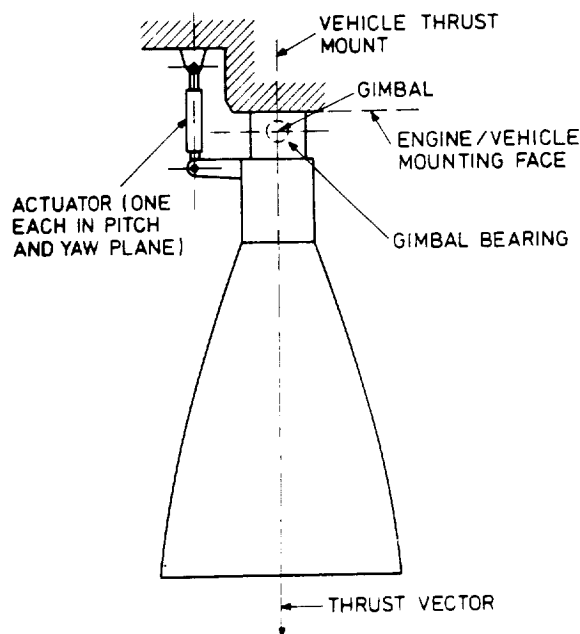
5.6   Conclusions and Recommendations

The mission will be using two types of propellants and thrusters. A monopropellant, hydrazine, will be used in the Martin Marietta designed thrusters. A series of twelve thrusters, along with reaction wheels, will control the attitude, three axis stabilization, and slewing requirements for the mission. Four MBB thrusters will use a bipropellant, Monomethylhydrazine and nitrogen tetroxide, to perform velocity changes and maneuvering. A total propulsion subsystem mass is estimated to be 3610.3 kg. This includes propellant and engine masses.

One of the major problems with the propulsion is the uncertainty of the effects on the spacecraft due to external forces. For example, the effects of solar activity, solar winds, solar radiation, and gravity effects of the Sun, depend on the year the mission is launched and the distance from the Sun. Other forces include, gravity gradients from other celestial bodies such as the Earth, 433 Eros, and other asteroids in close proximity to Eros, and the collision of micrometeors on the spacecraft. All of these must be corrected by using thrusters and reaction wheels. A more detailed analysis must be performed using both computer simulations and model testing to obtain the necessary data needed to correct for these external forces.

6.0   Guidance, Navigation, and Control (GN&C)

6.1   System Requirements

The overall Guidance, Navigation, and Control (GN&C) requirements for any mission are: establish and maintain the necessary course to accomplish the mission goals. These general requirements can be defined more specifically in terms of orbital mechanics (establishing the flight path) and dynamics and control (maintaining the flight path).

The specific requirements this mission places on the Attitude Sensing and Control (ASC) subsystem can further be divided into cruise phase and rendezvous phase, each of which places unique demands on the system's capabilities. During cruise, the main objective of ASC is to maintain communications with ground control by keeping the spacecraft pointed in a very specific direction at all times. When course corrections, defined by the orbital mechanics of the mission, are required, the ASC system must be able to provide them. During rendezvous and landing, ASC is required not only to maintain communications with Earth, but also to safely and accurately control the spacecraft to a secure landing. The potential complexity of the maneuvers at rendezvous thus make this the most demanding mission phase for the ASC designers to accomodate.

6.2   Orbital Mechanics

The main goal of the orbital mechanics subsection of the mission is to precisely determine the flight trajectory, transfer windows, and attitude maneuvers necessary to complete the mission. The resulting information from this analysis is then used by many of the subsystems as a part of their design parameters. The most immediate use of the information is by the GN&C subsystem, which is responsible for maintaining the flight parameters established by the mission analysis. Table 6.1 lists how some other subsystems use the information from the mission profile.

Table 6.1: System Interdependencies with Orbital Mechanics.

Subsystem	Influencing Factors

Propulsion	Velocity changes for:
	    Launch
	    Transfer and Rendezvous
	    Return and Capture

Communications	Maximum Transmission Distance Spacecraft orientation to point antenna Communications interference from Sun
Scientific Instrumentation	Required orientation for instruments
Thermal Control	Orientation toward and distance from Sun

With these factors in mind, analysis was begun on how mission parameters could be selected to minimize the cost requirements of these subsystems.

6.2.1 Transfer Optimization

With the selection of the destination (433 Eros) already made, designing the mission profile by varying this parameter is not possible. Attention is first focused on the propulsion subsystem, with the intent of minimizing the transfer velocity requirements. This, of course, translates directly into propellant (and cost) savings.

In a paper from the joint AAS/AIAA Astrodynamics Specialist Conference [17] global optimum ΔV characteristics for several asteroids were presented. Table 6.2 is an excerpt from this paper, listing the best available launch windows and characteristics between 1993 and 2010.

Table 6.2:   Possible Mission Windows (Lau, C.O. and Hulkower, N. D., "On the Accessibility of Near-Earth Asteroids," AAS/AIAA Astrodynamics Specialist Conference, Vail, Colorado, Aug. 12-15, 1985.)

Launch Date	Launch Energy $(km/s)^2$	Arrival Date	Post Launch ΔV (km/s)
01/20/93	28.17	06/28/94	3.560
01/21/00	29.66	07/14/01	4.491
01/21/07	31.17	11/03/07	3.353

It was decided that while the second opportunity had the highest ΔV, it was the closest of the three to the expected launch date. One drawback common to each of the three orbits considered is the need for a mid-course correction. For the orbit chosen, it occurs on the 281st day of the transfer. An inspection of the orbital parameters of Eros shows that this maneuver corresponds to an inclination change at the ascending node of Eros' orbit. The orbital parameters of Eros are as follows [18]:

$$
\begin{aligned}
a &= 1.4583155 \\
e &= 0.22228695 \\
i &= 10.826580 \\
\Omega &= 303.73856 \\
\omega &= 178.58421 \\
M &= 209.78952
\end{aligned}
$$

Ecliptic and Equinox — 1950.0

Epoch 1991 — December 10.0 ET

JD 2448600.5

With the information on the launch and rendezvous dates, reconstruction of the complete transfer becomes little more than a two-point boundary value problem. A program was developed to simulate the entire mission, keeping track of the relative positions of the Sun and Earth, with the intentions of using this information for the other subsystems. As stated earlier in Table 6.1, the position of these two bodies during the mission will play a considerable role in the communications and thermal control areas.

6.2.2 Mission Profile

The mission profile consists of a small number of large-scale transfer maneuvers, and a large number of small-scale attitude maneuvers for communications and other instrumentation alignment. In this section the focus is placed on the transfer maneuvers — their magnitude, direction, and timing. Table 6.3 contains a more complete list of the mission profile.

Table 6.3: Characteristics of Large Scale Mission Profile (Lau, C.O. and Hulkower, N.D., "On the Accessibility of Near-Earth Asteroids," AAS/AIAA Astrodynamics Specialist Conference, Vail, Colorado, Aug. 12-15, 1985.)

Date of Launch	01/21/00
Launch Energy $(km/s)^2$	29.66
Maneuver Date	10/29/00
Time of Flight (days)	540
Date of Arrival	07/14/01
Post-Launch DV (km/s)	1.172
Time of Flight (days)	394
Date of Arrival at Earth	01/24/03
Length of Mission (days)	1099

From the data above, it can be seen that the total ΔV for the round trip from LEO to LEO is approximately 13 km/s. Figure 6.1 shows the shape of the spacecraft's transfer orbit from the Earth to Eros. One characteristic of the orbit is that it is greater than a 360 degree transfer. The spacecraft re-traces the first portion of its flight approximately 520 days after launch.
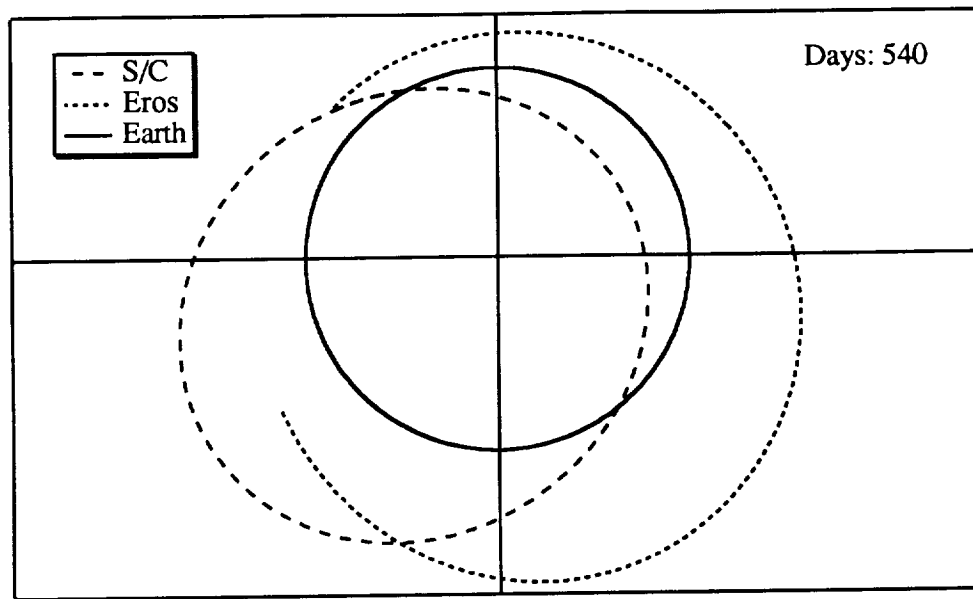
Figure 6.1: Shape of Spacecraft Transfer from Earth to Eros

6.2.3 Other Subsystem Considerations

As stated earlier, one of the functions of the orbital analysis is to determine certain parameters of use to the other subsystems. The transfer ΔVs and maneuver dates for the propulsion and navigation systems have already been determined. At this point consideration must be given to the thermal and communication systems. One of the requirements common to both of the above mentioned subsystems is the known position of the Sun relative to some body fixed axis system on the spacecraft. For the thermal subsystem, it is desirable to know the Sun's direction to regulate the amount of radiative heat transfer that occurs. For the communications subsystem, both the position of the Sun and the Earth must be known, so that predictions can be made as to if, when, and for how long communications may be impaired by an occultation. Figure 6.2 shows how the in-plane angular position (relative to the spacecraft) of Eros, the Earth, and the Sun vary throughout the 540 day transfer. Because of the low inclination of Eros, the intersection of the Sun's path with that of the Earth on the

graph is sufficient to warrant concern about communications at selected times during the flight.

6.2.4 Recommendations

The analysis tools used for the orbital mechanics portion of the mission are about 85% complete. Only slight additions and modifications to the program are needed to allow for the generation of more useful data that can be used by the other subsystems. One change which should be made is in determining the orbit from the boundary conditions (Launch and Rendezvous). This portion of the analysis was actually done in a separate program, requiring the data to be transferred by hand into the main program. By combining these it would allow for a more direct method of reproducing the necessary orbit. The analysis was also performed only on the Launch/Rendezvous portion of the mission. It is also necessary that it be done for the return trip. Again, if these two programs are joined, the return trip analysis will consist of no more than reversing the initial and final conditions of the problem.
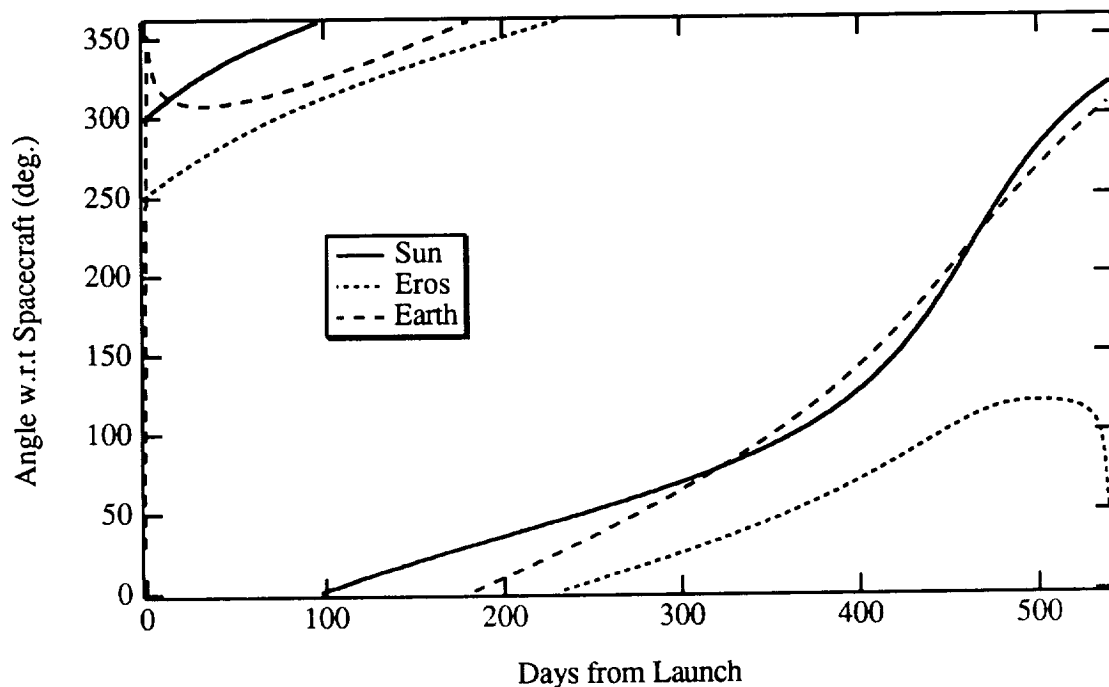
Figure 6.2:   In-plane angular positions of the Earth, Sun, and Eros during 540 day transfer

Another improvement which should be made is to take the calculation of the relative positions of the Earth and Sun one more step. Right now the reference frame is anchored to the radius vector of the spacecraft. To allow for the useful translation of their coordinates to the other systems, it is necessary that the final frame be fixed to the spacecraft as mentioned earlier. Once this last frame is incorporated, a multitude of useful (and necessary) information, such as thrust vectors for attitude maneuvers, and the aforementioned tracking and instrumentation pointing maneuvers can be defined.

6.3 Mission Maneuver Profile (MMP)

Once the orbital mechanics of the mission have been determined, a list of maneuvers from launch to recovery must be made which will then define the specific requirements for the hardware of the GN&C subsystem. Table 6.4 gives the Mission Maneuver Profile (MMP), with initial sizing of the larger maneuvers and stationkeeping pointing accuracy requirements. As will be shown in the following sections, these requirements constitute the limiting cases which need to be examined in the selection and sizing of the spacecraft's GN&C hardware.

6.4 Attitude Sensing and Control (ASC)

This topic includes spacecraft stabilization, attitude determination, and attitude control. Unlike orbital mechanics, which deals largely with the theoretical analysis involved in the definition of the MMP, ASC primarily handles the more particular issues of hardware selection and sizing. The requirements for the ASC subsystem are derived from (or simply taken from) the MMP.

Table 6.4: Mission Maneuver Profile (MMP): From LEO Parking Orbit to Recovery

1. Reorient spacecraft for thrust into transfer orbit
2. Thrust to transfer orbit
3. Reorient for communications -- stationkeeping (3-8 mrad)[1]
4. Reorient for midcourse correction ($\approx 90°$ slew)[2]
5. Perform midcourse correction (10.8° plane change)
6. Reorient for communications -- stationkeeping (3-8 mrad)[1]
7. Reorient for rendezvous course correction (slew for retrograde thrust?)
8. Perform rendezvous course correction(s) (thrust to target orbit)
9. Slow to match Eros orbit as altitude above Eros approaches 2.5km; select 3 most promising landing sites
10. Reorient to "orbit" about Eros over most promising landing site; compensate for rotation of scanning platform, perform detailed scan
   -> If site proves unsatisfactory, go to next of three most promising, repeat
   -> If all three sites prove unsatisfactory, repeat step 9
11. Rotate to keep landing area in sight
12. Land
13. Keep stable on ground (if torques from drill exceed expected levels)
14. Launch from Eros
15. If fuel, time allow, perform maneuvers required for detailed mapping (steps 9,10)
16. Reorient for departure
17. Thrust to return transfer orbit
18. Reorient for communications -- stationkeeping (3-8 mrad)[1]
19. Reorient for midcourse correction and perform
20. Reorient for communications -- stationkeeping (3-8 mrad)[1]
21. Reorient for thrust to LEO recovery orbit ($\approx 180°$ slew)[3]
22. Thrust to LEO recovery orbit
23. Reorient for communications -- stationkeeping (3-8 mrad)[1]

1: Pointing requirements for stationkeeping are based on the requirements given for the Apollo (8 mrad) and Galileo missions (3 mrad) [19,20]
2: See orbital mechanics section for details on requirements of midcourse correction.
3: Size of this maneuver based on: (1) the communications hardware and main thruster are located on opposite "ends" of the spacecraft and (2) the assumption that that the spacecraft will be pointing almost exactly in the direction of the burn. If (2) is untrue, maneuver will be smaller

6.4.1 Spacecraft Stabilization

A number of different factors influence the choice of stabilization method for any given spacecraft. Environment, scientific instrumentation, communications, and mission duration all must be considered in the design of a spacecraft's stabilization system.

First of all, the pointing accuracy requirements for communications purposes must be considered. This is an especially crucial issue for interplanetary missions, when a very small error in pointing angle may cause complete "blackout" of the communications system. The stationkeeping requirements for this mission, as listed in the MMP, are currently estimated at

3 and 8 milliradians (0.17° to 0.5°), based on similar requirements for the Galileo and Apollo missions, respectively [19,20].

This mission will use three-axis stabilization. There had been some debate about whether to use three-axis stabilization or a dual-spin method, Table 6.5 describes briefly the differences between the two types of systems. The debate arose largely due to the possibility of including in the scientific payload certain instruments which were either required or *preferred* to be mounted on a constantly spinning platform. However, the inclusion of such a platform would increase the overall complexity of the spacecraft, whether or not it decreased the particular complexity of the scientific payload, as the platform would have to be despun in any event for landing and sample acquisition. In addition, the techniques and technologies of dual-spin stabilization have only recently "come of age" for interplanetary missions (such as Galileo). Three-axis stabilization systems, on the other hand, have been used with great regularity and reliability in interplanetary flight for many years. Thus, the decision for three-axis stabilization was made based on overall system simplicity, known reliability and accuracy for interplanetary missions, and continuity of mission design.

Table 6.5: Three-axis and Dual-Spin Stabilization (Wertz, J.R. and Larson, J., eds., <u>Space Mission Analysis and Design</u>, 1991, Kluwer Academic Publishers, Inc., Dordrecht, The Netherlands, Table 11-5, p. 309 and Table 11-6, p.311)

	Three-Axis	Dual-Spin
Accuracy	0.001° - 1° or more	0.3° - 1° or more
Maneuverability	Limited only by size and type of actuators	Momentum vector along spun axis very stiff
Pointing Options	No constraints	Limited by articulation on despun section of spacecraft
Sensor Options	Depends on accuracy required; starsensors, IMUs	Depends on accuracy required; starscanners, sunsensors may be adequate; also IMUs
Lifetime Limits	Propellant Sensor Bearings	Propellant Sensor and Despin Bearings

Once the stabilization technique had been determined, the corresponding hardware had to be selected and sized. For this mission, momentum wheels will be used as the primary stabilization actuators, with monopropellant thrusters as back-up and to desaturate the wheels when necessary. Table 6.6 gives a description of a few different types of stabilization hardware including some of their advantages and disadvantages which were considered in the final selection.

Table 6.6: Three-Axis Stabilization Hardware (Wertz, J.R. and Larson, J., ed., Space Mission Analysis and Design, 1991, Kluwer Academic Publishers, Inc., Dordrecht, The Netherlands; also Knorren, H. and Lange, T., "Modular Design and Dynamic Tests on Active Bearing Momentum Wheels", Automatic Control In Space, Proceedings of the 9th IFAC Symposium, 1982)

	Power (W)	Mass (kg)	Performance
Reaction Wheels	10-110	2-20	0.01-1.0 Nm 0.4-400 Nms
Momentum Wheels	5-120	8.9-13.4	30-150 Nms
CMGs	90-150	> 40	25-500 Nm
Hydrazine Thrusters	N/A	Variable	0.5-9000 N

As previously discussed, the communications for this mission demand very accurate stationkeeping capabilities. The stabilization actuators must be able to maintain that pointing accuracy of 3-8 mrad despite the presence of disturbance torques acting on the spacecraft. These disturbance torques come from a number of sources, both internal and external. For this mission, the two sources of disturbance torques most likely to be the limiting cases are (1) torque due to solar pressure (external source) and (2) torque due to the rotation of the scanning platform during rendezvous and approach (internal source). The second of these is discussed in more detail in the section on control during rendezvous and landing (6.4.4).

On interplanetary missions such as this one, where the spacecraft spends the majority of its lifetime not in near proximity to a major gravitational, magnetic, or aerodynamic gradient, the torque due to the pressure exerted on the spacecraft by the solar radiation

generally becomes the dominating external torque. Griffin and French [21] give the following equation for calculating the solar radiation pressure torque:

$$T = rA(1 + K)(I_s / c)$$

where r = distance between center of mass and center of optical pressure (≈ 0.1m)
A = area of spacecraft normal to sun (≈ 5 m^2)
K = spacecraft reflectivity (≈ 0.5)
I$_s \approx 1400$ W/m^2 at 1 AU (estimated to be ≈ 1000 W/m^2 at 2 AU)
c = 2.9979x10^8 m/s

Using the values given above, the disturbance torque due to solar radiation pressure was calculated to between 2.5x10^6 and 3.5x10^6 Nm.

Wertz and Larson [8] give a simple expression for estimating the required angular momentum capacity for a momentum wheel based on knowledge of the limiting external disturbance torque (gives accuracy to one degree):

$$H = (10)(T)(\text{quarter orbit period})$$

Unfortunately, it is not mentioned whether or not this equation works only for Earth-orbiting spacecraft — which are predominantly influenced by gravity-gradient and magnetic torques — or for heliocentric as well. In any event, using this equation, the requirements for the angular momentum of the momentum wheels would be somewhere between about 30 and 100 Nms, both of which values are in the practicable ranges of the wheels studied for this mission. Based on this number, the final selection of momentum wheel configuration, from Knorrchen and Lange's paper on the Magnetic Bearing Momentum Wheel (MBMW) with variable rotor mass and variable rotation [21], was made. The wheels each have a mass of 13.4 kg, a peak power requirement (at power-up) of 120 W and steady-state power requirement of 7 W, a maximum nominal speed of 8000 rpm, with corresponding angular momentum of 150 Nms. This is well above the predicted values of 30-100 Nms referred to above, but because of the uncertainty in those calculations, the higher angular momentum was selected.

6.4.2 Attitude Determination

The requirements for accurate attitude sensing for an interplanetary mission are relatively well defined. The main dilemma in this area is the selection of specific types of sensors to meet accuracy requirements.

The basic configuration of the attitude control system for this mission will consist of two or more strapdown Inertial Measurement Units (IMUs) equipped with accelerometers as well as gyro assemblies in order to determine both the translational and rotational position of the spacecraft. Because of gyro drift, the inertial reference for the IMUs will need to be reset periodically. Sunsensors and starsensors, which are too slow in most cases to be used continuously, will be used for this purpose. In the interest of keeping the mission as a whole both as reliable and as inexpensive as possible, the current configuration of the attitude determination hardware consists of two sunsensors (one high accuracy, one low accuracy for back up), two starsensors (ibid.), and three IMUs. Table 6.7 lists the masses, accuracies, and power requirements for all five types of sensor.

Another intriguing possibility for attitude and position determination is described by Van der Ha and Caldwell in their paper on the integrated on-board and ground-based computer attitude reconstruction system used on the HIPPARCOS mission (ESA, 1988) [27]. This system combines on-board sensing and control with ground-based attitude reconstruction and prediction. This combination detects deviations from the planned flight path and required spacecraft orientation, which can give the mission more accurate and reliable station-keeping capabilities. However, as continuous use of a ground-based reference would require a great deal of computer and communications time, using this type of system for the primary attitude determination would probably interfere with the transmission of scientific data — especially during landing and sampling — and thus would be detrimental to the mission as a whole. On the other hand, several recent missions have demonstrated the value of having as many back-up systems as possible, and the implementation of a HIPPARCOS-type integrated system could be an excellent reserve system.

Table 6.7: Attitude Determination Hardware. (Connolly, A. et. al., "Synopsis of Optical Attitude Sensors Developed by ESA," Automatic Control In Space, Proceedings of the 9th IFAC Symposium, 1982, pgs. 257-264; also Wertz, J.R. and Wiley, J.L., editors, Space Mission Analysis and Design, 1991, Kluwer Academic Publishers, Inc., Dordrecht, The Netherlands, Table 11.12, pg. 323.)

Sensor	S/C Stabilization	Accuracy	Mass (kg)	Power (W)
IMU[1]	three-axis	≈0.003 °/hr random drift	20.0[2]	75.0[2]
High Accuracy Sun Sensor[3]	three-axis	0.01-0.05 arcsec	≈ 10	≈ 15
Multipurpose Sun Sensor[4]	three-axis	≤ 0.04°	1.65	10.4
Image Dissector Tube Star Tracker (IPS)[5]	three-axis	0.67-0.95 arcsec	12.0	22
Star Mapper	Spin or three-axis[6]	≤ 1 arcmin	≈ 2	≈ 10

1: An example of an IMU "package" is described in detail in Reference [24].
2: No mass or power requirement given in [24]; Estimate from data in Wertz and Larson, [8].
3: This sensor is described in detail in Reference [25].
4: Sensor recommended for various Earth orbits. Not specifically designed for heliocentric orbits. This sensor is described in detail in Reference [26].
5: This sensor was developed in 2 versions, one highly accurate for use in the Spacelab Instrument Pointing System (IPS), the other smaller and less accurate for EXOSAT (Both Earth orbiting).
6: This sensor was originally developed for a spacecraft spinning at 10 rpm. Later studies showed that it was relatively easy to modify control algorithm for approximately non-spinning (1 rev per 100 min) spacecraft.

6.4.3 Attitude Control

In selecting and sizing the attitude control hardware, the MMP must be inspected for two things: the smallest necessary maneuvers (i.e., the pointing accuracy requirements), and the largest necessary maneuvers. The determination of the type of attitude control system is dependent upon both of these; in fact, most spacecraft almost have two separate attitude control systems — one for stationkeeping and one for large slewing maneuvers. This mission will be no different.

For station-keeping, the same momentum-biased wheels used to stabilize the spacecraft can be used to correct minor deviations in orientation, with monopropellant thrusters used as both backup stabilization actuators and desaturation (or "momentum dumping") devices for the momentum wheels. The dilemma arose with the selection of the primary actuators to be used for larger maneuvers: either a Control Moment Gyroscope (CMG) or thrusters.

This dilemma, along with the long-term debate about stabilization methods, led to an interesting idea. During cruise phase, the stiff momentum vector of a dual-spun spacecraft could be very beneficial to mission stability. Despinning the spun platform at rendezvous would give the spacecraft a large amount of excess momentum, which could then be used to spin up a CMG. With this approach, the quick, precise, and large maneuvering capabilities potentially necessary at landing could be easily handled by the CMG, while during cruise phase to and from Eros, thrusters could handle the maneuvering requirements.

However, as can be seen in Table 6.6, CMGs are not only very massive, but require a great deal more power than momentum wheels at steady-state. Because rendezvous and landing is already one of the peak power times, the addition of a CMG, to be used exclusively during this phase, could represent an unacceptable level of increase to the power budget, and possibly merit an increase in the capacity (and therefore size) of the power system *in addition* to the increases already made in the mass budgets for the CMG. This consideration along with the increased complexity and instability of the system due to spinning-up and despinning the platform and the CMG at different times during the mission, led the design back to the most simple system possible: spacecraft stabilization to be achieved using momentum wheels, and large slewing maneuvers to be controlled with hot-gas (hydrazine) thrusters.

Sizing of the thrusters, as discussed in further detail by the propulsion group, was based primarily on the larger maneuvers required as given in the MMP. A margin of safety

was added to the propellant mass, such that additional maneuvering at rendezvous would be possible if it became necessary.

6.4.4 Control During Rendezvous and Landing

Although this area currently remains the most undefined topic in the design of the GN&C subsystem, there are a number of issues in the process of landing the spacecraft which have been explored. Looking again at the MMP, the maneuvers to be made during the process of rendezvous and landing are:

10. Reorient to *"orbit" about Eros* over most promising landing site; *compensate for rotation of scanning platform*, perform detailed scan
      -> If site proves unsatisfactory, go to next of three most promising, repeat
      -> If all three sites prove unsatisfactory, repeat step 9
11. *Rotate to keep landing area in sight*
12. *Land*

The italicized phrases are the areas of the most concern to the ASC group. They are addressed in more detail below.

It is uncertain exactly what orbiting about Eros would consist of at this point beyond a combination of linear thrust and slow "pitching" to keep the spacecraft on a somewhat circular path over the same spot on a rotating body (Eros). It is assumed that this maneuver will not last for more than about 5-10 min at a time. However, rotating to keep the final landing area in sight could very easily take a lot more time and energy than rotating with Eros to select the candidates for the landing area.

This spacecraft has, as part of its scientific instrumentation, a scanning platform similar to the one used on the Cassini mission which uses several different types of scans (visible, ultra-violet, laser radar) to detect hazards — such as boulders and pits — on potential landing sites. The platform is located at the end of a boom off one side of the spacecraft, and rotates to achieve a wider range of "vision." Because the scanning platform, described in detail by the scientific instrumentation group, moves independently of the

spacecraft, it will exert torques on the main body of the spacecraft, which must be balanced for stability. In addition, the spacecraft will have to compensate for the powering-up of the scanning platform — and thus presumably the spinning-up of the platform's actuators — during step 8 or 9 of the MMP.

In order to utilize the information from the scanning platform, a number of algorithms must be developed to process the data. For example, in order to determine the orientation of the spacecraft with respect to Eros, a program will need to process the data from the scanning platform, which will indicate *its* position relative to Eros, as well as its inertial position, and then examine the spacecraft's inertial position and deduce from those three pieces of information where the spacecraft is relative to Eros. Also, an algorithm which will communicate that position to Earth will have to be written which takes into account the time delay inherent in any such interplanetary transmissions. This would be an especially crucial program in the event of a failure of the autonomous landing system (which in itself will be a challenge). An example of a time-delay compensation algorithm can be found in [28].

6.4.5 Mass and Power Budgets for ASC Hardware

Table 6.8 gives the mass and power budget for the ASC subsystem. It should be noted that the hardware included in this budget, as well as the numbers given, represent the "worst case scenario" for this subsystem. The numbers given in these budgets are estimates based on data given in Wertz and Larson [8], Flamenbaum and Anstett [26], and Connolly et. al. [23], and where appropriate were also referenced in Tables 6.6 and 6.7.

Table 6.8: ASC Mass and Power Budget

Device	Function	Mass (kg)	Peak Power (W)
2 IMUs	Attitude sensing	40.0[1]	150.0[1]
Sunsensors (Multipurpose, HASS)	Ref. for IMUs	15.0[1]	20.0[1]
Starsensors (IPS version, Starmapper)	Ref. for IMUs	30.0[1]	30.0[1]
4 Momentum Wheels	Spacecraft Stabilization	55.0[2]	350.0[2]
TOTAL		**135.0**	**550.0**

1: See Table 2.7.
2: From Reference [24].

6.4.6 Recommendations

The conceptual and preliminary design of the ASC subsystem has been performed. However, very few of the calculations made to date are better than educated guesses in equation form, although the major problems to be addressed have, at the very least, been defined. The next step in the ASC design would consist of performing the more detailed analyses required. The disturbance torques, for example, need to be determined with more accuracy, as well as the sensor mass and power budgets. The control algorithms for rendezvous and landing need to be designed and written, and could be simulated and studied in great detail.

7.0 Communications Subsystem

7.1 Requirements

Spacecraft communications require the use of advanced electronic techniques for both the Earth-based systems and the spacecraft systems. Size and weight constraints limit the design of the spacecraft communications system. The spacecraft's operating environment also plays a key role in the system design.

One of the communications system's primary objectives will consist of performing high-speed, two-way information transfers. The communications system will relay to Earth the spacecraft's health and position as well as scientific data and images. The spacecraft must receive messages from Earth such as attitude adjustments, in-orbit corrections, and emergency manual landing override commands, if necessary. To accomplish this objective, the system will require high frequencies and high data rates.

7.2 Communications Subsystem Description

7.2.1 Frequency Band Selection

The K_a band has the highest frequencies the spacecraft can achieve without exceeding economic constraints. Because low frequency bands are widely used in communications systems, the use of higher frequency bands will most likely ensure a high clarity signal. The communications system will use uplink and downlink frequencies of 30 GHz and 20 GHz, respectively [29].

7.2.2 The High-Gain and Low-Gain Antennae

The High-Gain Antenna (HGA) will have a 3.5 meter diameter. An antenna of this size will provide the large power output to input ratio required for high speed

communications. During launch, the HGA will be folded to fit into the launch shroud. After the spacecraft is ejected from the shroud, the HGA will unfold.

The Deep Space Network (DSN) can receive a signal with a minimum power intensity of 10^{-17} W/m^2. From this basis, the minimum radiated uplink and downlink powers for the high-gain antenna were determined.

The gains of both the spacecraft and the DSN antennae were calculated using the following equation:

$$GAIN = 10\log_{10}\left[0.55\left(\frac{\pi D f}{c}\right)^2\right]$$

where D is the antenna diameter, f is the signal frequency, and c is the speed of light in a vacuum.

The communications system will employ two low-gain antennae pointing opposite each other, providing a full 360° of coverage.

7.2.3 Data Transfer Rates

To accomplish high speed communications, a data rate of 1.544 Mbps will be required. Using this data rate plus a 200% overhead, the communications system will send a complete image every 65.2 seconds. The transmitted CCD images will be composed of a 1024 x 1024 pixel grid with each pixel containing 4 bytes of information. To accommodate the large data handling and storage requirements involved with the imaging equipment, the communications system will employ a Digital Tape Recorder (DTR) [30].

7.2.4 Signal Modulation

All signals will be modulated using Quadrature Phase Shift Keying (QPSK) which was chosen because of its proven reliability. For the required data rate and, using QPSK the required bandwidth will have a magnitude of 926,400 Hz [29].

7.2.5 Path Losses

Travelling through space and Earth's atmosphere, the signal will experience losses. The required power and the signal path loss are both functions of the 3 AU maximum distance between Earth and Eros. These path losses can be determined by the following equation

$$PATH\ LOSS = 20 log_{10}\left[\frac{4\pi S f}{c}\right]$$

where S is the distance transversed by the signal (3 AU maximum), f is the frequency, and c is the speed of light in a vacuum.

7.2.6 Mass, Power, and Data Rate Budget

The total mass and power of the communications subsystem is based on existing systems. Eighty percent of the total power is consumed by the HGA and the power amplifier. The most reliable, efficient, and frequently used power amplifier is the traveling wave tube amplifier (TWTA). A typical TWTA uses 19.715 Watts of power [30]. Table 7.1 details the specifications of the communications subsystem [31].

Table 7.1: Communications Subsystem Specifications (Bostian, C.W., and Pratt, T., *Satellite Communications*, John Wiley & Sons, New York, 1986.)

Total Mass		30.0 kg
Total Power		80.0 W
Uplink Frequency		30.0 GHz
Downlink Frequency		20.0 GHz
DSN Antenna Diameter		120.0 m
High Gain Antenna Diameter		3.5 m
High Gain Antenna Efficiency		0.55
Max. Data Rate		1.544 Mbps
Required Bandwidth		926.4 kHz
Spacecraft Antenna Power Radiated	Uplink	19.05 W
	Downlink	42.86 W
Spacecraft Antenna Gain	Uplink	58.23 dB
	Downlink	54.71 dB
DSN Gain	Uplink	88.93 dB
	Downlink	85.41 dB
DSN & Spacecraft Antenna Path Loss	Uplink	235.03 dB
	Downlink	231.51 dB

7.3 Conclusions and Recommendations

The communications system will consist of one high-gain antenna (HGA) measuring 3.5 m in diameter and two low-gain antennae which provide 360° of coverage. The communication transmission will use a high-frequency K_a band to maximize the signal's clarity. This communications system will modulate the signal using reliable Quadrature Phase Shift Keying (QPSK). A Digital Tape Recorder (DTR) will store the large amounts of data taken by the various imaging devices and transmit this data in packets manageable by the HGA.

8.0 Ground Support

8.1 Requirements

The spacecraft will require adequate Ground Support to ensure the mission's success. It must supply a sufficent communications link between the spacecraft and the Mission Operations Center (MOC).

8.2 Ground Support Description

The mission will utilize the Deep Space Network (DSN) for ground support. Since the spacecraft must travel in interplanetary space, the DSN will provide adequate communications between Earth and the spacecraft. The DSN plays an important role in the mission, since it will collect and analyze all data sent back to Earth from the spacecraft. The DSN is operated for NASA by the Jet Propulsion Laboratory (JPL). DSN stations are located at three locations around the world to collect important data from space. These three installations forward commands to the MOC at JPL. Data rates of the DSN have increased over the years, and at present they are quite high. For example, in 1973, Mariner 10 achieved 117,200 bits per second (bps) from Mercury. At the distance from Eros to the Earth, the DSN should provide an excellent communication link between the spacecraft and MOC [32].

8.3 Conclusions and Recommendations

To ensure a successful mission, the spacecraft will rely on the DSN to fulfill its ground support communication needs.

9.0 Command and Data Handling (C & DH)
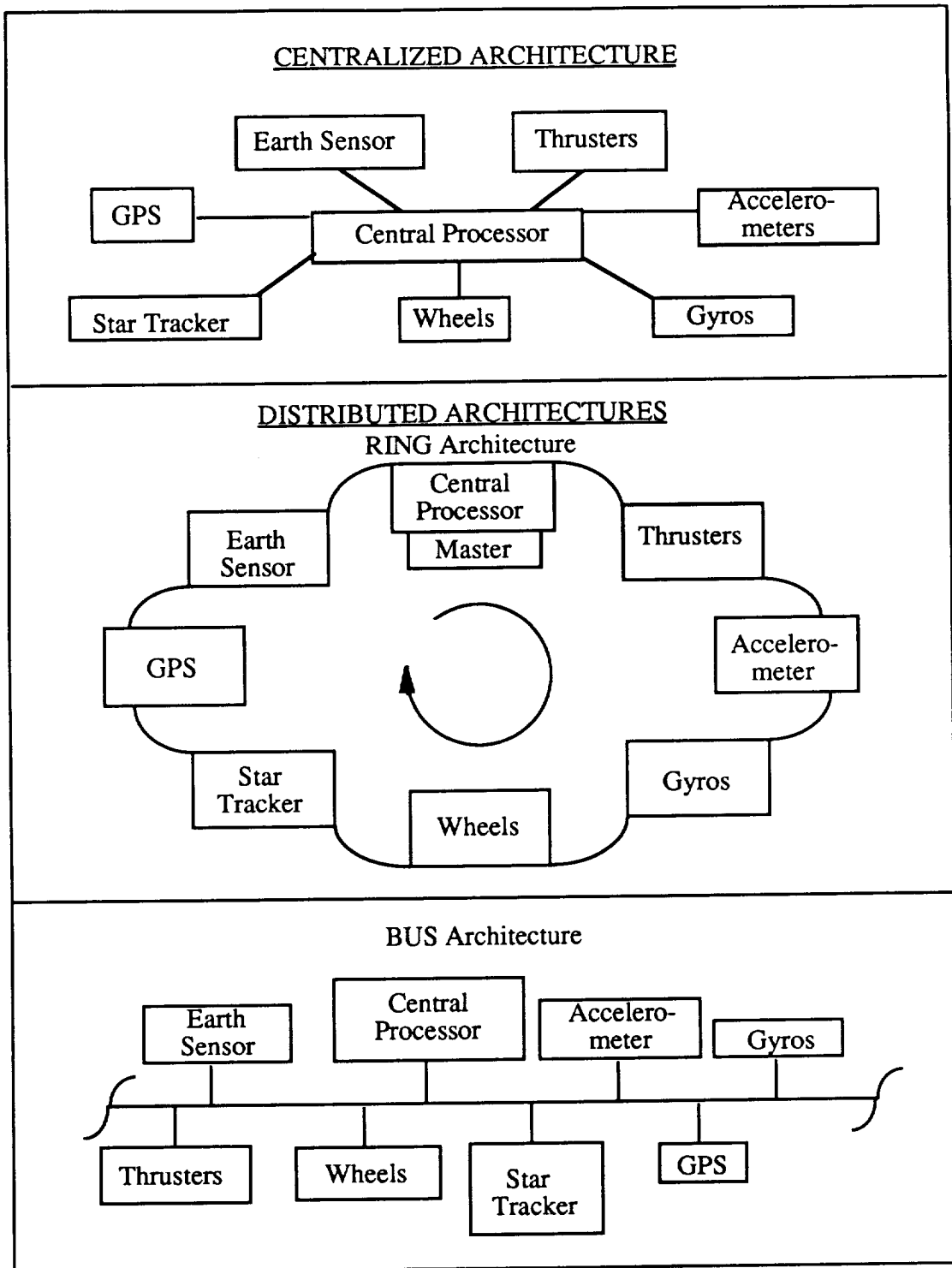
9.1 Requirements

The Command and Data Handling subsystem, often referred to as the brains of the spacecraft, is one of the most complex subsystems onboard. Defined by mission requirements and spacecraft parameters, C & DH interacts with all onboard subsystems through data and telemetry buses, and with ground control through communication downlinks. The C & DH subsystem is responsible for receiving and distributing data and commands; it also collects, formats, and relays standard operations telemetry and housekeeping to Earth. The extent of this subsystem's capabilities are severely limited by technology and cost. Due to these limitations, a rigid design procedure must be followed to ensure that the most simple system is developed to carry out all of the mission's tasks [8].

9.2 C & DH Architecture

The basic framework for a computer system is called the architecture. The architecture of the system is dependent on mission specifications and operational needs. There are two basic types of architecture, centralized and distributed. Figure 9.1 illustrates block diagrams for the two basic types. A new architecture type, which is finding increased usage, involves any combination of the two aforementioned types. This hybrid type architecture combines the best attributes of, and eliminates many of the major problems associated with, the constituent architecture types [8].

9.2.1 Centralized Architecture

Resembling a spider, the centralized architecture is perhaps the simplest to design. It consists of a central or hub processor and point-to-point interfaces with several remote units (Figure 9.1) [8].

CENTRALIZED ARCHITECTURE

Earth Sensor · Thrusters · GPS · Central Processor · Accelero-meters · Star Tracker · Wheels · Gyros

DISTRIBUTED ARCHITECTURES

RING Architecture

Central Processor / Master · Earth Sensor · Thrusters · GPS · Accelero-meter · Star Tracker · Wheels · Gyros

BUS Architecture

Earth Sensor · Central Processor · Accelero-meter · Gyros · Thrusters · Wheels · Star Tracker · GPS

Figure 9.1: Block Diagrams of Architecture Types. (Derived from Figures in Wertz, J.R. and Larson, W.J., eds., *Space Mission Analysis and Design*, Kluwer Academic Publishers, Norwell, MA, 1991.)

9.2.2   Distributed Architecture

The distributed architecture shows a different approach to computer design. There are two basic types of distributed architectures; they are the bus and ring configurations. The bus architecture makes use of a common interface, or bus, and all remote units share this. The ring architecture, as the name implies, is made up of a loop interface. Figure 9.1 illustrates examples of both types of distributed architectures; notice that there is no central hub, but there is a central or main processor [8].

9.2.3   Hybrid Architecture

As previously stated, the hybrid architecture is a combination of one or more of the other architecture types. Commonly, a ring, a bus, and a centralized architecture may be combined to create a rather effective hybrid. Such a hybrid combines the best attributes of all architecture types while eliminating many of the problems associated with each one.

9.2.4   Architecture Selection

Through analysis of the proposed mission requirements and spacecraft parameters, the hybrid architecture was selected. This architecture allows for a greater amount of flexibility than either a centralized or distributed architecture.

The following design is best suited for this spacecraft. At the subsystem level a centralized architecture will be utilized. This will involve connecting all of the subsystem sensors or data input/output devices to a central or hub processor. For the entire spacecraft, a two bus, branch-distributed architecture will be used. Each of the two buses will consist of a three bus interface. The three buses will be a command/data handler bus, a telemetry addition bus, and a telemetry data return bus. Four subsystem hubs will be interfaced on each bus branch. Finally, the communications portion of the C & DH subsystem architecture will be a ring architecture made up of the communications downlinks, the Telemetry and

Command Units (TCU's), and the system's main super interface. See Figure 9.2 for the

block diagram of this architecture [8].
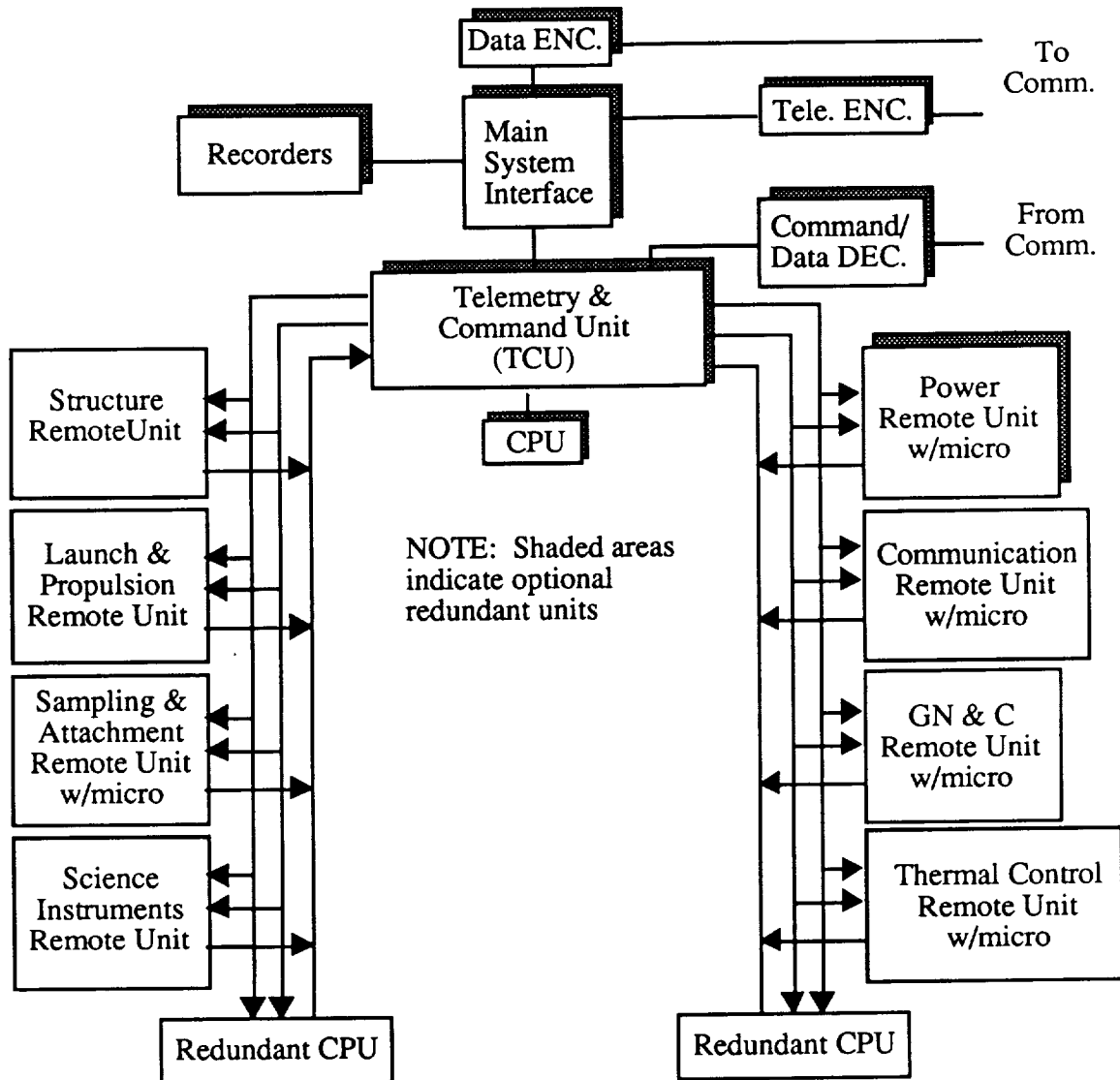
Figure 9.2: Block Diagram of Proposed Architecture

The architecture described in the previous paragraph was selected using a single

criterion. That criterion was maximum computing with maximum simplicity. Using the two

branch buses will distribute the system allowing subsystem processors to be near the

subsystem in question. This distribution allows for more subsystem units to be added, should they be needed, without overburdening the existing computers. It also reduces the risk of a single-point failure shutting the entire system down, which is a problem commonly associated with centralized architectures.

The subsystem hubs will add flexibility to the design constraints placed on each subsystem by giving each subsystem its own processor rather than rationing out processing space from a main computer to each subsystem.

This architecture also lends itself to modification for the structural constraints. By utilizing a central processor hub and two branch buses, the main processor can be placed in a central location within the spacecraft, and the subsystem processing units can be placed anywhere within the spacecraft. The only requirement that must be met involves the proper wiring of all units and the proper interfacing of the processors.

9.3   Hardware and Software

The selection of the computers and algorithms necessary to carry out the mission requirements involves a great deal of thought and computation. Criteria for this selection process can be broken down in to four questions:

- Is the system testable?
- Will the system accomplish the mission objectives?
- Does the system meet spacecraft parameters?
- Is the system reliable and cost effective?

These questions show a heavy reliance on unknown factors, such as subsystem data processing rates. Through the use of basic system analysis, many of these unknowns can be eliminated. By breaking the system into its fundamental units (subsystem hubs) and analyzing it unit by unit, each of these questions can be answered. The main factors affecting unit selection are mass, power, processing rates (bits/sec), and volumetric constraints.

The software requirements are vast. As the system takes shape, and more subsystems develop requirements, the software can be designed. Presently, the use of Assembly Language and Higher-Order Languages (HOL's) is projected. The HOL known as Ada appears to be the most versatile, able to handle general purpose, artificial intelligence and database management tasks. This language is a Department of Defense (DOD) Standard Language with extensive international acceptance. Table 9.1 lists some of the HOLs available and there characteristics. Notice that Ada is the only language found in all three of the primary processing applications. An additional requirement for Ada is an inference engine for artificial intelligence applications. There will be no artificial intelligence applications necessary within this mission's parameters; therefore the lack of an inference engine will not pose a problem [8].

Table 9.1: Table of Higher-Order Languages. (Wertz, J.R. and Larson, W.J., eds., *Space Mission Analysis and Design*, Kluwer Academic Publishers, Norwell, MA, 1991.)

Primary Processing Application	Common Higher-Order Languages and Their Uses	
General Purpose	Ada	DOD Standard Language; extensive international acceptance
	Jovial	DOD Language of 1970s
	Pascal	Ada precursor
	C	Used often for commercial development; well-supported development environment
	FORTRAN	Primarily Scientific and ground-based applications
Artificial Intelligence	LISP	Al - Object Oriented Language
	Prolog	Al - Object Oriented Language
	C	General purpose - inference engine needed
	Ada	General purpose - inference engine needed
Database Management	Ada	Can be used for embedded systems
	dBase	Database language; not for embedded systems
	Oracle	"
	Rdb	"

C - 3

The actual algorithms needed to make this subsystem a success are quite extensive. Their discussion would require a great deal of research and computer engineering development. Note that the actual development of these algorithms is beyond the scope of this project and only generic references to the nature of the required software are possible.

9.3.1 C & DH Inventory and Cost Analysis

Using basic estimation techniques found in Reference 8, a subsystem inventory was established. See Table 9.2 for the listing of subsystem requirements for mass, power, and volumetric displacement respectively. Notice that four of the subsystem units have been defined. These particular systems, the CPU, redundant CPU's, TCU's, and the recorders were selected as temporary stand-ins. The final selection of hardware will be a very long process and does not fall within the scope of this design project.

Based on estimation algorithms found in Reference 8, research and development (R & D) and first unit production costs were determined. Using the estimated mass of 121.35 kg and the algorithms, which maxed out at 112 kg, R & D could cost $27.8 million. The first unit production cost is a little less at $15.3 million. All values are subject to change as the final design of the subsystem is completed. More information will be available as research continues, and decisions will be made with regard to the particular computers necessary to accomplish the mission objectives.

Table 9.2: Mass, Volumetric, and Power Budgets for C&DH

Subsystem Equipment		Mass (kg)	Volume (cc)	Power (W)
Propulsion & Launch	1 RU* (21 boards)	5.24	7920.96	8.45
Thermal Control	1 RU (21 boards)	5.24	7920.96	8.54
• ME** (8 boards)		2.00	2676.00	18.55
Guidance, Navigation and Control	1 RU (21 boards)	5.24	7920.96	8.54
• ME (8 boards)		2.00	2676.00	18.55
Power	1 RU (21 boards)	5.24	7920.96	8.45
• ME (8 boards)		2.00	2676.00	18.55
• Redundant Unit (29 boards)		7.24	10596.96	27.00
Sampling & Attachment	1 RU (21 boards)	5.24	7920.96	8.45
• ME (8 boards)		2.00	2676.00	18.55
Science Instruments	1 RU (21 boards)	5.24	7920.96	8.45
Structure	1 RU (21 boards)	5.24	7920.96	8.45
Communications	1 RU (21 boards)	5.24	7920.96	8.45
• ME (8 boards)		2.00	2676.00	18.55
Main CPUs	ITEK/ATAC —	11.30	12900.00	50.00
• Redundant Unit	16ms	11.30	12900.00	50.00
Redundant CPUs	CDC/469	4.50	1400.00	20.00
• Redundant Unit		4.50	1400.00	20.00
Telemetry & Command Units	TCUs (10 boards)	2.49	3853.44	8.75
• Redundant Unit (10 boards)		2.49	3853.44	8.75
• Possibly use CDC/469 CPU				
Super Interfaces		2.49	3853.44	8.75
• Redundant Unit		2.49	3853.44	8.75
Recorders	Odetics DDS5000	9.07	14450.00	40.00
• Redundant Unit		9.07	14450.00	40.00
Encrypter/Decrypter Units		2.49	3853.44	8.75
TOTAL		121.35	164111.84	451.10

*Remote Unit
**Microprocessor Extension

9.3.2 Hardware Selection Modification Idea

For most subsystems, a high degree of redundancy is required to ensure the success of the mission. All redundant units are listed as optional when the final design is proposed. Most of the time the term optional implies a requirement, but design constraints limit the use of all optional equipment. In all cases, the redundant unit is a duplicate unit. This allows for easy transfer of processing from the failed unit to the back-up unit. Looking back to Figure

9.2, an interesting development can be noted. The subsystem hubs do not have a redundant unit, the exception being the power hub. In an attempt to save on volumetric, mass, and volume budgets, a single redundant CPU (RCPU) was chosen. Not only does this cut down on the aforementioned budgets, but it increases the processing capabilities of the redundant unit. By acting as a central hub for the failed subsystems, this RCPU can process telemetry, collate data, and, in general, cut down on processing time. Since the power subsystem shows the potential for multiple failures (i.e., power spikes, short circuits, etc.), a redundant unit on top of the RCPU has been proposed. This redundant unit ensures that power subsystem operations will continue even if there is a multiple failure within the subsystem.

9.4   The Concept of Autonomy

Most spacecraft have a need for some level of autonomy. This concept simply describes the spacecraft's ability to function without outside assistance (i.e., ground control). Such needs may arise when there is a break in communications or when the spacecraft is eclipsed by a large body in space (i.e., a planet, or an asteroid).

For this mission a high degree of spacecraft autonomy is recommended to ensure the proper completion of the mission. In order for this to be achieved, a rather complex algorithm needs to be developed. This algorithm will be able to determine system failure, correctly utilize back-up systems, and establish an alternate course of action, as well as recognize the need for autonomous operation (i.e., the spacecraft loses communications with Earth, necessitating the use of internal control rather than ground control). This spacecraft autonomy would not be entirely complete. An override command structure will be utilized to permit ground control to take over at any time.

A decrease in communication requirements for power can be achieved by increasing the level of spacecraft autonomy. Such an increase would allow the spacecraft to operate with a minimal use of ground facilities. For instance, the spacecraft could operate under its

own control until it reaches asteroid proximity; then it could turn control over to ground control for final command guidance.

9.5   Conclusions and Recommendations

A highly autonomous, hybrid architecture utilizing HOL software has been chosen as the best possible candidate for this mission's computer system. This system will minimize risks of failure and increase security of operation without ground control help.

The recommendations for this subsystem are not all-inclusive. The need exists for research into hardware and software packages. This research does not fall within the scope of this project and would require detailed design by computer engineers. For the most part, the groundwork has been laid for a highly viable computer system. When the final decisions are made regarding the hard/software of this subsystem, a multifunction, high-capacity operating system will be the culmination of the research done to produce a subsystem capable of completing the mission.

10.0 Thermal Controls

10.1 Requirements

All spacecraft components must be kept within specific temperature ranges to ensure their proper operation. Thermal control of the asteroid sample return spacecraft is critical for the success of the mission. The thermal control of the spacecraft will be regulated by means of both active and passive methods. The passive controls consist of the use of various surface coatings to control the absorption and emmitance of radiation both inside and outside the spacecraft. Active methods of thermal control include the use of heat pipes, solar radiators, and louver mechanisms. The spacecraft will make the best use possible of off-the-shelf technology with the use of new materials where needed. The primary reason for using existing technology is the reliability of such systems.

The primary concern of the thermal subsystem is to maintain stable temperatures for all spacecraft components throughout all phases of the mission. Not only must the thermal controls prevent overheating of some components, it must prevent freezing of others. Thermostats will be placed in these areas so that the spacecraft's on-board computer will be able to autonomously control the thermal heaters.

Overheating in such areas as the drill and power supply are also the primary concern of the thermal subsystem. To prevent excessive amounts of heat to be conducted throughout the spacecraft during drill operation, a combination of several thermal controls shall be used. These include heat pipes, thermal blankets, and the use of radiators to dissipate the heat generated.

10.2 Temperature Ranges

Initially, a list of primary equipment needed on the spacecraft was compiled. From this list, components requiring heat addition and those requiring heat extraction were formed and tabulated. Additionally a list of thermal operating ranges was compiled in order to find

an overall operating range for the entire spacecraft. Table 10.1 shows typical equipment temperature limits that can be expected for the asteroid sample return mission.

Table 10.1: Typical Equipment Temperature Limits. (Agarwal, Brij N., *Design of Geosynchronous Spacecraft*, Prentice-Hall Int., London, 1986, p.266)

Subsystem/Equipment	Nonoperating/Turn-on (°C)	Operating (°C)
Communications		
Receiver	-30/+55	+10/+45
Input multiplex	-30/+55	-10/+30
Output multiplex	-30/+55	-10/+40
Traveling Wave Tube Amps	-30/+55	-10/+50
Antenna	-170/+90	-170/+90
Electric power		
Solar array wing	-160/+80	-160/+80
Battery	-10/+25	0/+25
Shunt assembly	-45/+65	-45/+65
Attitude control		
Earth/Sun sensor	-30/+55	-30/+50
Angular rate assembly	-30/+55	+1/+55
Momentum wheel	-15/+55	+1/+45
Propulsion		
Solid apogee, motor	+5/+55	-----
Propellant tank	+10/+50	+10/+50
Thruster catalyst bed	+10/+120	+10/+120
Structure		
Pyrotechnic mechanism	-170/+55	-115/+55
Separation clamp	-40/+40	-15/+40
Drill	N/A	N/A

10.3 Passive Controls

Many passive controls are being considered for use on the spacecraft. These include: selective surface coatings, optical solar reflectors, second surface mirrors, multi-layer insulation blankets, thermal radiators, and a cold rail system.

10.3.1 Selective Surface Coatings

Selective surface coatings, such as paint, can be used to regulate the heat flow by varying the coating material throughout the spacecraft. Theses coatings regulate the heat

flow by adjusting the absorbtivity and emissivity in desired regions. Matte-black paint will be used on all internal spacecraft components to maximize heat exchange with other on-board equipment on the spacecraft. A white epoxy paint will be used primarily on the parabolic antenna surface to minimize temperature fluctuations which cause physical distortion [34]. However, there are also other forms of selective surface materials.

Optical solar reflectors (OSR) and second surface mirrors (SSM) act as thermal regulators on the outside of the spacecraft. OSR and SSM are similar, except that the OSR have fused silica glass with silver backing as opposed to flexible plastic sheets used in SSMs. Because the OSR and SSM have low absorptivity and high emmitance rates, they are ideally suited for limiting infrared radiation absorption in units that require low operating temperatures, such as batteries. The OSR and SSM would be used in conjunction with louvers to help control heat in temperature sensitive areas of the spacecraft [34].

Degradation of the selective surface coatings can, and will, occur from several effects. These include charged particles, high vacuum, and ultraviolet radiation from the Sun [33]. Since the SSM degrade more rapidly, and the duration of the mission is not known yet, the choice of which material to be used is not known.

10.3.2 Multi-Layer Insulation (MLI)

Multi-layer insulation blankets are used to reduce heat loss between the spacecraft and its surrounding environment. Placement of the blankets is around three primary areas. The first area is the outside of the spacecraft which will primarily face the Sun. Doing this will minimize the solar radiation absorption. The second area is around the propulsion system to help prevent freezing of the propellant. Lastly, it is also placed around the apogee kick motor to prevent exposing the spacecraft to high temperature fluxes during orbit injection [34]. At times when the spacecraft is at distances in excess of 1.5 AU's from the Sun, the thermal blankets will work more as an insulator in order for the spacecraft's components to remain within operating temperature limits given in Table 10.1.

MLI's are constructed with multiple layers of aluminized Kapton or Mylar, separated by Dacron mesh which prevents temperature flux due to conduction between the aluminized layers [34]. Many times the outermost layer of the MLI's are covered with a layer of indium-tin oxide which will make the MLI electrically conductive. The purpose of this is to prevent electrostatic charging on the MLI and the associated discharge [34].

10.3.3 Cold Rails and Cold Plates

Cold rails that are used in active subsystems diffuse heat sources along the rail. Cold rails are often used in conjunction with heat pipes [35]. This combination allows larger quantities of heat to be conducted more effectively than either method alone. The heat pipe/cold rail system, also known as a cold plate, is typically located in high temperature regions in the spacecraft where the equipment can be mounted directly onto the rail, as in Figure 10.1. The heat absorbed by the cold plate is then transported to a radiator for dissipation [8]. Cold rails are typically made of an aluminium alloy giving the combination not only good thermal conduction characteristics, but also providing structural support. However, beryllium is being considered by the structures team as a primary structural material. While not providing as high a thermal conductivity as some aluminium alloys, it is still suitable for the mission.
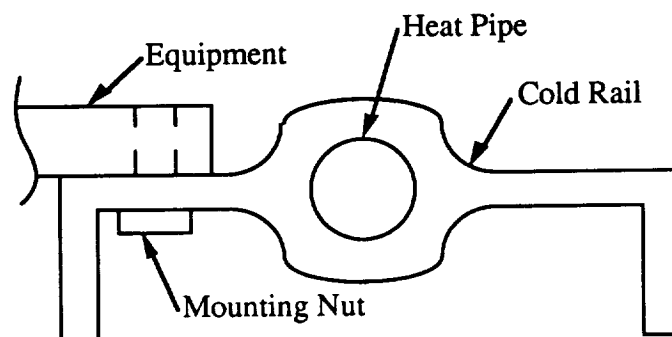

Figure 10.1: Heat Pipe/Cold Plate Combination (Tawail, M., *Heat Pipe Applications for the Space Shuttle*, AIAA 7th Thermophysics Conference, San Antonio, TX, April 10-12, 1972.)

10.3.4 Advanced Radiator

For the phases of the mission where large quantities of heat will need to be dissipated, such as during the drilling of the core sample, the possible use of a multi-plate Advanced Radiator (AR) is planned. Used in conjunction with the planned heat pipe system of the drilling/attachment section of the spacecraft, the AR is designed to handle up to 50 times more of a heat load than the conceptual Advanced Moisture and Temperature Sounder (AMTS) for a given heat load. When compared to the VISSR radiator, the AR dissipated more heat for either a constant surface area or weight [36]. Both the AMTS and VISSR are other conceptual radiators mentioned briefly by Bard [36].

The AR consists of several layers of radiator material each surrounding the next, see Figure 10.2. The AR concept allows heat to be conducted and radiated through each of the plates but only the outer most plate is directly exposed to solar radiation. This design improves the AR efficiency greatly. Because of this design, the AR is a much more efficient than a standard radiator panel.
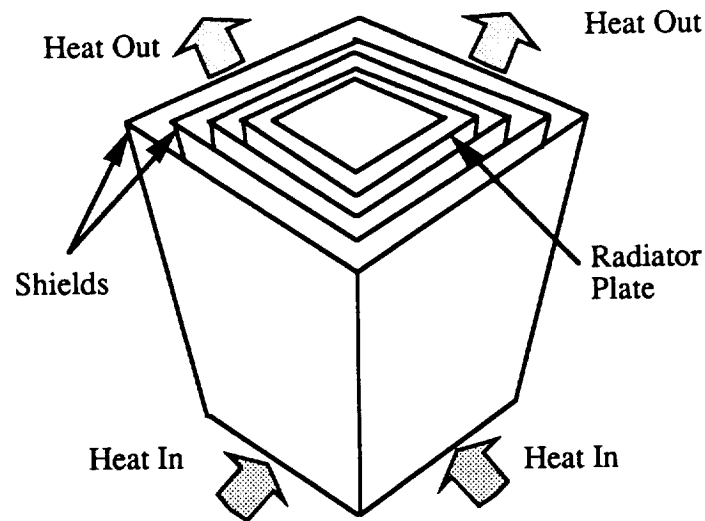

Figure 10.2: Diagram of Advanced Radiator Concept (Bard, S., *Advanced Radiative Cooler with Angled Shields*, AIAA 16th Thermophysics conference, Palo Alto, CA, June 23-25, 1981)

10.4   Active Controls

10.4.1   Heat Pipes

The heat pipe is a simple, yet effective means of transferring large quantities of heat over short distances. Heat pipes operate by conduction of heat with the use of a carrier fluid enclosed within a hollow pipe containing some form of wick as shown in Figure 10.3. In the high temperature region of the heat pipe the fluid is vaporized and moves towards the cooler region where it condenses and is transported back to the hot region via capillary pressure.
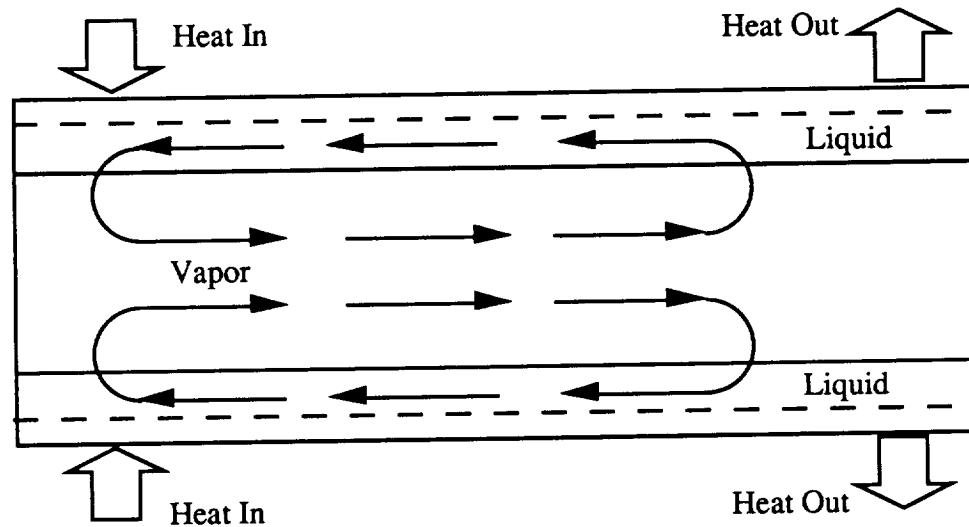
Figure 10.3: Schematic diagram of a Heat Pipe (Agrawal, Brij, *Design of Geosynchronous Spacecraft*, Prentice-Hall Int., London, 1986, p.299)

The material used as the working fluid primarily depends on the operating temperature range of the components in question. For lower temperature ranges, materials such as ammonia, freon, or other phase changing materials can be used. At higher temperatures liquid metals are generally used [37]. This is done effectively with the high latent heat of vaporization of the carrier fluid. The primary locations for the heat pipe system will be in the areas of the drill motor, and the spacecraft power supply.

10.4.2 Thermal Heaters

The thermal heaters are generally resistors fed with an electric current from the spacecraft power supply. Thermal heaters will be located in areas such as the propellant tanks, thrusters, valves, propellant lines, and batteries. Thermostats are used in conjunction with the heaters to regulate fine temperature control [8]. They can be controlled autonomously, via a ground control mode, or in a continuous-on mode [33].

For areas of the spacecraft that will require continuous heating, the use of Light-Weight Radioisotope Heater Units (LWRHU), similar to those used on the Galileo probe, are being considered. These would provide 0.56 W/g of radioisotope, typically Plutonium-238. The use of a 1-Watt heater would provide a small thermal increment to satisfy the needed thermal environment of the spacecraft components [38].

10.4.3 Louvers

Louvers, used in combination with optical solar reflectors or second surface mirrors, will be used to control fine temperature regulations such as in the region of the batteries. Depending on the amount of internal power generated and the external heat flux from the Sun or Earth, the louvers can vary the absorption to emmisivity ratio of the spacecraft. This is important during certain phases of the mission where more heat will need to be dissipated. The louvers operation is often controlled with the use of a spring loaded, bimetallic strip which, as the temperature varies, adjusts the position of the louvers [33]. A schematic diagram of the louver mechanism is given in Figure 10.4.
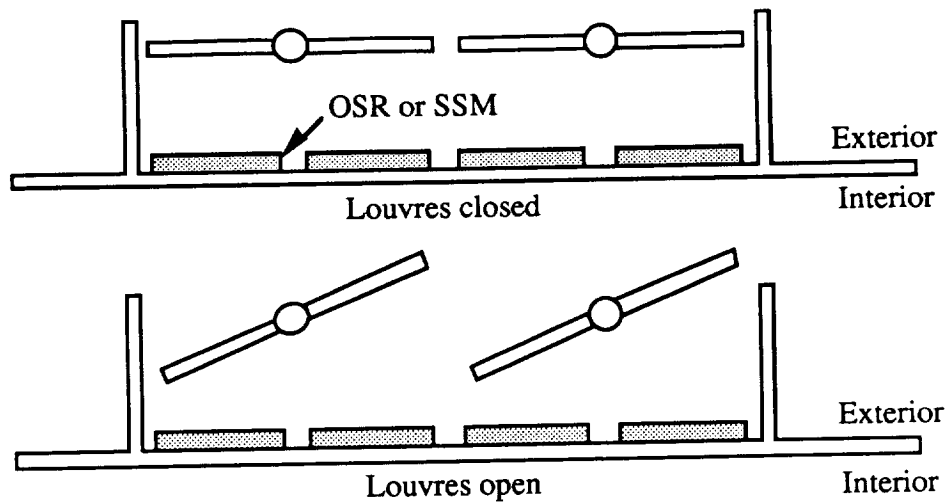
Figure 10.4: Louver Mechanism (Berlin,P. *The Geostationary Applications Satellite*, Cambridge University Press, New York,1988, p. 89)

10.5   Placement of Thermal Controls

Using the energy balance equation given in Wertz and Larson [8] on page 381:

$$P_{out} = P_{in} + P_{internal}$$

the solar flux, f, was calculated using:

$$f = L\left(4\pi d^2\right)^{-1}$$

where L is the luminosity of the Sun and d is the distance away from the Sun in meters. Using these equations and distances provided in Section 6.2, the average temperatures of the spacecraft were calculated for various portions of the mission. These temperatures are given in Table 10.2.

Table 10.2: Various Average Temperatures of the Spacecraft (with and without Thermal Blankets)

Location	w/ Thermal Blankets (°C)	w/o Thermal Blankets (°C)	Notes
Near-Earth	+11	+65	
En-route	-58 to +11	-17 to +65	
Eros	-58	-17	No drilling
Eros	+3	+56	With drilling

It should be noted that these temperatures represent the average temperature of the entire spacecraft as a whole. These numbers do not represent temperatures of specific subsystem components. Such calculations are beyond the scope of this report. However, the thermal controls for each of the major areas of the spacecraft will be discussed.

Since the temperatures given in Table 10.2 do not represent the localized temperatures of each of the spacecraft components, specific thermal controls should be used throughout the spacecraft in order to hold each component within the temperature parameters given in Table 10.1. A brief schematic diagram of the placement of thermal controls throughout the spacecraft is shown in Figure 10.5.

10.5.1 Heat Dissipation for the Power Supply

Thermal dissipation for the spacecraft power supply will primarily depend on the final design choice. The primary design being considered is the use of Radioisotope Thermal Generators (RTG's) in combination with a series of batteries. Also being considered for use as a primary power supply for the spacecraft is the Dielectric Isotope Power Supply (DIPS). While both will require some form of thermal radiator, the RTG radiator requires a considerably smaller radiator area than the one required for a DIPS system. For a typical 5 MW DIPS generator, a 46 m^2 radiator plate will be needed [7]. A possible redesign of such a large radiator plate would be the use of several smaller radiator plates containing heat pipes.

Since the DIPS system operates using a liquid metal as a working fluid, this fluid could be fed directly into the heat pipe system reducing the overall mass (size) of the thermal radiator [39]. A major drawback to this method is with possible extreme heating of the working fluid resulting in too much of the fluid being located in the condenser section of the heat pipe and not within the generator itself. Another option for dissipating large quantities of heat from the power supply would be to improve existing radiators available.
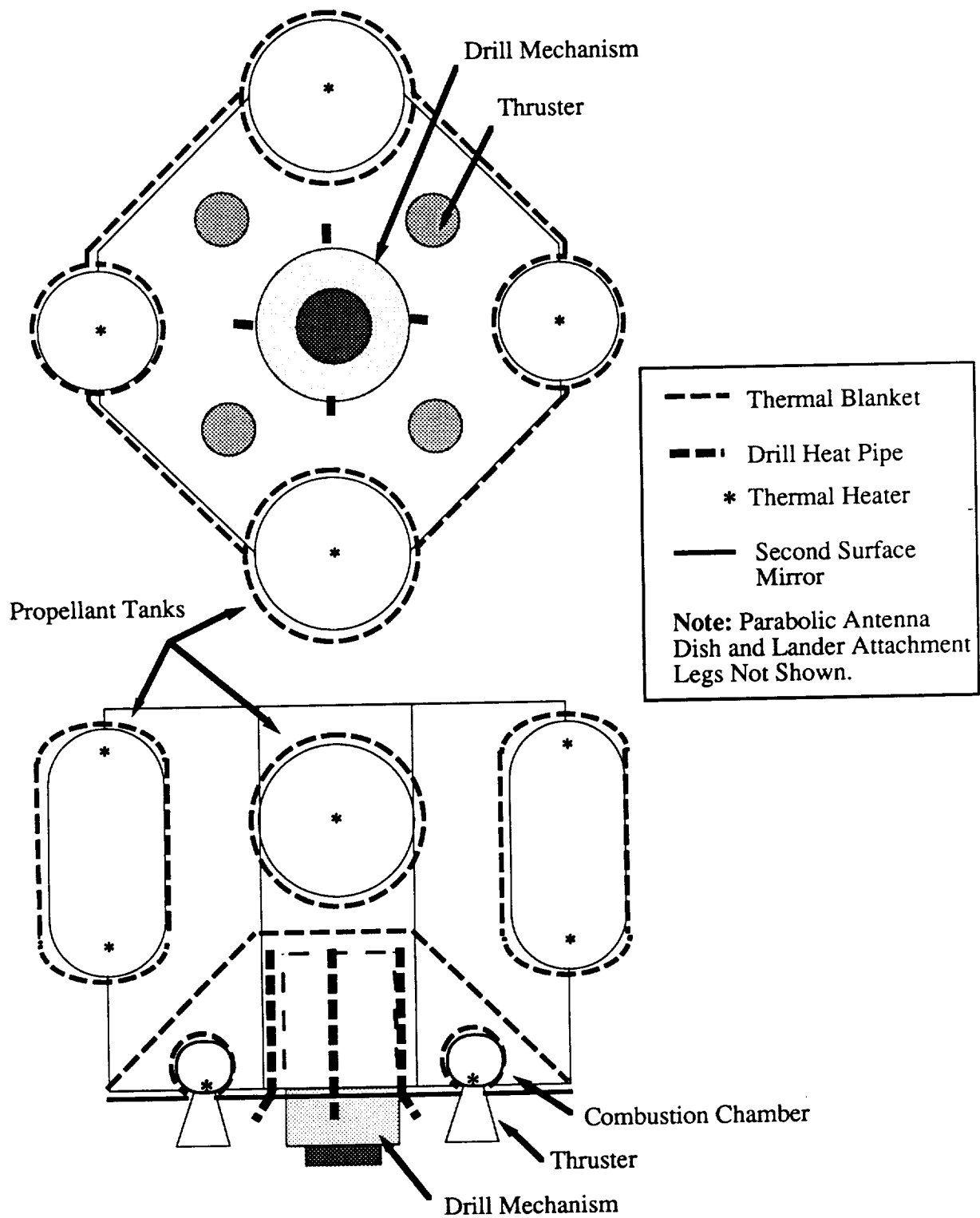
Figure 10.5: Thermal Control Design for the SASR Spacecraft

The optimum radiator material would consist of a high conductivity, high infrared emissivity, and low solar absorpivity material. Copper was found to have the highest conductivity of the materials listed in Wertz and Larson [8]. The material having one of the lowest absorption to emission ratios is white epoxy paint. Thus having a copper radiator with a coating of white epoxy would be desirable. Unfortunately the high mass of the copper material makes it impractical for an entire radiator. A conceptual solution to this could be the use of a copper tape weaved around evenly spaced heat pipes enclosed in an aluminium alloy matrix coated in a white epoxy paint. This combination provides the conductance of the copper throughout the radiator while utilizing the low weight of the aluminium alloy. Such a radiator configuration is shown in Figure 10.6.
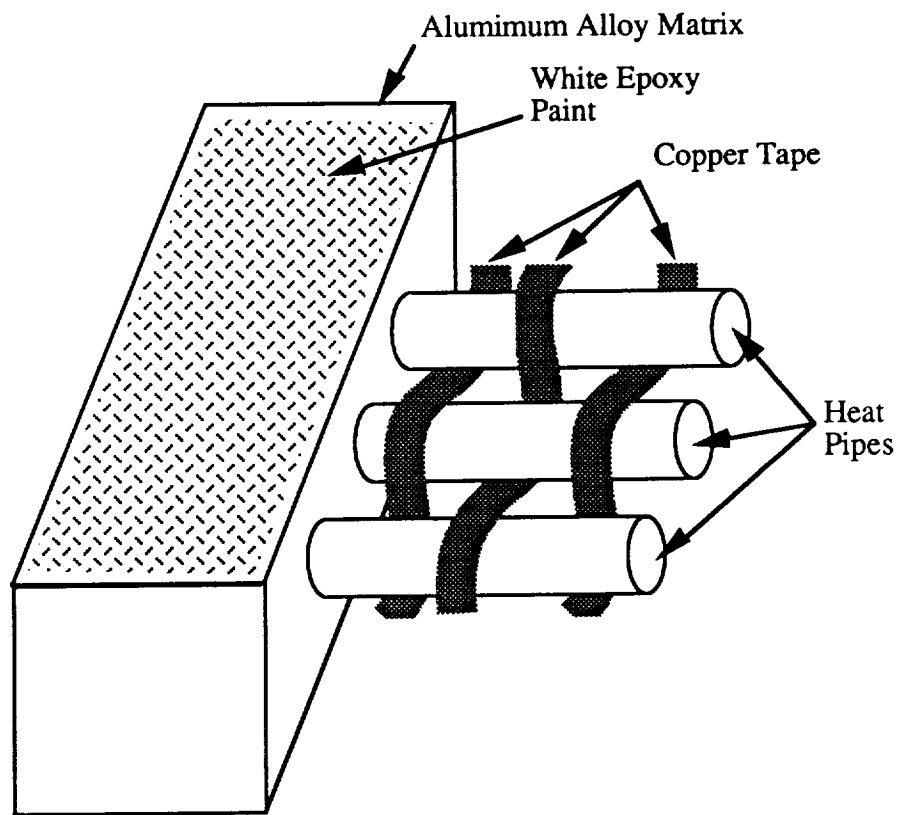
Figure 10.6: Conceptual design of Thermal Radiator

The copper tape weaved around the heat pipes would allow greater conduction of the heat away from the heat pipes which would be further conducted through the aluminium and finally radiated into space. The aluminium alloy surrounding the heat pipes would also provide protection for the heat pipes from micrometeor impacts.

Possible problems for such a system would be the differences in the coefficients of thermal expansion of the aluminum and the copper. This problem could arise not only in space but also in the processing of the radiator itself. The radiator plate could however be assembled with the application of the aluminium matrix by using plasma vapor deposition. The exact details to this process are not known at this time but will be examined.

10.5.2 Propulsion System

In order to maintain the operating temperatures for the hydrazine, nitrogen tetroxide, and monomethylhydrazine propellants used in this spacecraft, several precautions must be taken so the propellants do not freeze or experience excessive heating. Since the majority of the spacecraft mission will be at distanced greater than 1 AU from the Sun, each of the propellant tanks will be fitted with thermal blankets and electric thermal heaters. Additionally, each propellent tank will be fitted with thermostats so that the spacecraft's computer can monitor the temperatures of the propellents.

The propellent lines, thrusters, and valves will also be fitted with electric thermal heaters and thermostats to prevent freezing of the propellent lines. At times when the propellent tanks are beyond the given thermal parameters, heat will be conducted away from the tanks via the spacecraft structure where the tanks are to be mounted.

The main spacecraft thrusters, shown in Figure 10.5, are contained within a region of the spacecraft where high temperatures are expected. Therefore, this area will be completely surrounded with thermal blankets and second surface mirrors to act as a thermal barrier to minimize the heat flow between this area and the rest of the spacecraft.

10.5.3 Drill Mechanism

The drill mechanism for the asteroid sample extraction will generate the single greatest amount of heat for the spacecraft while on the asteroid. For this reason several thermal components shall be used to control this heat generation.

As with the primary spacecraft thrusters, the drill mechanism will be enclosed in an area which contains a thermal barrier of thermal blankets and second surface mirrors, to protect the rest of the spacecraft from excessive heating. The drill itself will be fitted with four aluminum heat pipes which will use water as a working fluid. This combination of materials should transfer an adequate amount of heat away from the drill into space.

The aluminum material in the heat pipe will conduct 205 W/m°C [37] while the rest of the excess heat will be removed via the working fluid. The useful range of temperatures for water as a working fluid are from 30°C to 200°C [37]. While the minimum temperature for water is considerably above the average temperature of the spacecraft while en-route to the asteroid, the fluid will be kept from freezing with the use of electric heaters located along the heat pipe. The heaters will be regulated by the spacecraft's computer via thermostats so that the water will not freeze nor vaporize while the drill is not in use.

The base of the spacecraft will be fitted with a large second surface mirror (SSM). There are two main reason for this. First, the SSM will be used to prevent the heat dissipation by the heat pipes from being reabsorbed by the spacecraft. Second, the SSM will act as added protection for the spacecraft from debris impacts while the drill mechanism is in operation.

10.5.4 Scientific Equipment

Many of the scientific equipment designated for this mission can be held within their temperature parameters with the use of thermal blankets, heaters, or radiator panels. The exception to this is the Visual Infrared Mapping Spectrometer (VIMS). The VIMS must be kept at an approximate temperature of -193°C. This will require the use of a Radiative

Cryogenic Cooler (RCC) and Sun-shield (Figure 10.7) similar to the one used on the Galileo probe. The RCC has been designed to provide refrigeration to the array of visual and infrared detectors. Details of this system are given in the report by Morris [39].
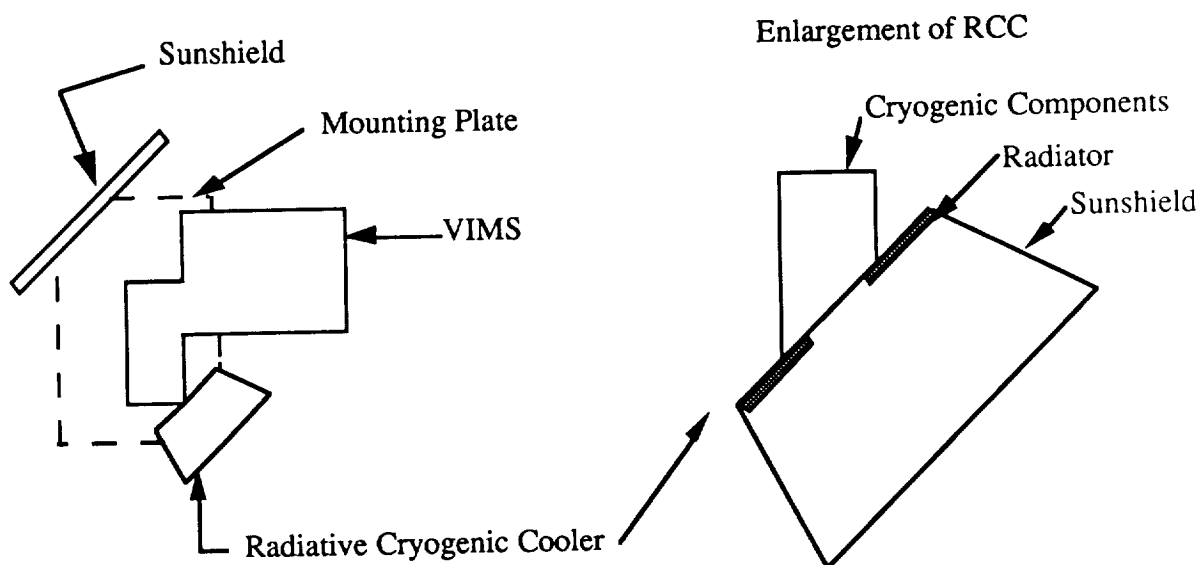
Figure 10.7: VIMS Radiative Cryogenic Cooler (Cafferty, Thomas T., *Radiative Cryogenic Cooler for the Near-Infrared Mapping Spectrometer for the Galileo Jupiter Orbiter*, AIAA 16th Thermophysics Conference, Palo Alto., June 23 - 25, 1991)

10.5.5 Asteroid Sample

Beyond the survival of the spacecraft, the most important function of the thermal subsystem is to ensure the return of the asteroid sample in as near the original state as possible. The primary concern being the heating of the sample as the return spacecraft nears Earth. The sample return container will be fitted with extensive thermal blanketing to minimize the heat flow to the sample. To try and maintain low temperatures, a cryogenic cooling system will also be incorporated into the sample return container. Thermostats will be used to control the activation of the cryogenic cooling system.

10.6   Recommendations

There has been a great deal of information gathered on the ways of controlling the thermal environment onboard the spacecraft. However, more detailed work can be done to improve the system. This includes running a thermal analysis program to find the temperatures at all locations in the spacecraft at any time during the mission. Through the use of a computer thermal modeling program, the thermal controls of the spacecraft can be optimized, thus reducing the thermal cost parameters. These include the minimization of the mass and power consumption of the subsystem.

11.0 Scientific Payload

11.1 Requirements

This mission requires that the collection of scientific data should be divided into three distinct phases. These are the cruise phase, the rendezvous phase, and the on-site phase. The cruise phase will consist of the time period between departure from Low Earth Orbit (LEO) and target sighting at an altitude of around 1 million km. Upon sighting of Eros, the rendezvous phase of the mission will begin. This phase will continue until the spacecraft is anchored in position on the surface of the asteroid, at which time the on-site phase will commence. Each of these mission phases will possess its own specific requirements.

11.1.1 Cruise Phase Requirements

The scientific requirements during the cruise phase will be to study many of the important features of the interplanetary space between the Earth and Eros. The scientific instrumentation should provide a means to study the physical characteristics of the solar wind plasma, interplanetary magnetic fields, and micrometeorite particles. The instruments must take data continuously throughout this phase in order to provide a complete and detailed picture concerning the nature of the interplanetary space along the spacecraft's trajectory.

11.1.2 Rendezvous Phase Requirements

The rendezvous phase of the mission will require the most intense usage of the scientific payload. Requirements of this phase will include: detailed imaging over a wide range of wavelengths, surface compositional measurements, and the analysis of the interaction of the asteroid with the interplanetary environment (i.e. magnetic field, solar wind, etc.). In addition, the instruments must assist in the determination of a landing site that is both safe and desirable. Efforts will also be made to accurately determine characteristics of Eros such as its mass, diameter, albedo, and spin rate. It will be necessary to employ a

variety of diverse instruments in order to obtain the required information. Following the on-site phase, the spacecraft will execute further topographical mapping of Eros' surface contingent on the remaining propellant supply.

11.1.3 On-Site Phase Requirements

Once anchored securely on the asteroid, the scientific requirements will consist of: surface images in the vicinity of the vehicle, local magnetic field measurements, micrometeorite population analysis, and seismic measurements. The instruments will perform all of the required measurements before implementation of the drilling process since drill-generated vibrations would greatly inhibit instrument performance.

11.2 Scientific Instrumentation Description

11.2.1 Plasma Spectrometer (PLS)

The Plasma Spectrometer (PLS) will study the solar wind plasma existing in the interplanetary environment and analyze this plasma's interaction with Eros. The instrument comprises a multi-sensor plasma analyzer and uses electrostatic deflection to measure the ion and electron velocity distributions. The PLS can make measurements over an energy range of 1 eV to 50 keV and a mass range of 1 AMU to 50 AMU. Angular resolution is approximately 2° in one plane and 20° in another (orthogonal) plane. The energy resolution will allow measurements of supersonic flows. The PLS will occupy a place on a turntable located at the end of a boom [41].

11.2.2 Magnetometer (MAG)

A Magnetometer (MAG), located on a 10 m long boom, will measure the magnetic field found in interplanetary space and determine how this field interacts with Eros. The

MAG may aid in the asteroid's compositional determination by interpreting Eros' effect on the (otherwise near uniform) magnetic field.

The MAG will take measurements at regular intervals (as often as possible) during all three mission phases to better determine the characteristics of both the unaltered and the altered magnetic fields. It will have a resolution of 0.01 nT and an absolute accuracy of 0.1 nT [42].

11.2.3 Dust Analyzer (DA)

The spacecraft will utilize a Dust Analyzer (DA) during all three scientific phases. The DA's objectives will include: measuring the density of dust particles around Eros and in the space between Earth and Eros; and determining the mass, speed, and electrical charge of individual dust particles. The DA will contain an impact plasma detector to count individual impacts. This instrument will be located on the same turntable boom as the PLS.

11.2.4 Solid State Imaging (SSI)

The spacecraft will employ the Solid State Imaging (SSI) equipment during the rendezvous phase to obtain visual spectrum images for both scientific purposes (such as albedo measurements) and landing site determination.

The SSI system will employ two charge-coupled devices (CCDs) each comprised of identical, two-dimensional pixel arrays (1024 x 1024). Both instruments will be mounted on a High-Precision Scanning Platform (HPSP) [42]. The narrow angle camera will have a field of view of 11.42° x 11.42° with a focal length of 50 cm. The wide angle camera will have a field of view of 22.62° x 22.62° and a focal length of 25 cm. Spectral resolution, achieved by filters, will range from 200 to 11000 nm.

The spacecraft will utilize the narrow-angle camera during the high altitude segments of the rendezvous phase (from one million km altitude down to 100 km). Use of the wide-

angle camera will begin at 100 km altitude and continue through landing site selection and the on-site mission phase.

Because the SSI system will take a large amount of data at one time, a Solid-State Recorder (SSR) may need to be employed. The SSR will record the data and trickle it to Earth in manageable segments.

11.2.5 Visual and Infrared Mapping Spectrometer (VIMS)

The Visual and Infrared Mapping Spectrometer (VIMS) is a remote sensing tool which simultaneously images an area in hundreds of wavelengths in the visual and infrared spectrum (0.35 to 5.1 μm). The selected VIMS will be based on proposed design specifications for the Comet Rendezvous and Asteroid Fly-by (CRAF) mission (Figure 11.1) and mounted on the HPSP. The VIMS will require an operating temperature of 80 K because higher temperatures will affect the infrared measurements [43].
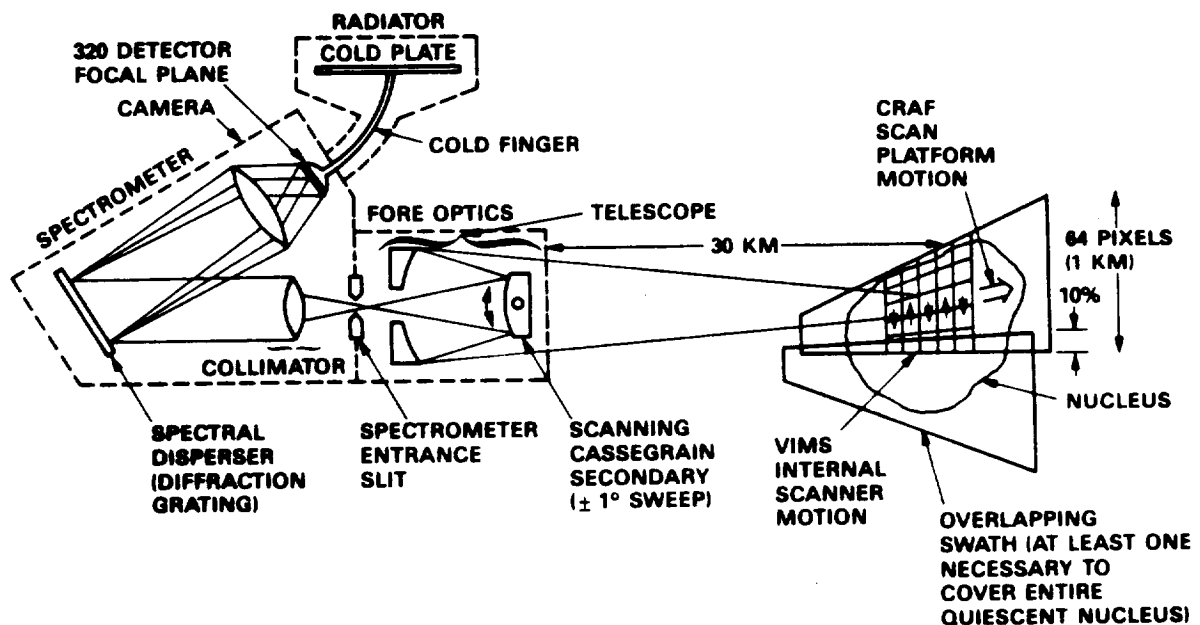
Figure 11.1: CRAF VIMS (Wellman, J.B., et al, "Visual and Infrared Mapping Spectrometer (VIMS): A Facility Instrument for Planetary Missions," *Proceedings SPIE*, San Diego, CA, Vol. 834, pp. 213-221.)

During the rendezvous phase, the spacecraft will use the VIMS to determine Eros' surface composition (mineral concentrations, ice patches, etc.). While adding to the complete picture of Eros, this data may also aid in determining an ideal landing site.

11.2.6 Ultraviolet Spectrometer (UVS)

An Ultraviolet Spectrometer (UVS) will image and identify surface elements such as SO_2, NH_3, and O_3 which emit in the ultraviolet (UV) spectrum (1150 to 4300 angstroms). This instrument will also be located on the HPSP.

11.2.7 Laser Radar (LADAR)

The spacecraft will employ a Laser Radar (LADAR) system for surface scanning during the landing site selection segment of the rendezvous phase. The LADAR design is similar to one proposed for a comet approach and landing system for the Rosetta/Comet Sample Nucleus Return [44]. The instruments that constitute the LADAR system are an ND:YLF pulsed-diode transmitter, an avalanche photodiode receiver, a 10x beam expander, a 5x common telescope, and two 2° wedge scanning prisms. The LADAR instrumentation will be mounted on the HPSP. Table 11.1 summarizes many of the important characteristics of the LADAR system.

Table 11.1: LADAR Instrument Characteristics (Bonsignori, Roberto and Luca Maresi, "Sensor System for Comet Approach and Landing," *Proceedings SPIE*, Orlando, FL, Vol. 1478, pp. 76-91, 1991.)

Pulse duration	2 ns
Pulse repetition frequency	400 Hz
Beam Divergence	40 μrad
Horizontal Resolution	1 m (at 2.5 km altitude)
Range Accuracy	10 cm

11.2.8 Radio Science (RS)

The Radio Science (RS) experiments will utilize radio emissions to and from the spacecraft to determine factors such as gravitational field strength, solar wind interaction, and charged particle characteristics. Eros must be in occultation with the spacecraft and Earth for the RS experiment to work.

11.2.9 Seismometer (SEIS)

A seismometer (SEIS) will measure seismic events occurring during the on-site phase of the mission. Because vibrations caused by the drilling process may invalidate any seismic readings, the SEIS operation will be limited to the time periods during which the drill is not operating.

11.3 Mass, Power, and Data Rate Budgets

Tables 11.2, 11.3, and 11.4, summarize the mass, power, and data rate budgets for the scientific payload, respectively. These numbers were determined either by direct calculation or by comparison of the instrumentation that has been previously designed to accompany other spacecraft missions such as Galileo, CRAF, and Cassini.

Table 11.2: Scientific Payload Mass Budget

Instrument Name	Mass (kg)
Plasma Spectrometer (PLS)	12.5
Magnetometer (MAG)	7.0
Dust Analyzer (DA)	5.0
Solid-State Imaging (SSI)	33.0
Visual and Infrared Mapping Spectrometer (VIMS)	23.5
Ultraviolet Spectrometer (UVS)	8.0
Laser Radar (LADAR)	26.9
Radio Science (RS)	6.3
Seismometer (SEIS)	7.0
Total	129.20

Table 11.3: Scientific Power Requirements By Phase

Instrument	Cruise (W)	Rendezvous (W)	On-Site (W)
PLS	14.5	14.5	---
MAG	3.1	3.1	3.1
DA	2.0	2.0	2.0
SSI	---	30.0	30.0
VIMS	---	9.1	---
UVS	---	6.5	---
LADAR	---	59.0	---
RS	---	---	---
SEIS	---	---	2.0
TOTAL	19.60	124.20	37.10

Table 11.4: Maximum Scientific Payload Data Rate Requirements By Phase

Instrument	Cruise (Kbps)	Rendezvous (Kbps)	On-Site (Kbps)
PLS	16.0	16.0	---
MAG	3.6	3.6	3.6
DA	0.024	0.024	0.024
SSI	---	120.0	120.0
VIMS	---	32.0	---
UVS	---	4.0	---
LADAR	---	640.0	---
RS	---	---	---
SEIS	---	---	2.0
Total	19.624	815.624	125.624

11.4 Role of Science Instruments in Landing Site Selection

The act of autonomous landing site selection will involve considerable coordination between the scientific instruments, the Command and Data Handling System (C&DH), and the Guidance, Navigation, and Control System (GN&C). The spacecraft will utilize both a passive system (CCD imaging) and an active system (LADAR scanning) to complete this task.

At an altitude of 2.5 km, the spacecraft will enter orbit with Eros, maintaining its

position over a specific surface location. At this time, the SSI system will photograph an area

of the surface (1 km x 1 km) directly beneath the spacecraft. The C&DH system will analyze

the reflectance imagery by using a shadow detection algorithm to detect large depressions or

protrusions on the surface [45]. This algorithm (which is still in the developmental stages)

will create a hazard map from which it will identify up to three potentially safe landing zones,

each having a 30 m radius. The LADAR system will then scan these areas for surface

gradients until one is found that presents no likely hazards. This scanning process may take

as long as two to three minutes. Once this site is found, the information will be relayed to the

GN&C system which will then begin the landing process. If no safe landing zone is

discovered, the spacecraft will maneuver to an alternate location and repeat the passive/active

scanning process. Figure 11.2 shows this sensor approach [46].
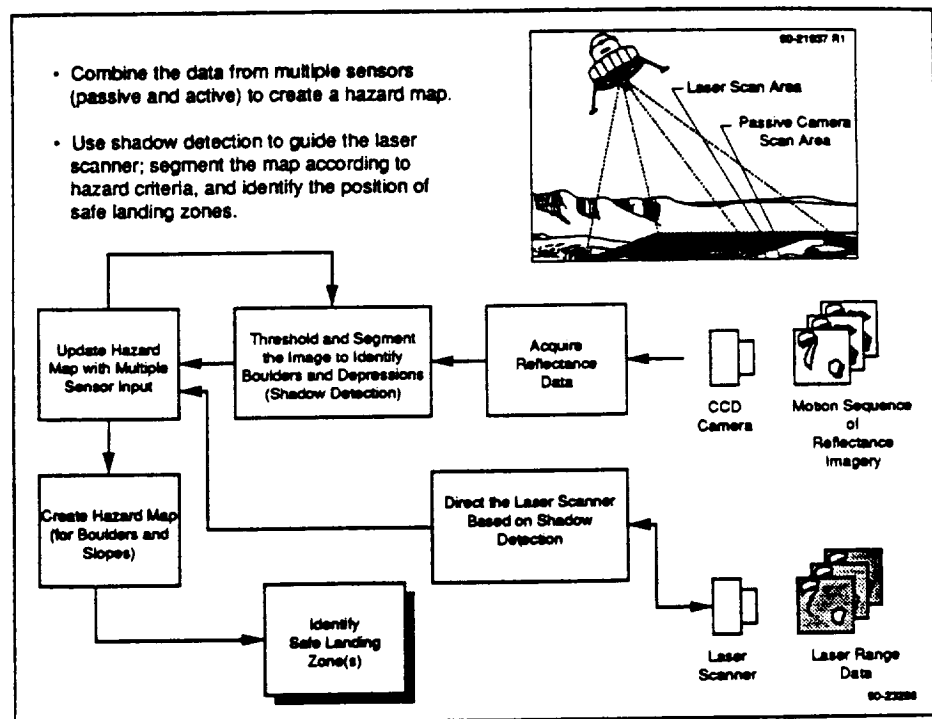
Figure 11.2: Passive/LADAR Sensor Approach (Gleichman, K., Tchoryk, P., and Sampson, R.E., "Application of Laser Radar to Autonomous Spacecraft Landing," *Proceedings SPIE*, Los Angeles, CA, Vol. 1416, pp. 286-294.)

11.5   Recommendations

The spacecraft will contain a scientific payload capable of taking a diverse and extensive amount of data throughout all phases of the mission. Spectrometer and Solid-State Imaging experiments will image the ultraviolet to infrared spectral range to determine Eros' surface composition. A magnetometer, plasma spectrometer, and dust analyzer will examine the environment along the spacecraft's flight path as well as around Eros. A seismometer will obtain seismic activity measurements occurring on the asteroid. If the propellant supply permits, the imaging instruments will generate detailed maps of the surface.

Utilizing a laser radar system for autonomous landing site detection is a concept in the early design stages. While showing great promise, this system requires further research, development, and testing.

12.0   Attachment and Sample Collection

12.1   Requirements

Attachment is that phase of the mission where the spacecraft lands and then physically attaches itself securely to the asteroid. This is an essential and crucial phase of the mission since the core drill will be imparting extremely large torques and vertical forces on the spacecraft. A regolith sample will be obtained using a method similar to ocean floor sample collection, while a 10 kg solid core sample will be obtained using a coring drill designed specifically for this mission.

Based on discussions with Dr. J. Koehler, Department of Earth and Mineral Sciences at the Pennsylvania State University, and subsequent research into material properties and drilling equipment, it was determined that there are many unresolved problems associated with attachment to the surface as well as with sample collection. The major problem is that the properties (especially hardness) of the rock are virtually unknown. Since the asteroid is in a vacuum, impurities such as water do not exist in the asteroid material. Absence of these impurities make the molecular bonds much stronger; thus a material with known properties on Earth could be conceivably many times harder in the vacuum of space [47]. For this reason, it is believed that present drilling technology is not suitable for the specified mission. The following discussion is therefore conceptual in nature. Further discussion of the problems with attachment and drilling is described in subsequent sections. Therefore this design is presented on the assumption that the asteroid properties, when discovered, will allow attachment and drilling to take place.

12.2   Regolith Sample

A series of remote sensing tests will be run prior to landing on the asteroid; this will allow for appropriate sample site selection. A complete description of the instruments used is covered in section 11.0. When the remote sensing of the asteroid is complete and all the

results are interpreted, two different sample sites will be chosen based on their different characteristics. The first is terrain which would resemble small rock fragments or regolith soil, the other is solid rock with a flat surface in order to make an actual landing for core drilling. When a desired regolith soil section is selected from the asteroid data, the initial sampling will start. Positioned above the asteroid, the spacecraft will take three regolith samples using sampling methods similar to those used in ocean floor sample collection. The concept uses the idea of back charges. Three cylinder shaped sample collectors (30.5 cm in length and 5.08 cm in diameter for 6.5kg of regolith samples) are released at low velocities toward the selected region. Upon contact, back charges are set off driving the collectors fully into the regolith soil. The samples are then reeled back into the spacecraft by tethers which are attached to them. These are the first of the two different types of samples which will be brought back to Earth for analysis. Each sample will be stored in its own stainless steel container to protect it from contaminants. The next method requires that the surface be flat and composed of solid material in order to land and attach to the asteroid.

12.3 Attachment and Landing

Since there is a very weak gravitational field on the asteroid as compared to the Earth or Moon, attachment is a vital part of the operation. Using the remote sensing, a relatively flat landing site will be found. Once above this site, thrusters will be fired with low thrust pulses to direct the spacecraft toward the asteroid surface. The foot-pads will be constructed from an energy-absorbing aluminum honeycomb and the legs will contain shock absorbers in case of a hard landing. Crushable blocks will be placed on the underside of the spacecraft in the event of touchdown in a rocky terrain.

Once the spacecraft is on the asteroid, it will have to withstand relatively large amounts of torque and external forces during drilling. The lander will have four legs with a wide base in order to distribute the torques more evenly. To fasten the lander to the asteroid, a sensor/spike system was chosen. Sensors located on the underside of the foot-pads

determine when the lander has made contact with the asteroid. The signals from these sensors trigger the back charges located on top of the spikes, and each of these spikes are driven deep into the solid rock. This will occur only after all four legs have touched down. Thrusters will again be fired, this time high level thrusts, to offset the force of the asteroid surface on the penetrating spikes. These spikes are driven through the feet of each of the legs and are approximately 0.4 meters long and five centimeters in diameter. Each foot will contain three spikes that are barbed to insure a secure fit. This will prevent the lander from separating from the asteroid and also provide stability during drilling operations.

The methods of attachment described here assume that material properties will be known. This is of course essential in the determination of attachment spike material and charges to be used. Due to the expected extremely high downward force (i.e., 22.2kN) and torques (approx. 4000 Nm) imparted by the drilling apparatus, proper attachment is the most crucial phase of the mission. It should be noted that this method of attachment assumes that the rock will not fragment during spike insertion. If this is expected to occur after material properties are known, an alternate method of attachment will need to be investigated.

12.4   Subsurface Sampling

12.4.1   Solid Core Sample

When the spacecraft is fully attached, the next sample will be taken by the use of a core drill. Stored within the spacecraft, the drill will be lowered to the asteroid surface along its frame support track, see Figure 12.1. The drill bit will be composed of black industrial diamonds in order to cut through the solid core material, currently the hardest bit material used on Earth. Steel is the material to which the drill bit will be attached. Current research is being conducted for the use of ceramics for this procedure. The actual core sample that will be taken will be 5.08 centimeters in diameter and approximately 1.5 meters deep.
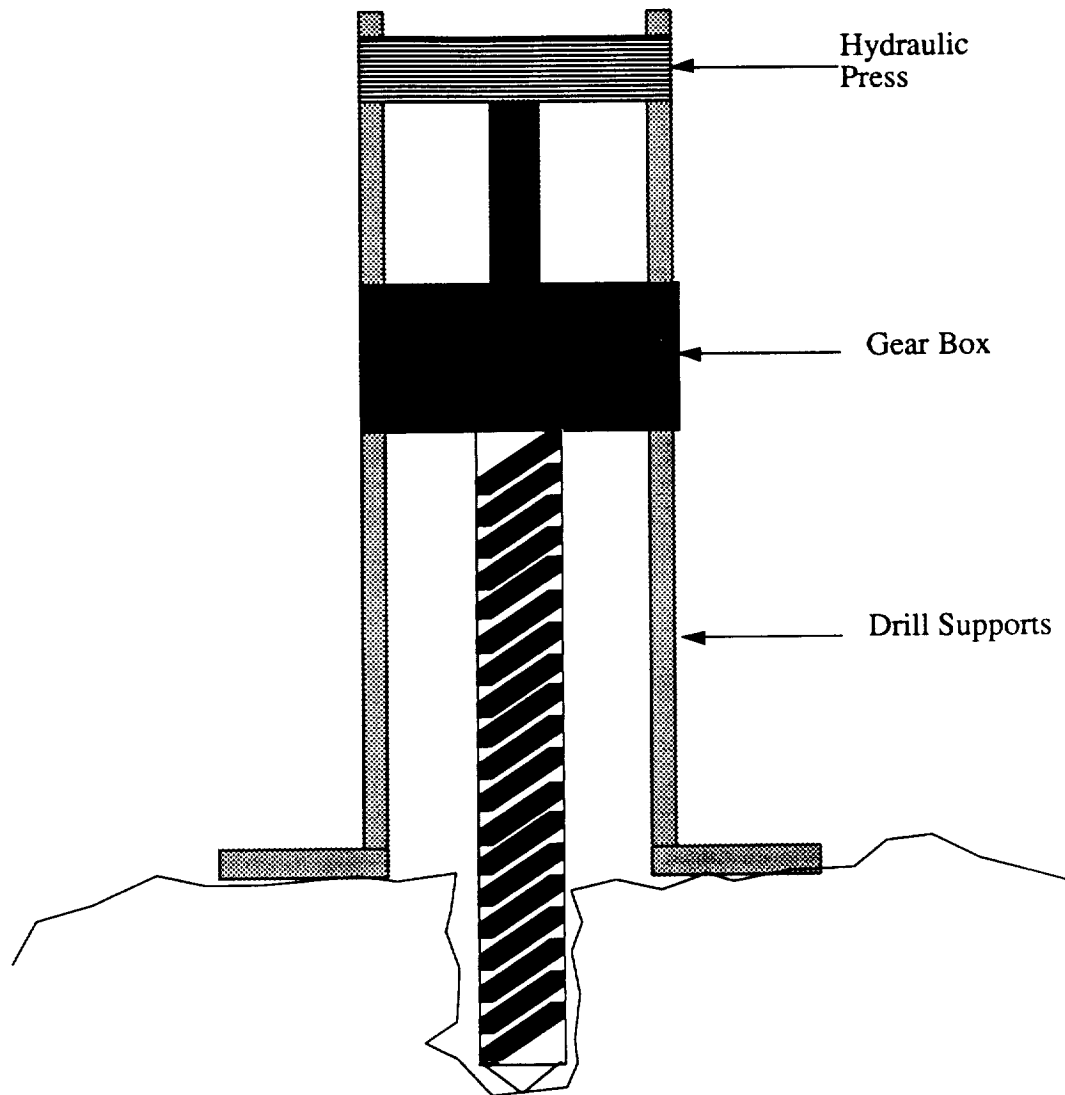
Figure 12.1: Drilling Apparatus

These dimensions are based on obtaining a single 10 kg sample of material with estimated density of 3.5 g/cm^3. In order to generate the high torques and downward thrust, it was estimated that the motor needed will require at least 7.5 kW of power. The weight of most industrial drills range from a couple hundred to several thousand pounds depending on the downward thrust and torques needed. Since we are limited by launch mass constraints, it was determined that this drill could not exceed 1000 kg. This drill will need to generate torques that will exceed 4000 N-m and an opposing force of about 22.2 kN. In order to generate the

necessary downward thrust, a hydraulic press system will need to be utilized, see Figure 12.1. On Earth these consist of bulky systems of levers that are not suitable for space missions having mass and size constraints. Such a hydraulic system will need to be developed specifically for this mission.

Once drilling is complete the sample will be retrieved. The entire drill casing will be retrieved and stored in the return vehicle. Upon reaching the return module, the drill bit will be removed and an endcap will replace it to seal the sample for the return to earth. The sample retrieval casing will be made from stainless steel in order to preserve the sample from contaminants.

12.4.2 Problems with Core Drilling

There are several drawbacks to this method which need to be addressed in order to explain why it never performs as it is expected. The major drawback is that there is a problem with the left over particles which remain during the drilling process (similar to saw dust when cutting wood). On Earth, air is forced down the core sample which in turn forces the left over particles to escape out the sides of the hole. In space there is no atmosphere and the fragments will stay in the hole and increase the friction on the drill. As these particles build up, they tend to have a bonding type attraction; they can stop the drill far sooner than would be predicted. Since time is not a large concern, the following procedure for removal of the particles is proposed. Drilling will occur in approximately thirty second intervals. After each interval, the drill will be raised and a burst of high pressure gas, Hydrazine from the propulsion system, will be directed into the hole through small channels in the drill casing, located between the outer casing and the sample retrieval pod, see Figure 12.2. This will force the particles out so that drilling can begin again. Since the bottom of the spacecraft is already protected by the crushable honeycomb, these particles are not considered a threat. Additionally, since the drilling is only in thirty second bursts, overheating of the bit should not be a problem. Assuming approximately 0.32 cm penetration in each drilling interval, the

total drilling time will be approximately 4 hours. This does not account for the time when the drill is being raised and lowered or when the particles are being removed.
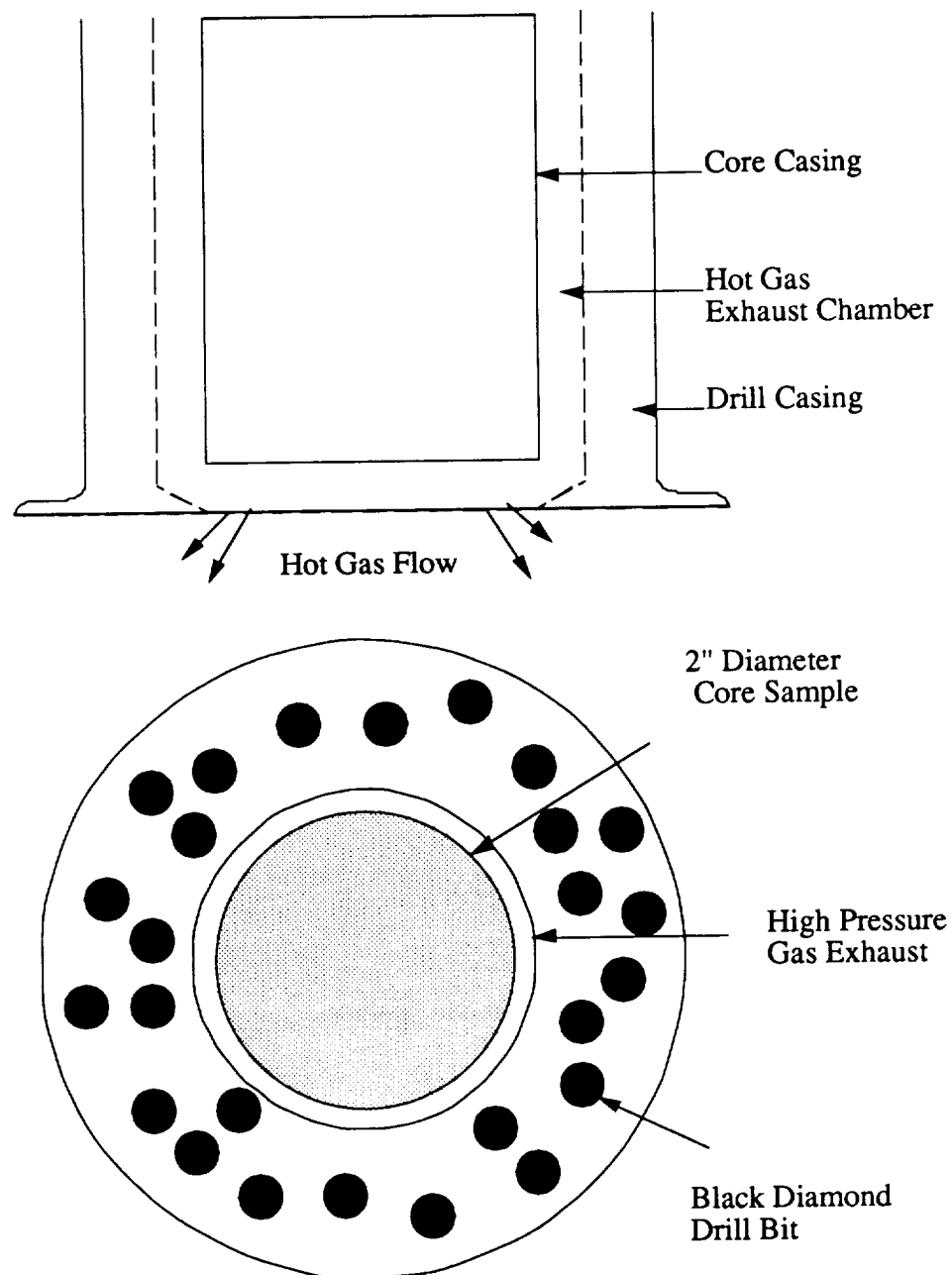
Figure 12.2: Drill Bit Design

It should be noted again that knowledge of the material hardness is essential for the success of the entire mission and that obtaining a core sample may, in fact, not be possible with present drilling technology [47]. This reality was observed when the push tube core drills failed to retrieve solid rock samples from the moon [48].

12.5   Conclusions and Recommendations

As previously stated, determination of material properties is essential in designing the attachment and drilling equipment. Current experiments are being conducted where materials are placed in vacuum for extended periods of time. This procedure is done to extract impurities, such as water, in order to simulate materials found in space. Since this process changes the material's molecular bonds, this process could conceivably take many years. It is therefore recommended that smaller scale missions initially retrieve regolith samples before a full scale drilling operation is undertaken. From these samples a closer representation of the core material could be obtained.

Assuming drilling will be possible, a specific drilling apparatus needs to be developed. The major technologies that need to be advanced are the thrust producing mechanism (or hydraulic press) and harder more durable drill bits.

13.0 Retrieval

13.1 Requirements

The retrieval method will require safe and efficient recovery of the samples from LEO.

13.2 Retrieval Description

For the final leg of the journey, the spacecraft must descend through the atmosphere and return the sample to the Earth. The Space Shuttle will retrieve the spacecraft from LEO. By this method, the spacecraft would not require the added mass of a heat-shields, and parachutes. Space Shuttle retrieval, would entail the spacecraft entering Low Earth Orbit (LEO) and remaining their until the Shuttle can perform the retrieval. This retrieval method will require an additional mount on the spacecraft which could support the force of the Shuttle's robot arm as it pulls the spacecraft into the cargo bay. Then the Shuttle will carry the spacecraft back to Earth inside the cargo bay. This will require additional propellant to place the spacecraft into a suitable LEO and to perform the necessary maneuvers to rendezvous with the Space Shuttle. Another important consideration is also the availability of the Space Shuttle. However, the spacecraft can wait in LEO for an extended period of time, since the sample would most likely not be extensively affected by a long wait time until the Space Shuttle can perform the retrieval.

13.3 Conclusions and Recommendations

The sample will remain in LEO until the Space Shuttle can perform a convenient retrieval. The wait-time in LEO will highly depend on Shuttle availability.

14.0 Cost Analysis

14.1 Requirements

There are several reasons why a cost analysis section should be done. Two of those reasons are to use a budget to restrict how much money can be spent on certain areas or for informational purposes only. The first situation, that of working within the strict guidelines of a budget, seems to be more realistic. However, for this mission project, a cost analysis section is being done for informational purposes. This will help provide a comparison between this objective and those done in the past.

There are two main requirements for the cost analysis. They are that the final cost is reasonable and that the cost analysis methods that are used to find the final figure be feasible to use. The methods that were used in this cost analysis fall within these requirements.

14.2 Subsystem Cost Breakdown of the Spacecraft

Using the cost analysis models given in Wertz and Larson [8] and Cyr [49], a complete list of spacecraft systems and equipment was compiled. Using this list of subsystems, a spreadsheet was developed to calculate the cost of the spacecraft and life cycle cost. The major categories of subsystems for the cost analysis spreadsheet and their costs are shown in Table 14.1.

14.3 Discussion of Spreadsheet

There are four parts to the spreadsheet. The first is the Research, Development, Testing, and Evaluation (RDT&E) cost for the space segment portion. These costs are acquired from the actual researching and testing of prototypes for the various subsystems on the spacecraft. Most of these cost estimates are based on mass and power, which makes the computations easy to do since the details of each area are easy to develop.

Table 14.1: Cost Analysis Breakdown (FY92$M). (Wertz, J.R. and Larson, W.J., *Space Mission Analysis and Design*, Kluwer Academic Publishers, Norwell, MA, 1991 and Cyr, K., "Cost Estimation Methods for Advanced Space Systems," NASA Johnson Space Center, 1988.)

Space Segment Cost — Research, Dev., Testing, & Eval. (RDT&E)		Space Segment Cost — First Unit	
Communications		Communications	
Antenna	3.77	Antenna	0.88
Electronics	10.29	Electronics	5.27
Spacecraft Bus		Spacecraft Bus	
Structure/Thermal	35.87	Structure/Thermal	6.39
Tracking, Telemetry, & Control	30.71	Tracking, Telemetry, & Control	16.87
Attitude Determination	38.80	Attitude Determination	10.01
Power	328.11	Power	17.68
Drill Mechanism	142.67		
Propellant	125.24	SUBTOTAL	57.09
Scientific Instruments	44.83		
Software	380.88		
SUBTOTAL	1141.16		

Ground Segment Cost		Total Cost	
Development		Space Segment Cost	
Software	189.89	RDT&E	1141.16
Equipment	169.81	First Unit	57.09
Facilities	37.73	Ground Segment Cost	
Management	37.73	Ground Station	919.39
Systems Engineering	62.89	Ground System Operation and Support	611.26
Product Assistance	31.45	Launch Segment	115.70
Integration & Test	50.31		
Logistics	31.45	TOTAL COST	2844.60
Operations and Maintenance			
Maintenance	307.13		
Contract Personnel	1.00		
SUBTOTAL	919.39		

The second part is the First Unit Cost for the spacecraft. This is the cost that the actual subsystems on the spacecraft will have. Again, most of these cost estimates are based on mass and power.

The next section is also broken into several segments. They are Operations and Maintenance and Development. These figures are approximate costs that will be induced

from the ground portion of the mission. Most of these calculations will be based on the required amount of computer code for the ground segment.

The final part , the total life cost, is the sum of the first three parts. In addition, areas that were not included in the space segment or the ground segment, such as launch segment cost are included in the life cycle cost.

14.4   Cost Estimation Methods

To complete the cost analysis spreadsheet, two cost estimation methods were used. The first method, Cost Estimation Relationship (CER) was taken from Wertz and Larson [8] and the other method uses an equation taken from Cyr [49].

14.4.1   Cost Estimation Relationship

The primary method for the cost estimation was the Cost Estimation Relationship, CER. This method uses different equations for different subsystems and uses a parameter, such as mass, as the input value.

14.4.2   Cost Estimation Equation

This method was used to compute approximate costs for subsystems that were not included in Wertz and Larson [8]. These subsystems are the drill mechanism, propellant, and scientific instruments. The equation found in Cyr [49] is:

$$Cost = 0.000172 \left(Q^{0.5773} \right)\left(W^{0.6569} \right)\left(58.96\,C \right)\left(1.0291^{(Y-1900)} \right)\left(G^{-0.3485} \right)$$

where Quantity is the number of elements and test articles procured, Weight is the dry weight of the element, Culture is a measure of mission difficulty, Year is the year of the launch, and Generation is a measure of subsequent variations on a basic design. The output, Cost, includes researching and testing and the procurement cost. However, the costs for the drill

mechanism, propellant, and scientific instruments subsystems shown in the RDT&E section contain the First Unit costs also.

14.5   Results of the Cost Analysis

As Table 14.1 illustrates, the final estimated cost for this spacecraft program is $2844.60 million dollars for the fiscal year 1992. Compared with older interplanetary spacecraft systems, such as the Pioneer program, this cost appears very high. (The approximate cost for the Pioneer spacecraft bus was $33.12 million in fiscal year 1992 dollars. [8]) However, the cost of the spacecraft seems realistic since it can be expected that more expensive equipment, such as the drill mechanism and power supply, are needed to complete the mission requirements. The Pioneer spacecraft did not require a drill and the amount of power that the asteroid sample return spacecraft does. Almost half of the total cost of the spacecraft is due to the RDT&E segment. If more off-of-the-shelf technology would be used, the RDT&E cost would drop significantly, dropping the total cost also.

14.6   Recommendations

Even though the two methods used to estimate the spacecraft cost worked well, more work can still be done to develop an analysis method that would better approximate the mission cost. Expanding the analysis to include minor subsystems and components would greatly increase the accuracy of the cost estimate.

15.0   Conclusions and Recommendations

This mission design proposal represents only the initial stages of the design process and offers a sound argument for the near-term feasibility of such a project. However, further research will have to be conducted in many of the crucial design areas. In particular, the drilling system and the autonomous landing system will require development and testing since they have not been employed on previous spacecraft. In order to better understand the drilling requirements, it is recommended that a regolith sampling mission be undertaken before the core sample-retrieval is attempted. In addition, the computer algorithms which control these systems must also be developed and tested.

16.0 References

[1] Isakowitz, S.J., *International Reference Guide to Space Launch Systems*, AIAA Publications, Washington, D.C., 1992.

[2] Devore, R., Personal communication, Packet containing General Brochure and EFC Data Sheets, Electrofusion Corporation, February 7, 1992.

[3] Buden, D., et al. "The Stafford Commission Synthesis Group Evaluation of Power for the Space Exploration Initiative." Proceedings of the 26th Intersociety Energy Conversion Engineering Conference. Vol. 2. Boston, MA, August 4-9, 1991, pp. 28-32.

[4] Hartman, R.F., "Modular RTG Technology Status," Proceeding of the 25th IECEC, Vol. 1. Reno, NV, August 12-17, 1990, pp. 235-238.

[5] Armijo, J.S., et al., "SP-100- The National Space Reactor Power System Program in Response to Future Needs," Proceedings of the 26th IECEC, Vol. 2, Boston, MA, August 4-9, 1991. pp. 21-27.

[6] Darooka, D.K., "Ten Kilowatt to Multimegawatt Modular Space Power System Using Stiring Engine," Proceedings of the 25th IECEC, Vol. 5, Reno, NV, August 12-17, 1990, pp. 224-230.

[7] Determan, W.R., "SNAP-DYN: Concepts for Multikilowatt Space Power Applications," Proceeding of the 23rd IECEC, Vol. 3, Denver, CO, July 31-August 5, 1988, pp. 203-213.

[8] Wertz, J.R. and Larson, W.J., *Space Mission Analysis and Design,* Kluwer Academic Publishers, Norwell, MA, 1991.

[9] Labat, J. and Goualard, J., "Preliminary Study of Rechargeable Lithium Cells for Space Applications," Proceedings of the European Space Power Conference, vol. 1, Madrid, Spain, October 2-6, 1989, pp. 271-273.

[10] Sullivan, R.M., et al., "The Delta 181 Lithium Thionyl Chloride Battery," Proceedings of the 26th IECEC, vol. 3, Boston, MA, August 4-9, 1991, pp. 384-386.

[11] Deligiannis, F., et al., "Performance Characteristics of Lithium Primary Cells After Controlled Storage," Proceedings of the 26th IECEC, vol. 3, Boston, MA, August 4-9, 1991, pg. 395.

[12] Standlee, D., "The Hubble Space Telescope Battery Background," The 1990 NASA Aerospace Battery Workshop, Huntsville, AL, December 4-6, 1990, pp. 691-704.

[13] Kenny, B.H., et al., "Analysis of Space Power System Masses," Proceedings of the 25th IECEC, vol. 1, Reno, NV, August 12-17, 1990, pp. 484-486.

[14] Detwiler, R.C. and Smith, R.L., "Galileo Spacecraft Power Management Distribution System," Proceedings of the 25th IECEC, vol. 1, Reno, NV, August 12-17, 1990, pp.446-451.

[15] Sutton, G.P., *Rocket Propulsion Elements; An Introduction to the Engineering of Rockets*, John Wiley & Sons, New York, NY, 1986.

[16] Tinmat, Y.M., *Advanced Chemical Propulsion*, Academic Press, Inc., Orlando,FL, 1987.

[17] Lau, C.O. and Hulkower, N.D., "On the Accessibility of Near-Earth Asteroids," AAS/AIAA Astrodynamics Specialist Conference, Vail, CO, August 12-15, 1985.

[18] *Ephemerides of Minor Planets*, Institut Teoreticheskoi Astronomii, Akademiia Nauk SSSR, 1947-, Leningrad, Izd-vo "Nauka," Leningradskoe otdelenie, 1947-.

[19] Stephenson, R.R., "The Galileo Attitude and Articulation Control System: A Radiation-Hard, High-Precision, State-of-the-Art Control System," *Automatic Control in Space 1986*, Proceedings of the 10th IFAC Symposium, Toulouse, France, June 24-28, 1985, J.P.Chretien, editor, Pergamon Press, New York, 1986, pp.83-90.

[20] Thompson, R.C., Aerospace 401B class notes, The Pennsylvania State University, February 4, 1992.

[21] Knorrchen, H. and Lange, T., "Modular Design and Dynamic Tests on Active Bearing Momentum Wheels," *Automatic Control in Space 1982*, Proceedings of the 9th IFAC Symposium, Noordwijkerhout, The Netherlands, Jun 5-9, 1982, P.Th.L.M. van Woerkom, editor, Pergamon Press, New York, 1983, pp.459-465.

[22] French, J.P. and Griffen, M.D., *Space Vehicle Design*, AIAA Education Series, Washington, D.C., 1991.

[23] Connolly, A., Fabbricotti, M., Kruythoff, P.N., Menadri, A.S., and Underwood, P., "Synopsis of Optical Attitude Sensors Developed by ESA," *Automatic Control in Space 1982*, Proceedings of the 9th IFAC Symposium, Noordwijkerhout, The Netherlands, June 5-9, 1982, P.Th.L.M. van Woerkom, editor, Pergamon Press, New York, 1983, pp.257-264.

[24] Amieux, J.C. and Muller, G., "Space Borne Attitude Measurement Units," *Automatic Control in Space 1982*, Proceedings of the 9th IFAC Symposium, Noordwijkerhout, The Netherlands, June 5-9, 1982, P.Th.L.M. van Woerkom, editor, Pergamon Press, New York, 1983, pp.417-421.

[25] Bokhove, H., "A High Accuracy Sun Sensor," *Automatic Control in Space 1982*, Proceedings of the 9th IFAC Symposium, Noordwijkerhout, The Netherlands, June 5-9, 1982, P.Th.L.M. van Woerkom, editor, Pergamon Press, New York, 1983, pp.265-272.

[26] Flamenbaum, S. and Anstett, P., "Multipurpose Sun Sensor Using a CCD Detector," *Automatic Control in Space 1982*, Proceedings of the 9th IFAC Symposium, Noordwijkerhout, The Netherlands, June 5-9, 1982, P.Th.L.M. van Woerkom, editor, Pergamon Press, New York, 1983, pp.273-282.

[27] Van Der Ha, J.C. and Caldwell, S.P., "Hipparcos Precise Attitude Determination: A Balance between On-Board and On-Ground Capabilities," *Second International Symposium on Spacecraft Dynamics*, Proceedings of an ESA Symposium, Darmstadt, FRG, October 20-23, 1986, ESA SP-255, December,1986, pp.385-393.

[28] Delpech, M. and Maurette, M., "Feasibility of Time Delay Compensation for a Space Teleoperation Task," *Automatic Control in Space 1986,* Proceedings of the 10th IFAC Symposium, Toulouse, France, June 24-28, 1985, J.P.Chretien, editor, Pergamon Press, New York, 1986, pp.279-285.

[29] *Mars Sample Return Mission: Two Alternate Scenarios,* NASA/USRA Advanced Design Program, Final Report, The Pennsylvania State University, June 1991.

[30] Gordon, G.D. and Morgan, W.L., *Communications Satellite Handbook,* John Wiley & Sons, New York, NY, 1989.

[31] Bostian, C.W., and Pratt, T., *Satellite Communications,* John Wiley & Sons, New York, 1986.

[32] Morrison, D., *Voyages to Saturn,* Scientific and Technical Information Branch, National Aeronautics and Space Administration, Washington, D.C., 1982.

[33] Agrawal, B., *Design of Geosynchronous Spacecraft,* Prentice-Hall Int., 1986.

[34] Berlin, P., *The Geostationary Applications Satellite,* Cambridge University Press, 1988.

[35] Tawail, M., "Heat Pipe Applications for the Space Shuttle," AIAA 7th Thermophysics Conference, San Antonio, TX, April 10-12, 1972.

[36] Bard, S., "Advanced Radiative Cooler with Angled Shields," AIAA 16th Thermophysics Conference, Palo Alto, CA, June 23-25, 1981.

[37] Dunn, P. and Reay, D., *Heat Pipes,* Pergamon Press, 1982.

[38] Johnson, E. and Zocher, R., "Galileo Light-Weight Radioisotope Heater Units Design and Safety Analysis," Los Alamos National Laboratory, NM, 1990.

[39] Morris, J., "Thermic Energy Conversion and Metallic-Fluid Heat Pipes: High Power Densities from High-Temperature Material Interactions," AIAA 16th Thermophysics Conference, Palo Alto, CA, June 23-25, 1981.

[40] Cafferty, T., "Radiative Cryogenic Cooler for the Near-Infared Mapping Spectrometer for the Galileo Jupiter Orbiter," AIAA 16th Thermophysics Conference, Palo Alto, CA, June 23-25, 1981.

[41] Yeates, C.M., et al, "Galileo: Exploration of Jupiter's System," National Aeronautics and Space Administration, Washington, D.C., 1985.

[42] "CASSINI: Saturn Orbiter and Titan Probe," National Aeronautics and Space Administration / European Space Agency, Washington, D.C., October 1988.

[43] Wellman, J.B., et al, "Visual and Infrared Mapping Spectrometer (VIMS): A Facility Instrument for Planetary Missions," *Proceedings SPIE,* San Diego, CA, Vol. 834, pp. 213-221.

[44] Bonsignori, R. and Luca, M., "Sensor System for Comet Approach and Landing," *Proceedings SPIE,* Orlando, FL, Vol. 1478, 1991, pp. 76-91.

[45]   Reiley, M.F., Carmer, D.C., and Pont, W.F., "3-D Laser Radar Simulation for
        Autonomous Spacecraft Landing," *Proceedings SPIE*, Los Angeles, CA, January
        23-25, 1991, Vol. 1416, pp. 295-303.

[46]   Gleichman, K., Tchoryk, P., and Sampson, R.E., "Application of Laser Radar to
        Autonomous Spacecraft Landing," *Proceedings SPIE*, Los Angeles, CA, Vol. 1416,
        pp. 286-294.

[47]   Personal conversations with Dr. J. Koehler, Department of Earth and Mineral
        Sciences, The Pennsylvania State University, January-April 1992.

[48]   Elden, J. and Coste, P., "The Challenge of Sample Acquisition in a Cometary
        Environment," Structures and Mechanisms Division, Mechanical Systems
        Department, ESTEC, Noordwijk, Netherlands, ESA Journal 1991, Volume 15.

[49]   Cyr, K., "Cost Estimation Methods for Advanced Space Systems," NASA Johnson
        Space Center, 1988.

Volume III

Multiple Asteroid Sample Return Mission

The Pennsylvania State University

Department of Aerospace Engineering

MULTIPLE ASTEROID SAMPLE RETURN MISSION

by

Christopher Adams, Andrew Aldo, Paul Cotter, William Churley, Marc DiPrinzio, Timothy Dombkowski, Kevin Donahue, Joseph Gagliardino, Paul Glad, Michael Gilroy, John Hawkins, Matt Lear, Mark Pickenheim, Scott Ritenour, Peter Selby, David Smuck, Mark Wright, Joseph Zambetti

June 1992

Abstract

A multiple asteroid sample return mission is proposed incorporating future technologies into the design. This mission utilizes a nuclear-electric, low-thrust propulsion system and a tethered probe in order to retrieve multiple samples from each asteroid. The spacecraft will rendezvous with the asteroids Euterpe, Psyche, and Themis (types Stony-Iron, Metallic, and Carbonaceous, respectively), and return the samples, via a lander, to low Earth orbit for recovery by the Shuttle or its replacement. The transfer orbits, reactor size, and propellant mass were defined with NASA's QuickTop 2 (QT2) program. The spacecraft will use an optical communications system that, compared to conventional systems, has smaller transmission hardware, lower mass, higher data rates, and also consumes less power. The reusable landing gear will adapt to uneven surfaces, cushion the landing impact, and keep the spacecraft vertical for drilling. The drill system will make use of several devices to keep heating and power requirements low, such as an augering device to remove the heated drilling debris. This system would also allow for a new drill stem to be used for the retrieval of each sample. The spacecraft mass is 15,800 kg; therefore, a Titan IV will be used to reach Low Earth Orbit (LEO), and a low-thrust spiral trajectory will be followed until Earth escape.

Table of Contents

List of Figures

List of Tables

1.0   Introduction

1.1   Mission Rationale

An asteroid sample return mission has been previously proposed by several research institutions, including the National Aeronautics and Space Administration and The Massachusetts Institute of Technology [1,2]. The need for such a mission is driven by a continuous depletion of the Earth's scarce resources (i.e., precious metals, ores, and water). Since little is known about the chemical properties of asteroids, there is a need to explore their composition in order to evaluate possible resource substitutes and to contribute to the overall knowledge of the scientific community.

1.2   Proposed Mission

This report proposes a scientific sample return mission to three of nine possible asteroids which are located in the asteroid belt (see Figure 1.1). Several asteroids were evaluated based on their orbit eccentricity, distance of nearest Earth approach, and angle of inclination relative to the Earth's ecliptic. The proposed design will incorporate a main spacecraft/lander configuration. The main spacecraft/lander configuration will rendezvous with three asteroids to acquire surface core samples. The main spacecraft is responsible for transporting the lander to the asteroid, maintaining a continuous data link during sampling, and returning the sample. After reaching the asteroid, the main spacecraft portion of the vehicle will be responsible for defining the asteroid's topography, gravitational field, and spin rate before the lander is sent to explore its surface. The lander will then descend to the surface of the asteroid while still being attached to the main spacecraft by a tether. On the asteroid, several tests will be performed to disclose the chemical composition of the surface and core. After removing three core samples, the lander will return to the main spacecraft. All transmittable data will be relayed back to Earth by a high-gain antenna. The entire

vehicle will then travel to two more asteroids and finally relay the asteroid core and dust samples back to Earth.

1.3   Spacecraft Subsystems

The subsystems of the spacecraft detailed in this report include: orbital mechanics; launch vehicle; spacecraft structure; propulsion; power; guidance, navigation, and control; communications; command and data handling; thermal control; micrometeoroid protection; landing gear; and sample extraction.
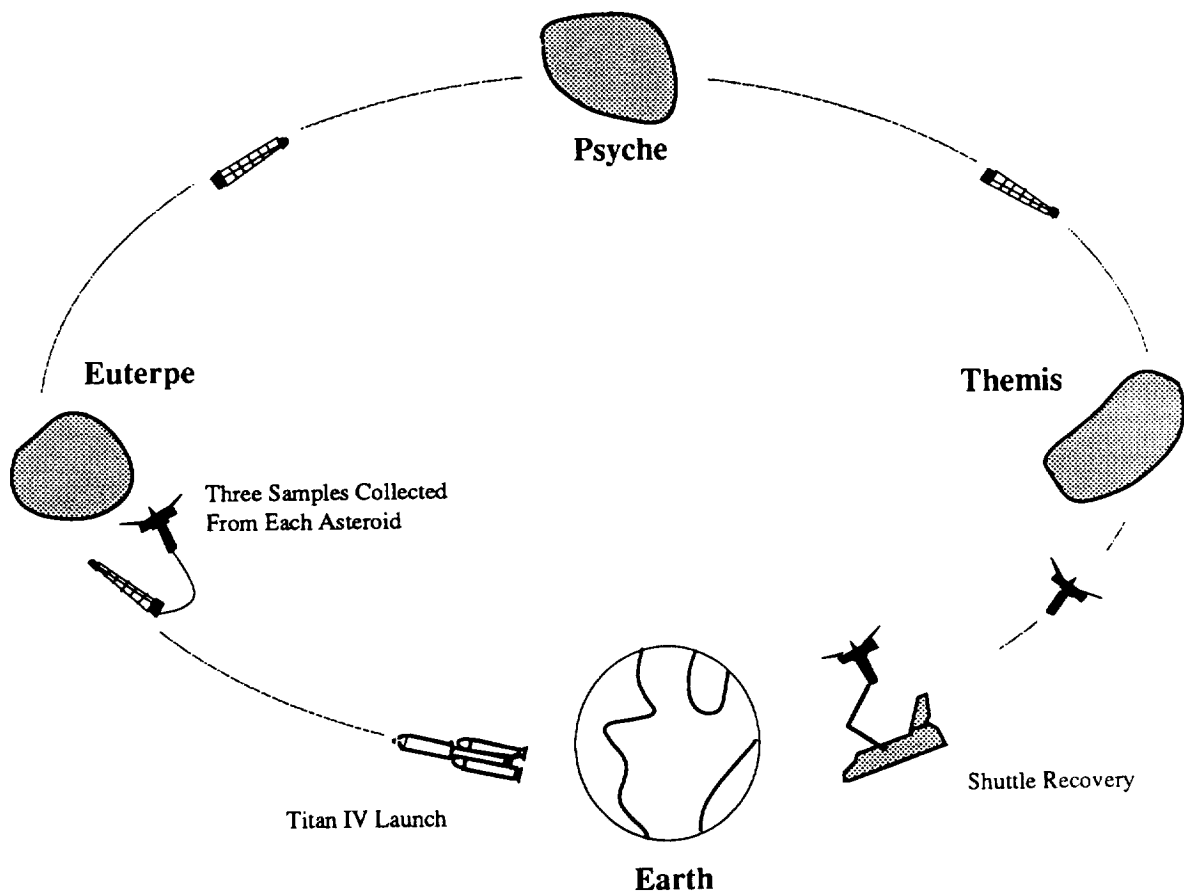
Figure 1.1:   Mission Scenario

2.0 Orbital Mechanics

2.1 Requirements

The orbital mechanics calculations are performed in order to achieve two main goals. First, the mission duration should be minimized, and second, the total spacecraft mass must be kept as low as possible. This is a very difficult task because of the high number of inter-related variables in the calculations. Effects of reactor mass and power, thruster mass, specific impulse (I_{sp}), thrust level, propellant mass, target ephemeris data, the mission's structure, and total time must all be considered to acquire a workable solution.

Minimum reactor, shielding, propellant, and thruster masses are required to keep mission costs low and launch possibilities reasonable. Thus, it is highly desired that the total spacecraft mass be under 17,450 kg, the maximum mass that a Titan IV can carry to LEO [3]. It is common for the design of a low-thrust spacecraft to incorporate dozens of thrusters; therefore, these thrusters contribute significantly to the total spacecraft mass. Minimum thruster implies that a minimum number of thrusters be used, thus reducing the spacecraft complexity and increasing reliability. In addition, using the optimal I_{sp} is desired to balance the total mass of the reactor and the propellant.

Keeping the total travel time to a minimum is also highly desired, after all, the sooner that results are obtained, the better. Even more importantly, however, lower mission time increases overall mission reliability due to continuous wear on all the spacecraft's subsystems. For shorter mission times there is less concern about micrometeoroid bombardment, reactor failure or propellant depletion, mechanical failure of movable parts, and in general, use of the spacecraft parts beyond their recommended lifetime.

Ultimately, the orbital mechanics calculations must provide a means to rendezvous with the three target asteroids long enough for the desired scientific data and samples to be acquired.

2.2 Introduction

Orbital mechanics calculations will include traveling from LEO to Earth escape, rendezvous with the three target asteroids, the return to Earth's sphere of influence, and finally the return to LEO. Since an ion propulsion system will be used, low-thrust calculations must be performed for all legs of this mission. Though this method of propulsion has never been used for a space mission, extensive research has been performed concerning the orbital mechanics calculations necessary for such missions. A brief explanation of these methods is outlined below, along with an explanation of NASA's QT2 program, a low-thrust orbital mechanics calculation tool, and its application to this mission.

2.3 Basic Concepts of Orbital Optimization

Since the concept of the low-thrust trajectory was first proposed, researchers have been attempting to optimize this type of transfer through a variety of means. These researchers are mainly seeking to decrease both the flight time and the required propellant of a given mission. As with any orbital optimization problem, there are two ways to get a solution, either by directly integrating the equations of motion, or by simplifying the equations to obtain an approximate analytical solution. Because the thrust is constant, the energy of the orbit is always changing; therefore, the orbital elements are slowly changing as well. Due to this gradual procession, perturbation methods lend themselves well to the integration of the problem. Black [4] points out, however, that when numerically calculating the full equations of motion, the amount of computation required for transfers involving many revolutions is prohibitive, and numerical errors rapidly become unacceptably large. Thus, another approach involves slightly simplifying the equations of motion and then integrating these newly derived equations.

For low-thrust trajectories, a common technique involves developing a 'fast/slow timescale' solution. This method involves optimizing the change in the orbital elements for one or a few revolutions, thereby obtaining a control law for the slow timescale problem.

This control law is then integrated into the fast timescale problem and applied over many revolutions until the minimum time solution is found. This results in greatly decreased computational time, while retaining a higher degree of accuracy then when more gross assumptions are used in an analytical solution. The only problem with integration is that the calculated solution is only valid for those specific initial conditions; therefore, the entire set of calculations must be carried out again for even a slightly different set of values. The following subsection examines an analytical solution for low-thrust trajectories.

2.4   An Analytical Solution of Low-Thrust Trajectories

Black [4] developed a simplified analytical solution describing low-thrust transfer orbits, and then compared the results to direct integration of a corresponding simplified set of equations of motion. At low thrust levels, the analytical solution was found to be acceptable. As the thrust increased, however, the deviation between the analytic and integrated solutions grew unacceptably large. In addition, the error increased with more revolutions of the spacecraft; this is due to the larger number of iterations that must be performed. In actuality, each calculation is an approximation, and the inherent errors in these calculations grow over time; this effect is seen in Figure 2.1. Two other major points come from his work. First, the results imply that a minimum propellant solution, which is different from a minimum time solution, can be developed. Basically, if the thruster is turned off and on at appropriate times, then the minimum propellant solution can be found. Second, it is estimated that the analytical solution calculates one revolution 90 times faster than the integrated solution [4].
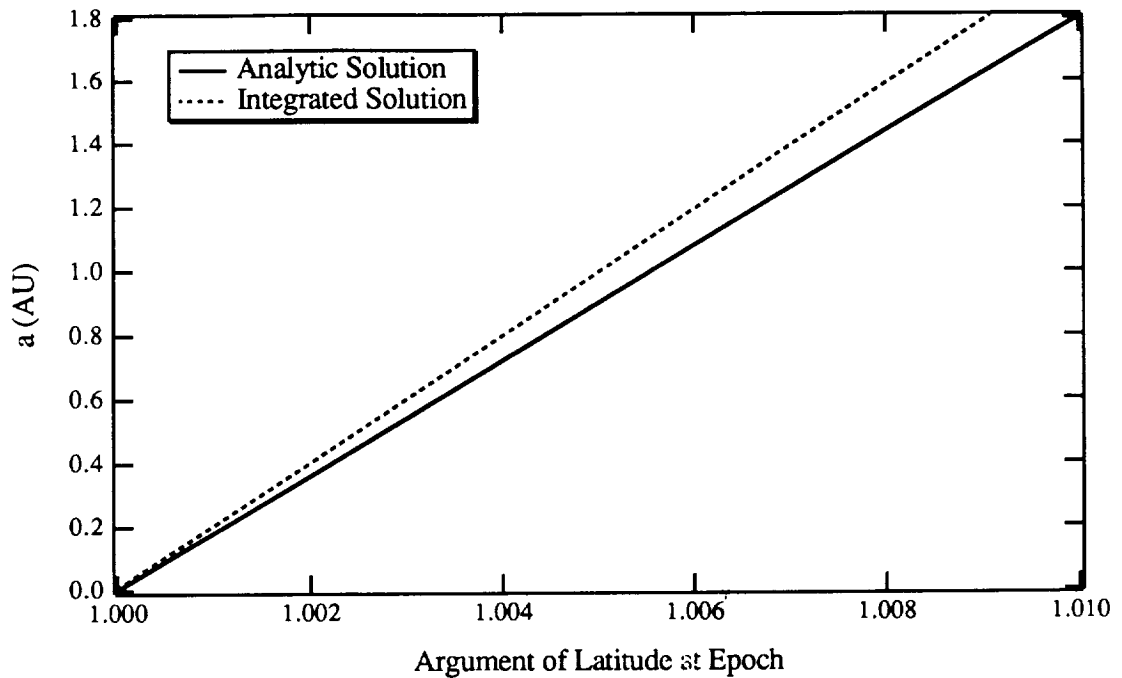
Figure 2.1: Semi-Major Axis Versus the Argument of Latitude at Epoch. [Black, T., "Optimal Low-Thrust Transfer Using a First Order Perturbation Model," M.S. Thesis, Air Force Institute of Technology, Wright Patterson Air Force Base, June, 1985.]

2.5   Asteroid Selection

The target asteroids were selected on the basis of type and accessibility, with secondary consideration being given to size. The data on the chosen target asteroids is summarized in Table 2.1 [5]. The types of asteroids chosen were S (Stony-iron), C (Carbonaceous), and M (Metallic). These types were selected because they are the most common; therefore, this mission should bring back information applicable to most of the asteroids in the Solar System. In addition, these asteroids were chosen because their orbits have a low inclination and similar semi-major axes. This will keep the total ΔV requirement to a minimum. Also, these asteroids are fairly large, and may be easier to track than smaller asteroids. Information on these large asteroids will be useful if mining becomes a high priority in the future since it is more economically sensible to set up mining operations for a longer duration (i.e., on a larger asteroid).

III - 6

Table 2.1: Target Asteroids. [Bender, D. F., "Osculating Orbital Elements of the Asteroids," Jet Propulsion Laboratory, 1979.]

Name	Number	Type	Diam. (km)	a (AU)	e	i (deg)	Ω (deg)	ω (deg)	Mean Anomaly (deg)
Euterpe	27	S	118	2.35	0.17	1.59	94.39	355.79	239.19
Psyche	16	M	249	2.92	0.14	2.09	150.13	226.24	251.13
Themis	24	C	246	3.13	0.13	0.76	35.65	112.19	235.88

* @ Julian Date 2443800

2.6   QuickTop 2 Capabilities

The QuickTop 2 program and the Chebytop system were acquired from NASA Lewis Research Center to perform the orbital mechanics calculations for this mission. QT2 is a driver for the Chebytop system, which is essentially a mass tracking program with major variables being travel time, launch dates, and reactor power for given home and target ephemeris data [6].

QT2 has a large number of capabilities; only those used for this mission are described below. First, during one run, QT2 can be told to sweep through the specified values of one parameter, while optimizing another variable and holding all remaining ones constant. This is very useful for manually optimizing travel time, departure date, or arrival date. Unfortunately, QT2 does not automatically optimize travel time or departure date. On separate runs, however, QT2 can automatically optimize I_{sp}, reactor power, and reactor mass specific power with all other variables held constant. User defined ephemeris data can be input for both home and target. Predefined launch vehicles can be used for launch and departure from Earth's sphere of influence, such as the Titan IV. Also, low-thrust spiraling can be used to leave Earth's gravity instead of a launch vehicle with an upper stage. The total firing duration of the thrusters in one leg of the mission can be set; this is useful for defining the maximum instantaneous thrust, and for ensuring that thrusters are not used longer than their specified lifetime [6].

QT2 will optimize both legs of a mission from Earth to one asteroid and back [6]. However, the proposed mission involves three asteroids, and therefore, four total mission legs. Due to this, the program must be used in a much more complicated manner to obtain actual trajectory data.

2.7   Orbit Calculations Using QuickTop 2

This mission requires four different transfer orbits; leg 1 is from Earth to Euterpe, leg 2 is from Euterpe to Psyche, leg 3 is from Psyche to Themis, and leg 4 is from Themis to Earth. The QT2 code was run for each leg, and a 'patched solution' was determined. This may not represent the minimum total time or propellant mass, since each individual leg is optimized as opposed to the mission as a whole. However, it will serve as an initial estimation of the optimized trajectory.

The first step is to enter ephemeris data for the target asteroids. Since the gravitational pull of even the largest asteroids is nearly negligible, the spacecraft cannot rely on gravity to keep it orbiting around the asteroid. Therefore, the spacecraft must 'match' orbits with the target asteroid at the time of arrival to ensure that the asteroid will be near during the entire observation time. Essentially, the asteroid and spacecraft will be co-orbiting the Sun. During this period, maneuvers will be made to maintain a close, yet safe, distance from the asteroid, and the tethered probe will be deployed. The dynamics of a spacecraft with a tethered lander involve some interesting and complicated analyses, but they will not be covered in this report.

Next, the total invariant spacecraft mass plus a first guess of variable mass was entered. The variable mass includes reactor, shielding, propellant tanks, and thruster masses. The program then calculates propellant mass; everything else is considered invariant spacecraft mass. Also, it was assumed that an I_{sp} of 10,000 seconds would be attainable. Then, the program was run to determine the appropriate reactor mass for each leg of the journey. The appropriate reactor mass was that which would get a total spacecraft mass,

including thousands of kilograms of reactor shielding and hundreds of kilograms of thrusters, across that specific leg of the journey as quick as possible and at a desirable date.

This program must be run in reverse order (leg 4, 3, 2, and 1); the reason for this is best understood by an example. Suppose the program were run for leg 1 and then for leg 2. The propellant requirement determined by the second run would affect the conditions in the first run. Therefore, leg 4 was analyzed first, followed by legs 3, 2, and 1.

Unfortunately, due to limited total spacecraft mass and limited thrust per thruster, the travel times turned out to be fairly large (see Table 2.2). Although launch dates were input over ranges sometimes as great as six years, the total stay time at all the asteroids totaled 6.9 years (also summarized in Table 2.2). This data was acquired after performing hundreds of runs on QT2, most often varying trip time and departure dates.

Table 2.2: Results of the Orbital Mechanics Calculations.

Event	Start Date (MM-DD-20YY)	Duration (days)	Propellant (kg)	Thrusting Time (days)
Leg 1	03-20-02	2401*	2581*	1946*
Euterpe stay	10-15-08	514	0	0
Leg 2	03-13-10	783	1037	782
Psyche stay	05-04-12	1347	0	0
Leg 3	01-11-16	1000	1146	864
Themis stay	10-07-18	650	0	0
Leg 4	07-18-20	2091*	2105*	1587*
TOTAL	04-09-26**	8786*	6869*	5179*

* includes geocentric spiraling
** LEO arrival date

Once the propellant requirement was calculated for legs 3 through 1 of the journey, the total propellant tank mass was calculated. This was then added to the total spacecraft mass required for the fourth leg, with a mass margin of error of 200 kg. This leg was then refined to yield a final total spacecraft mass, power, and fourth leg travel time as well as

departure and arrival dates. This information was then used in calculating final trajectories for legs 3 through 1. All four transfer trajectories are shown in Figure 2.2, along with first point of Aries, the Sun, and the initial target asteroids.

The resultant mass of the spacecraft was too great for an upper stage to be used on a Titan IV. Therefore, the spacecraft will spiral from LEO to a heliocentric orbit, and on to Euterpe. The additional propellant and tank mass for the geocentric spiraling phase has been incorporated into the spacecraft total mass. Unfortunately, after extended efforts, a rather large travel time of 24 years resulted. This could be lowered by altering the chronological order of asteroids visited, or by visiting different asteroids altogether. The mission design only considered visiting the asteroids in the order of Euterpe, Psyche, and Themis.
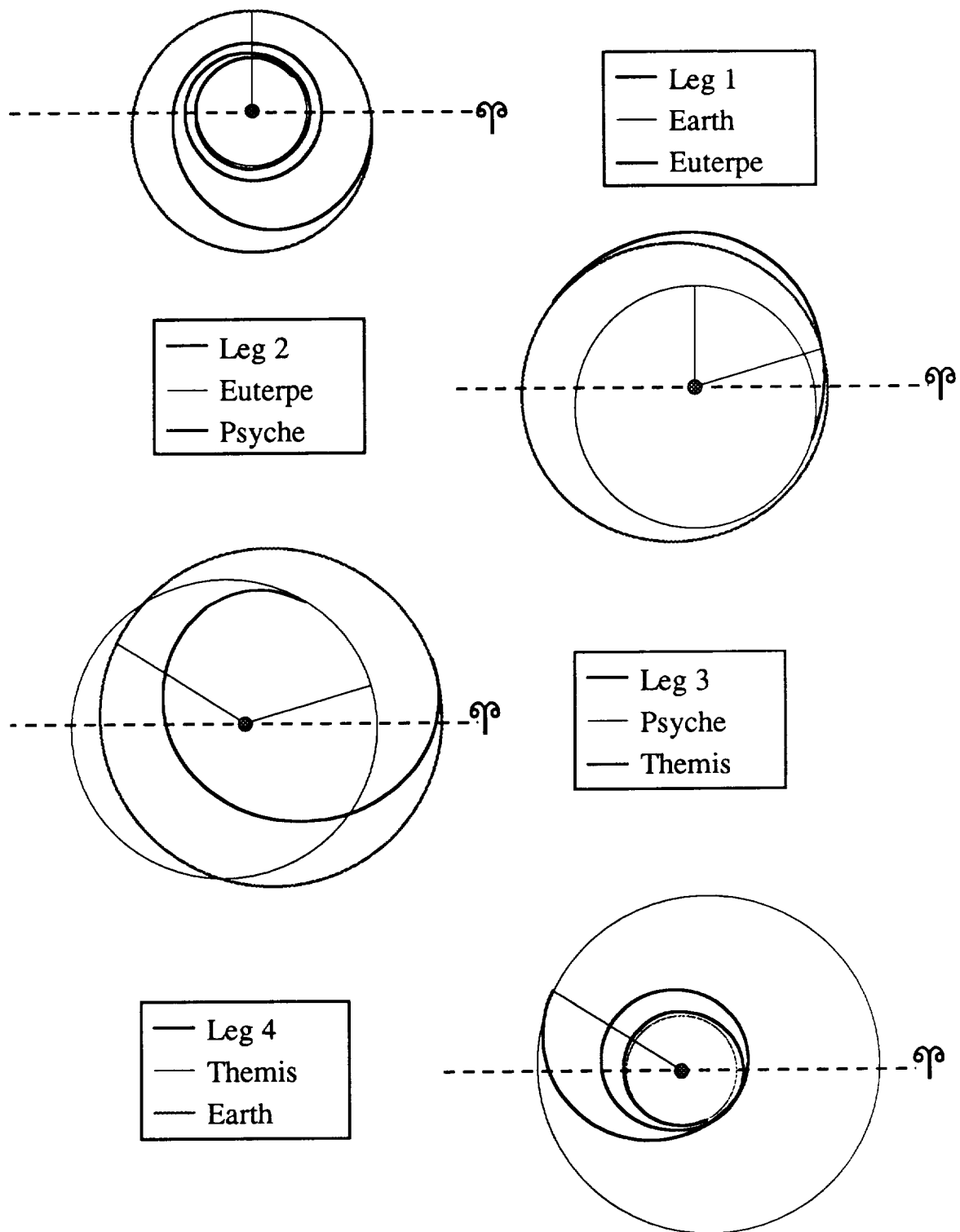
Figure 2.2: Transfer Trajectories. [Ephemeris data taken from: Bender, D.F., "Osculating Orbital Elements of the Asteroids," Jet Propulsion Laboratory, 1979.]

2.8   Conclusions and Recommendations

It is obvious that it would be highly desirable to reduce the total travel time, the asteroid stay time, and the total spacecraft mass. Perhaps the I_{sp} of 10, 000 seconds could have been varied more thoroughly to find an optimal balance between reactor mass and propellant mass. It was found that lower I_{sp}'s result in a higher required instantaneous thrust, and this very dramatically increases the total number of thrusters required; this in turn greatly increases the spacecraft mass. Thus, much more propellant is required, and the total spacecraft mass can be doubled if the I_{sp} is reduced too low. As a result, reducing I_{sp} could increase the total trip time to an even more undesirable number; this also implies an increase in the number of thrusters (and thruster mass) because of limited thruster lifetime. The limiting factor is not the huge total mass (even though this increases cost greatly, it is physically possible to use a larger launch vehicle), but the unacceptable complexity of hundreds of low-thrust thrusters, bringing the mission reliability down to nearly zero.

Using a larger launch vehicle and thrusters that can handle more thrust would result in a more desirable total trip time. Also, thrusters with a longer lifetime would reduce spacecraft mass and provide a shorter trip time. It is also quite possible that a different size reactor could have produced a more favorable solution. Changing the ephemeris data, by visiting different asteroids or the same asteroids in a different order, could also produce more desirable results.

3.0   Launch Vehicle

3.1   Requirements

The choice of launch vehicle is dependent on the particular mass, size, and desired initial orbit of the payload. The mass of the spacecraft before launch is 15,800 kg. The stowed spacecraft is approximately 16 meters long with a maximum diameter of 4.5 meters. Furthermore, the mission profile dictates that the spacecraft begin its journey from LEO.

3.2   Total Spacecraft Length

To keep the vital components of the spacecraft at a safe distance from the reactor, a 20 meter truss has been designed. This results in a total spacecraft length of over 25 meters; which is too long to fit in any existing launch vehicle. Therefore, the truss will be collapsed for the launch phase and extended while in LEO. The minimum spacecraft length of 16 meters is therefore determined from the length of the remaining components, specifically 2.5 meters for the reactor and shielding, 2.5 meters for the main spacecraft body, and 11 meters for the large reactor radiator panels.

3.3   Launch Vehicle Selection

There are currently only two American launch vehicles capable of accommodating the spacecraft. One is the expendable Titan IV, and the other is the reusable Space Shuttle. The Titan IV can lift a payload 5 meters wide and 23 meters long with an overall mass of 17,450 kg to LEO. The Space Shuttle can place a 4.5 meters wide by 18.0 meters long payload weighing 22,765 kg into the same orbit [3].

The Space Shuttle is not, however, a feasible alternative since NASA is not willing to carry a nuclear reactor in the cargo bay. In addition, the Space Shuttle will cost approximately 25% more than the Titan IV [3].

This leaves only the Titan IV as the only feasible American launch vehicle. Figure 3.1 shows the spacecraft, with the truss collapsed, in a Titan IV faring. If, however, a major accident or problem develops which will prevent the use of the Titan IV, an alternate launch vehicle must be used. This alternative will be the European Space Agency's Ariane 5, built by Arianespace; its first flight is scheduled in 1995. The Ariane 5 can accommodate a 4.57 meters wide and 18 meters long payload with a mass of 18,000 kg which makes a rough equivalent to the Titan IV [7].

3.4   Conclusions and Recommendations

The Titan IV launch vehicle has been selected to boost the spacecraft into LEO. The Ariane 5 has been named as an alternative launch vehicle if the Titan IV is for some reason unavailable. The cost for a Titan IV is $214 million (FY 2002) [3].
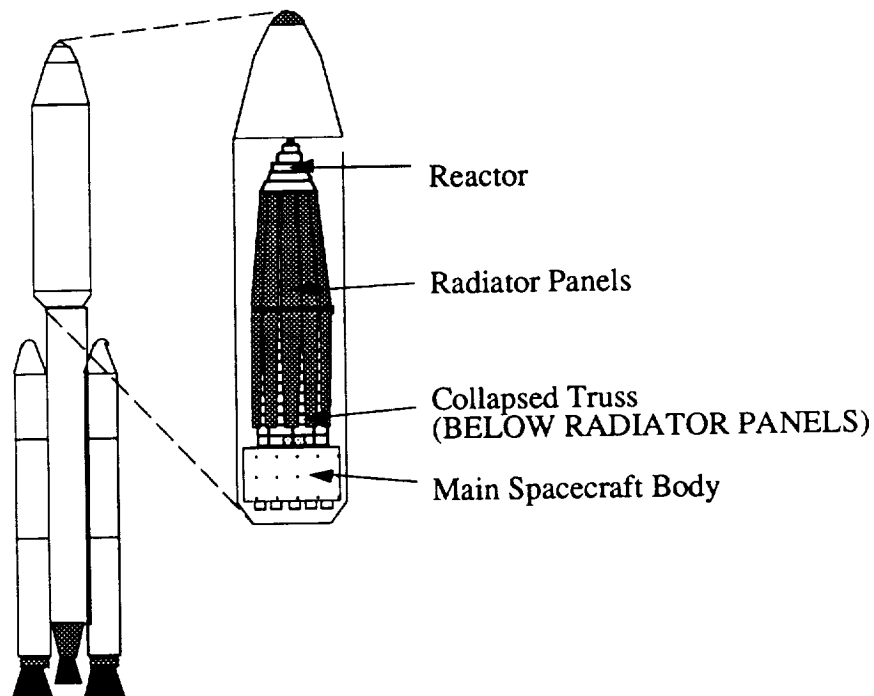
Figure 3.1: Collapsed Spacecraft in Titan IV Fairing

4.0   Structural Subsystem

4.1   Main Spacecraft

The use of composite construction is important in the spacecraft industry because of weight and strength bonuses. Composite materials are used in this mission to construct a truss to connect the nuclear reactor to the rest of the spacecraft, and to design a monocoque torus to hold the propellant and components of the mission.

Special considerations are necessary for composite applications in space however. Composite parts cured on Earth experience an 'out-gassing' effect due to the vacuum of space. It should be possible to specially prepare the composite materials with a coating to prevent or minimize this effect. Also, coverings need to be considered for minimizing micrometeoroid impacts.

4.1.1   Truss Structure

The basic structural design of the spacecraft is a direct result of the need to keep a nuclear reactor about 20 m from the onboard systems and instruments. Other proposed low-thrust designs have used a truss to connect the reactor to the bulk of the spacecraft. This idea was expanded from utilizing a narrow triangular or square truss to a conical truss connecting the outer edge of the reactor assembly to the outer edge of the base of the spacecraft.
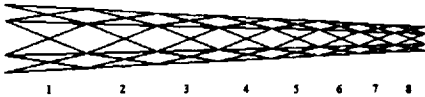
By using the ANSYS computer finite element package, a preliminary design was obtained for the spacecraft structural skeleton. Six main spars with cross members were used to connect a double torus cage at the base of the craft to the reactor at the top (see Figure 4.1). The upper cage at the base will hold the propellant for the mission. The lower cage will contain all components of the mission except those needed to be mounted on booms such as communication systems. For analysis, lumped mass elements were placed at the top of the truss to simulate the reactor and radiator panels while similar elements were used equally around the cage at the base to simulate propellant and spacecraft system mass. A maximum

angular acceleration was estimated on the largest moment possible from a typical control moment gyro. A factor of safety of 1.5 was used with a preliminary factor of 10 to include dynamic effects (net safety factor of 15). Members will be fabricated from Hercules graphite/epoxy and were sized to prevent the first Euler buckling mode. Tubular members were analyzed for the ability to deploy the truss after injection into LEO. The resulting structure is detailed in Table 4.1.
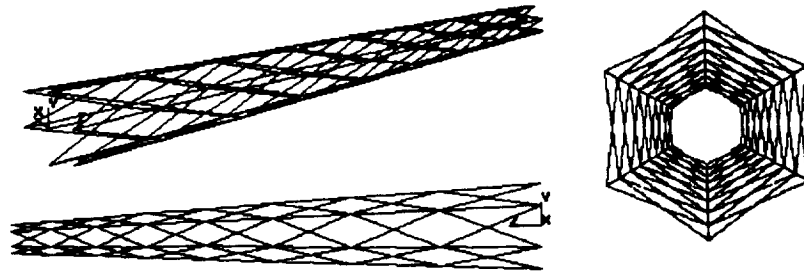
Figure 4.1: Frame Skeleton of Main Truss

Table 4.1: Truss Sizing

	Member Radius (mm)	
Section Number	Main Spar	Cross-Member
1	14.7	9.30
2	13.7	9.05
3	12.1	8.50
4	11.2	8.45
5	9.51	7.82
6	8.94	7.85
7	6.70	7.55
8	6.23	7.13
Total Mass of Truss		**35.8 kg**

4.1.2 Torus Structure

Advanced composite shells consist of strong, fibered sheets of material oriented in specific directions separated by a core usually made of foam or honeycomb as in Figure 4.2. The outer sheets provide strength and stiffness while the core provides shear resistance and greatly increases buckling loads. This design is essential to the aerospace industry since composites are a modern technology with significant strength and weight improvements over conventional materials having applications in all aerospace vehicles.

By using a composite element available on the ANSYS finite element package, multilayered and multidirectional shells can be analyzed for an application. For this mission, it is necessary to design a shell to enclose the spacecraft components, propellant storage purposes, and for anchoring of the landing craft (see Figure 4.3).
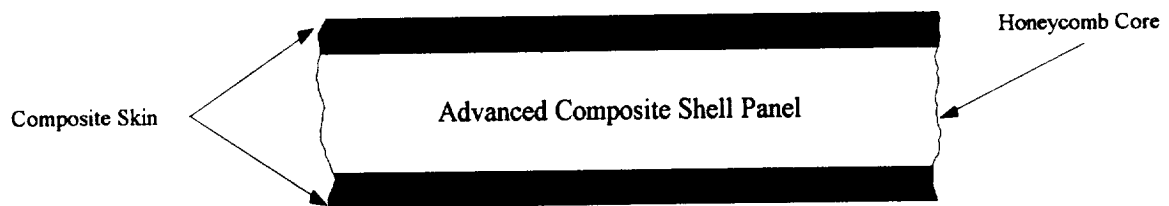
Figure 4.2: Typical Composite Shell
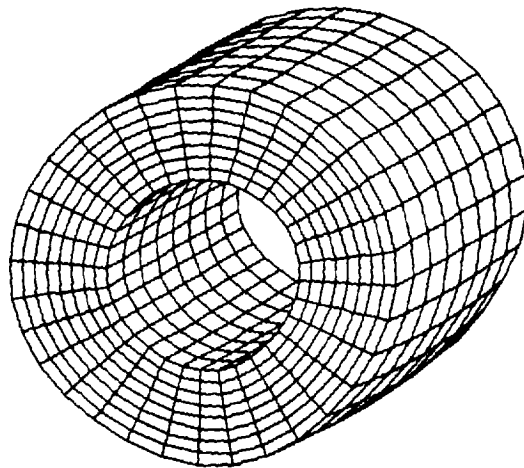
Figure 4.3: Torus Shell

It is also necessary to carefully consider material selection. Graphite/Epoxy is commonly used in aircraft, however less stiff Kevlar composite is more tolerant of damage. Material choice is important for the shell of the spacecraft on this particular mission. Micrometeoroid damage can be anticipated and an outer layer of thin aluminum and foam core or similar material will be added over the torus shell design adding a buffer zone to significantly lower composite impacts. A monocoque design with a graphite/epoxy sandwich surrounded by a buffer zone to minimize impacts was chosen. This configuration will provide a strong and light structure that will house all instruments and systems, provide propellant storage, and house the lander vehicle at its center.

4.1.3   Deployment

The truss structure will be stowed at launch so that the spacecraft torus and nuclear reactor are rigidly secured in the bay of the launch vehicle. After initiation of LEO, the truss powered by batteries will be commanded to deploy. A series of tests will be performed to check the health of the vehicle after the launch. When properly tested, the spacecraft will be sent into an escape trajectory. At this time the nuclear reactor will be started and battery power will no longer be needed.

4.2   Lander Vehicle

The mission will employ a small landing craft to obtain all core samples from prospective asteroids. The vehicle will be stored at the center of the main torus on a retractable mechanism for deployment.

4.2.1   Structure

The mission will employ the lander vehicle depicted in Figure 4.4 to extract core samples from chosen asteroids. The lander will have a rigid truss frame to support the drilling equipment. This truss frame will be made of Hercules graphite/epoxy similar to the

main spacecraft truss. A composite skin will cover this hexagon shape truss in a cylindrical fashion. The composite skin material will be a graphite/epoxy sandwich with a honeycomb material separating the composite layers, similar to the torus structure. This will protect the internal components from dust and debris which may result from drilling. The drill will be located at the centerline of the lander while the barrel-like storage compartment containing the samples will be slightly off center. This will leave one empty storage cylinder from which the drill can pass through at the centerline.
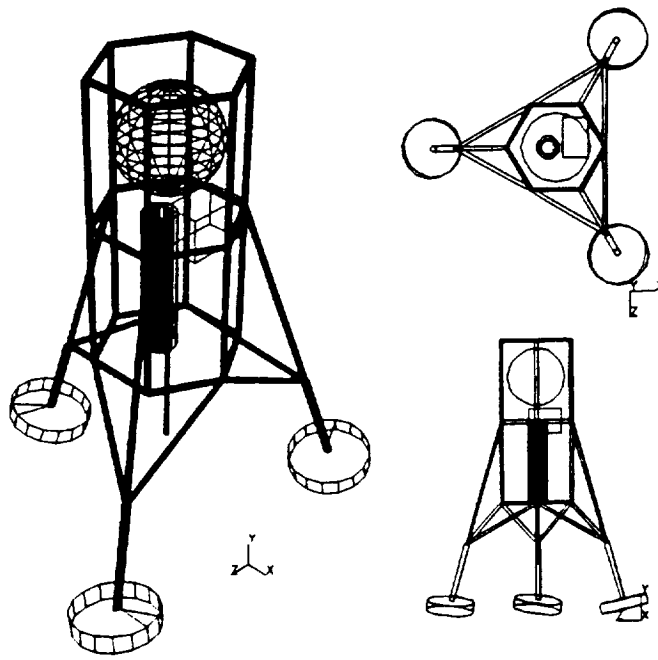
Figure 4.4:   Lander Configuration

Scientific instruments will be located toward the top of the lander vehicle with the exception of an altimeter, which will be located near the bottom, assisting with guidance, navigation, and control. Batteries will be onboard the lander to power a transmitter to be used once the lander is jettisoned from the main spacecraft into LEO. This will aid in the Shuttle recovery portion of the mission. A spherical tank will be located in the upper portion

of the lander, which will store xenon propellant. This supply will be used by thrusters located at strategic positions on the lander.

Retractable landing gear will be used on the lander vehicle. This landing gear will consist of three legs which will fold down from the sides of the lander. These legs will be equipped with sensors to determine the current position of the landing gear. This is necessary in the event of a failure in one or more of the legs to fully retract. If this should occur, safety abort mechanisms will detach the legs, since there will not be enough clearance to fit the lander in the torus structure with the any of the legs down. Backup mission scenarios may be developed in case of such a failure, such as taking the remainder of the samples at the current asteroid before detaching the landing gear.

4.2.2 Attachment

Power to the lander vehicle will be supplied through a umbilical tether which will connect the lander with the main spacecraft. This cable will be 0.5 to 1 km in length. It will be stored in a cylindrical compartment located in the back of the torus structure. The tether will be wound to minimize storage space as well as for simplicity in collecting the excess once the lander is secure and inside the torus. This tether will supply power and provide a data link to and from the lander as well as providing a physical means to reel the lander back to the main spacecraft in the event of any navigational problems. Another technique employed in this mission is attaching the lander vehicle to the main spacecraft with a retractable boom. This boom will work like a power antenna on an automobile. At the tip of the boom a disk will be mounted which will actually connect with the lander. The umbilical tether will be located inside the boom to avoid being tangled throughout the mission. This boom will extend a safe distance outside the torus structure where the lander will either detach or dock. Once the lander is secured, the boom will retract, pulling the lander inside the torus. This will reduce any potential problems such as collision with the main spacecraft.

4.3 Structural Conclusions and Recommendations

Using ANSYS finite element analysis, a mass estimate for a graphite/epoxy spacecraft structure was obtained. Placement of subsystems on the spacecraft bus needs to further considered. Also, mass estimates of the lander vehicle are provided although further analysis is needed to finalize the design. Mass and cost estimates are provided in Table 4.2.

Table 4.2: Structure mass and cost estimates

	Mass (kg)	Cost ($M)
Main Truss	35.8	198.53
Torus Shell	140.0	81.00
Lander Frame	45.0	93.81
TOTAL	**220**	**373.34**

5.0 Propulsion Subsystem

5.1 Propulsion Requirements

The propulsion system chosen for this mission must meet demands such as thrusting for long time periods (8-15 years), utilizing high I_{sp}, and having complete control of thrusting at all times. This system must be able to transport the spacecraft from Earth to the asteroids and back meeting these criteria.

5.2 Low-Thrust Propulsion

A low-thrust propulsion system will satisfy the requirements of the mission. A high-thrust propulsion system has relatively low I_{sp} values. For this mission, the low-thrust system is more feasible. The low-thrust system will utilize an array of thrusters powering them with an electric power plant. The SP-100 has been selected as the powering unit for the thrusters and is discussed further in Section 6.0.

5.3 Thrusters

The thrusters used on the spacecraft must provide high I_{sp} and still provide enough thrust for the mission. Several types of thrusters were analyzed including DC arc jet, resistojet, and ion-thrusters.

Both the DC arc jet and the resistojet have very complicated network systems consisting of various components. DC arc jets have short burn duration availability, yet offer higher thrust than most electric thrusters [8]. Resistojet thrusters use a multi-propellant system which complicates the system further and has a high I_{sp} degradation rate [9]. These facts make the ion-thruster most feasible for the mission.

Ion-thrusters work by introducing neutral propellant atoms into an ionization chamber where they are ionized using an intense electric field [10]. This will produce positively charged propellant ions which pass through a magnetic field and are then accelerated by a

screen-accelerator potential difference. Through this process, the ions become a high-velocity exhaust stream. A schematic of a Kaufman ion-thruster is shown in Figure 5.1.
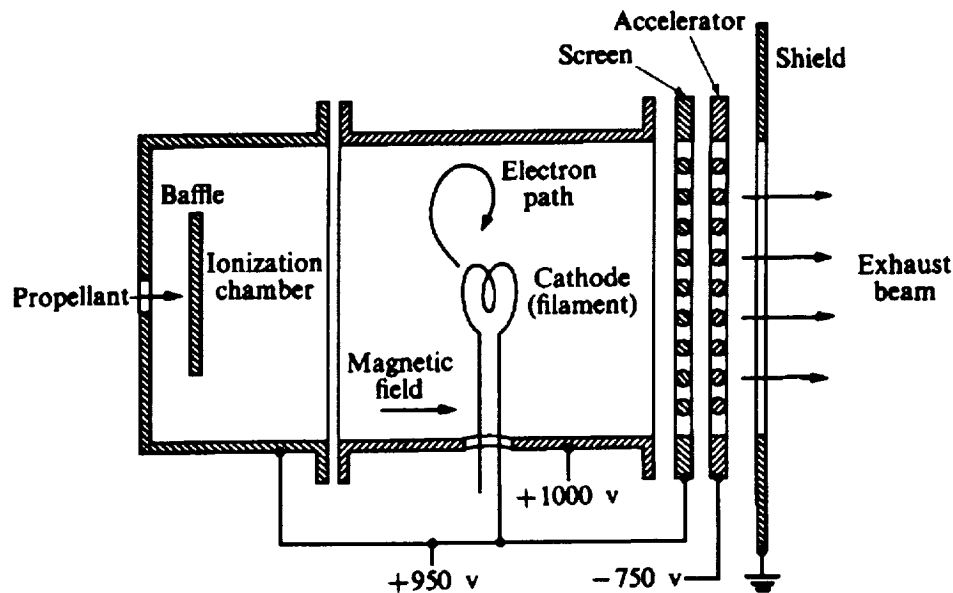
Figure 5.1: Schematic of Kaufman Thruster. [Hill, P. and Peterson, C., *Mechanics and Thermodynamics of Propulsion*, Addison-Wesley Publishing Co., 1992]

Multiple thrusters must be carried for two reasons. First, ion-thrusters have an optimum size due to constraints of maximum ionization while maintaining minimum thruster wear. An optimized thruster can be seen in Figure 5.2.

From the scale of the figure, the size of a thruster is relatively small, roughly 6 inches by 6 inches in cross-section. An ion-thruster's size cannot be increased to produce greater thrust [10]. The second requirement affecting the number of onboard thrusters needed on the spacecraft is the thruster lifetime prediction versus the thruster burn time. Similar to an engine spark plug, repetitive electrical arcing wears the metal of the anode and cathode. Once the wear becomes too great the thruster will no longer work efficiently. Just as spark plugs need to be replaced in a car, additional thrusters must be carried in the event of necessary thruster replacement. Ion-thrusters have a predicted lifetime of about 10,000 hours of use or approximately 1.1 years. A mission that required 3.3 years of thrusting would require a minimum of 3 sets of thrusters. In addition to the required number of thrusters,

there should be some redundancy in the system in case of thruster failure. A typical mission that required 3.5 years of thrusting might require 4 or 5 sets of thrusters for success. The thrusters chosen for the mission each produce 0.8 mN of thrust, have an I_{sp} of 10,000 sec., and a lifetime of approximately 300 days [11].
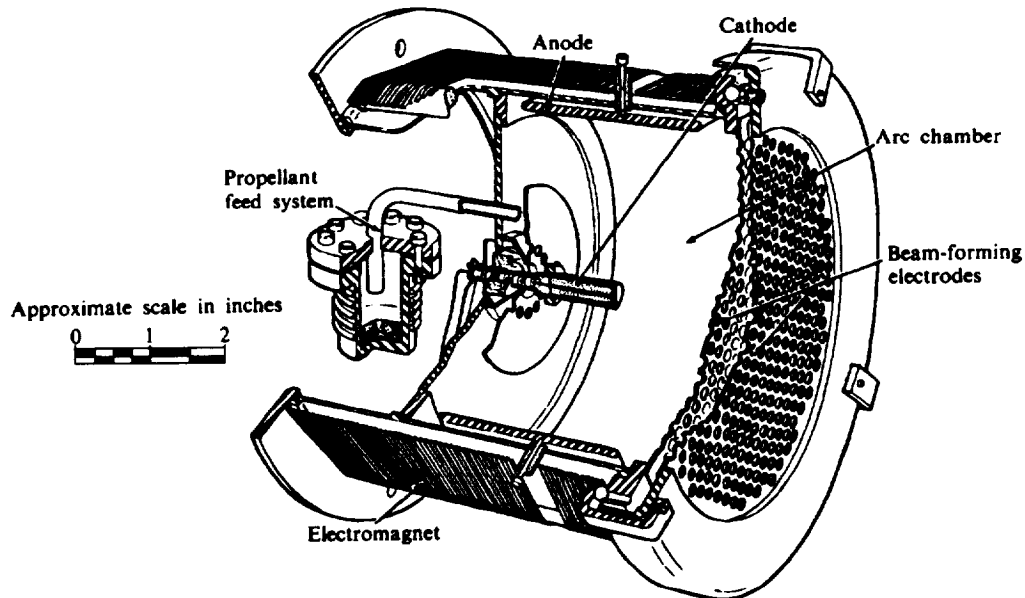
Figure 5.2: Low-Current Ion-thruster. [Hill, P. and Peterson, C., *Mechanics and Thermodynamics of Propulsion*, Addison-Wesley Publishing Co., 1992]

5.4   Low-Thrust Propellant

The propellant chosen for this mission is xenon. It was chosen because it offers high efficiency, is readily available, and is relatively safe to work with. Figure 5.3 shows the relationship between specific impulse and efficiency. The specific impulse for this mission is assumed to be 10000 sec which is based on current thruster research. Xenon also offers a high-thrust to power ratio as can be seen in Figure 5.4. This figure can be extrapolated for the specific impulse used for this mission. It also has a much higher boiling point than the other propellants considered for this mission [11]. This is particularly important because the mass of propellant needed for the mission is large (800 kg) and storage space is limited. Therefore the xenon will need to be stored on board the spacecraft in the liquid phase.
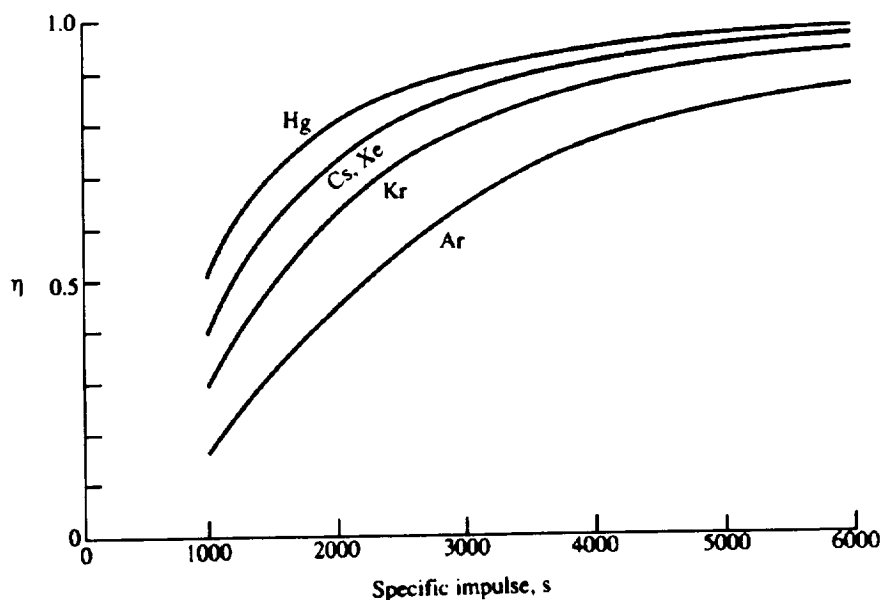
Figure 5.3: Ion-Thruster Efficiencies. [Hill, P. and Peterson, C., *Mechanics and Thermodynamics of Propulsion*, Addison-Wesley Publishing Co., 1992]
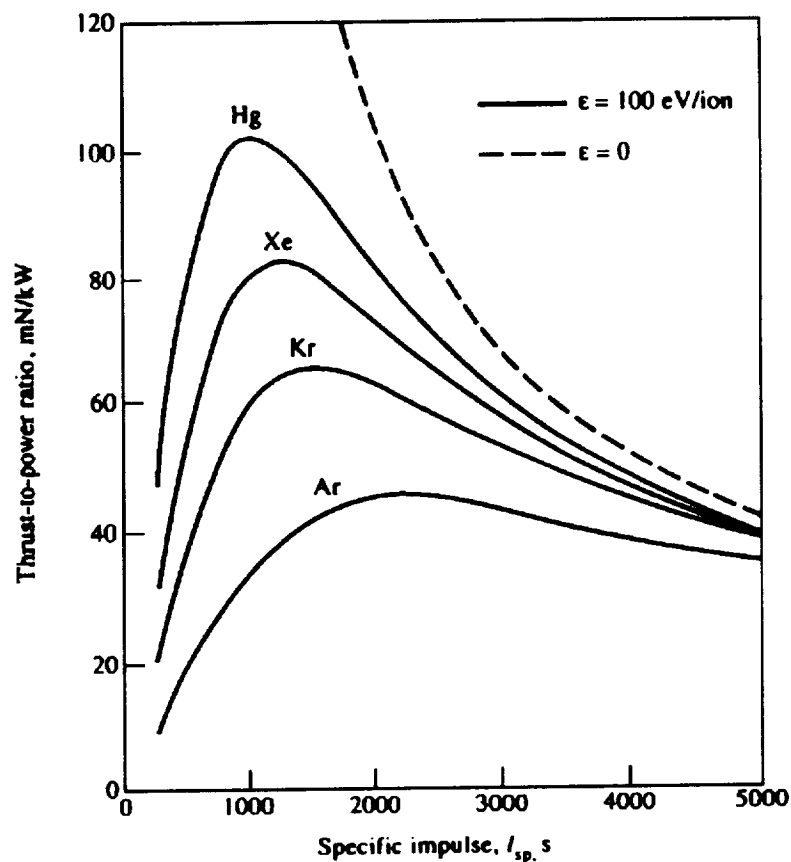
Figure 5.4: Thrust-to-power ratios for high-performance ion propulsion subsystem operated on various propellants. [Hill, P. and Peterson, C., *Mechanics and Thermodynamics of Propulsion*, Addison-Wesley Publishing Co., 1992]

III - 25

5.5 Propulsion Conclusions and Recommendations

The number of thrusters as well as the mass of propellant were determined using the QT2 program. If parameters of the orbital mechanics are altered, estimates are subject to change.

Future work would include more intricate analysis in the system layout, specifically including the plumbing network, pressure tanks, fuel storage, and propulsion network configuration. A thruster capable of producing higher thrust levels or able to sustain longer periods of operation should be explored. Power and mass estimates have been completed for the individual thrusters and thruster control units [11]. Estimates have also been computed for the miscellaneous components of the propulsion section. Cost estimates were derived from the NASA Advanced Cost Estimate program [12]. These values can be seen in Table 5.1.

Table 5.1:   Propulsion Budget.

	Mass (kg)	Power (Watts) per unit	Units used at one time	Total Units	Cost (million $)
Ion-Thruster	8/unit	13600	4	80	108.3
Thruster Control Unit	12/unit	15800	2	40	103.3
Propellant tanks, piping, controls, etc.	680	—	—	—	10
Total	**1800**	**86000**			**221.6**

6.0   Power Systems

6.1   Power System Requirements

The mission layout will require the spacecraft to have long thrust times in low-thrust orbital transfers. An onboard system that can power the ion-thrusters will need to be carried throughout the mission for a number of important reasons. The primary stipulation for an onboard system is to provide an ample power supply to all spacecraft systems such as communications, guidance navigation and control, and scientific experimentation. A secondary reason for the onboard system is to provide a necessary power source to operate the ion-thrusters. It was also necessary to take into account the power supply for the lander. This topic will be discussed in greater detail further along in the section.

A number of different types of power systems were considered for the asteroid sample return mission. From the many first reviewed, two unique systems were selected for further consideration. The two systems, solar and nuclear, both exhibited important features essential towards the success of the mission. Each system was considered on the basis of power output, cost, reliability, and the ability to be tailored to fit the mission. The next section details the final selection and the reasons for the selection.

In addition to the primary power system, an auxiliary power system was designed. The system would consist of a type of battery back-up for the main spacecraft and a small battery back-up for the lander. This topic will again be discussed in greater detail later.

6.2   Primary Power System

The primary power system was studied with two separate power configurations in mind. The first configuration was a solar power system which would use solar arrays similar to those proposed for Space Station Freedom. The power produced by a solar power system would be reduced as the spacecraft travels away from the Sun. This is caused directly by a reduction in the Sun's light intensity, which is proportional to the inverse square of the radial

distance. Primarily due to the increasing power loss, a solar power system was not considered for this mission. If the mission involved the inner Solar System, this type of system would be more feasible. The second power system under consideration was a space nuclear reactor. A nuclear power source would allow the mission to utilize a constant supply of power throughout the mission. The reactor, however, has yet to be implemented on any mission and therefore some risk might arise in using an untested system. Nevertheless, with all the possible ramifications of using a nuclear power source, the advantages far outweigh the disadvantages. The design of the reactor is discussed in detail in the following section.

6.2.1   Nuclear Reactor

A nuclear power source was selected to be used as the primary power supply since the system would not have power losses during the mission. For safety reasons it will be necessary to send a nuclear powered spacecraft to Earth escape velocity before the reactor can be activated. One possible reactor concept that is being considered is the General Electric SP-100 reactor, shown in Figure 6.1, which has a 10 year predicted full-power life [13]. The reactor is a closed system, i.e. there is no radioactive waste emitted, and it works by heating liquid lithium as it is pumped through the core and then using a Rankine conversion system to transform this heat to usable power. The Rankine conversion cycle utilizes potassium as the conversion fluid. The cycle, running at full power conversion, has an estimated efficiency of 20.8% [14]. This value is understood to be relatively low, however, the conversion cycle has not yet been optimized. Lithium will be used as the primary reactor coolant which allows the reactor to remain inactive until escape velocity is achieved. The reason for this inherent safety in the reactor design is that the reactor core is encased in a solid block of lithium at launch. If a launch accident did occur, the reactor core would remain safe and intact. Once activated, excess heat from the reactor would have to be dissipated by radiator panels so the reactor would not overheat. In addition, the reactor will include a redundant shutdown system such as movable reflector elements and beryllium pins

that could be inserted into the reactor core. The core's inherent reactivity feedback also would assist in reactor core stabilization in the event of the core becoming supercritical. The inherent reactivity feedback is the negative feedback produced by the reactor core's thermal expansion properties. As the reactor core superheats, its volume increases due to the thermal expansion.
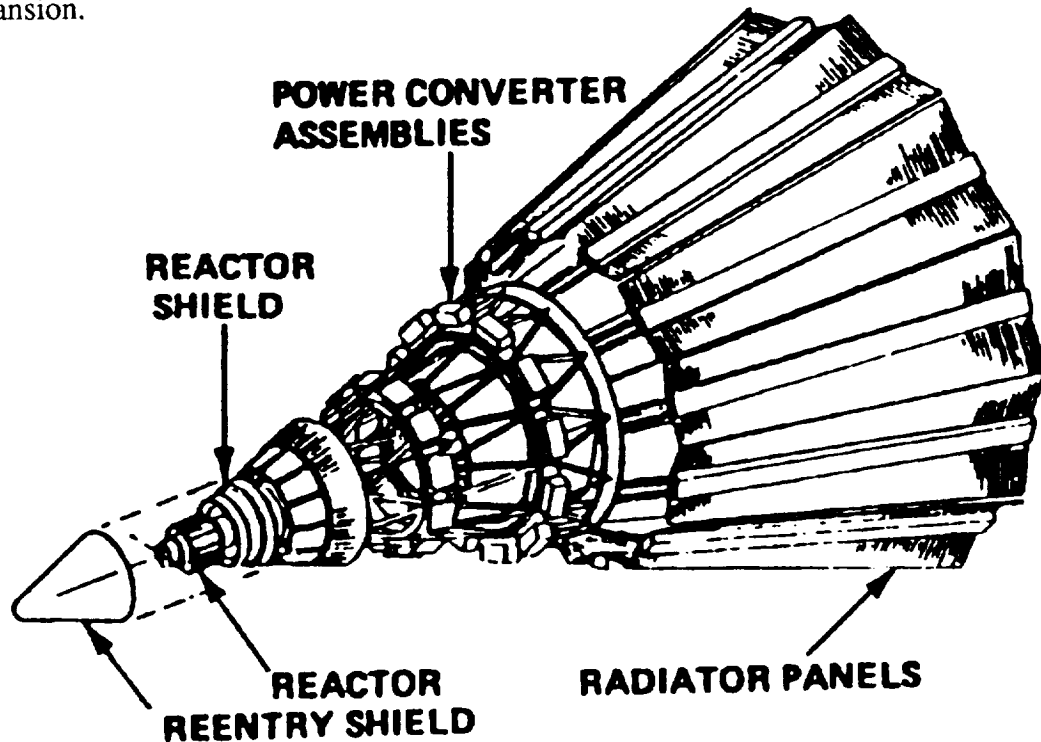
Figure 6.1: SP-100 Nuclear Reactor and Shielding Assembly. [General Electric Space Nuclear Power Tutorial, conducted at NASA Lewis Research Center, May 29-31, 1991]

The mass of an SP-100 reactor depends on the power output generated by the reactor, the reactor's separation distance, and the maximum radiation dosage of the spacecraft [14]. The results of the study are shown in Figure 6.2. A number of different reactor/structure design configurations were investigated. Each configuration places the reactor at a different distance away from important payloads. The configurations also placed an appropriate amount of shielding near the reactor to ensure safe radiation levels. Configurations 1 and 3 have a 20 m separation between the reactor and spacecraft while configurations 2 and 4 have

a 40 m separation. Also, configurations 1 and 2 allow for a radiation dosage of 7.5×10^4 rad over the calculated 10 year life span of the reactor while configurations 3 and 4 allow for a dosage of 5.0×10^5 rad over the same period. The specific mass of the power system is plotted as a function of the power output and specific mass decreases with increasing power due to economies of scale.
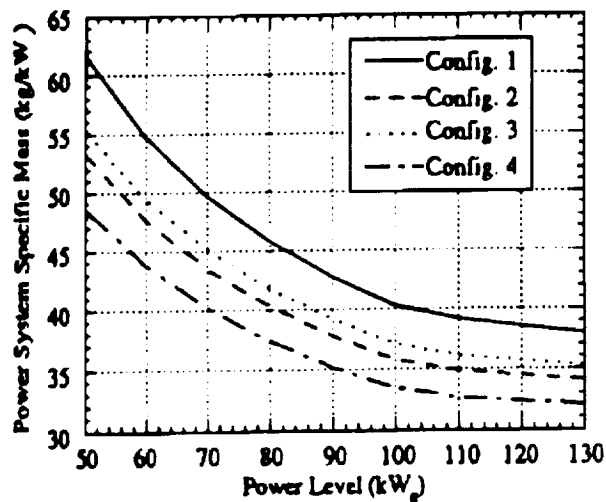
Figure 6.2: Specific Mass of SP-100 Reactor for Varied Power Output. [General Electric Nuclear Power Tutorial, conducted at NASA Lewis Research Center, May 29-31, 1991]

6.2.2 Reactor Safety

The safety of the mission has drawn a good deal of questioning in the area of nuclear safety. The question of radiation release always surfaces when the topic of nuclear power is brought up. The idea of launching a nuclear reactor into the Earth's atmosphere is even more questionable. These questions and others were considered during the final selection of a suitable power system. The design of the General Electric SP-100 reactor has exhibited many important safety features which allow the reactor to perform safely even under adverse conditions. Space nuclear systems have had recent examples of safety judgments from the Galileo and Ulysses launches. The SP-100 design can be compared to the design of these two missions. The reactor design took into consideration the most probable accidents during

III - 30

launch and Earth fly-by. The reactor was designed to remain intact and subcritical during accidents. In the remote chance of inadvertent reentry, the reactor was designed to perform an essentially buried impact. A detailed study of the reactor's safety has been performed on a number of other accident scenarios, however, the likelihood of such accidents is very minute. The General Electric SP-100 reactor is accepted as the future of space nuclear power. The safety, power output, reliability, and overall acceptance are the overwhelming reasons why the reactor was the final selection for the power system for the mission.

6.3   Auxiliary Power

The mission will require an auxiliary power source to supply the spacecraft with the necessary power before the nuclear reactor is brought on-line. This energy source needs to be large enough to supply power to the spacecraft until the reactor is deployed and operational. A set of batteries will be used to provide the power needed. Two different types of batteries were considered for the mission. The first can be labeled as a primary battery source. The battery selected for the primary source was a lithium thionyl chloride battery configuration. This configuration permits the battery to expend the power at a moderate rate in only a matter of hours. The lithium thionyl chloride battery would be used to allow for housekeeping communications and for the deployment of the truss structure. A secondary battery source would be used as a back-up to the nuclear power source. This would only be used in the case of a reactor shutdown or other such problems.

The lander will also require a power source to supply the necessary power to the various systems. Again, a lithium thionyl chloride battery configuration would be used to supply power for basic housekeeping duties. A secondary battery configuration will also be needed when the lander is released from the main spacecraft in Earth orbit for retrieval by the Space Shuttle. This battery configuration would utilize a nickel cadmium (NiCd) cell to store power generated from the nuclear reactor. The battery would then be switched on during the release of the lander. The primary reason for the selection of the NiCd was the batteries long

life span and the extensive database of the system. Also, the NiCd battery is space-qualified in a large pool of missions.

6.4 Power System Conclusions and Recommendations

The GE SP-100 nuclear power reactor was chosen for use on this mission since it is specifically being developed for applications in space. Nuclear safety has been considered and is under further consideration in the development of the power system. The power system was mainly chosen for nuclear electric powered propulsion. The SP-100 is still being developed therefore all mass, power, and cost estimates are subject to change. In Table 6.1 the mass characteristics of the system are given.

Table 6.1: Power Subsystem Mass and Cost Estimates

Functional Subsystem	Component	Total System Quantity	Current Mass Estimate (kg)	Cost (million $)
Reactor	Fuel Pins	1	1215	21.343
	Reactor Vessel and Internals	1	745	30.875
	Reflectors	12	485	51.459
	Safety Rods	3	95	27.683
	Reentry Shield	1	175	22.176
	Total Assembly		2715	153.536
Shield	Neutron Shield	1	900	18.641
	Gamma Shield	1	730	16.495
	Thermal Control Structure	1	985	20.532
	Structure/Vessel	1	670	15.731
	Total Assembly		3285	71.399
Combined Total			**6000**	**224.935**

7.0   Guidance, Navigation, and Control

7.1   Requirements

Several devices will be needed to ensure that guidance, navigation, and control requirements are met during all phases of the mission. Many maneuvers, including midcourse corrections, station keeping, orbit injections, and attitude stabilization will take place during the mission. A maneuver involving the separation of the main spacecraft and the lander will occur at the asteroid. After the surface mission has been completed, the lander will rendezvous and dock with the main spacecraft. These maneuvers will require three-axis control and reaction control systems. Sensors monitoring the position and velocity of the spacecraft will be required to facilitate the arrival at the asteroid.

7.2   Sensors

The navigation and attitude control of the main spacecraft and lander will be handled by an Inertial Measurement Unit (IMU), which will directly measure linear and rotational accelerations. From the acceleration measurements the rotational and linear velocities and positions will be calculated. The IMU will be backed up by two digital Sun sensors and an integrated focal plane star sensor on the main spacecraft. Earth sensors are not useful on interplanetary missions because of the low luminosity of the Earth. During parts of any trajectory away from the Sun, which has intensities of 12 orders of magnitudes greater than the Earth, the Sun falls into the field of view of the Earth sensor, which will also render this type of sensor inoperable. Thus, for trajectories away from the Sun, some other celestial object, such as Canopus which is approximately 90 degrees away from the sunline, is preferable as a reference point [15]. A telescope will be used on both vehicles as a long-range sensor. The telescope on the main spacecraft will be locked onto the expected position of the asteroid and will be used in a way similar to a star tracker. A radar range-rate sensor will serve as the mid-range sensor for the main spacecraft and lander. This radar sensor will

have a range of one meter to three kilometers, and will be used to determine control responses necessary to achieve orbit with the asteroid. Corrections needed to maintain the orbit will be determined with assistance from the horizon sensor. A laser range finder will function as the short range sensor and will also backup and verify the distances of the radar sensor.

7.3   Main Spacecraft Controls

Control moment gyroscopes (CMG), which are capable of producing high torque, will be used to control the attitude of the main spacecraft. The main spacecraft will also have a monopropellant hydrazine (N_2H_4) thruster system for midcourse corrections and trajectory adjustments. Hydrazine thrusters were chosen because of a long heritage, and their thrust level is sufficient for the needs of this mission. Sixteen main thrusters will be used to control the main spacecraft. They will be fixed along two of the principal axes, four thrusters on each arm, and will only be able to fire at an angle perpendicular to a principal axis. There will be eight backup thrusters aligned out of the principal planes. These thrusters will be attached to a ring, allowing changes of the thruster firing angle in 5 degree increments. Each set of two thrusters will be able to backup four of the single position thrusters in case of failure. Placement of the thrusters is shown in Figure 7.1.

7.4   Lander Controls

Four cold-gas thrusters located on the top of the lander will be used for docking and maneuvering purposes. Cold-gas thrusters were chosen so as to reduce the amount of thermal shielding needed during docking maneuvers with the main spacecraft. Four hydrazine thrusters mounted on the bottom of the lander will control the descent and lift off from the asteroid. There will also be a hydrazine thruster mounted on each side of the lander to control lateral movement during operations on the asteroid. The placement of the thrusters on the lander can be seen in Figure 7.2.
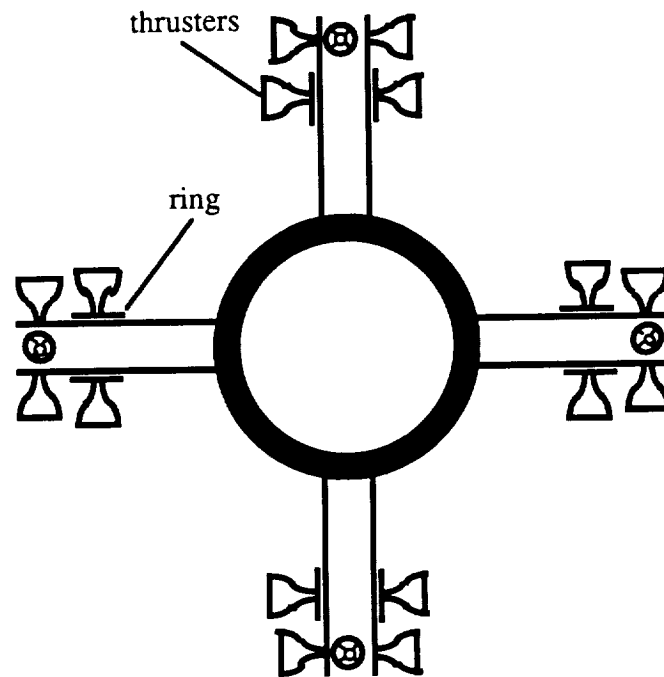
Figure 7.1: Main Spacecraft Cross-sectional view detailing thruster placement
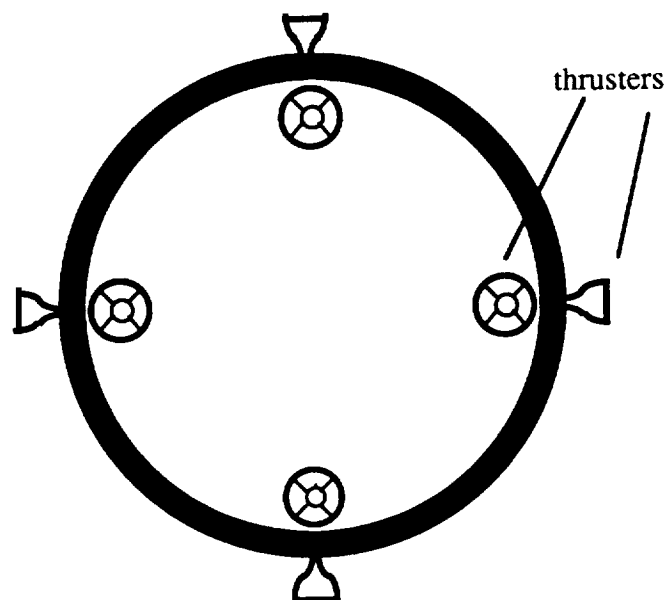
Figure 7.2: Lander — top/bottom view of thruster placement

7.5   Mass, Power, and Cost Budgets

The following tables (Tables 7.1, 7.2, and 7.3) contain mass, power, and cost budgets for the guidance, navigation, and control of the main spacecraft and lander. The cost budget was developed using the formulas found in Reference 3. Hydrazine thrusters were calculated at approximately double the cost of normal cold gas thrusters.

Table 7.1:   Guidance, Navigation, and Control Subsystem - Main Spacecraft (Wertz, J.R. and Larson, W.J., *Space Mission Analysis and Design*, Kluwer Academic Publishers, Dordecht, The Netherlands, 1991.)

	Units	Mass/Unit (kg)	Power (W)
IMU	1	15	100
Sun sensor	2	2	3
Star mapper/tracker	1	5	12
Radar sensor	1	10	5
Laser range finder	1	5	10
Telescope	1	5	3
CMG	1	50	120
Hydrazine thruster	24	0.5	10
Propellant		105	
TOTALS		**211**	**263**

Table 7.2:   Guidance, Navigation, and Control Subsystem - Lander (Wertz, J.R. and Larson, W.J., *Space Mission Analysis and Design*, Kluwer Academic Publishers, Dordecht, The Netherlands, 1991.)

	Units	Mass/Unit (kg)	Power (W)
IMU	1	15	100
Horizon sensor	1	3	8
Telescope	1	5	3
Radar sensor	1	10	5
Laser range finder	1	5	10
Hydrazine thruster	8	0.5	3
Cold gas thruster	4	0.5	2
Propellant		5	
TOTALS		**49**	**131**

Table 7.3: Cost Analysis for Main Spacecraft and Lander Guidance, Navigation, and Control (Wertz, J.R. and Larson, W.J., *Space Mission Analysis and Design*, Kluwer Academic Publishers, Dordecht, The Netherlands, 1991.)

Component	Mass (kg)	RDT&E (FY92$M)	First Unit (FY92$M)
Attitude Determination	80	24.44	6.72
Attitude and Reaction Control	70	13.15	4.28
Additional Costs			
Advanced Technology			
Star Tracker		3.18	1.70
SUBTOTAL		**40.77**	**12.70**
Multiplication Factor for Heritage (0.6)			
TOTAL		**24.46**	**12.70**

7.6 Recommendations

Hydrazine thrusters were chosen over xenon ion gas thrusters due to heritage and thrust levels. They are cheaper than the xenon ion gas thrusters, and the cost of a separate fuel tank is minimal when compared to the cost difference. The development of most of the equipment used for guidance, navigation, and control can be facilitated using existing technology.

8.0 Communications Subsystem

8.1 Requirements

This mission will require more power and pointing precision than a low Earth orbiting satellite. The communication system will have to be able to send and receive data at distances up to 4.54 AU; this will have a profound effect on the selection of the communication architecture. Low power, and especially low mass, are also important design criteria. A power requirement under 100 watts is desirable, though with the very large supply of power from the nuclear reactor, this is not a stringent design criterion. Still, low mass and volume is desirable so that the spacecraft can be launched on a reasonable launch vehicle. A mass under 200 kg and a small or highly collapsible antenna is desired. Data rates of 10 to 100 kilobits per second (kbs) are required.

8.2 Omni-Directional Antenna

During launch the spacecraft main communication subsystem will not be powered up. For communications during the launch phase an omni-directional antenna will be used to relay telemetry and command data. Once LEO has been reached the optical communication system will be powered up, checked-out, and utilized for the remainder of the mission. The omni will no longer be used.

8.3 Communications System Selection

RF and optical interplanetary communication systems were compared. The RF system proposed would involve an upgrade of the Cassini X-Band (8.4 GHz) configuration to Ka-Band (32 GHz) configuration, eliminating the use of X-Band completely [16]. However, the slightly reduced mass and power would still require a fairly large, three meter, antenna. The nuclear power source used to drive the thrusters, would also pose a problem for the RF communication system. For these reasons, an optical communication system will be

implemented. The short wavelengths of optical signals will substantially increase the data rate capability.

8.4 Optical Transceiver Package

There are two major components of an optical communications network. The first is the optical transceiver package (OTP) aboard the spacecraft. The second consists of the Earth orbiting relay station, (EORS) [17].

This system was originally intended for interplanetary missions. The design requires the communication subsystem to have high data rate capabilities, small size and low power requirement. The OTP contains a single, eleven inch aperture telescope (as opposed to the 3 meter antenna dish of the Cassini configuration), which is used for both uplink reception and downlink data transmission. An illustration of the OTP is shown in Figure 8.1. Pointing of the telescope will be accomplished with milliradian accuracies to place the Earth in its field-of-view. The precise tracking and pointing is accomplished by fine steering imaging optics within the unit. The total mass of the optical system is 52.4 kg. The power required for the optical system is only 57 Watts as compared to the 86.8 Watts required for the Cassini configuration. Mass and power summary are broken down by the major components as seen in Table 8.1. The mass allocations were optimized within the constraints of the functional requirements, materials, environments and cost [18].

The communications system can use an EORS or communicate directly to an Earth relay station. The maximum distance for this Earth orbiting relay station is 10 AU, which is more than ample for this mission requirement of 4.54 AU. Downlinking can be done in precise rates of 10 kbs, 30 kbs, and 100 kbs with a bit error probability of 10^{-3}. A five microradian laser beam at a wavelength less than 2.0 microns transmits at an average of 10 Watts. Platform stability is controlled so that the transmitted beam is pointed to the OTP by open-loop pointing,with zero point loss. To receive, EORS has a clear aperture of 10 meters

with a 1 microradian field-of-view. A photomultipier-based, direct detection system is used

for the receiver. More information on EORS is given in Table 8.2 [18].
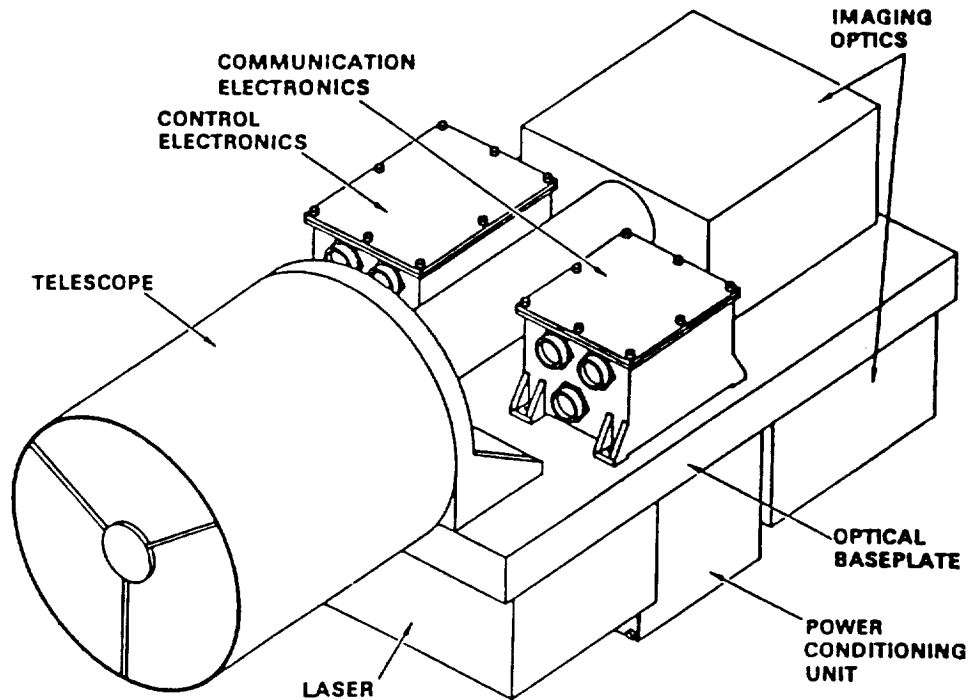
Figure 8.1: Optical Transceiver Package (Isometric View). [Lambert, S. G., et al., "Design and Analysis Study of a Spacecraft Optical Transceiver Package," Final Report, JPL Contract 957061 with McDonnell Douglas Corp., August 19, 1985.]

Table 8.1: Mass and Power Summary for the OTP. [Lambert, S. G., et al., "Design and Analysis Study of a Spacecraft Optical Transceiver Package," Final Report, JPL Contract 957061 with McDonnell Douglas Corp., August 19, 1985.]

Item	Mass (kg)	Power (W)
• Electro-Optics Assembly		
Telescope (11 in.)	8.2	—
Imaging Optics Assembly	6.1	2.0
Laser Assembly	9.1	4.0
Detector Assembly	0.5	0.4
Earth Tracker	2.1	4.6
• Electronics		
Comm. Electronics	4.1	7.7
Control Electronics	5.7	14.5
Power Conditioner Unit	8.9	17.1
Structure/Wire/Misc.	7.7	6.7
TOTAL	**52.4**	**57.0**

Table 8.2: Earth Orbiting Relay Station (EORS) Characteristics. [Lambert, S. G., et al "Design and Analysis Study of a Spacecraft Optical Transceiver Package," Final Report, JPL Contract 957061 with McDonnell Douglas Corp., August 19, 1985.]

Aperture Size	10 Meters Effective
Detector Field-of-View	1 mrad
Receiver	Photomultiplier Based
Direct Detection Quantum efficiency	30%
Transmit Power	10 Watts, Average
Transmit Divergence	5 mrad Diameter
Pointing Loss	Zero
Pointing	Capable of Open Loop Pointing 5 mrad Beam at OTP

There are certain criteria that the spacecraft subsystems must meet so that the OTP will operate with the designed accuracy. First, the spacecraft attitude must have precision control within 2.0 milliradians. This will allow for accurate pointing of the OTP telescope to the Earth. If this criteria is not met, a larger telescope field-of-view would be necessary, meaning a gimbaled telescope with larger area. This would result in greater mass, volume, and cost. Command data is designed to be sent to the spacecraft via optical uplink for decoding, then to the OTP, so one location of decoding is necessary. System acquisition time is calculated to be less than three seconds [18].

8.5   Dynamic Environmental Effects

Knowledge of dynamic environmental effects is essential to ensure mission survivability. The OTP can be effected by various aspects of space environment. Micrometeoroid encounter probabilities are based on Galileo Orbiter estimates. The component most susceptible to meteoroid damage is the telescope mirror. Since the OTP boresight is to be pointed toward Earth opposite the velocity vector, minimum shielding is required [18].

OTP has been designed for maximum protection against gravitational, magnetic, electrical, and thermal radiation at 10 AU's. The thermal subsystem includes a heater to keep the OTP temperature in its operating range [18].

The OTP design has five specific background noise sources. These consist of uplink to OTP from EORS, Earth background radiation, off-axis sunlight scattering on the detector, Earth tracker, and downlinking. OTP is capable of compensating for all of these effects [18].

8.6   Optical Transceiver Package Components

The two major components of the OTP consist of an electro-optics assembly and electronics assembly. The electro-optics assembly contains a telescope, imaging optics, downlink laser, Earth tracker head assembly, and beacon communication detector. The electronic assembly consists of a power unit, a communications electronic assembly and a control electronics assembly [18].

In the electro-optics assembly, the telescope is fixed mounted and collects the beacon and Earth radiation and relays it to the imaging optics. The laser used in the OTP for uplinking and downlinking, consists of a frequency doubled Neodymium Yttrium Argon Gas (Nd:YAG) Laser. The maximum range of the uplink/downlink system is 10 AU, which is more than ample for this mission requirement of 4.54 AU. There are three distinct down link rates, 100 kbs, 30 kbs, and 10 kbs. The Earth tracker head is an array detector used for point-ahead and Earth tracking functions. The communications electronics system performs pulse position modification while supplying output data from the spacecraft [18].

Control electronics are used for Earth tracking capabilities. These consist of controlling all OTP modes of operation that are interfaced with the spacecraft attitude reference system and Earth tracker error signals. A power conditioner unit provides all prime power conditioning for various components in the OTP system. The optical design has a Cassegrain 11-inch defraction limited telescope coupled in an image optics assembly. Beam steering mirrors and optical relay elements control vernier tracking and transfer the transmit

laser energy to the telescope, while also transferring received energy to the correct detectors [18].

8.7 Electronics Design

There are three assemblies that make up the electronic configuration. These assemblies provide control, communication, and power conditioning functions. The control electronics provide the acquisition and tracking function. The Communications Electronic Assembly controls the communication functions of coding/decoding and modulating/demodulating. The Power Conditioner Unit converts the spacecraft power to the required secondary voltage levels, provides redundancy switching mechanism and heater control, as well as command and telemetry interfaces [18].

8.8 Conclusions and Recommendations

The optical communication system will meet mission requirements as described by the Cassini mission that will be deployed in 1997. The power and mass required for this subsystem are 57 Watts and 52.4 kg, respectively. The optical communication system requires 29.8 less Watts and 60 less pounds than the proposed upgrade of the Cassini communication configuration. The system also has a higher data rate capability than the Cassini configuration. Unfortunately, this system has not been tested in the space environment. The total cost of the communications system is approximately $157.6 million (FY 2002). This cost estimate was calculated using the Cost Estimation Methods for Advanced Space Systems [12].

9.0   Command and Data Handling

9.1   Requirements

The computer system will monitor the daily housekeeping of the main spacecraft and rendezvous and docking related data from the lander. Everything from attitude determination and control to power management will be controlled by this system. This system will analyze data from the GN&C sensors and apply appropriate thrusters to correct any errors. The CPU will use a system called MAX, which is a high-speed general purpose multicomputer for space applications. Rendezvous and docking will be monitored by a separate MAX [19,20].

9.2   Monitoring of the Spacecraft from the Ground

The Spacecraft Monitoring and Control Software (SMCS) will be composed of approximately 20 subsystems which range from low-level utility routines through the middleware systems to the major monitoring and control software. The main functions of the system are to monitor, display and archive spacecraft telemetry, prepare commands, and produce hard copies of experimental data. Of special interest in the case of the SMCS are the database files, telemetry processing, telecommanding, and archiving of data [19].

9.2.1   Database Files

The SMCS has to rely on the contents of one or more databases for its operation. These range in complexity from the file giving the definitions of each display (parameters, axis limits, colors, etc.) to a list of addresses of experimenters who require hard copies of data.

A standard VAX text editor will be used to update these files. For efficiency, some of them will be compiled into another format for easier access [19].

C-4

9.2.2 Telemetry

The telemetry processing will have to be received from a Data Capture and Staging Subsystem (DACS), which is transmitted across a Transmission Control Protocol/Internet Protocol (TCP/IP) communications interface. The SMCS requests data from the DACS either in real time or recall mode. The incoming telemetry will arrive at Earth in Standard Format Data Units which consists of a header and a 128 byte frame of spacecraft data. These frames must be collected until a whole format of telemetry is complete. The number of frames needed to make up a format is dependent on the type of data (2 for engineering, 32 for scientific). Each format of telemetry produces a Processed Telemetry Record (PTR) which is made available for display and archiving. The DACS will be configured to hold approximately three days of telemetry data. This data can be received from the DACS in four ways. The first is real-time data, which is received directly from the spacecraft. Real-time data, however, must be processed as quickly as possible so that any problems can be detected. The second method is playback. Playback data is recorded onboard and then received interleaved with real-time data. It is stored on disks for processing at a later date. The third way is recall data which is real-time data received at the ground-station, but which, for some reason, was not passed through to SMCS. The final technique is recalled playback data. This is playback data which was not passed through when originally received and is processed as normal playback data [19].

9.2.3 Telecommanding

A schedule of commands is built up using a standard text editor to give a list of data. A day's worth of commands, along with any contingency procedures, will be included in one file. The schedule is made up of four main types of spacecraft commands. The first command is on/off commands which are mainly used for power supply switching. The second type is the fixed-bit pattern memory load commands, and the third is memory load commands with variable input data. Last is the block commands which are made up of sub-

blocks that can contain commands to schedule/deschedule onboard processes. When the command schedule is verified, it is stored on disk until needed. When required for uplink, the processed schedule will be converted into NASA standard command frames and transferred onto tape [19].

9.2.4 Archiving of Data

Data will be stored on circular Short History Files (SHF) which holds the last fifteen day's worth of data. Any playback data will be inserted into the correct place in the file. For these reasons the SHF are circular, the oldest data being overwritten by the newest, and have fixed time slots for each record [19].

9.3 Main Computer Processor

After investigating the many processors available today, a high speed, general purpose multicomputer was selected. This processor is faster, uses less power, and has a higher density than any other processor available. The processor, called MAX, is also best suited for the multiple tasks that will be expected from the computer subsystem.

All MAX's strengths coincide with the requirements of the computer system. MAX possesses sophisticated concurrency support for times when the spacecraft is at an asteroid and many subsystems are operating at once. It also features fault tolerance, which provides redundancy and includes control systems to monitor errors. This will maintain the mission should correctable failures arise. The system is tailorable to any requirements of the mission and has on-line repairability.

Additional qualities the MAX incorporates into its design are: dual processor design, direct memory access, separate local bus and memory for each central processing unit, and two speed data transmission. The transmission can be either conventional multi-tasking and input/output at low levels, or data flow programming at high levels of transmission. The

other improvements to this processor, which are more suited to be discussed in the rendezvous and docking section, also contributed to its selection [20].

9.4 Rendezvous and Docking Processor

Because Rendezvous and Docking (RVD) requires very demanding performance from a computer processor, the main spacecraft will also include a separate rendezvous and docking processor. Rendezvous between the lander and the asteroid, and the lander and the main spacecraft will be monitored by this processor. The RVD processor has the capability to run the software dedicated to monitoring and control of the GN&C, support and management of the standard telemetry package, and managing information related to RVD. This processor will also monitor sensor data acquisition and processing; estimation; position, attitude and thruster control; and the docking mechanism (between the lander and main spacecraft). After a review of the processing required for an RVD maneuver, it was determined that high computing, interface, memory size, and reprogramming capabilities are essential to the success of this maneuver [3].

Another MAX system has been selected as the RVD processor because it contains a floating point unit (FPU) co-processor for advanced mathematics, tailored for real time application; prioritization of responses; and all the qualities explained in the preceding section. The RVD processor will also be a redundancy for the main computer. The special requirements of an RVD processor and how the MAX meets these requirements will be examined in detail in the following sections [20].

9.4.1 Computing Requirements

The RVD processor will derive "measurements" of the spacecraft from sensor output. It will estimate the position from current measurements and the previously estimated state. It will also drive the spacecraft in a given trajectory and attitude by a set of forces and torques on the spacecraft frame. Finally, the processor will compute the relative orientation of the

docking frame with respect to the target's rotating frame, since the attitude of the target is an inertial one. The MAX's FPU co-processor is capable of these computations [20,21].

9.4.2   Memory Size and Reprogramming Capability

A memory size of 0.5 Mbytes will be needed to store the software for the RVD processor. MAX has a memory size of 32 Mbytes [20]. All data collected during the RVD maneuver will be stored while the sampling portion of the mission continues and will then be transmitted to Earth during the travel time between asteroids.

Any reprogramming of the computer must be done from Earth. If reprogramming is necessary the MAX has on-line repairability. Due to the transmission lag-time, checks of the software must be performed two to three weeks prior to the RVD maneuver. This verification time depends on the accuracy and power of the long-range sensors. Earlier detection of the asteroid by the long-range sensors will allow more time to verify the software and make any necessary corrections [21].

9.4.3   Interface Requirements

The RVD processor will interface with the main computer and the GN&C system to obtain the needed telemetry and communication data. Since the RVD processor and main processor are the same this will not be a problem. The GN&C interface will guide the spacecraft to the proper location and give accurate attitude, velocity, and distance measurements. For a successful RVD maneuver, the interface between the RVD processor and the other spacecraft subsystems must have a high level of performance [21].

9.5   Architecture of the Onboard Computer

The computer system aboard the spacecraft can utilize one of three different architectures. The first is centralized architecture. This type of architecture has point-to-point interfaces between processing units and a single management computer. Even though

this type of architecture will have a large wiring harness, it is very reliable. When a failure along one interface occurs, the other processing units and interfaces are not affected. The second type of architecture is bus architecture. The bus architecture uses a common data bus which all the processors share. The third type, ring architecture, establishes a way to arbitrate bus control. The ring architecture allows for adding more nodes with only a minor effect on the central processor. Unlike the centralized system, the ring system may allow a failure along one interface to affect other interfaces.

The MAX hardware architecture uses a bus structure configuration because the system will be fully decentralized (sharing no memory between modules) and there can be any number of identical processing modules. Other features of the bus include global system time synchronization; round-robin access during heavy loading and multiple access during light loading; and fully distributed operations. The bus architecture can be seen in Figure 9.1 [20].
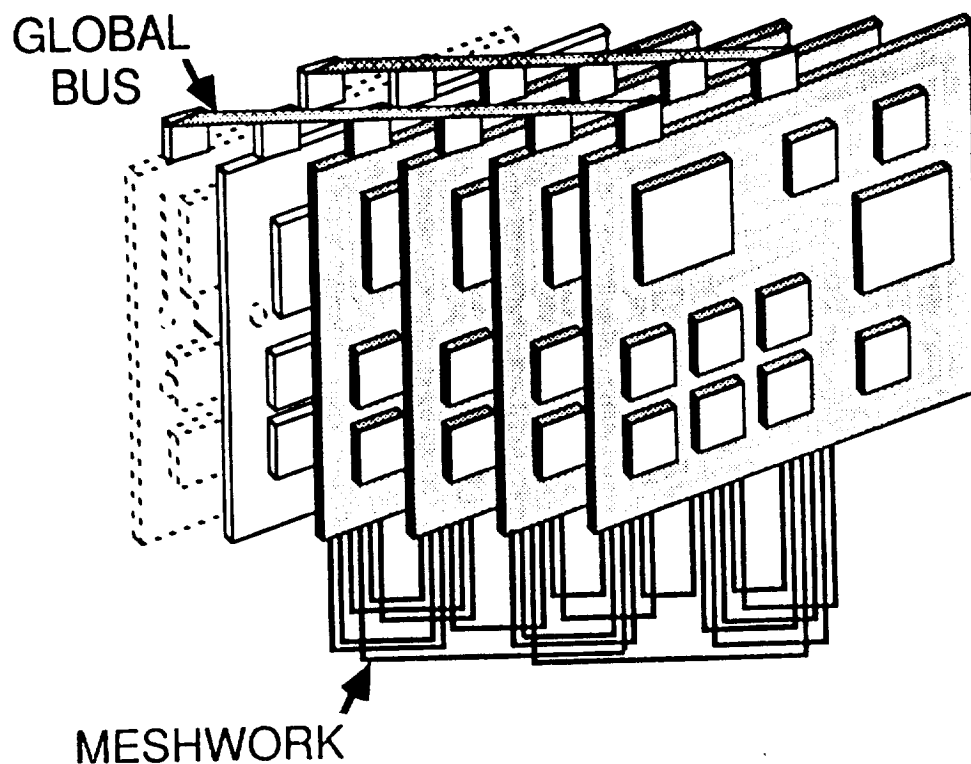
Figure 9.1: MAX Hardware Architecture [Bolotin, G., "Computer Sciences and Data Systems, Vol. 2", *NASA-CP-2459-Vol 2*, March 1987, pp. 250-275.]

9.6 Mass, Power, and Cost Budgets

The following tables contain mass, power, and cost budgets for the computer subsystem of the main spacecraft. The masses of the remote units and the formulas for developing the cost budget came from Reference 3.

Table 9.1: Computer Subsystem [Wertz, J.R. and Larson, W.J., *Space Mission Analysis and Design*, Kluwer Academic Publishers, Dordecht, The Netherlands, 1991.]

	Units	Mass/Unit (kg)	Power (W)
CPU	2	11.3	30.0
Telemetry and Command Unit	2	2.49	8.75
Remote Units			
GN&C	1	5.24	8.45
Propulsion	1	5.24	8.45
Communications	1	5.24	8.45
Scientific Instruments	1	5.24	8.45
Power	1	5.24	8.45
Sampling	1	5.24	8.45
TOTAL		**56.53**	**119.45**

Table 9.2: Cost Analysis for Computer [Wertz, J.R. and Larson, W.J., *Space Mission Analysis and Design*, Kluwer Academic Publishers, Boston, MA, 1991.]

Component	Mass (kg)	RDT&E (FY92$M)	First Unit (FY92$M)
Computer System	56.53	19.51	12.09
Multiplication Factor for Heritage (1.1)			
TOTAL		**21.46**	**12.09**

9.7 Recommendations

Though the MAX processor has no heritage, many of its features are tailored exactly to meet the needs of the mission. Its large memory and ability to compute advanced mathematics make it suitable as the RVD processor. The second processor will be a redundant system because of the modularity and fault tolerance in the MAX system. Its multiple co-processors allow it to handle the needs of several subsystems simultaneously. This processor was the best of those examined at handling the needs of the mission.

10.0 Thermal Control

10.1 Requirements

The thermal control subsystem will maintain the spacecraft within the operating temperatures of the structure and each of the subsystems. It must radiate excess heat produced by the subsystems while controlling the amount of radiation absorbed (primarily solar radiation). Different operating temperatures for the various components and interaction of the components with the thermal control system can make their temperatures difficult to maintain. The thermal control system must operate for the duration of the voyage. Two major types of thermal control systems were investigated: passive and active. A summary of the techniques often used for the thermal control of spacecraft is given in Table 10.1.

10.2 Passive Systems

Passive systems are advantageous because they are lighter, less costly, require less power, and have no moving parts. The one major disadvantage of passive systems is their inability to adequately control temperatures during large changes in solar intensity and intermittent use of equipment having high power consumption. Some passive systems considered include paints, coatings, multilayer insulation, and heat pipes [22].

10.2.1 Paints and Coatings

Paints and coatings are used on the surface of a spacecraft to establish a balance between the heat absorbed and the heat radiated into space. Many types of paints and coatings have been tested and used on spacecraft. The major problems which must be overcome when considering the use of these materials are the solar absorptance, infrared emittance, and degradation due to solar radiation. Some of the materials best suited for and most used in the space environment are: white paints, thermal coatings, and second surface mirrors.

Many white paints have been tested on spacecraft both in near-Earth orbits and in interplanetary space. Of these zinc oxide in potassium silicate (Z-93) and treated zinc oxide in silicone (Z-13G) have shown marked stability over long durations of exposure to radiation in both the laboratory and on spacecraft such as the Mariner V and Lunar Orbiter IV [23]. Both paints show comparable results, degrading little over time. Results from near-Earth craft, however, have shown better results than the interplanetary craft. This is due to the constant exposure of the solar wind outside the Earth's magnetic sphere.

The Z-93 paint was selected for the surface of the lander because of its proven resistance to increased solar absorptivity over long time periods. Its change in solar absorptance was only 0.005 over a period of 1580 equivalent sun hours [23].

Table 10.1: Thermal Control Techniques [Corliss, W.R., *Scientific Satellites*, U.S. Government Printing Office, Washington, D.C., 1967.]

	Technique	Advantages	Disadvantages
Surface paints and coatings (passive)	Stripes, patches, polka dots	Simplicity of application	Nonuniform surface temperatures; difficult with large vehicles
Surface property control (passive)	1. Mirror finish and controlled thickness of coating 2. Surface treatment by chemical baths 3. Sandblasting	1. Control absorptance to emittance ratio over wide range 2. Uniform coating, suitable for large spacecraft 3. High temperature, stable	1. Precision technique, limited to small craft 2. Quality control 3. Quality control
Electric heaters, coolers (active)	Heaters, coolers, temp. sensing, power switching	Simplicity, flexibility of control	Reliability problem, power available for temperature control
Movable external surfaces (active)	Louvers, Maltese cross (movable surface) actuated by bimetal elements	Controls temp. over a wide range of inputs, requires no heater power	Incident sunlight on louvers may pose problem, bearing failures, launch vibrations
Variable internal heat paths (active)	Actuators vary radiation to outer surface by bimetal elements, bellows, or louvers	Efficient use of vehicle's waste heat, requires no heater power	Require compartments insulated from shell

Another thermal coating under consideration was aluminized teflon. Long-term tests on this material have shown it to be very stable under solar radiation following an initial decrease in its solar absorptance. Aluminized teflon also has a lower solar absorptance than many other materials and has a stable infrared emittance rate [24].

A second surface mirror which has proven its effectiveness is the Optical Solar Reflector (OSR). It consists of fused silica with second surface silver. Though it must be bonded to the substrate via adhesives or mechanical fasteners, its low weight per unit area (0.056 g/cm^2) and low solar absorptance to emittance ratio (0.059) make it a competitive choice as a coating [25]. Its low absorptance to emittance ratio also allows it to serve as a radiator.

10.2.2 Multilayer Insulation

The multilayered micrometeoroid shield used on this lander will consist of fiberglass silicone layers with polyurethane foam as a spacer between the layers. This shielding will provide insulation for the internal systems of the spacecraft and will keep heating due to solar radiation within tolerable limits when used with the low absorptance, high emittance second surface mirror and white paint.

10.2.3 Cold Plates and Heat Pipes

Another option examined is the use of cold plates and heat pipes. They allow for the transfer of heat from high temperature to low temperature regions and can be designed to operate as passive systems, having no moving parts.

Both systems operate by absorbing thermal energy. A cold plate absorbs thermal energy via a phase change device. As it absorbs energy from electrical equipment, the phase-change material, usually a paraffin, melts. It then cools, transferring the heat to the cold plate when the equipment is inactive. For a passive system, the cold plate is connected directly to

a radiator to allow for the dissipation of excess heat whereas an active system contains fluid being circulated through passages leading from the cold plate to the radiator [3].

Heat pipes are enclosed systems which operate by absorbing heat through one end of the pipe, vaporizing the working fluid within. The vapor flows to the opposite end of the pipe where it cools and condenses. The liquid is then returned to the evaporator end by flowing through a wick. They are characterized by: high thermal conductance, the tendency of the condenser surface to operate at uniform temperature, and the possibility of variable conductance. Heat pipes as passive systems can be designed with variable conductance by using a noncondensable gas to regulate the condensing area. This allows for a nearly constant source temperature over a wide range of heat input [26]. The major source of failure of heat pipes is incompatibility of the working fluid, wick, and wall materials.

Heat pipes were chosen over cold plates because they can be designed for variable conductance. Heat pipes for space applications commonly use aluminum alloys for the wall material and ammonia as the working fluid. The heat pipes used for this mission will consist of an aluminum wall, ammonia, and a stainless steel multiarterial wick. Argon has been chosen as the non condensable gas for controlling the conductance. Heat pipes consisting of these materials have been proven effective by past usage [26]. The wick is designed to have multiple arteries to allow the pipe to operate should an artery fail due to vapor or gas blockage. The wick configuration is shown in Figure 10.1.

Stainless steel former

mesh lining inner wall and artery
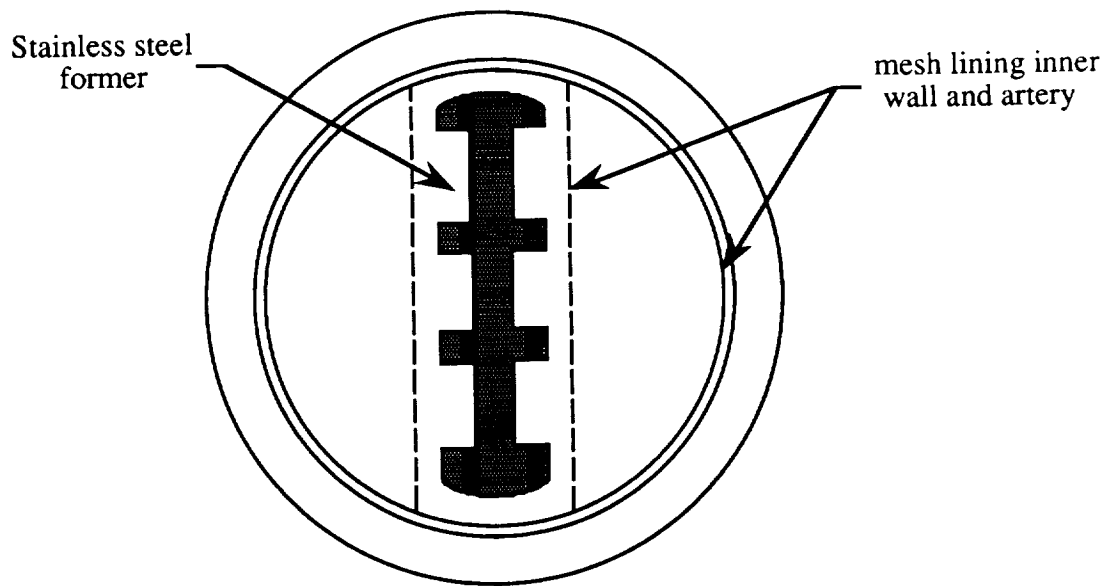
Figure 10.1: Arterial Wick [Dunn, P., and Reay, D.A., *Heat Pipes*, Pergamon Press Inc., Elmsford, New York, 1978.]

10.3 Active Systems

Active systems are useful in situations requiring large dissipations of energy and for systems requiring little temperature variation [3]. Because they include moving parts, active systems can pose reliability problems, especially on long-duration missions. The higher weight and power requirements can also be a problem when these must be kept to a minimum to reduce costs. Electrical heaters were considered as solutions for keeping the subsystems within their operating temperatures as were heat pipes with thermal switches and deployable radiators. Those subsystems with stringent temperature requirements could be placed in ovens, or insulated compartments, with electrical heaters to carefully control the temperature.

10.3.1 Deployable Radiators

In the instance that if more radiating surface should be needed than could be provided by fixed radiators, a flexible, deployable radiator was considered. These can be stowed in compact units during launch and deployed in space. Their mass savings is also

attractive because they do not require extensive structural support [27]. Two types of flexible radiators have been developed: soft tube and hard tube. The soft tube radiator has transport tubing that deploys by unrolling inflatable tubes on either side of a flexible panel. The hard tube radiator uses radiator tubes wound in a helical spring configuration, forming a cylinder. It deploys with the energy stored in the spring.

Although they are attractive from a mass standpoint, these radiators were not chosen since the proposed spacecraft does not have a large power output and second surface mirrors will provide the radiating surface needed.

10.3.2 Electric Heaters and Active Heat Pipes

Because of the decreased reliability associated with active systems and the extra power required to run these systems, electric heaters and active heat pipes were discarded in favor of the lighter, more reliable passive systems. Variable conductance heat pipes can also control the temperature of heat sources with varying power output.

10.4 Recommendations

Due to the scientific importance and the long duration of the proposed mission, materials and systems which have proven their effectiveness have been chosen for the thermal control of the spacecraft. Active systems have been discarded in favor of lighter weight, more reliable passive systems. The systems chosen for the thermal subsystem are Z-93 white paint, variable conductance heat pipes, and a second surface mirror consisting of fused silica with second surface silver.

The total mass of the thermal subsystem is estimated to be approximately 125 kg. This includes a safety factor for any changes in the design which may be needed. Since no active systems will be used for the thermal control, the power consumption of this subsystem is zero. The cost estimate of further development and evaluation of the chosen materials and systems is $16M FY92.

11.0 Meteoroid Protection

11.1 Requirements

The threat posed by meteoroid impact is still not well understood, especially in regions beyond the Earth and its orbital radius. Using radar, visual, and satellite observations, several estimates of the particle flux in deep space have been made. Most of these place the meteoroid flux at four to ten times greater than those near Earth, but inside the asteroid belt it could be as much as a hundred times greater. Meteoroid impact defense selection was based upon a mechanism's ability to protect against the three major impact effects — penetration, surface alterations, and spallation — without adding excessive mass.

11.2 Penetration

The most obvious hazard associated with meteoroid impacts is hull penetration. Both the explosive force and the secondary impacts from the fractured wall particles can cause catastrophic damage to internal systems. In past missions (Voyager, Galileo) the probability of such strikes was so low that hull strengthening was too "weight expensive" to be worthwhile; however, according to estimates by Dr. Fred Whipple [28], an unprotected spacecraft near the asteroidal belt could expect as many as three penetrations a day.

11.3 Surface Alterations

External cracking and cratering of the surface could eventually lead to failure either from stress concentration around the crater lip or from future impacts in the same region. The near continuous micrometeoroid (meteoroids with mass $\leq$ 0.025 g) bombardment has been experimentally shown to cause small surface layer losses over time [29]. Although these losses are very small, in a heightened flux environment they could be as large as 200 angstroms per year. Considering that thermal and optical systems can be significantly altered by a loss of only 0.1 microns, even such small changes are significant.

Problems have also been seen with composite structures. The high temperatures of hypervelocity impact tend to cause delamination and adhesive breakdown [30], and some, including graphite, crush easily under even low-speed impacts.

11.4 Spallation

Even a non-penetrating strike could still cause significant internal damage through spallation. Upon impact a compression wave forms in the target material and travels towards its inner surface. If this wave is strong enough, the inside surface will rupture leaving the wall cracked and weak, while ejecting fragments toward sensitive, unprotected internal systems. Weaker waves could produce destructive vibrational amplitudes in ceramic components or cracks in any welded joints throughout the spacecraft.

11.5 Recommendations

To protect against these hazards either the skin may be thickened to present a larger barrier to incoming particles or a thin bumper-spacer scheme may be used. Increasing the thickness tends to have great weight penalties while still not providing a suitable defense against spallation and vibrational damage; however, with the same material thickness and some advanced materials, the weight efficiency may be increased up to 16 times that of a thickened outer wall. The bumper technique attempts to deflect low energy particles and to arrest the higher energy particles before they impact the spacecraft inner surface. The initial strike occurs on an outer high-strength wall. Any penetrating, spalling fragments, or dangerous vibrations are then met by a thicker area of foam which should sufficiently dissipate the energy to a safe level. By not exposing the spacecraft face to the incoming micrometeor, any surface cracking or spallation is eliminated.

Since high flux rates and high-energy particles are expected in the asteroidal region, an additional bumper-spacer layer will be required to protect from penetration with a 95% certainty. The materials chosen were a fiberglass-silicone bumper and a polyurethane spacer.

Many tests have been performed with this construction [31], and it proved to be the best and most weight efficient defense. A comparison of some other alternatives is shown in Table 11.1, and a cross-section of the design is shown in Figure 11.1.

Table 11.1: Comparison of Various Meteoroid Protection Materials (tested at 10 km/s particle velocity and shield thicknesses of 0.033 in.) (Pipitone, S.J., "Effectiveness of Foam Structures for Meteoroid Protection," *NASA Contractor Report*, 1964.)

Bumper		Spacer		
Material	Weight (lb/ft^2)	Material	Weight (lb/ft^2)	Penetration of Hull?
fiberglass-silicone	0.17	polyurethane	1.2	No
Dacron-Butyl	0.42	flexible latex foam	6.0	No
aluminum (2024)	0.17	none	—	Yes
aluminum (2024)	0.31	polyurethane rigid foam	4.0	Yes
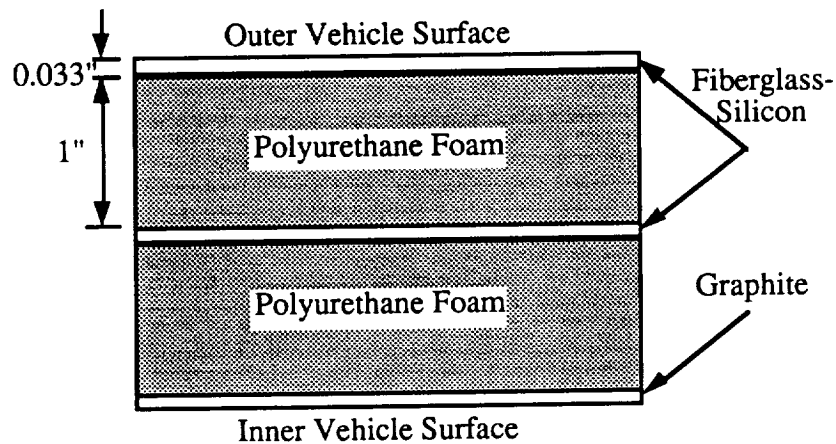
Figure 11.1: Bumper - spacer design concept

Because this mission is a prelude to future asteroid exploration and since no accurate model for meteoroid flux outside 1 AU is available, measurements of meteoroid impacts should be carried out. The best detection method is a simple sounding board - microphone apparatus. If the flux of dangerous meteoroids is found to be sufficiently high, future missions may need to travel out of the ecliptic plane where fluxes are believed to decrease drastically with increasing inclination.

Assuming a total spacecraft surface area of 102.5 ft^2, the bumper protection scheme will weigh approximately 281 lbs. If a sounding plate of total test area of 25 ft^2 is placed over the shield an additional 10 lbs. will be added.

12.0   Scientific Instruments

Because the main purpose of this mission is to obtain information about the composition of asteroids and their future worth for mining purposes, scientific experiments are a high priority.   Most of the asteroidal material study, however, will take place on Earth, where more detailed experiments can be carried out.   If such experiments were to be performed on the spacecraft or at the sampling site, the mass and power restrictions would far outweigh any benefits that might be gained.

Some on-site testing may prove valuable, in the event that the sample is damaged, destroyed, or contaminated upon return.   Only small, inexpensive tests will be performed.   A spectrometer will be used to determine the rough composition of the asteroid.   Magnetic field strength measurements will also be taken with an on-board magnetometer [22].   If future missions are to be manned, radiation counts will also be needed and these will be found via a Geiger counter.

In order to find a safe landing site, and to provide additional information on asteroid structure, radar will be used to provide detailed surface maps.   Radar was chosen over the many other available systems because its performance is independent of reflected light, it is very accurate, and it can cover larger areas than optical methods.

Additionally, as stated in the section on micrometeoroid shielding, a reliable model of meteoroid flux rates and masses is essential to missions into the asteroidal belt.   This data will be gathered by a simple microphone - sounding board apparatus.

The total mass and the total cost of the recommended scientific instruments are 120 kg and 180 million dollars, respectively.   These systems will also require 250 W of power to run.
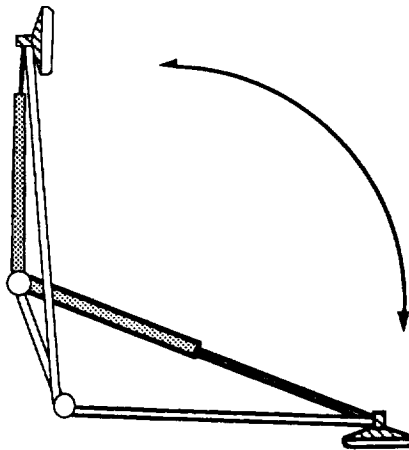
13.0 Landing Gear System

13.1 Requirements

Touchdown on the asteroid will be an extremely crucial part of the mission. Therefore, much care was taken in designing the landing gear. The legs must be capable of being stored during transport and then deployed to hold the lander in a vertical position. A vertical orientation is desired to ensure proper drill alignment. Consequently, the landing gear must be flexible and have the ability to adapt to a variety of terrain [32]. In addition, lightweight landing gear are desirable to keep the overall mass of the spacecraft as low as possible. It is not necessary for the landing gear to support much weight since the gravity on the asteroids will be negligible. Therefore, the primary function of the landing gear is to provide stability. Stability during the drilling phase is very important and for this reason the landing pads must have the ability to anchor to the asteroid surfaces. By anchoring to the surface, the lander will be prevented from twisting due to the drill's torque.
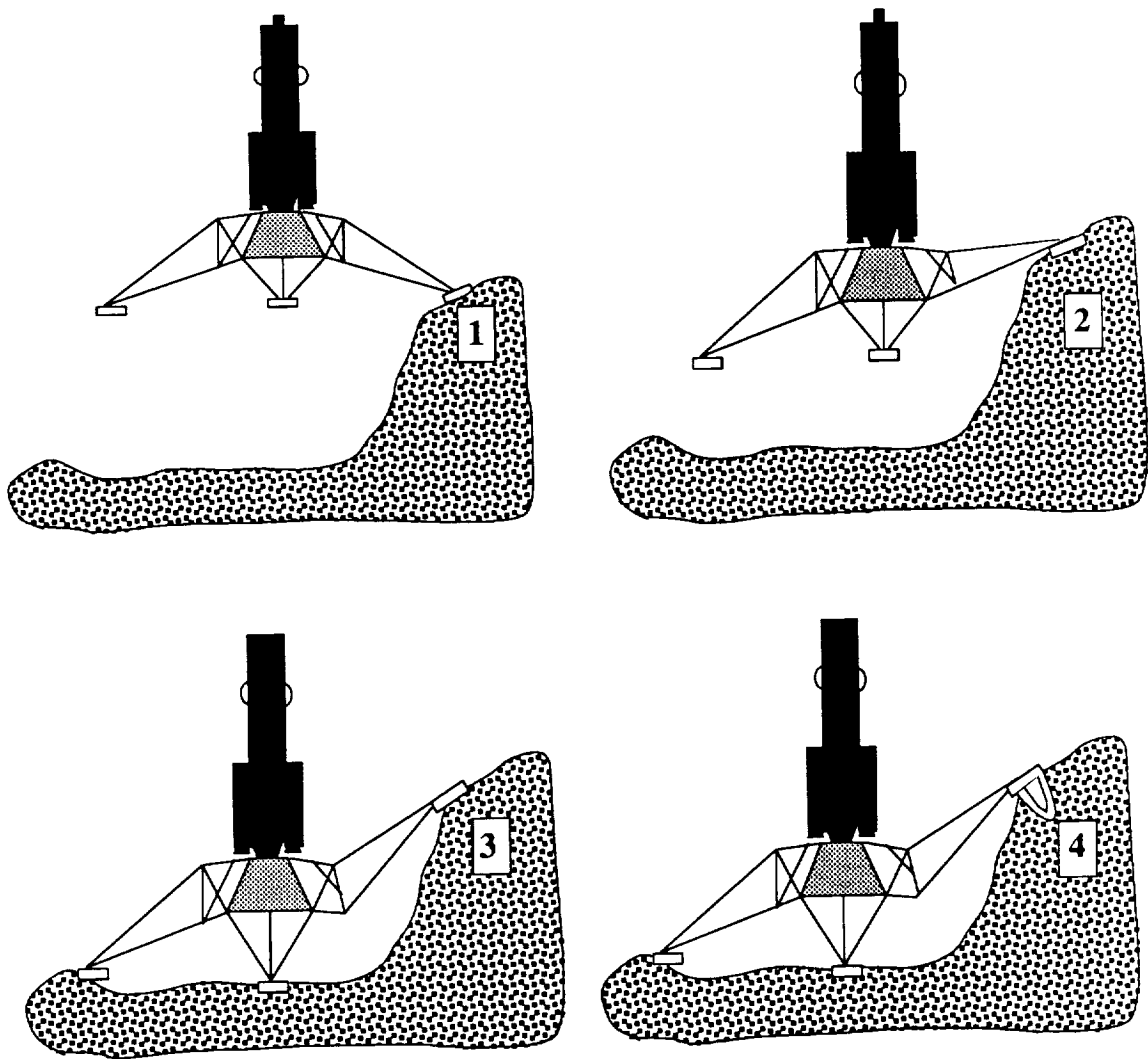
13.2 Landing Gear

The design of the landing gear structure is relatively simple and resembles the configuration used in the Apollo program. The system will be composed of three legs; Figure 13.1 illustrates the basic design of the landing gear articulation. The upper strut is a spring loaded telescoping member. During transport, the legs will be folded against the body of the lander. Upon rendezvous with the asteroid, the legs will be released and allowed to extend to their landing position. The landing gear is equipped with sensors on the bottom of the landing pads which are linked to the central processing unit of the main spacecraft. With this system, the landing gear will be able to adapt to the unpredictable surface irregularities on an asteroid. The lander will be able to land in a vertical orientation without the use of an expensive and heavy active suspension system [32].

Figure 13.1: Landing Gear Articulation. [Angell, D., et al., "Lunar Polar Coring Lander," University of Texas, May 4, 1990.]

13.3 Operation of the Landing System

As the lander reaches the terminal portion of its descent, the computer begins waiting for input from the pressure sensors at the bottom of the landing pads. Once a signal is received from a landing pad indicating that contact has been made, the computer commands the upper telescoping arm of the leg to unlock. The leg will then be free to move without resistance. As the spacecraft continues to slowly descend, it maintains vertical orientation by firing the attitude control thrusters. When a second landing pad signals that it has touched down, the computer commands the upper telescoping arm of that leg to unlock and allow the leg to move. Finally, after the third leg signals that it has touched down, the computer commands the upper arms of all three legs to re-lock in their current positions (see Figure 13.2). As the lander descends, the computer checks the percentage of the full articulation of each leg continuously. If full articulation of any one of the legs is reached before one of the other legs touches the surface, the computer commands the lander to thrust upward and outward. The lander will avoid a failed landing and make a short hop to a new landing site and try the procedure again. Figure 13.3 illustrates the control loop [32].

Figure 13.2: Potential Landing Scenario Illustrating the Adaptability of the Landing Gear to Uneven Surfaces. [Angell, D., et al., "Lunar Polar Coring Lander," University of Texas, May 4, 1990.]
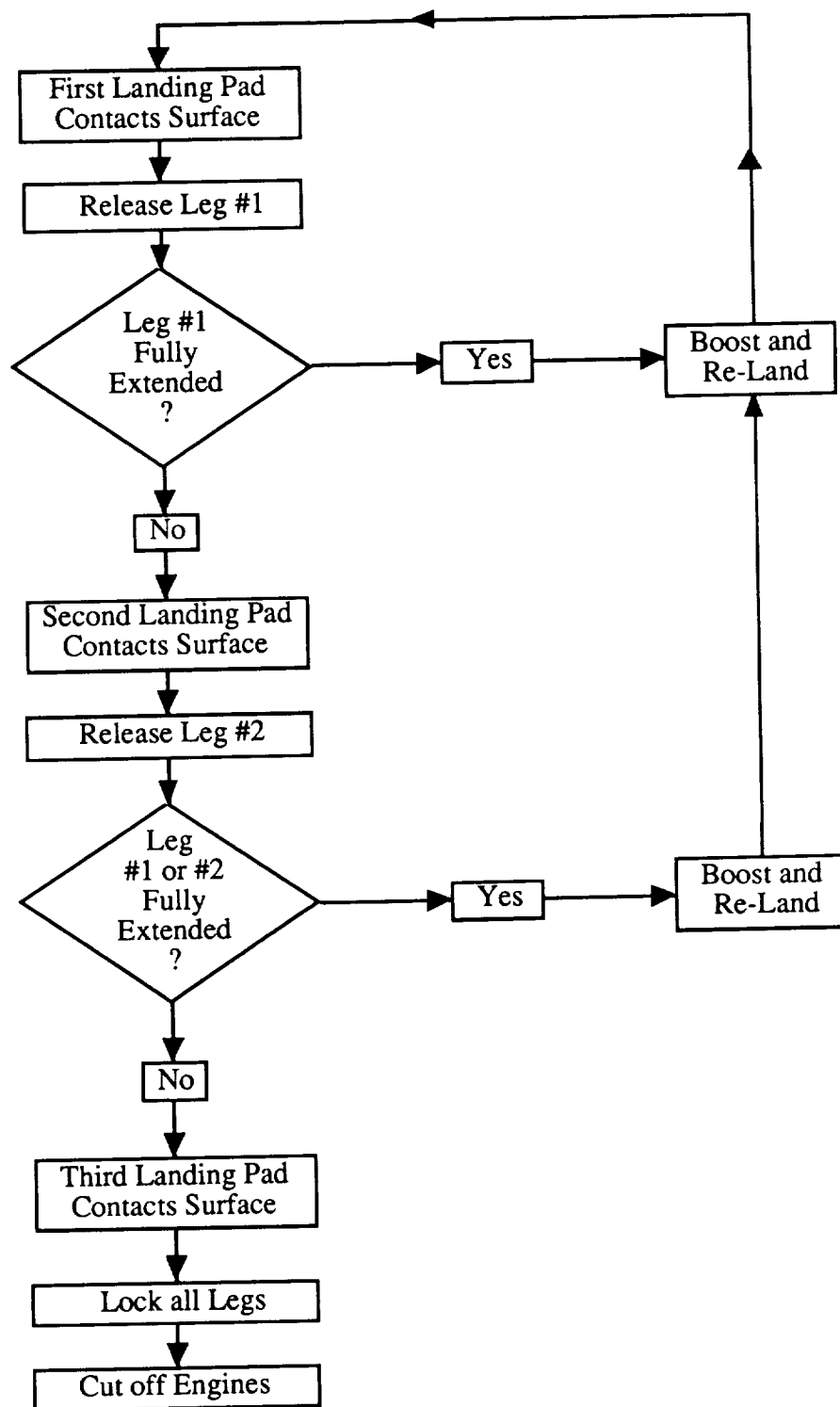
Figure 13.3: Landing Gear Control Loop. [Angell, D., et al., "Lunar Polar Coring Lander," University of Texas, May 4, 1990.]

13.4 Anchoring Devices

During the drilling process it is necessary to maintain proper drill-hole alignment. If the drill stem and hole become misaligned, the power consumption of the drill will increase significantly and the penetration rate will drop off rapidly. To guarantee proper drill-hole alignment, it is necessary to prevent the lander from moving during the drilling process. To accomplish this task, each landing pad will have four small drills mounted inside it. When the lander has successfully landed, one drill inside each landing pad will be activated. These three drills will deploy and penetrate the surface of the asteroid, thereby anchoring the lander to the asteroid. Thrusters on the top of the lander will force it against the asteroid while the anchoring drills are operating, thus insuring successful penetration of the anchoring drills. The lander is to land in three different places on three different asteroids, and therefore the small drill bits in the landing pads will inevitably wear out. For this reason, each landing pad will have four anchoring drills. One drill in each landing pad will be utilized for all three landings on each asteroid. The fourth anchoring drill on each landing pad will serve as a backup. Figure 13.4 illustrates a landing pad [32].

Side View   Top View
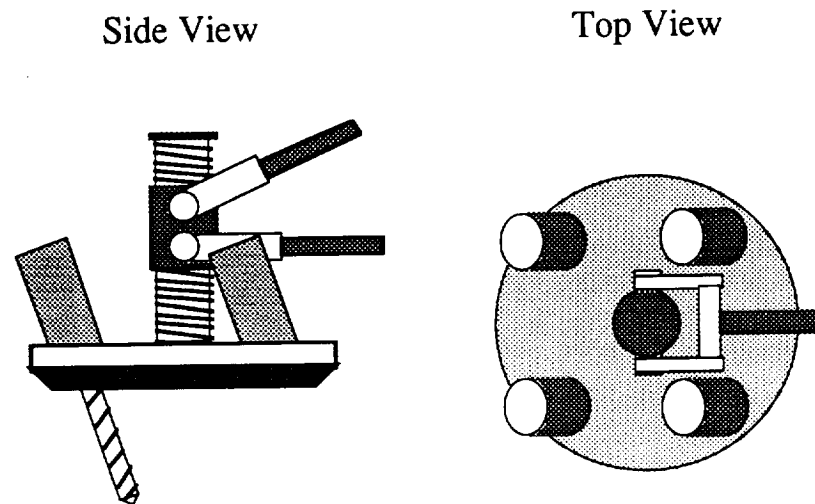
Figure 13.4: Landing Pad. [Angell, D., et al., "Lunar Polar Coring Lander," University of Texas, May 4, 1990.]

13.5 Conclusions and Recommendations

The landing gear design will meet the requirements described in section 13.1. The mass of the landing gear was estimated at about 15 kg [32]. The estimated cost of this system was found to be approximately $69.4 million (FY 2002) [12].

To improve the landing gear design further it would be desirable to select the materials to be used in the landing gear. As stated earlier, the landing gear does not need to support much weight, but its stiffness is important for stability. Therefore, a composite material such as graphite/epoxy might be used for its excellent stiffness characteristics and light weight.

14.0   Coring Method and Design

14.1   Requirements

Due to the harsh space environment and variety of rock formations, several design and performance constraints have been specified to obtain pristine core samples. Each of the core samples are to be approximately one meter in length. Preferably, the cores should be removed in one piece, with very little damage or contamination. Thus, the coring apparatus and lubricants must only minimally affect the physical properties of the samples. Also, the apparatus must be able to protect the core samples from damage and contamination during the transport back to Earth. The storage system should be able to accommodate a total of nine samples, and the samples should be stored in such a manner that their place of origin can be easily traced [33].

The coring apparatus must be totally automated, self-maintaining, and be required to operate in a vacuum. The coring bit must be able to withstand the dry drilling conditions as well as the large temperature differences due to the heat generated during the drilling process. Additionally, the apparatus must be lightweight to minimize transportation costs, yet durable and as efficient as possible [34].

14.2   Sample Size Considerations

From terrestrial geochemical studies, with most types of advanced instrumentation for chemical and isotropic analysis of geologic materials, samples exceeding 0.1-1.0 grams in mass cannot be analyzed directly but must be subsampled. These sampling procedures are quite complicated, but will ensure limited sampling errors. Thus, the sample size should be minimized as far as possible in order to be able to return as many different samples as possible. Nevertheless, the samples should be large enough to be representative. Therefore, as stated in [18], a core sample of approximately 2.5 cm in diameter by 1 meter was determined to be large enough to permit measurement of the important physical properties.

Assuming an approximate density of 3500 kg/m^3, the mass of a single sample was determined to range from 1-3 kg depending on the surface material compositions [35]. This would also minimize the total mass to be returned to Earth [36,37].

14.3   Drill Design

The drill is required to be fully automated and very robust. It must also be able to core in a variety of rock formations as well as withstand the harsh environment of space [32].

Due to a combination of axial crushing and rotary removal of debris, a rotary-percussion drilling technique was considered. This combination of percussion and rotation would allow the drill to break through hard surfaces and provide the cutting action while forcing drill debris out of the hole. This method produces a lower bit temperature as compared to a diamond rotary coring method [32,38].

A tungsten carbide bit was chosen over a diamond bit. This selection was made because a diamond bit is limited by heat constraints and the inability to sustain a percussion action. Also, due to the dry drilling conditions, the diamond bit has a tendency to dull quickly in very hard rock formations. Whereas, the tungsten carbide bit was found able to withstand the high temperatures caused by friction associated with dry drilling [32].

The coring assembly, shown in Figure 14.1, consists of a coring bit and a core barrel, which are both located at the end of the drill stem. The core barrel is a hollow tube designed to receive and retain the core sample as the bit drills into the asteroid. Due to the harsh conditions and treatment that the core barrel and drill stem must withstand, such as the high abrasion from the walls of the drill hole, high temperatures, lack of lubrication, and percussive impacts, the drill stem and core barrel will be made of titanium or similar material. To reduce the undesired build-up of friction caused by the contact of the regolith with the walls of the drill stem, the drill bit would be slightly larger in diameter than the stem. This would allow for space between the drill stem and drill wall. Since the cuttings from the drilling can carry up to 80% of the heat generated during the coring process, quick removal of

these cuttings would reduce the heat transferred into the core by 60% and prevent any possibility of the coring apparatus from jammed during the coring process. Thus, helical augers implemented on the outer wall of the stem will provide debris removal from the bottom of the drilling hole. An intermittent flow of xenon gas blown down the hole could also aid in the removal of the debris, and provide some lubrication and cooling of the drill bit. Several one-way gates at the bottom of the stem would prevent the core from sliding out during retrieval of the sample [32].
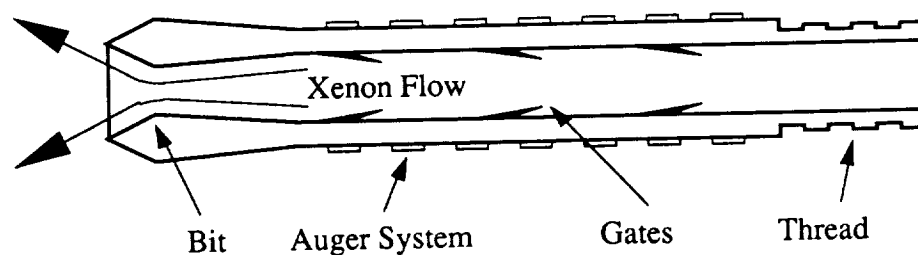

Figure 14.1: Drill Stem Assembly. [Angell, D. et. al., "Lunar Polar Coring Lander," University of Texas, May 4, 1990.]

An electric motor will have numerous functions during the coring process. These functions include supplying a downward reciprocating axial force and transferring torque to the drill stem. A mechanical gearing device will be used to vary the drilling rotation rate. It will also allow the drill to share its power between the axial, percussive motion, and the torque. Lubrication of these parts should be achieved by a solid lubricant, such as sulfur steel or a silicon coating. This would reduce the risk of contamination of the core samples. To reduce the bulk and mass of the drilling structure, hoisting of the sample will be provided by the same mechanism used to drive the drill stem. With the percussive motion ceased, the system will simply be put into reverse. However, the rotary motion of the drill will be maintained to reduce friction [32].

14.4 Drill Stem Storage Cylinder

Since several samples are to be taken, core sample containers will store the extracted samples. As mentioned earlier, the drill stem will be used to drill into the asteroid, as well as to receive and retain the sample for storage. Thus, the design will include a total of ten drill stems. Nine of the drill stems will be used to retrieve the desired samples, while the tenth drill stem will be included in the event one of the other nine drill stems fail. Due to the harsh conditions that are inflicted upon the drill bit during the dry drilling procedure, the bit will have a tendency to dull quickly and may be close to its melting temperature after the coring process. Therefore, using different drill stems for each sample would allow a new drilling bit to be used. Also, by changing the drill stem after each drilling procedure, the chance of contaminating other samples with the same drill bit will be lessened. The drill stems will be positioned in a circular arrangement as seen in Figure 14.2 [33].
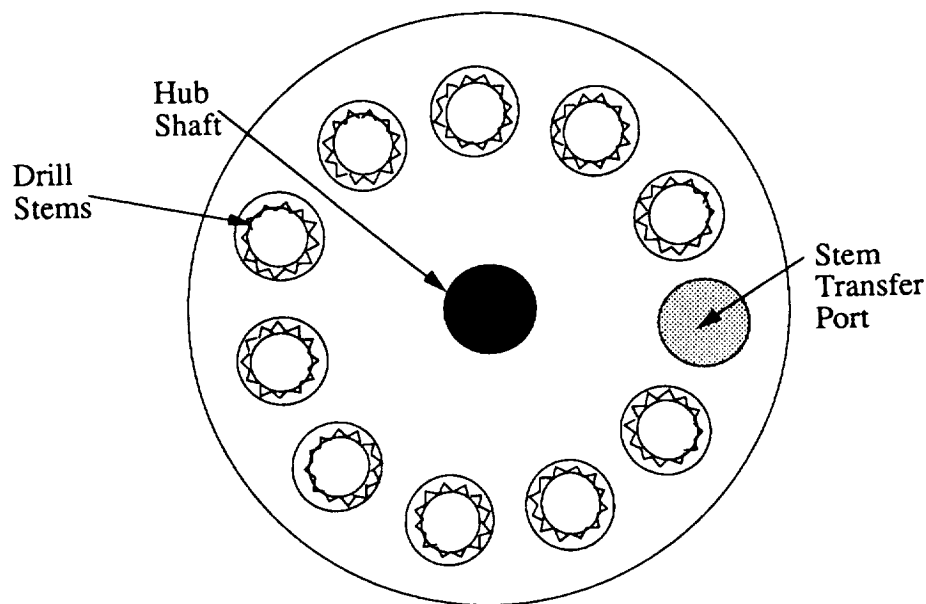
Figure 14.2: Drill Stem Storage Cylinder. [Angell, D., et. al., "Lunar Polar Coring Lander," University of Texas, May 4, 1990.]

14.5 Drilling Operation and Procedure

Each drill stem will be stored in a rotating turret similar to a revolver. The hub shaft, which the revolver-like turret rotates on, aligns an empty drill stem with the drill shaft. Then, the driller shaft attaches itself to the drill stem, and the vertical transfer drive assembly of the drill removes the stem from the turret. Next, the drill stem is aligned with the stem transfer port in the turret assembly and on the lander. Once the proper alignment is achieved, the drilling process can begin, and the drill stem is lowered towards the asteroid's surface. Throughout the drilling process, xenon gas will be blown down the hole intermittently to aid in flushing out any debris, while the core barrel receives the sample. After the one meter sample is obtained, with the percussive action ceased, the drill motor will be put into reverse to extract the sample. Finally, the drill stem with the core sample will be placed back into the turret. For the other samples, the turret will rotate so the drill shaft can be aligned with an empty stem. Once the drill shaft and stem are aligned, the procedure will be repeated [32].

14.6 Penetration Rates and Power Requirements

Table 14.1 illustrates the anticipated average power requirements and rate of penetration for various types of solid rock. These suggested values are dependent on the type and size of motor used; therefore, they are subject to change. The total amount of energy required is for a one meter drilling process, including extraction of the sample.

Table 14.1: Coring Penetration Rates and Power Requirements. [Angell, D. et. al., "Lunar Polar Coring Lander," University of Texas, May 4, 1990.]

Material	Penetration Rate (cm/min)	Specific Energy Density (W-hr/m)
Pumice	300	8
Unsorted cohesive conglomerates	150	16
Vesicular basalt (50% porosity)	12	150-200
Dense basalt ($1760 \, kg/cm^3$)	3	900-1200

14.7 Subsystem Mass Estimates

An estimated mass of the entire coring apparatus, including the drill stems and storage cylinder, is illustrated in Table 14.2. The masses are approximations from other similar coring and storage devices.

Table 14.2: Coring Apparatus Mass Estimates. [Duke, M.B., et al., "Manned Mars Missions: Working Group Papers," NASA, May 1986, and Chugh, C. P., *Manual of Drilling Technology*, A. A. Balkema Publishers, Rotterdam, 1985.]

Component	Estimated Mass (kg)
Motor	38
Gear Box	30
Drill Stem Assemblies	62
Drill Stem Storage Revolver	25
Miscellaneous	5
TOTAL	**160**

14.8 Conclusions and Recommendations

Details for this coring apparatus design require further development. The estimated cost of the system was determined to be $329.25 million (FY 2002) [12]. Future research would include an analysis to determine the torque required of the coring apparatus. This constraint will then have to be utilized in the design of the electrical motor and the mechanical gearing device needed to drive the drill. A structural analysis should also be performed to determine the stresses which the drill stem assembly would encounter during the coring process. This would ensure that the drill stem assembly would be manufactured from the appropriate materials, such as lightweight titanium. Also, a method or device to cut off or fracture the core sample from the bottom of the drilled hole is necessary for the extraction of the sample. Additionally, a control system to coordinate the coring process should be defined and developed.

15.0 Conclusions and Recommendations

This mission will provide several asteroid samples from the three most common types of asteroids. Information from these samples will teach us about the constituents of much of the solar system, and will reveal secrets of the solar system's origin.

Unfortunately, this mission is 24 years long, making the reliability very questionable. This could be reduced by selecting different target asteroids. Perhaps smaller, near-Earth asteroids would allow for smaller travel and stay times.

Although the optical communications system is not a space-tested design, it is lighter, smaller and requires less power, than conventional communications systems. This system is currently being developed and will provide more than ample communication rate and range. The GN&C system will use a combination of hydrazine thrusters, cold gas thrusters, and Inertial Measurements Units. Cold gas thrusters on the lander are utilized to reduce the thermal protection necessary on the main spacecraft. The hydrazine thruster can supply the appropriate thrust level and have a proven heritage. Temperature of the spacecraft will be controlled by a passive thermal system. Heat pipes with multiarterial wicks with ammonia as the working fluid will be used. Multiarterial wicks will reduce the chance of system failure due to impurity build-up over time. An advanced multicomputer called MAX will be used as both the main computer system as well as the rendezvous and docking system. The MAX system is lighter, requires less power, and has a greater capacity for adaptation than any existing processor. This system is still under development but shows great potential. Micrometeoroid protection will utilize a two bumper technique. This technique has proven to be 95% effective. This system will also act as thermal insulation for the spacecraft. The drill system will retrieve three samples from each of three asteroids as well as protect the samples. To do this the drill has been designed to operate in the harsh environment of space and to be able to drill through the very hard asteroid surface. The landing gear has been designed to adapt to uneven asteroid surfaces and to secure the lander to the surface for the

drilling process. The legs will hold the spacecraft nearly vertical so that the drill will penetrate as deeply as possible. Small anchoring drills will be employed on the landing pads to ensure a secure grip on the surface.

The GE SP-100 nuclear power reactor was reactor was chosen for use on this mission since it is specifically begin developed for application in development of the power system. The power system was mainly chosen for nuclear electric powered propulsion. The SP-100 is still being developed therefore all mass, power, and cost estimates are subject to change.

Using ANSYS finite element analysis, a mass estimate for graphite epoxy spacecraft structure was obtained. Placement of subsystems on the spacecraft bus needs to be researched further. Also, mass estimates of the lander vehicle are provided although further analysis is needed to finalize the design.

Because the Titan IV can carry 15,800 kg and accommodate a spacecraft 16 m long by 4.5m in diameter, the Titan IV will be used to launch the spacecraft. The Shuttle, or its replacement, will be used to return the lander and the samples to Earth.

The number of thrusters as well as the mass of propellant were determined using the QT2 program. If parameters of the orbital mechanics are altered, estimates are subject to change.

Future work would include more intricate analysis in the system layout, specifically including the plumbing network, pressure tanks, fuel storage, and propulsion network configuration. A thruster capable of producing higher thrust levels or able to sustain longer periods of operation should be explored. Power and mass estimates have completed for the for the individual thrusters and thruster control units. Cost estimates were derived from the NASA Advanced Cost Estimates program.

The combination of these subsystems is hoped to produce a reliable spacecraft that will gather data about the Solar System that has never been obtained before. Furthermore, exact details must be developed and figures for cost, mass, and power may vary slightly in the final design.

16.0 References

[1] Adams, C., "Design Study for Asteroidal Exploitation," The Massachusetts Institute of Technology, Lexington, Massachusetts, August 1985, pp. 1-33.

[2] Isbell, D., and Lawler, A., "NASA Budget Funds All Sectors, Snarls Science Projects, Space News, Army Times Publishing Co., Springfield,.VA, Vol. 2, No. 34, October 7-13, 1991, p. 10.

[3] Wertz, J.R. and Larson, W.J., Space Mission Analysis and Design, Kluwer Academic Publishers, Dordecht, The Netherlands, 1991.

[4] Black, T., "Optimal Low Thrust Transfer Using a First Order Perturbation Model," Thesis, Air Force Institute of Technology, Wright Patterson Air Force Base, June, 1985.

[5] Bender, D.F., "Osculating Orbital Elements of the Asteroids," Jet Propulsion Laboratory, 1979.

[6] Riehl, J.P., and Mascy, A.C., "QT2: A New Driver for the Chebytop System," NASA, Cleveland, OH, February, 1990.

[7] Lenorovitz, J.M., "Campaign Begins for Ariane 5 Orbital Satellite Launch Customers," Aviation Week and Space Technology, October 28, 1991.

[8] Deininger, W.D., Design and Performance of an ArcJet Nuclear Electric Propulsion System, Jet Propulsion Laboratory, AIAA-87-1037, May, 11 1987.

[9] Morren, W. and Soney, J., 2000 hour Cyclic Endurance Test of a Laboratory Model Multipropellent Resistojet, NASA Lewis Research Center, Cleveland, OH, AIAA-87-0993, May 11-13, 1987.

[10] Hill, P. and Peterson, C., Mechanics and Thermodynamics of Propulsion, Addison-Wesley Publishing Co., 1992.

[11] Shimada, S., Takegahara, H., and Kimura, H., Ion Engine System For North-South Station Keeping of Engineering Test Satellite VI, Mitsubishi, Kamakura, Japan, AIAA-87-1005, May 11-13, 1987.

[12] Cyr, K., "Cost Estimation Methods for Advanced Space Systems," NASA/Johnson Space Center, 1988.

[13] General Electric Space Nuclear Power Tutorial. Conducted at NASA Lewis Research Center, May 29-31, 1991.

[14] Hack, K.J., George, J.A., and Riehl, J.P., Evolutionary Use of Nuclear Electric Propulsion, NASA Lewis Research Center, Cleveland, OH, AIAA 90-3821, September 25-28, 1990.

[15] Wilson, A., Interavia Space Directory 1989-1990, Intervia SA, 1989.

[16] "Outward to the Beginning: The CRAF and Cassini Missions of the Mariner Mark 2 Program," Jet Propulsion Laboratory, 1988.

[17] Lesh, J.R., "Deep Space Optical Communications Development Program," Jet Propulsion Laboratory, California Institute of Technology, January 1987.

[18] Lambert, S.G., et al., "Design and Analysis of a Spacecraft Optical Transceiver Package," Final Report, JPL Contract 957061 with McDonnell Douglas Corporation, August 19, 1985.

[19] Hamer, P.A., and Snowden, P.J.,"Ulysses Spacecraft Control and Monitoring System",*Journal of British International Society*, Vol. 44, No. 7, July 1991, pp. 317-329.

[20] Bolotin, G.,"Computer Sciences and Data Systems, Volume 2", *NASA-CP-2459*, Vol. 2, March 1987, pp. 250-275.

[21] Gerli, C., and Longoni, F., "The RVD Mission: The On-Board Data Processing Requirements",*Proceedings of the 1st European In-orbit Operations Technology Symposium*, Darmstadt, W. Germany, November 1987, pp. 87-93.

[22] Corliss, W.R., *Scientific Satellites*, U.S. Government Printing Office, Washington, D.C., 1967, pp. 356-365.

[23] Millard, J.P., "Results from the Thermal Control Coatings Experiment on OSO-III," *AIAA Progress in Astronautics and Aeronautics: Thermal Design Principles of Spacecraft and Entry Bodies*, Vol. 21, 1969, pp.769-795.

[24] Lucas, J.W., *Fundamentals of Spacecraft Thermal Design*, Jet Propulsion Laboratory, 1972, pp. 123-133.

[25] Greenberg, S.A., Vance, D.A., and Streed, E.R., "Low Solar Absorptance Surfaces with Controlled Emittance: A Second Generation of Thermal Control Coatings," *AIAA Progress in Astronautics and Aeronautics: Thermophysics of Spacecraft and Planetary Bodies*, Vol. 20, 1967, pp. 297-314.

[26] Dunn, P., and Reay, D.A., *Heat Pipes*, Pergamon Press Inc., Elmsford, New York, 1978.

[27] Fletcher, L.S., Heat Transfer and Thermal Control Systems, University of Virginia, 1978, pp. 243-262.

[28] Whipple, F.L., "Dust and meteorites," *Astronautics 7*, August 1962, pp. 40-42.

[29] Davison, J.R., "Space Debris Hazard Evaluation," *NASA Technical Notes*, 1963.

[30] Pipitone, S.J., "Effectiveness of Foam Structures for Meteoroid Protection," *NASA Contractor Report*, 1964.

[31] Beller, W., "'Bumper' May Cure Meteoroid Hazard," *Missiles and Rockets*, November 6, 1961.

[32] Angell, D., et al., "Lunar Polar Coring Lander," University of Texas, May 4, 1990.

33)

[33] Collins, D., et al., "Microcoring Apparatus," Advanced Design Program, Georgia Institute of Technology, March 18,1989.

[34] Akins, J., et al., "Core Sample Extractor," Georgia Institute of Technology, 1989.

[35] Weast, R.C., ed., "Handbook of Chemistry and Physics," 65th Edition, Chemical Rubber Company, 1985.

[36] Koeberl, C., et al., "Sampling Mars: Analytical Requirements and Work to Do in Advance," Institute of Geochemistry, November 16-18, 1987.

[37] Korotev, R.L., and Haskin, L.A., "Some Lessons from Apollo for a Sampling Strategy on Mars for Understanding the Origin of the Ancient Igneous Crust and the Composition of the Mantle," Department of Earth and Planetary Sciences and McDonnell Center for the Space Sciences, Washington University, November 16-18, 1987.

[38] Chugh, C.P., *Manual of Drilling Technology*, A. A. Balkema Publishers, Rotterdam, 1985.

[39] Duke, M.B., et al., "Manned Mars Missions: Working Group Papers," NASA, May 1986, and Chugh, C. P., *Manual of Drilling Technology*, A. A. Balkema Publishers, Rotterdam, 1985.